UNIVERSITY OF SOUTHAMPTON

FACULTY OF NATURAL AND ENVIRONMENTAL SCIENCES
SCHOOL OF OCEAN AND EARTH SCIENCES

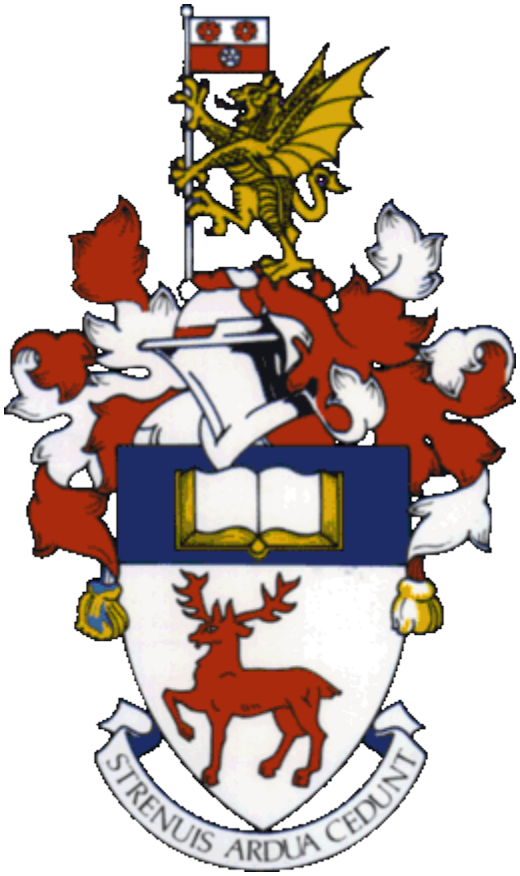

NUTRIENT UTILISATION BY *TRICHODESMIUM*
CHARACTERISATION OF MOLECULAR AND PHYSIOLOGICAL PROCESSES

by
DESPO POLYVIOU

Thesis for the degree of Doctor of Philosophy
August 2016

Despo Polyviou:
Nutrient utilisation by *Trichodesmium*
Characterisation of Molecular and Physiological Processes

Supervised by:

Prof. Thomas S. Bibby, Prof. C. Mark Moore,
Dr Andrew Hitchcock, Dr Martha Gledhill and Prof. Matt Mowlem

I dedicate this book to the three people who have made me who I am today:

My brother, who taught me that shoes need to be taken for walks and that you can be anyone you like to be (be that a fairy tale character or a cool animal.

My mum, the strongest person I know, who taught me what love is, what patience is, and who believed in me when no one else did (not even me).

My dad, who inspired my love for the sea, and taught me to never cease searching both inside and around me.

“I ca’n’t believe that!” said Alice

“Ca’n’t you?” the Queen said in a pitying tone.

“Try again: draw a long breath, and shut your eyes.”

Alice laughed. “There’s no use trying,” she said:

“one ca’n’t believe impossible things.”

“I daresay you haven’t had much practice,” said the Queen. “When I was your age, I always did it for half-an-hour a day.

Why, sometimes I’ve believed as many as six impossible things before breakfast.”

Through the Looking-Glass
Lewis Carroll

UNIVERSITY OF SOUTHAMPTON

ABSTRACT

FACULTY OF NATURAL AND ENVIRONMENTAL SCIENCES
School of Ocean and Earth Science

Doctor of Philosophy

NUTRIENT UTILISATION BY *TRICHODESMIUM*:
Characterisation of Molecular and Physiological Processes

By Despo Polyviou

The activity of photosynthetic cyanobacteria capable of nitrogen (N_2) fixation (diazotrophs) strongly influences oceanic primary production and global biogeochemical cycles. The niche of these organisms extends mainly across low latitude oligotrophic oceans, largely deficient in nitrate, where they introduce 'new' nitrogen (N) to the system. In these regions the abundant marine cyanobacterium *Trichodesmium* spp. accounts for a significant proportion of the fixed N flux.

Despite fixation of N, the availability of phosphorus (P) and iron (Fe) remain a constraint to the activity and biogeography of diazotrophs. The genome of *Trichodesmium* has therefore been shaped to provide intricate adaptive strategies optimising growth under both P and Fe depletion. Characterisation of these strategies can provide information that will enhance the understanding of the organism's biogeography in the contemporary and future ocean.

In this work, molecular and physiological techniques are employed to study nutrient uptake pathways, and the metabolic response of *Trichodesmium erythraeum* IMS101 (*Trichodesmium* hereafter) to nutrient limitation. The current lack of an established system for genetic manipulation of this organism inhibits direct functional characterisation of proteins. To circumvent this, the model cyanobacteria *Synechocystis* sp. PCC 6803 (*Synechocystis* hereafter) is used as a vehicle for the heterologous expression of *Trichodesmium* genes.

Using this technique, the suggested contribution of *Trichodesmium* to an emerging oceanic P redox cycle is first explored. A four-gene cluster (*ptxABCD*), that encodes a putative ABC transporter (*ptxABC*) and NAD-dependent dehydrogenase (*ptxD*), is demonstrated to be responsible for the organism's ability to utilise the reduced inorganic compound phosphite. The presence and expression of this gene cluster is also confirmed in diverse field metagenomic and metatranscriptomic datasets further confirming its role in *Trichodesmium* species.

Pathways of Fe utilisation are also investigated. Through heterologous expression the function of a currently employed Fe stress biomarker, protein Tery_3377 (IdiA), which is homologous to both Fe^{3+} transporters (FutA2-like) and intracellular proteins with protective function under Fe stress (FutA1-like), is elucidated. Fusing the signal sequence of this protein to GFP revealed its periplasmic localisation, and its expression in *Synechocystis* mutants of both *futA1* and *futA2* paralogues further supported involvement in Fe^{3+} uptake, providing evidence for its function as an Fe transporter in *Trichodesmium*.

Finally, a physiological experiment was performed to determine the significance of direct physical contact with Saharan desert dust for acquisition of Fe by *Trichodesmium*. It is demonstrated that cell surface processes are fundamental in dust-Fe utilisation by this organism and transcriptomic analysis identifies a number of unique genes regulated under different Fe and dust regimes including putative cell-surface proteins not previously studied in *Trichodesmium*.

Combined, these studies have revealed a diverse array of molecular and physiological strategies potentially employed by *Trichodesmium* to survive and thrive on the ephemeral supplies of nutrients encountered in oligotrophic oceans, an attribute that facilitates its significant contribution to biogeochemical cycles.

Table of Contents

Chapter 1 1

1.1 The importance of marine primary production 1

1.2 Nutrients in the ocean 3

1.2.1 Phosphorus 6

1.2.2 Iron 8

1.2.3 Paradigms of nutrient limitation 9

1.3 Marine Diazotrophy 10

1.3.1 The players 10

1.3.2 Oxygen avoidance 16

1.4 Living with less- lessons from marine microorganisms 18

1.4.1 Cellular strategies to cope with P stress 18

1.4.2 Cellular strategies to cope with Fe stress 22

1.4.3 Trophic life strategies- Genomic minimalism or maximalism? 27

1.5 Omics and Detection of stress responses 28

1.6 Significance of molecular data in ocean science 31

1.7 Thesis plan 32

Chapter 2 35

2.1 Strains and growth conditions 35

2.1.1 *E. coli* 35

2.1.2 *Trichodesmium* 35

2.1.3 *Synechocystis* 39

2.2 Physiological measurements 40

2.2.1 Photosynthetic physiology 40

2.2.2 Growth 41

2.2.3 Chlorophyll *a* 42

2.2.4 Statistical analysis 42

2.3 Methods for molecular analysis 42

2.3.1 Nucleic acid extractions and quality control 42

2.3.2 DNase Treatment and cDNA synthesis 44

2.3.3 Polymerase Chain Reaction (PCR) conditions 45
2.3.4 Agarose gel electrophoresis 46
2.4 Generation of genetically modified strains 48
2.4.1 Approaches 48
2.4.2 Techniques 53
2.5 Protein Immunoblotting and Crystallisation 55
2.5.1 Immunoblotting 55
2.5.2 Purification and crystallisation 55
2.6 RNA sequencing 57
2.6.1 Library preparation and sequencing 57
2.6.2 Statistical analysis 58
2.7 Bioinformatic analysis 59
2.7.1 Analysis of the Dust-$FeCl_3$ *Trichodesmium* transcriptome 59
2.7.2 Investigation of omic datasets from other studies 59
2.8 Epifluorescent and confocal microscopy 60
2.8 Phylogenetic analysis 60
Chapter 3 63
3.1 Introduction 63
3.2 Results and discussion 66
3.2.1 Phosphite as a source of P for *Trichodesmium* 66
3.2.2 Description of the *Trichodesmium* putative *ptx* genes 68
3.2.3 Regulation of *ptx* gene expression in *Trichodesmium* 69
3.2.5 Heterologous expression of *Trichodesmium ptxABCD* in *Synechocystis*. 73
3.2.4 Environmental prevalence of *ptx* genes in *Trichodesmium* 77
3.3 Conclusions and further discussion 78
Chapter 4 81
4.1 Introduction 81
4.2 Results and discussion 84
4.2.1 Bioinformatic analysis of Tery_3377 84
4.2.2 Tery_3377 cellular localisation 89
4.2.3 Mode of Tery_3377 export to the periplasm 92
4.2.4 *Synechocystis futA* mutants generation and physiology 94

4.2.5 Expression of Tery_3377 in *Synechocystis* mutants 96
4.2.6 Protein purification and crystallisation 100
4.3 Conclusions and further discussion 103
Chapter 5 107
5.1 Introduction 107
5.2 Experimental design 110
5.3 Results and discussion 112
5.3.1 Experimental controls 112
5.3.2 Dust as a source of iron- the role of cell surface contact 113
5.3.3 RNA sequencing results- An overview 119
5.3.4 RNA sequencing technique validation 125
5.3.5 Differentially regulated processes and genes 126
5.3.6 Responses to $FeCl_3$ and dust additions- Pairwise comparisons 130
5.3.7 Markers of iron limitation. Confirmation of the cellular Fe state. 133
5.3.8 Transcriptomic response of major processes across the experimental treatments. 135
5.3.9 Regulatory DNA 154
5.3.10 Other metals 159
5.4 Conclusions and further discussion 160
Chapter 6 167
6.1 Introduction 167
6.2 Main findings and concluding remarks 168
6.2.1 Better characterisation of nutrient uptake systems 168
6.2.2 Dust/$FeCl_3$ effects on photosynthesis 175
6.2.3 Is it more than just the concentration of nutrients? The problem with biomarkers of iron limitation 177
6.2.4 Non-coding RNA- A role in the response of *Trichodesmium* to dust 179
6.3 Final discussions 180
Appendix 183
Bibliography 193

List of Figures

Figure 1.1: Phytoplankton activity and downstream interactions with the ocean system. 2
Figure 1.2: The link between nutrients and primary production in the ocean. 5
Figure 1.3: Interactions of phosphorus and iron forms with the biotic and abiotic environment in the ocean. 7
Figure 1.4: Marine diazotrophy in nutrient limited oceans. 11
Figure 1.5: Trichodesmium morphology. 14
Figure 1.6: Strategies of N2 fixation-photosynthesis segregation 17
Figure 1.7: The Phosphorus and Iron uptake and utilisation pathways in microorganism 21
Figure 1.8: The cellular information flow and interactions with the environment. 29
Figure 2.1: Generation of deletion mutants. 48
Figure 2.2: pFLAG vector map.. 50
Figure 2.3: Generation of the GFP tagged signal sequence strains 52
Figure 3.1: Growth and physiology of *Trichodesmium* in different P regimes 67
Figure 3.2: The arrangement of the *ptxABCD* genes in *Trichodesmium* 68
Figure 3.3: Gene expression analysis in response to P source 70
Figure 3.4: Expression of genes along the *ptx* and *phn* clusters. 72
Figure 3.5: Confirmation of strain generation 74
Figure 3.6: Growth of *Synechocystis* with phosphite requires all four *ptx* genes 75
Figure 3.7: Strains of *Synechocystis* grow unevenly on phosphate 76
Figure 4.1: Current model of the localisation of *Synechocystis* Fut paralogues. 83
Figure 4.2: Maximum likelihood phylogenetic analysis of Tery_3377 homologues from selected bacteria. 86
Figure 4.3: The GFP tagged-signal sequence strains. 90
Figure 4.4: Localization of signal sequence-GFP constructs in *Synechocystis*. 91
Figure 4.5: Identification of GFP expression in *Synechocystis* strains. 93
Figure 4.6: Localization of the *Trichodesmium* Tery_3377 signal sequence-GFP constructs in *Synechocystis*. 93
Figure 4.7: *Synechocystis* Δ*futA1* and Δ*futA2* deletion mutants were generated 94
Figure 4.8: Physiology of FutA mutant strains in *Synechocystis*. 95
Figure 4.9: Expression of FutA1 and FutA2 in *Synechocystis* deletion and complemented mutants 96
Figure 4.10: Photosynthetic physiology of strains under Fe stress. 96
Figure 4.11: Growth rate of strains under Fe stress. 99
Figure 4.12: Size Exclusion Chromatography (SEC) of Tery_3377 101
Figure 4.13: Purification and crystallisation of Tery_3377. 102
Figure 5.1: The experimental design. 110
Figure 5.2: Experimental design to assess possible differential dissolution of nutrients from dust enclosed or not enclosed in dialysis tubing 111
Figure 5.3: Assessment of potential dialysis tubing effects when included in the experiment 112

Figure 5.4: Assessment of potential inhibitory effect of the dialysis tubing on abiotic dust-chemical dissolution. 113
Figure 5.5: Growth of *Trichodesmium* under different Fe regimes. 114
Figure 5.6: *Trichodesmium* filament physiology under different Fe regimes. 116
Figure 5.7: *Trichodesmium* photosynthetic efficiency (F_v/F_m) under different Fe regime .. 117
Figure 5.8: Trichodesmium functional absorption cross section of PSII (σ^{PSII}) during growth under different Fe regimes 118
Figure 5.9: Gene numbers and GO annotation coverage 120
Figure 5.10: Distribution of the number of genes expressed across different levels of reads/gene 120
Figure 5.11: Gene expression clustering across treatments and replicates 121
Figure 5.12: Comparison of differential expression across the experimental treatments . 122
Figure 5.13: Clustering demonstrates patters of differential expression across all genes and treatments. 123
Figure 5.14: Validation of the RNAseq results using quantitative RT-PCR (qPCR). 126
Figure 5.15: GO enrichment in differentially expressed genes. 128
Figure 5.16: The balance of positive and negative changes in gene expression. 131
Figure 5.17: Comparisons of transcriptomic changes due to additions of Dust and $FeCl_3$. 132
Figure 5.18: Iron uptake across the inner and outer cell membranes.. 136
Figure 5.19: Gene expression of various components of putative Fe uptake pathways in *Trichodesmium*. 140
Figure 5.20: Changes in transcription of genes involved in the process of photosynthesis. 142
Figure 5.20: Transcriptomic response of subunits involved in the photosynthetic electron transport chain. 146
Figure 5.22: Gene expression of putative outer membrane proteins. 151
Figure 5.23 : Representative expression across the *Tery_08xx* cluster. 153
Figure 5.24: Representative expression profile along the *Trichodesmium* twintron arrangement. 156
Figure 5.25: Expression of the *Trichodesmium* twintron across the experimental treatments 157
Figure 5.26: Expression of the *Trichodesmium* diversity generating retroelement.. 158
Figure 6.1: Iron and Phosphorus uptake by *Trichodesmium*.. 169
Figure 6.2: The prevalence /expression of the ptx gene cluster in marine cyanobacteria *Trichodesmium* and *Prochlorococcus* 171
Figure 6.3: The hypothesised response of the photosynthetic electron transport (PET) chain to Fe limitation in *Trichodesmium*. 176
Figure A.1 Clustered expression patterns across the four experimental treatments 191

List of Tables

Table 1A: Characteristics of the major diazotrophic cyanobacteria groups. 12
Table 1B: Sources of iron accessible to *Trichodesmium*. 25
Table 2A: Bacterial strains used for experiments. 36
Table 2B: Modified (m) YBC-II media recipe 37
Table 2C: Modified YBC-II trace metal composition compared to standard YBC-II. 38
Table 2D: BG-11 media recipe. 38
Table 2E: Fast Repetition Rate fluorometer settings 40
Table 2F: Description of physiological parameters recorded. 41
Table 2G: RNA extracted- quality control and concentrations. 44
Table 2H: Genes analysed by qPCR, amplicon and primer information 48
Table 2I: Plasmid generated in this study 50
Table 2J: Buffers used for Tery_3377 protein extraction 57
Table 2K: Tery_3377 homologues included in the phylogenetic analysis 61
Table 3A: The different forms and oxidation states of phosphorus in the ocean.. 64
Table 3B: Details of the *ptx* homologous genes in *Trichodesmium* 69
Table 3C: The expression of phosphite (*ptx*) and phosphonate (*phn*)-metabolism genes in *Trichodesmium* transcriptomes. 70
Table 3D: Putative Pho box promoter binding sequences associated with P-metabolism involved genes. 73
Table 3E: Environmental prevalence of *ptx* genes in *Trichodesmium* 78
Table 4A: Phenotypes previously reported in *Synechocystis* Δ*futA1* and Δ*futA2* mutants 82
Table 4B: IdiA/FutA/Fbp homologues of selected bacteria. 85
Table 5A: Clustering of differentially expressed genes in 10 distinct patterns across experimental treatments. 124
Table 5B: The top20 differentially expressed genes presented is descending order of statistical significance (P-value). 129
Table 5C: Expression of suggested biomarkers of iron limitation.. 134
Table 5D: The *Trichodesmium Tery_08xx* operon components 154
Table A1: Primer sequences used for genetic modification 184
Table A2: The 50 top differentially expressed genes in the transcriptomic analysis 186
Table A3: The 50 most highly expressed genes in the transcriptomic analysis 188

Acronyms

ANOVA Analysis of variance

ATP Adenosine triphosphate

BLAST Basic local alignment search tool

cDNA Complementary deoxyribonucleic acid

Chl-α Chlorophyll-α

DIP Dissolved inorganic phosphorus

DNA Deoxyribonucleic acid

DNase Deoxyribonuclease

DOP Dissolved organic phosphorus

DTT Dithiothrietol

EDTA Ethylenediaminetetraacetic acid

FRRf Fast Repetition Rate fluorometer

gDNA Genomic deoxyribonucleic acid

GLM General linear model

HNLC high nutrient low chlorophyll

IPTG Isopropyl β-D-1-thiogalactopyranoside

kDa Kilodalton

MIQE Minimum information for publication of quantitative real-time PCR experiments

mRNA Messenger ribonucleic acid

NADPH Nicotinamide adenine dinucleotide phosphate

NCBI National center for biotechnology information

NRQ Normalised relative quantity

NTC No template control

OP Organophosphorus

ORF Open reading frame

PAGE Polyacrylamide gel electrophoresis

PCR Polymerase chain reaction

PIP Particulate inorganic phosphorus

Pn Phosphonate

POC Particulate organic carbon

polyP Polyphosphate

POP Particulate organic phosphorus

PSI Photosystem I

PSII Photosystem II

qPCR Quantitative polymerase chain reaction

RFC Relative fold change

RNA Ribonucleic acid

rRNA Ribosomal ribonucleic acid

RT-PCR Reverse transcription polymerase chain reaction

ROS Reactive oxygen species

SEA Singular enrichment analysis

SOD Superoxide dismutase

I, Despo Polyviou declare that this thesis, and the work presented in it are my own

Nutrient utilisation by *Trichodesmium*-Characterisation of Molecular and Physiological Processes

I confirm that:

- This work was done wholly or mainly while in candidature for a research degree at this University.
- Where any part of this thesis has previously been submitted for a degree or any other qualification at this University or any other institution, this has been clearly stated.
- Where I have consulted the published work of others, this is always clearly attributed.
- Where I have quoted from the work of others, the source is always given. With the exception of such quotations, this thesis is entirely my own work;
- I have acknowledged all main sources of help;
- Where the thesis is based on work done by myself jointly with others, I have made clear exactly what was done by others and what I have contributed myself;

Parts of this work have been published as:

Polyviou, D., Hitchcock, A., Baylay, A. J., Moore, C. M. and Bibby, T. S. (2015), Phosphite utilization by the globally important marine diazotroph *Trichodesmium*. Environmental Microbiology Reports, 7: 824–830. doi:10.1111/1758-2229.12308

Signed: _____

Date: _____

Acknowledgements

I am determined that if someone was to rip off this page and place it on the opposite side of the scale to the rest of the book the scale would shift towards the side of the single page. Through it, I want to acknowledge the people that I travelled with along the path that lead to the point I stand now. For no matter how fulfilling it is to reach a destination, the road and the adventures you have with people along the way is what makes you, as a person and as a scientist.

First and foremost, I would like to express my gratitude to my supervisors: Thomas Bibby, my advisor and mentor for inspiring me to become a scientist and supporting me every step of the way. Having the special ability to distinguish when it was time for each, he guided me when I needed guidance and encouraged me to lead my own way when I was ready. Mark Moore, for his clarity of thought and good advice. Having him stand behind me always made me feel safe and confident in our research endeavours. Andrew Hitchcock, for teaching me everything I know from holding a pipette to making bacteria glow fluorescent green, and without whom this thesis would never have been possible.

Special thanks go to my examiners Maeve Lohan and James Murray for making my viva examination a pleasant experience and their useful corrections and comments on this work.

I also thank Martha Gledhill for although she had to migrate at the beginning of my PhD she first managed to pass on some of her infectious enthusiasm for chemistry, which sometimes makes you dance in the lab. I am also grateful to Ben Van Mooy for taking me out of the lab and teaching me some real oceanography.

Thanks to all that I had the luck to produce amazing science with. Joe Snow, the protein expert, whose thesis was incredibly useful while writing this book, and Alison Baylay, the DNA expert, who was patient with me and present whenever I needed her, either for scientific advice or to just have coffee and cake. I thank Moritz Machelett and Ivo Tews for teaching me how to make pretty pink crystals. I am also grateful for Mark Hopwood's determination to convert me to chemistry. I enjoyed the stimulating discussions we shared in 166/09 and the sleepless nights of science in Crete.

I am indebted to Nicola Pratt who helped me get started and continued helping me thereafter and John Gittins for providing his expert advice when needed. I am also appreciative of all the people I had the pleasure to work next to in the lab including Andreas the single other member of the DnA team for simply being awesome, Nathan, Wladimir, Sophie, Tommy, Harry, Dok, and Annie.

I am grateful to James for taking me along on his adventures and showing me new things. He gave my life forward momentum and would be happy to know that towards the end of this book I started to take regular 'fast walks'. Thank you also goes to my friends and especially Nina, Giang and Glaucia for the fun we had together and their support whenever it was needed, Nicole for always being there, Iordanis for bringing a piece of home to the office, and all my officemates for making NOCS a more pleasant place to work.

Finally, I thank my family and especially my grandparents for passing me their thirst for knowledge, and encouraging me to take advantage of all the opportunities that they themselves were never offered.

Work for this PhD was supported by the Graduate School of the National Oceanography Centre Southampton, the Natural Environmental Research Council and the A.G. Leventis Foundation.

Chapter 1
Introduction

1.1 The importance of marine primary production

Marine microbial life is of foremost importance in catalysing oceanic biogeochemical cycles which are bi-directionally linked to the global climate. Phytoplankton accounts for about half of the global annual primary production through photosynthetic fixation (Box 1) of ~48.5 Pg of carbon every year (Field et al. 1998; Falkowski et al. 2004). Via a process referred to as the marine biological carbon pump (Fig. 1.1) fixed organic carbon is exported from surface waters to depth, with a fraction subsequently stored within marine sediments. Since climate changes over glacial/intergalacial periods correlate to the atmospheric CO_2 concentrations, which can be explained by the activity of the biological carbon pump (Sigman & Boyle 2000), it is vital to understand the efficiency of, and limiting factors controlling these process in the context of rapidly changing climatic conditions. As a more direct consequence, perturbations to oceanic primary productivity can also affect fisheries production (Blanchard et al. 2012) and consequently food security.

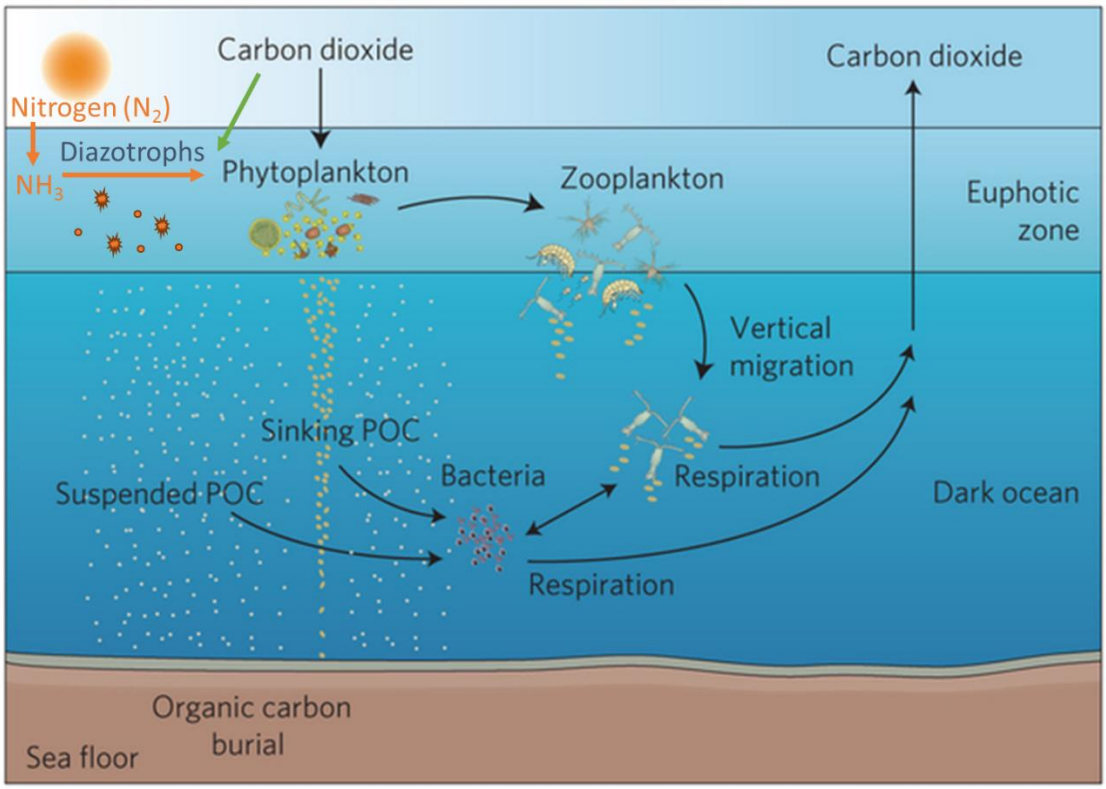

Figure 1.1: **Phytoplankton activity and downstream interactions with the ocean system.** The biological carbon pump is powered by growth of autotrophic organisms through atmospheric CO_2 drawdown and carbon fixation. Nitrogen (N_2) fixation enhances primary production either directly though growth of photosynthetic diazotrophs or through the release of fixed N in the surrounding environment. Particulate organic carbon (POC) is consequently exported from the euphotic zone to the ocean sediment. Some POC escapes from this downward flux and is recycled, becoming available to support regenerated production. (Figure adapted from Herndl & Reinthaler 2013).

Although marine macrophytes account for a significant proportion of coastal photosynthetic activity, in the open ocean CO_2 fixation is dominated by unicellular autotrophs (Duarte 2009, p.10). These are a diverse group composed primarily of the eukaryotic microalgae groups: coccolithophores, dinoflagellates and diatoms, as well as prokaryotic marine cyanobacteria (Simon et al. 2009). Ancestors of the latter were the first organisms capable of oxygenic photosynthesis, a process that lead to the oxygenation of the oceans at the end of the Pre-Cambrian period (Kaufman 2014). They include *Synechococcus* and *Prochlorococcus*, major contributors to oceanic primary production (Liu et al. 1997; Partensky et al. 1999; Scanlan 2003), and nitrogen fixing organisms such as *Trichodesmium* and *Crocosphaera* (Carpenter et al. 1992).

Box 1: PHOTOSYNTHESIS

Phytoplankton drive the biological carbon pump through the process of photosynthesis, during which light and carbon dioxide (CO_2) are utilised for the production of organic matter.

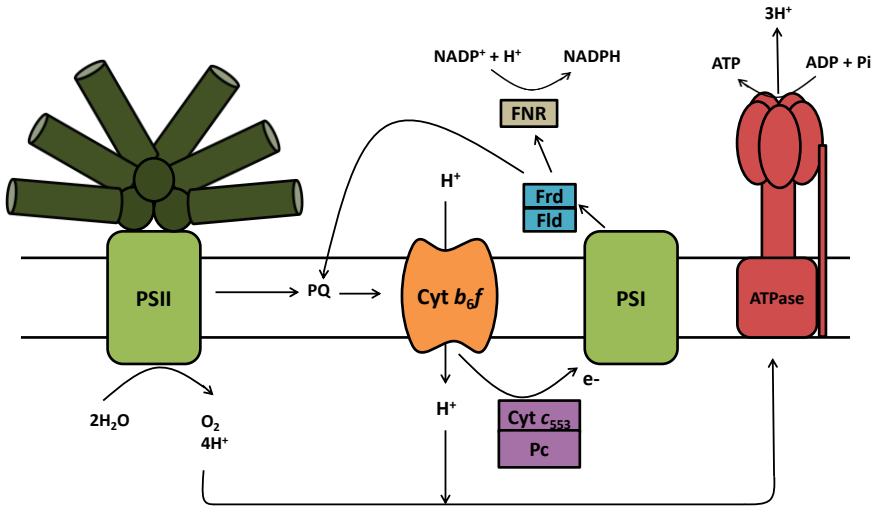

At the thylakoid membranes photosystem II (PSII) utilises light energy to oxidise water (H_2O) and reduce plastoquinone (PQ) starting a chain of electron transport that continues from PQ to cytochrome b_6f (Cyt b_6f) and from Cyt b_6f to plastocyanin (PC) or cytochrome c_{553} (Cyt c_{553}) before they reach the second light- absorbing protein complex of photosynthesis, photosystem I (PSI). PSI will facilitate electron transfer to ferredoxin (Frd) or flavodoxin (Fld) which will in turn reduce ferredoxin-NADP+ reductase (FNR) the protein generating the reductant NADPH.

During electron transport a proton (H^+) gradient is generated across the thylakoid membranes (from photolysis of H_2O by PSII and shuttling of H^+ across the thylakoid membrane by cyt b_6f) which is utilised by the F_1F_o ATP synthase to drive the formation of ATP from ADP and P_i.

ATP and NADPH are subsequently used for the assimilation of CO_2 to organic matter and to drive cellular metabolic processes.

1.2 Nutrients in the ocean

Vast areas of the ocean, referred to as oligotrophic, are depleted in the macronutrients nitrogen (N) and phosphorus (P) and therefore limit primary production (Fig. 1.2) (Moore et al. 2013). A group of prokaryotic microorganisms, referred to as diazotrophs, have developed the ability to take up inorganic dinitrogen (N_2) from their environment and reduce it to two molecules of ammonia (NH_3) (Box 2) which can be consequently utilised for growth and to carry out essential metabolic processes. This drives CO_2 fixation by

autorophic diazotrophs directly, but also 'new nitrogen' is released through cell exudates and cell death/decay and becomes available to other photosynthetic organisms (Fig. 1.1). N_2 fixing microorganisms (Sec. 1.3.1) are a key component of biogeochemical cycles driving a significant amount of new production (480–960 Tg C yr^{-1}) in oligotrophic regions (Mahaffey et al. 2005). Globally 100-200 Tg of new nitrogen is introduced to the ocean system per year (Karl et al. 2002).

Box 2: NITROGEN FIXATION

The process of N_2 fixation (diazotrophy) is fundamental in the marine environment as it sustains primary production in oligotrophic regions of the ocean.

Through this process nitrogen gas (N_2) from the atmosphere is converted to ammonia (NH_3). The enzyme nitrogenase, an enzyme inactivated by oxygen (O_2), is required for the catalysis of this reaction. The stability of N_2 due to its triple bond renders N_2 fixation an energetically costly process:

$$\mathbf{N_2 + 8H^+ + 16ATP + 8e^- \rightarrow 2NH_3 + H_2 + 16ADP + 16P_i}$$

The identity of the single limiting nutrient controlling oceanic productivity over geological timescales has been the subject of a long scientific debate with P and N at the centre of it (Falkowski 1997; Tyrrell 1999). The 'geochemists view' is that as biological N_2 fixation can relieve organisms of external N requirements while there is no atmospheric source for P, supply of the latter will ultimately control the ocean's productivity over time (Redfield 1958; Tyrrell 1999). On the other hand, the 'biologists view' states that due to loss of fixed N through denitrification and/or anammox reactions, and as N appears at a deficit compared to P, in the surface oligotrophic tropical/subtropical oceans, production over long timescales will be controlled by the process of N_2 fixation (Falkowski 1997; Falkowski et al. 1998).

In reality the theory of nutrient limitation can be applied to different levels, from the smallest cellular level where a nutrient limits the activity/proliferation of a single cell at a specific moment in time and particular oceanic location, to restriction of productivity across the world oceans over long time scales. The term 'ultimate limiting nutrient' was coined to describe the latter (Tyrrell 1999). Between these two levels, a nutrient can restrict the growth of a community at a specific time and place and this is defined as the 'proximal limiting nutrient'. Therefore, P has been suggested to take the role of the ultimate limiting nutrient while N of the proximal limiting nutrient (Tyrrell 1999).

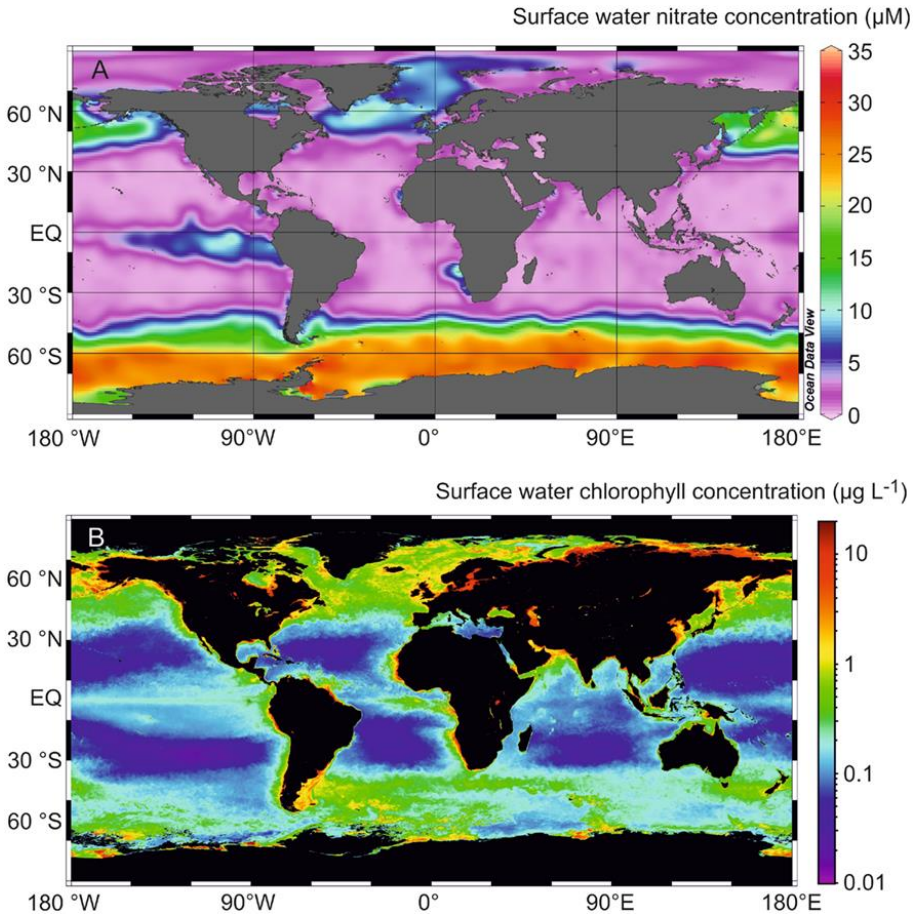

Figure 1.2: The link between nutrients and primary production in the ocean. (A) Concentrations of nitrate are depleted across the low latitude oligotrophic oceans and thus **(B)** limit primary production (chlorophyll concentrations). Chlorophyll concentration also remain relatively low in locations referred to as high nutrient-low chlorophyll (HNLC) regions which include the equatorial and subarctic Pacific Ocean and the Southern Ocean (figure from Gledhill & Buck 2012).

However, restriction of N_2 fixation through limitation of the micronutrient iron (Fe) complicates this justification (Martin 1990; Moore & Doney 2007; Moore et al. 2009; Martínez-Garcia et al. 2011) suggesting that this nutrient also has an important role in the control of oceanic primary production. In addition to that, Fe appears to have a direct control on productivity of large oceanic areas with high N and P concentrations such as the equatorial and subarctic Pacific Ocean and the Southern Ocean. These areas maintain low levels of primary production and are referred to as high nutrient-low chlorophyll locations (HNLC) (Fig. 1.2) (Martin et al. 1994; Boyd et al. 2000; Tsuda et al. 2003; Buesseler et al. 2004; Blain et al. 2007).

Limitation of marine nutrients P and Fe is briefly reviewed below taking into account speciation and complexation of these nutrients in the water as well as their biological importance and interactions with marine microorganisms (Fig. 1.3).

1.2.1 Phosphorus

Phosphorus is essential for the construction of phospholipid cell membranes and nucleotides used as the building blocks of (dioxy)ribonucleic acids (DNA and RNA) as well as nucleoside triphosphates (eg. ATP) that constitute the cell's energy currency. Although it is the 11th most common element in the Earth's crust it is mostly confined to the lithosphere from where weathering and riverine/aerial transfer delivers it to the oceans (Compton et al. 2000). Most (~75%) of the new P entering the ocean is in the form of particulate (> 0.2 μm) inorganic P (PIP) but some dissolved (< 0.2 μm) inorganic P (DIP) as well as particulate and dissolved organic P (POP and DOP) is also supplied (Compton et al. 2000). This P will be incorporated in growing cells (Fig. 1.3), travel through the food web and sink upon cell death, but a large proportion will be returned/remade available to the surface ocean largely as DIP through upwelling and lateral transfers (Mahaffey et al. 2004). Microbial transformations of P are numerous and support a complex cycle which is currently the subject of intensive research (reviewed by Karl 2014).

Characterisation of P forms, their concentrations and fluxes is challenging even when more than 50 analytical procedures are currently employed for their identification (Karl & Björkman 2001). Certain DOP/PIP molecules including most organophosphonates (Pn) (+3 valence state), reduced P compounds with a direct C-P bond which makes them more stable than organophosphates (+5 valence state, C-O-P bonds), resist hydrolysis which is used to quantify 'total P' leading to inaccuracies in the calculated concentrations. Another limitation to the methods is that organic P concentrations are calculated by subtracting phosphate (PO_4^{3-}) concentrations from the 'total P'. This disregards reduced inorganic P sources phosphite, PO_3^{3-} (+3 valence state), and hypophosphite, PO_2^{3-} (+1 valence state) which might be found in significant concentrations in aquatic environments (Pasek et al. 2014). In addition, PO_4^{3-} itself is hard to track at concentrations below 1nmol L^{-1} and fast turnover times of below 1 hour sometimes encountered in oligotrophic regions (Karl 2014).

From the information currently available we can induce that PO_4^{3-} concentrations vary across the surface oceans by more than 1000 fold and are heavily depleted at low latitudes. The DOP pool exceeds that of PO_4^{3-} often by more than 10 times and can be comprised by

25% of Pn (Clark et al. 1998; Kolowith et al. 2001; Karl 2014). Also, a significant proportion (up to 25%) of the dissolved P ocean inventory could be present as reduced inorganic P, PO_3^{3-} and PO_2^{3-} (Pasek et al. 2014).

Bottle incubation experiments have previously suggested that the ocean is limited or colimited (in combination with other nutrients) by PO_4^{3-} at locations such as the Central to North Atlantic and Pacific Oceans (Wu et al. 2000; Sañudo-Wilhelmy et al. 2001; Mills et al. 2004; Moutin et al. 2005; Mills et al. 2008). For the Atlantic Ocean this has been explained by an Fe influx providing an excess of the nutrient to the North, and therefore inducing P drawdown to limiting concentrations by growing diazotrophs (Wu et al. 2000; Moore et al. 2009). In contrast, P is more abundant in the South Atlantic where diazotrophs are limited by Fe (Moore et al. 2009).

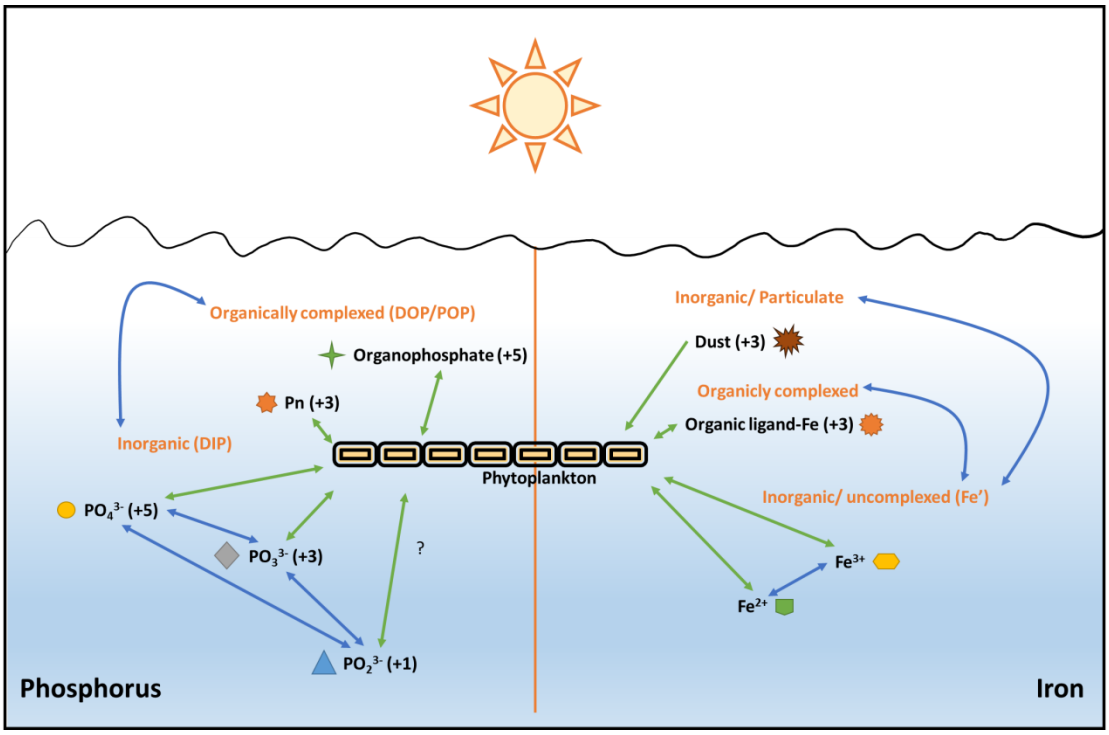

Figure 1.3: Interactions of phosphorus and iron forms with the biotic and abiotic environment in the ocean. Different forms of P (left) and Fe (right) in the ocean are interconverted due to physical and biological activities (blue arrows) and can be taken up/released by marine organisms (green arrows). Valence states of P and Fe forms are presented in brackets.

1.2.2 Iron

Iron is the fourth most common element in the earth's crust and is delivered to the oceans through fluvial and aerial sources as well as hydrothermal vents. Aerial dust deposition from the major deserts is the predominant input to the open oceans (Moore & Braucher 2008). At circumneutral pH and the oxidising conditions encountered in the ocean, Fe^{2+} is quickly oxidised to Fe^{3+} which has a much lower solubility and is more likely to precipitate out of the surface waters. This leaves the oceans highly anemic.

One factor affecting the solubility of dust Fe is mineralogy. Iron, which can constitute 4-7% of the total desert particle mass, is classified as either 'structural Fe' found in the crystal lattice of aluminosilicate minerals (clays, quartz and feldspars) or 'free Fe' in (hydr)oxides (hematite, magnetite, goethite). Mineralogy of dust varies depending on its source but clays make up ~48-82% of the dust mass, and although their Fe content is low (~2-23%) compared to (hydr)oxides (~58-77%), they have the largest contribution (96%) to dissolved Fe because of its higher solubility (Journet et al. 2008). The solubility of dust Fe, shown to vary between 0.01 and 80% (Mahowald et al. 2005), will also depend on several processes both atmospheric (Photo(chemistry), physical processing, transport and mixing) and oceanic (dissolved Fe concentrations, Fe-binding ligands, biological processes, particle adsorption and the kinetics of dissolution) (Baker & Croot 2010).

The majority (99%) of oceanic dissolved Fe (< 0.2 μm) was previously suggested to be organically bound (Gledhill & Berg 1994; Rue & Bruland 1995; Wu & Luther 1995; Gledhill & Buck 2012) but recent evidence suggests that a considerable amount could be present as inorganic dissolved colloidal (0.02-0.2 μm) Fe (Fitzsimmons et al. 2015). The organic Fe-binding ligands currently remain largely uncharacterised (Gledhill & Buck 2012) but their significance is paramount as they contribute significantly in maintaining Fe in solution and making it more liable to photoreduction (Barbeau et al. 2001; Wagener et al. 2008).

Iron is a critical element for growth of phytoplankton whose photosynthetic apparatus require as many as 23-24 Fe atoms (Shi et al. 2007). At the same time diazotrophs require ~2.5-5.2 times more Fe than non-diazotrophs (Sañudo-Wilhelmy et al. 2001) as nitrogenase, the enzyme responsible for N_2 fixation, requires an additional 38 Fe atoms per monomer. Potentially 80-90% of the cellular Fe-quota is associated with nitrogenase in some diazotrophs (Richier et al. 2012).

The potential importance of Fe in constraining primary production in the ocean was first stressed by John H. Martin in his 'Iron Hypothesis'. For more than 25 years his words: 'Give me half a tanker of iron and I will give you an ice age' stimulated the scientific community (Martin 1990). Multiple large scale Fe release experiments, as well as shipboard bottle incubation experiments were designed to test Martin's Hypothesis and confirmed the importance of Fe in HNLC locations (Boyd et al. 2007). In addition to these locations, growth of diazotrophs in various oligotrophic regions appears to be limited by Fe (Moore et al. 2009). More recently, the Iron Hypothesis was supported by data from a Subantarctic Atlantic sediment core indicating a connection between global cooling over geological time scales, productivity and desert dust fluxes to the ocean (Martinez-Garcia et al. 2014).

1.2.3 Paradigms of nutrient limitation

The first conceptual model used to describe nutrient limitation in the ocean was based on work by J. von Liebig who indicated how the scarcest nutrient can control the levels of production (Leibig's Law of the minimum) (de Baar 1994), and F. F. Blackman who extended this theory to the effect of a limiting factor on constraining photosynthesis and growth rates (Blackman's Law of limiting factors) (Blackman 1903).

More recent observations, that often additions of more than one nutrients can stimulate growth of phytoplankton, have introduced the concept of ocean 'colimitation' (Saito et al. 2008). This describes the situation whereby more than one nutrient simultaneously limit production. There are different scenarios through which colimitation can occur (Saito et al. 2008):

- Independent nutrient colimitation: The level of two nutrients can be reduced to equally minimal levels so as additions of both induce growth (Saito et al. 2008).
- Biochemically dependent colimitation: One nutrient limits the ability to acquire a different nutrient. An example of this is provided by new evidence indicating that Fe is a cofactor of the P utilisation enzyme alkaline phosphatase which is consequently controlled by the availability of both nutrients (Yong et al. 2014; Mahaffey et al. 2014).
- Biochemical substitution colimitation: Two nutrients can substitute each other in specific biochemical functions. An example is the occurrence of superoxide dismutase SOD proteins (involved in cellular defence against oxidative stress) with different element binding properties (Ni, Mn, Fe or Cu and Zn) (Wolfe-Simon et al. 2005).

1.3 Marine Diazotrophy

N_2 fixation, essential in maintaining primary production under N-limitation, is highly interlinked with the P and Fe biogeochemical cycles (Falkowski 1997; Moore et al. 2009). This necessitates a better understanding of the identity and ecological properties of diazotrophic species.

1.3.1 The players

The characterisation of contributors to oceanic N_2 fixation and their distribution is still underway. To this end, molecular techniques for the identification of the diversity and distribution of the conserved gene *nifH*, which codes for a subunit of the catalytic enzyme of N_2 fixation, nitrogenase, have been utilised for the past 2 decades (Zehr et al. 1998).

Diazotrophic capabilities are encountered in both cyanobacterial and non-cyanobacterial species. Heterotrophic diazotrophs, identified through *nifH* molecular analysis, appear to be widespread and at certain locations the dominant N_2 fixers (Farnelid et al. 2011). Their prevalence was indicated in environments such as the oxygen minimum zones and deep waters where photosynthetic organisms are not active (Halm et al. 2009; Fernandez et al. 2011; Farnelid et al. 2013). Diazotrophic cyanobacteria on the other hand, are found to dominate across the tropical and subtropical surface oceans (Fig. 1.4) (Stal 2009). They include filamentous species found between 26.5 to 30 °C and unicellular which can also exist in deeper, colder waters ranging between 15 and 30 °C (Moisander et al. 2010).

Unicellular cyanobacteria (UCYN)

These small (< 10 µm) diazotrophs (Goebel et al. 2007) were first identified at station ALOHA using the *nifH* technique (Zehr et al. 1998) and can be categorised in three groups: UCYN-A, UCYN-B, UCYN-C (Table 1A). Until recently, they have been generally overlooked but recent studies suggest a higher contribution towards the total diazotrophic community than previously assumed (Montoya et al. 2004). They are currently thought to fix and release N at rates similar to the more well studied diazotrophs (i.e. *Trichodesmium*) (Falcon et al. 2004; Berthelot et al. 2015, Martínez-Pérez et al. 2016) particularly in winter when conditions are not optimal for the latter (Goebel et al. 2007; Lee Chen et al. 2014).

The UCYN-A *Candidatus Atelocyanobacterium thalassa* have a highly streamlined genome lacking photosystem II (PSII) complexes and the ability to fix CO_2 (Zehr et al. 2008; Tripp et al. 2010; Bombar et al. 2014). They form symbiosis to the single celled Prymnesiophyceae

algae (Thompson et al. 2012; Hagino et al. 2013) with which they exchange 85-95% of their fixed N for carbon (Thompson et al. 2012; Krupke et al. 2015). New research indicates that different UCYN-A clades (UCYN-A1 and UCYN-A2) display 'partner fidelity' with their algae host (Thompson et al. 2014; Cornejo-Castillo et al. 2016). The cultivated group UCYN-B *Crocosphaera watsonii* found widespread in the ocean (Mazard et al. 2004; Hewson et al. 2009; Webb et al. 2009), can form symbiotic relationships with diatoms (Carpenter & Janson 2000; Foster et al. 2011) but is mainly free living and can form colonial aggregations (Foster et al. 2013). UCYN-C contains the free-living cultivated species *Cyanothece* (Reddy et al. 1993) and TW3 (Taniuchi et al. 2012) and the importance of this group was suggested in the recent VAHINE mesocosm experiment at the New Cledonian lagoon (Bonnet et al. 2016; Hunt et al. 2016).

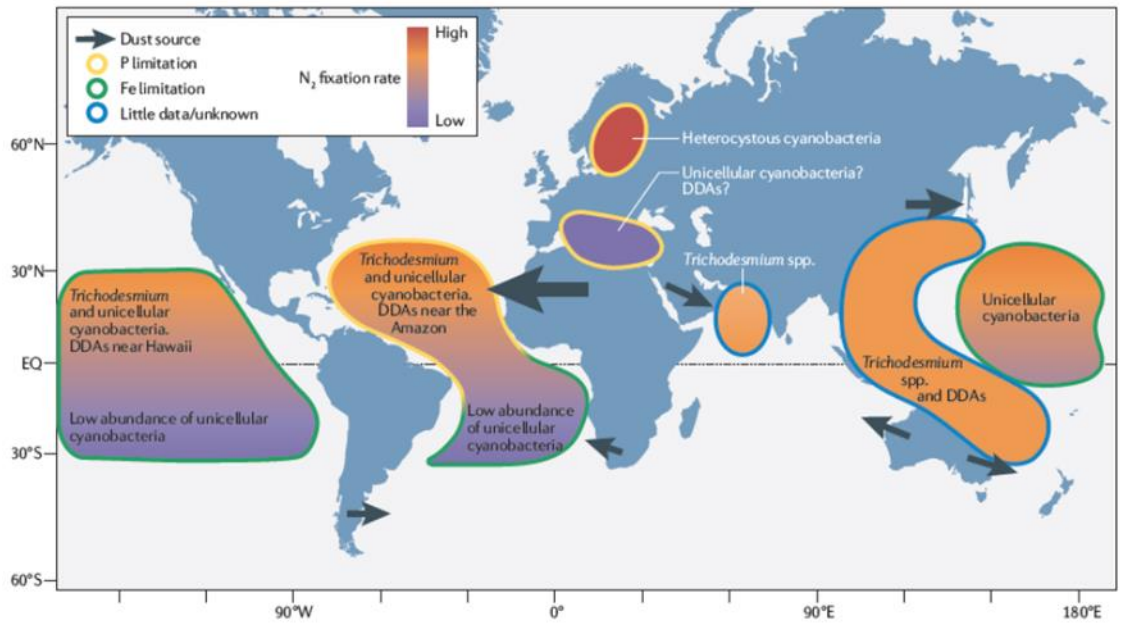

Figure 1.4: Marine diazotrophy in nutrient limited oceans. As nitrate by definition cannot limit diazotrophs, N_2 fixation thrives at low latitudes (rates indicated as fill colours), with *Trichodesmium* found across the majority of these regions. Other nutrients including iron (green outline), which is primarily supplied through Aeolian dust deposition (arrows), and phosphorus (yellow outline) are limiting diazotrophic growth (Sohm et al. 2011).

Filamentous nitrogen fixing cyanobacteria

DDA: Diatom Diazotroph Associations (DDAs) are composed of a diatom host and a diazotroph symbiont (*Richelia* and *Calothrix* lineages) (Table 1A) (Janson et al. 1999; Foster & Zehr 2006). They are hypothesised to be important contributors to organic carbon export from the surface ocean due to the heavy, high silicon containing diatom cell walls (Subramaniam et al. 2008).

The interactions between the host and diazotroph are intricate and presently not fully understood but recent data suggests that DDA formation is stimulated by low nitrate availability (Tuo et al. 2014). Symbiosis can be obligate or facultative (Peters & Meeks 1989; Kneip et al. 2007; Ran et al. 2010; Hilton et al. 2013) and the arrangement of the relationship varies: *Richelia* is found inside *Rhizosolenia* and *Hemiaulus* cells (Carpenter et al. 1992) while *Calothrix* is extracellular to *Chaetoceros* spp. and can be cultured independently (Foster et al. 2010). Surprising new evidence also identified an association of *Calothrix* to the abundant free living colonial diazotroph *Trichodesmium* (Momper et al. 2015). Different life strategies are controlled by- and have shaped- the genomes of the two diazotroph symbionts *Richelia* and *Calothrix*. The former possesses a streamlined genome compared to the latter, with genes involved in N metabolism lacking. This mechanism possibly ensures stability of N_2 fixation as the process is essential for the symbiotic partnership (Hilton et al. 2013).

Table 1A: Characteristics of the major diazotrophic cyanobacteria groups.

Diazotroph group	Morphology	Strategy of N_2 fixation	Lifestyle
UCYN-A *Candidatus Atelocyanobacterium thalassa*	Unicelluar	Spatial (host fixes C)	*Symbiotic* (host: Prymnesiophyceae)
UCYN-B *Crocosphaera watsonii*	Unicelluar	Temporal (N_2 fixation at night)	Free-living Symbiotic (host: diatoms)
UCYN-C *Cyanothece* spp	Unicelluar	Temporal (N_2 fixation at night)	Free living
DDA *Richelia* spp *Calothrix* spp	Filamentous	Spatial (form heterocysts)	Symbiotic (host: diatoms)
***Trichodesmium* spp.**	Filamentous/ Colonial	Combinatory (form diazocytes and fix at midday)	Free-living Epibionts

Similar to UCYN-A the diazotroph symbiont of DDAs transfers fixed N to the host which in the case of *Richelia* can amount to approximately 97% of the N_2 fixed (Foster et al. 2011). The benefit to the diazotroph symbionts is not currently clear as, unlike UCYN-A, they are fully capable of photosynthetically fixing their own carbon. It is possible, that transfer of additional carbon, or other nutrients, from the host to the diazotrophs, makes the symbiosis advantageous (Krupke et al. 2015).

<u>*Trichodesmium:*</u> *Trichodesmium* is widely distributed in an area covering approximately half of the earth's surface across the tropical and subtropical oceans (Fig. 1.4) and accounts for ~50% of the total marine N_2 fixation (Capone et al. 1997; Westberry & Siegel 2006). Two of the most important species are *T.erythraeum* and *T.thiebautii* with the former (isolated in 1991) (Prufert-Bebout et al. 1993) being the most well studied strain of this species.

Trichodesmium is polymorphic, found in filaments of ~100-200 cells that come together to form puff (Fig. 1.5Bi), tuft (Fig. 1.5Bii), and bowtie colonies (Table 1A). The colonies are referred to as consortia due to their function as microhabitats for an array of microorganisms clustered (at high densities compared to the surrounding water) in and around the colonies (Sheridan et al. 2002). These microorganisms include a diverse community of other cyanobacteria, heterotrophic bacteria, eukaryotes and phages (Hewson et al. 2009) which are distinct to the community of the surrounding environment (Hmelo et al. 2012). In addition, *Trichodesmium* colonies act as biological activity hotspots where epibionts potentially benefit from the N and carbon released from the *Trichodesmium* cells. Interactions within the consortia community appear to be central to the controls of nutrient utilisation, with quorum sensing shown to stimulate the expression of genes involved in P utilisation (Van Mooy et al. 2012).

First reports of *Trichodesmium* were recorded by Captain James Cook and Sir Joseph Banks on board HMS *Endeavour* on her first voyage (Banks 1770) and the organism was first described by Ehrenberg (1830) (Box 3). It is thought that the Red Sea was named from the colouration of the water during *Trichodesmium* blooms. These blooms are visible from space and remote sensing can now report they extend over distances of $\sim 5.4 \times 10^6$ km^2 (Westberry & Siegel 2006).

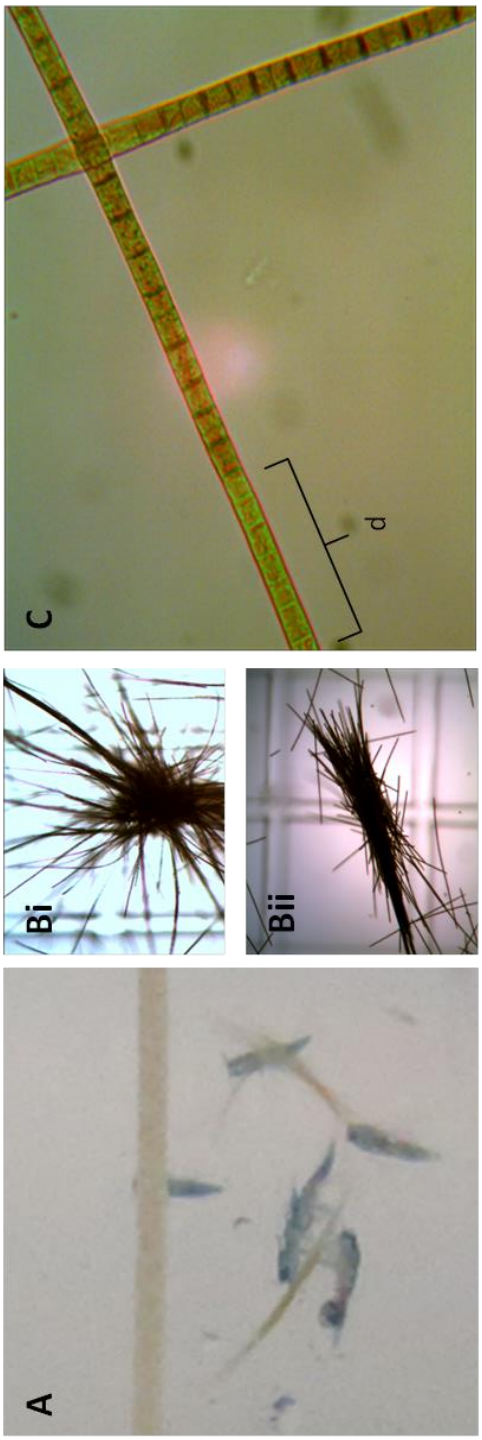

Figure 1.5: *Trichodesmium* morphology. (A) Copepods graze on *Trichodesmium* colonies in the environment (image taken during the PABST cruise in the Sargasso Sea). **(B)** *Trichodesmium* filaments come together to form colonies (puff (i) and tuft (ii) morphotype presented). **(C)** Lugol's stained *Trichodesmium* filaments visualised under light microscopy. Diazocytes (d) are recognised by their lighter, green colouration due to reduced carbohydrate storage compared

Trichodesmium blooms, which develop rapidly likely in response to nutrient influxes, significantly enhance N inputs to the surrounding environment while sequestering large amounts of atmospheric carbon (Capone et al. 1997; Lenes et al. 2001; Westberry & Siegel 2006; Luo et al. 2012). These blooms are observed to collapse rapidly (Rodier & Le Borgne 2008; Rodier & Le Borgne 2010; Bergman et al. 2013; Spungin et al. 2016) possibly due to viral activity (Hewson et al. 2004) or autocatalytic programmed cell death (PCD) likely stimulated by nutrient stress (Berman-Frank et al. 2004; Berman-Frank et al. 2007; Bar-Zeev et al. 2013; Spungin et al. 2016). Recent observations from the VAHINE mesocosm experiments indicate no significant changes in viral abundance but enhanced caspase activity during the *Trichodesmium* bloom demise in support of PCD being the mechanism of bloom termination (Spungin et al. 2016).

Box 3: First references to *Trichodesmium* blooms

"On December 10th I observed there the astonishing phenomenon of the bloody coloration of the entire bay which forms the harbour of Tor. The open sea outside of the coral reef which shunts off the harbour was colourless as usual. The short waves of the calm sea conveyed to shore a slimy mass which appeared blood-red in the sunlight and was deposited in the sand of the beach, so that at ebb tide the entire bay, which takes a good half hour to cross, was given a blood red border."

(Ehrenberg 1830) as referenced by (Carpenter et al. 1992)

"On the 15th of July (1843), the blazing sun of Arabia woke me abruptly, shining suddenly on the horizon without any dawn and in all its splendour. I leaned my elbows rather mechanically on a windowsill at the stern of the ship to seek a vestige of fresh night air before the heat of the day devoured it. It was my surprise to see the ocean astern of the ship coloured red as far as the eye could reach! I ran up on the deck and saw the same phenomenon on all sides."

Letter by E.Dupont in 1843 (Wille 1904) as referenced by (Carpenter et al. 1992)

"We sailed from Bahia. A few days afterwards, when not far distant from the Abrolhos Islets, my attention was called to a reddish-brown appearance in the sea. The whole surface of the water, as it appeared under a weak lens, seemed as if covered by chopped bits of hay… ...Their numbers must be infinite: the ship passed through several bands of them, one of which was about ten yards wide, and, judging from the mud-like colour of the water, at least two and a half miles long."

(Darwin 1909) The Voyage of the Beagle

Despite *Trichodesmium* rarely being found in sediments traps (Walsby 1992; Scharek et al. 1999; Chen et al. 2003), a strong downward pulse of organic matter has been suggested to follow PCD indicating a possible link of this process to the efficiency of the carbon pump (Bar-Zeev et al. 2013). In addition, recent evidence indicated export of carbon though non-diazotrophs (i.e. diatoms) that benefit from fertilisation of the surrounding waters, following *Trichodesmium* blooms (Bonnet et al. 2015). Indeed, *Trichodesmium* was reported to transfer twice as much fixed N_2 to non-diazotrophs (both heterotrophs and autotrophs) compared to unicellular diazotrophs (Bonnet et al. 2015).

1.3.2 Oxygen avoidance

The ability of diazotrophic cyanobacteria to fix N_2 clashes with the process of photosynthesis as O_2 produced during the latter is detrimental to nitrogenase. Therefore, mechanisms have evolved to segregate the two processes spatially, or temporally (Berman-Frank et al. 2003).

Spatial segregation is encountered in filamentous cyanobacteria which can form thick-walled, PSII-lacking cells referred to as heterocysts to accommodate N_2 fixation (Fig. 1.6). Both symbiotic diazotrophs like *Richelia* (Gomez et al. 2005) (Table 1A) and free-living like the freshwater model-cyanobacteria *Anabaena* (Kumar et al. 2010) employ this strategy. Unicellular diazotrophs on the other hand, do not have the luxury for division of labour between cells and therefore temporally segregate photosynthesis and N_2 fixation instead (Fig. 1.6, Table 1A). For example, *Crocosphaera* is a nocturnal N_2 fixer with a protein diel cycle that involves *de novo* synthesis of the NifH at the start of the scotoperiod when photosynthesis in not functioning (Saito et al. 2011). The same strategy is followed by *Cyanothece* (Toepel et al. 2008).

Unique amongst other diazotrophs, *Trichodesmium* employs a less strict variation of both modes of segregation simultaneously (Fig. 1.6, Table 1A). Although not heterocyst forming, ~15 % of each filament develops specialised nitrogenase containing (Berman-Frank et al. 2001) (but not terminally differentiated) cells with degraded gas vacuoles and glycogen granules (Sandh et al. 2012) arranged in zones of ~2-30 cells (Bergman et al. 2013) (Fig. 1.5C). At the same time, and although both photosynthesis and N_2 fixation occur during the photoperiod, it possesses its own circadian clock synchronising a midday downregulation of photosynthesis (low or negative O_2 evolution) (Berman-Frank et al. 2001) with enhanced O_2 scavenging mechanisms (respiration and Mehler reaction) (Kranz et al. 2009) and a peak in nitrogenase activity (Berman-Frank et al. 2001).

Trichodesmium's fixing strategy might be advantageous by allowing direct transfer of energy from photosynthesis to fuel N_2 fixation contrary to when the two processes are separated in time and thus utilisation of energy reserves is required (Staal et al. 2007). The flexibility of the non-terminally differentiated diazocytes as opposed to heterocysts could also be a benefit to survival in the rapidly changing oceanic conditions this organism encounters. It should be added, that an understanding of the controls on diazocyte formation and their mechanism of action could also be biotechnologically interesting in the field of algal biofuels as they could provide genetic engineering strategies coordinating aerobic and anaerobic chemical reactions.

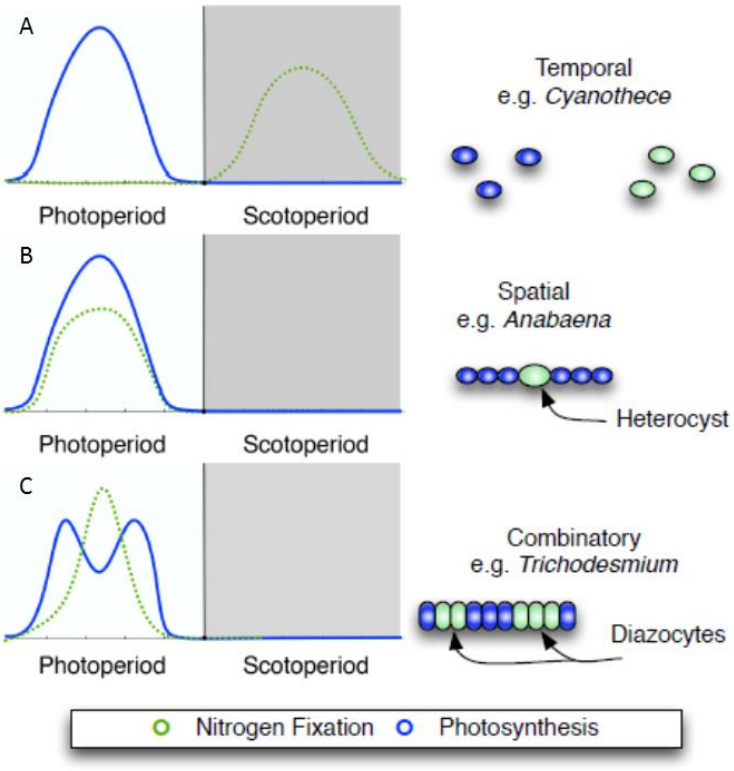

Figure 1.6: Strategies of N_2 fixation-photosynthesis segregation. Different groups of diazotrophs employ different approaches: **(A)** During temporal separation (e.g. in *Cyanothece*) N_2 fixation is carried out during the scotoperiod, **(B)** spatial separation (e.g. In *Anabaena*) involves specialised N_2 fixing cells (heterocysts), **(C)** while a combinatory strategy (in *Trichodesmium*) is observed when specialised but not terminally differentiated N_2 fixing cells (diazocytes) have their peak activity at midday when photosynthesis is depressed (figure from Snow 2014).

Despite all the advantages it confers *Trichodesmium's* synchronous N_2 and CO_2 fixation requires the maintenance of a higher cellular Fe quota (~66-87 µmol mol^{-1} carbon) compared to nocturnal N_2 fixers like *Crocosphaera* (~16 µmol mol^{-1} carbon) (Tuit et al. 2004) due to high Fe demands of both the photosynthetic and diazotrophic lifestyles (Geider & La Roche 1994; Shi et al. 2007).

1.4 Living with less- lessons from marine microorganisms

It has been previously discussed (Sec. 1.2) that P and Fe are key nutrients controlling the primary productivity of the oceans. Phytoplankton and amongst them diazotrophs whose ecological niche spreads across P limited oligotrophic gyres (Fig. 1.4) and their N_2 fixing qualities come at a cost of Fe, are forced to cope with the increased pressures. They therefore display a series of highly streamlined adaptations that ensure efficient use of the available nutrients. With focus on the globally important diazotroph *Trichodesmium* some of the adaptations of marine producers to low environmental P and Fe are reviewed below:

1.4.1 Cellular strategies to cope with P stress

Regulation: The regulatory mechanism coordinating the cells' response to low P is controlled by the Pho regulon first identified in *E.coli* (Wanner & Chang 1987). This functions through a two component system involving an inner membrane histidine kinase sensor (SphS/PhoR), and a transcriptional response regulator (SphR/PhoB). When P is unavailable to the transmembrane subunit it phosphorylates and activates the regulator which interacts with DNA sequences referred to as PHO boxes. Interestingly, even though *Trichodesmium* seems to be lacking the transmembrane SphS/PhoR component, the transcriptional regulator SphR/PhoB appears to regulate its PO_4^{3-}-deficiency response by inducing the transcription of transporters and enzymes for PO_4^{3-}, organophosphate, and Pn utilisation (Dyhrman et al. 2006; Su et al. 2007; Orchard et al. 2009).

Conservation of resources: A strategy employed during times of nutrient scarcity is the management of intracellular reserves to maintain cellular activity at the lowest possible nutrient expense. *Trichodesmium* cells growing with reduced concentrations of P have a lower P quota indicating that mechanisms of lowering the cellular requirements for the nutrient are employed by this organism (White et al. 2006a, 2010).

An example of such a mechanism is the substitution of P containing, phosphatidylglycerol (PG), with non-phosphorus containing, sulphoquinovosyldiacylglycerol (SQDG), membrane lipids under P-deficient conditions. This was characterised in laboratory cultures of *Trichodesmium* as well as for other major marine primary producers like *Synechococcus*, *Prochlorococcus*, the diazotroph *Crocosphaera*. (Van Mooy et al. 2009) and diatoms (Martin et al. 2011). Observations that the low P Sargasso Sea is characterised by a higher abundance of non-P lipids, lowering the P quota of organisms' lipid membranes compared to the South Pacific (Van Mooy et al. 2008; Van Mooy et al. 2009) reaffirm the significance of this strategy *in situ*.

Storage: Storage of cellular P as inorganic polymer polyphosphate (polyP) is thought to create luxury reserves of the nutrient in P-replete conditions for use during nutrient stress (Rhee 1973; Ault-Riché et al. 1998; Werner et al. 2005). However, *Trichodesmium* and other phytoplankton have been indicated to increase polyP concentrations in P-deficient conditions (Orchard et al. 2010a; Martin et al. 2014) for reasons not currently characterised.

Vertical migration: Diurnal vertical migration is a mechanism used by phytoplankton including diatoms and flagellates to access nutrients below the nutricline when they are depleted in surface waters (Eppley et al. 1968; Hall & Pearl 2011; Villareal et al. 2014). It is suggested that *Trichodesmium* uses cellular gas vesicles to regulate its buoyancy and acquire P at depth during the night, before rising to the surface to resume photosynthetic activity (Karl et al. 1992; Villareal & Carpenter 2003; White et al. 2006b).

P utilisation: As in many other organisms, PO_4^{3-} uptake by *Trichodesmium* appears to be mediated by the high affinity P specific transporter (Pst). The organism possesses homologs to the ABC transporter (PstABC) composed of the inner membrane components PtsA and PstC, the ATPase PstB and the PO_4^{3-} binding proteins PstS/SphX (Orchard et al. 2009) (Fig. 1.7). Interestingly, *sphX* was previously identified to be regulated by PO_4^{3-} concentrations while *pstS* was not. The two genes are colocalised in the genome but *sphX* is separated to *pstS* and the transporter genes *pstABC* by a 19 545 bp gap suggesting regulation by separate promoters (Su et al. 2007; Orchard et al. 2009). No homologues of the low affinity PO_4^{3-} transporter Pit (Fig. 1.6) have been identified in this species (Willsky et al. 1973).

Utilisation of organophosphorus (OP) is facilitated by enzymes that catalyse release of PO_4^{3-} which can consequently be internalised by the Pst transporter. In the case of

organophosphate these enzymes are alkaline phosphatases (APs) encoded by genes *phoX* and *phoA* (Fig. 1.7). *Trichodesmium*, which relative to the microbial community appears to be a better competitor for use of organophosphate compared to PO_4^{3-} (Orchard et al. 2010b), has one putative homologue of *phoA* (preceded by a Pho-box related promoter sequence) and two of *phoX* (only *phoX1* has Pho-box related promoter sequence). The expression of *phoA* and *phoX1* is upregulated under P limitation and AP activity was previously used to assess the organism's P state *in situ* (Dyhrman et al. 2002; Webb et al. 2007; Orchard et al. 2009).

APases can be found in the periplasm of marine bacteria but also intracellularly (Fig. 1.7) to facilitate organophosphate catabolism after direct uptake through Upg transporters (Luo et al. 2009). These transporters, first characterised in *E. coli*, are composed of the periplasmic binding UgpB, the inner membrane UgpAE and the ATPase UgpC (Overduin et al. 1988; Brzoska & Boos 1988) (Fig. 1.7), and appear to be abundant in the marine environment (Luo et al. 2009). No obvious homologous exist in *Trichodesmium*.

AP activity (APA) is a commonly used biomarker of P-limitation *in situ* (Sebastián et al. 2004a, 2004b; Dyhrman & Ruttenberg 2006; Sato et al. 2013), however, it only provides an overall community P-stress index, which due to taxonomic heterogeneity might not be representative of the efficiency of processes affecting biogeochemical cycles (Lomas et al. 2004). In addition, recent evidence suggests an even more critical pitfall of this technique as PhoX appears to require Fe for its production (Yong et al. 2014). This is problematic if AP activity is used to assess P limitation in a highly Fe variable environment (Mahaffey et al. 2014).

The predominant route for Pn catabolism is through the enzyme C-P lyase (Fig. 1.7) which acts to hydrolyse the C-P bond of a wide variety of substrates. Steps in better understanding the mode of the dephosphonation reaction have recently been made but the pathway is still not fully characterised (Kamat et al. 2011; Seweryn et al. 2015). The C-P lyase core components are encoded by genes *phnGHIJKLM* found in a gene cluster together with Pn ABC transporter genes *phnCDE*. In *E. coli* but not *Trichodesmium*, *phnF* and *phnNOP* thought to act as a transcriptional repressor and regulator respectively (Hove-Jensen et al. 2010, 2011), are also members of the C-P lyase cluster. The expression of the *phn* cluster is under the control of PO_4^{3-} concentrations in *Trichodesmium* and appears to be coordinated by the Pho regulon (Dyhrman et al. 2006; Su et al. 2007).

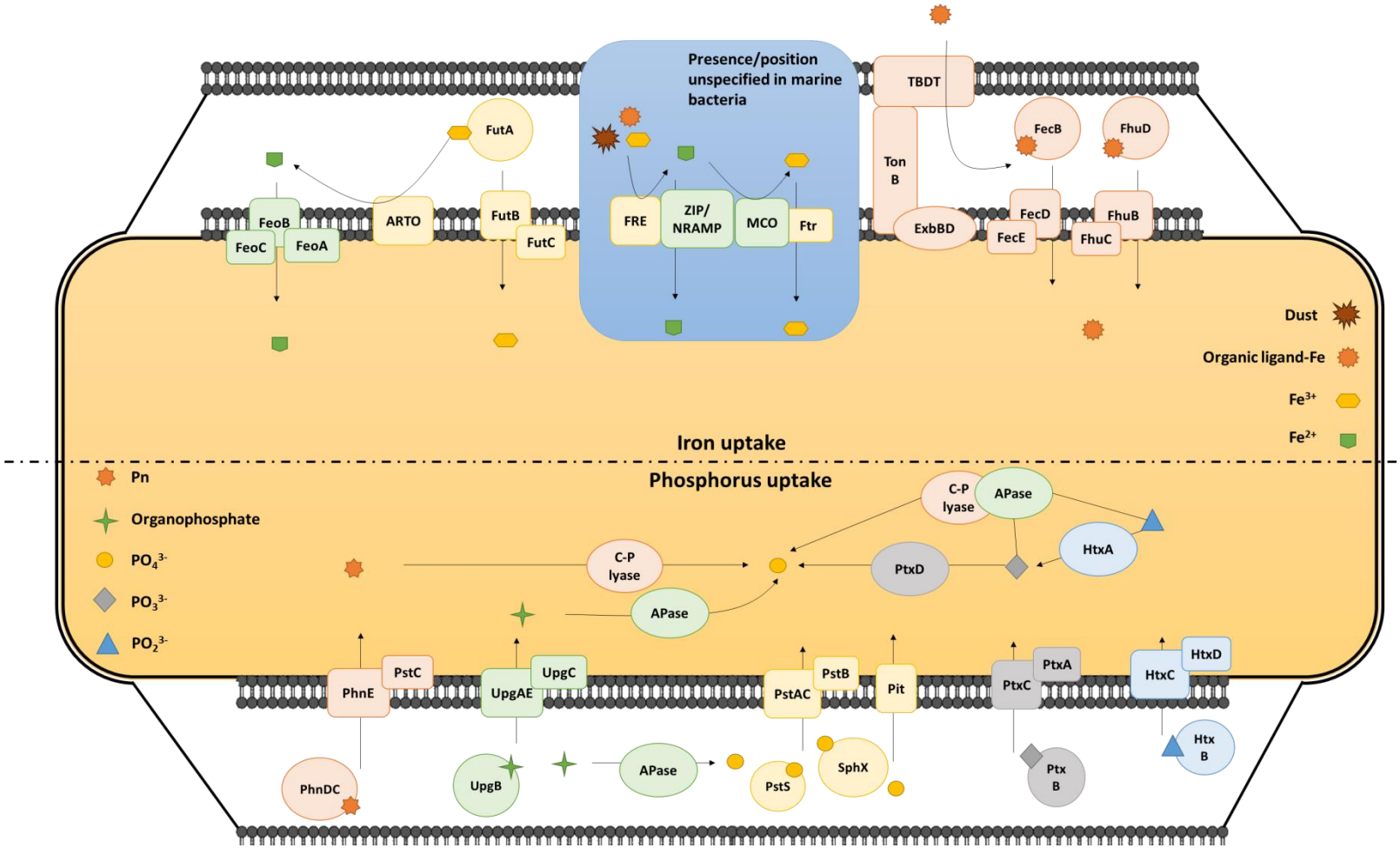

Figure 1.7: The Phosphorus and Iron uptake and utilisation pathways in microorganisms. Mechanisms of phosphate (PO_4^{3-}), phosphite (PO_3^{3-}), hypophosphite (PO_2^{3-}), organophosphate and organophosphonates (Pn) have been previously indicated to be employed for P utilisation. Similarly, phytoplankton is known to be able to utilise dust, organically bound iron and both reduced (Fe^{2+}) and oxidised (Fe^{3+}) free inorganic iron (Fe') by employing a broad spectrum of uptake pathways

In addition to the reduced organic form, P can possibly also be found in the ocean in its reduced inorganic state as PO_3^{3-} and PO_2^{3-} (Fig. 1.3). The potential prevalence of these sources in aquatic environments (Pasek et al. 2014) and their importance to *Trichodesmium* colonies which seem capable of both producing and possibly taking up PO_3^{3-} (Van Mooy et al. 2015) are currently not well characterised. Gene clusters for PO_3^{3-} (*ptx*) and PO_2^{3-} (*htx*) utilisation, first characterised in *Pseudomonas stutzeri*, are members of the Pho regulon in this organism. They include genes encoding ABC transporters (*ptxABC* and *htxBCD*) and enzymes NAD:phosphite oxidoreductase (*ptxD*) and hypophosphite dioxygenase (*htxA*) required for PO_3^{3-} and PO_2^{3-} oxidation respectively (Metcalf & Wolfe 1998; White & Metcalf 2004) (Fig. 1.7). It is worth noting that both of these reactions can potentially be carried out by C-P lyases and APases as well, although the reaction through PtxD is more energetically favourable.

Homologues of the *ptx* operon have recently been identified in marine cyanobacteria and diazotrophs, including *Trichodesmium,* and have been characterised to be responsible for PO_3^{3-} utilisation in *Prochlorococcus* MIT930 (Martínez et al. 2012). On the other hand PO_3^{3-} appears to be inaccessible or have a deleterious effect on microalgal species *Chlamydomonas reinhardtii*, *Botryococcus braunii* and *Ettlia oleoabundans* (Loera-Quezada et al. 2015). The ability of *Trichodesmium* to utilise PO_3^{3-} and the role of the *ptxABCD* homologous gene is further examined in Chapter 3 of this work.

1.4.2 Cellular strategies to cope with Fe stress

Regulation: The cellular response to Fe-limitation is coordinated by the ferric uptake regulator (Fur) which was first discovered in *E. coli* (Hantke 1981; Bagg & Neilands 1987a, 1987b). Fur binds to both DNA and Fe (Bagg & Neilands 1987a; Deng et al. 2015) and acts as a transcriptional repressor when the metal is abundant. Under Fe-deficiency it dissociates from DNA to allow activation of genes involved in the organisms' stress response (Lee & Helmann 2007; Osman & Cavet 2010). Despite its role as a repressor, Fur can also act as an activator directly or through interactions with regulatory small RNAs (sRNAs) (Delany et al. 2002; Massé & Gottesman 2002).

Conservation of resources: To reduce their cellular Fe demand marine microorganisms are known to replace Fe with non-Fe cofactors in certain enzymes and electron transporters. Examples are the electron transporters: ferredoxin which is replaced by flavodoxin

(LaRoche et al. 1996), and cytochrome c_{553} replaced by the copper containing plastocyanin (Peers & Price 2006).

Cells are also able to reduce Fe demands by regulating expression of multisubunit complexes. For example, under Fe-deficiency the ratio of photosystem I (PSI) to photosystem II (PSII) drops (Fraser et al. 2013; Snow et al. 2015). This preferential reduction of one photosystem compared to the other is a result of their differential demand for Fe: PSI binds 12 Fe atoms per monomer and is thus much more Fe demanding compared to PSII which binds 3 (Shi et al. 2007). To compensate for the reduction of PSI:PSII the PSI antenna protein IsiA is stimulated (Bibby et al. 2001; Shi et al. 2007; Richier et al. 2012; Ryan-Keogh et al. 2012; Fraser et al. 2013; Snow et al. 2015) resulting in an increase of PSI light harvesting efficiency by up to seven times (Yeremenko et al. 2004).

Low-Fe-stimulated replacement proteins and the genes that encode them have been previously used as biomarkers for detecting Fe-limitation in the field (Erdner & Anderson 1999; Lindell & Post 2001; Chappell et al. 2012; Saito et al. 2014). This is a valuable technique as the bioavailable pools of Fe are presently not clearly characterised. By circumventing or complementing Fe concentration measurements the use of biomarkers allows direct sensing of the organisms' perception of availability of the nutrient. However, care must be applied in interpreting the results as this proxy of Fe-limitation is not a direct measure of the N_2 and carbon fixation efficiencies.

Storage: Storage proteins are used to keep cellular Fe reserves for periods of low Fe supply. For example, ferritins are Fe storage proteins, which are widespread amongst bacteria, fungi, as well as plant and animal species, and form spherical complexes made of 24 subunits that can store 4500 Fe atoms (Andrews 1998; 2010). The related bacterioferritins, are only found in prokaryotes, and can sequester 2000 Fe atoms in their core. (Andrews 1998; 2010). They differ to ferritins in that they contain 12 hemes likely involved in Fe release (Yasmin et al. 2011). A third smaller protein complex from the same superfamily, termed 'DNA-binding protein from starved cells' or Dps, is found in prokaryotes and is made of 12 subunits that can store 500 Fe atoms (Castruita et al. 2006).

Studies have indicated the significance of Fe storage proteins in diatoms (Marchetti et al. 2009) and cyanobacteria for which bacterioferritins can associate with up to half of the cell's Fe reserve and are vital for survival under Fe stress (Keren et al. 2004). Recently a diel regulation of ferritins has been demonstrated in phytoplankton. This is possibly associated

with the replacement of damaged with *de novo* synthesised photosynthetic proteins during the dark period when they are not in use (Botebol et al. 2015). Securing released Fe in storage proteins during this process could be particularly beneficial during periods of Fe stress when external available pools are scarce and oxidative damage of photosynthetic machinery is augmented.

Fe utilisation: Highly efficient uptake mechanisms in cyanobacteria provide them with the ability to access various forms of Fe. Known accessible sources to *Trichodesmium* are presented in Table 1B. The uptake pathways that make these sources available are currently poorly characterized at the molecular level although such knowledge is important for understanding phytoplankton Fe homeostasis and its interaction with biogeochemical cycles.

The organic ligand pool of the surface oceans includes siderophores small chelating agents produced by bacteria and exported from the cell to bind Fe. Specialised transporters (TonB dependent transporters), subsequently take up the siderophore bound Fe (Neilands 1995). *Synechococcous* is the only marine cyanobacterial species identified to produce siderophores in addition to several marine heterotrophic bacteria (Ito & Butler 2005; Hopkinson & Morel 2009; Boiteau & Repeta 2015). Despite this, several phytoplankton species, and amongst them *Trichodesmium*, can engage in 'siderophore piracy' by utilising Fe from foreign siderophores (Achilles et al. 2003; Roe et al. 2012).

TonB-dependent transporters (TBDT) are composed of one or more outer membrane proteins utilising energy transferred by the periplasm-spanning TonB anchored on the plasma membrane. The energy transduction pathway starts with proteins ExbB and ExbD (forms homodimers with both ExbB and TonB in vivo) located in the plasma membrane (Ollis et al. 2009) where they utilise the proton motive force to induce conformational changes to TonB (Larsen et al. 1999; Brinkman & Larsen 2008; Ollis & Postle 2012; Ollis et al. 2012) (Fig. 1.7). The exact mechanism of energy transfer has not yet been elucidated. Although TBDTs involved in nickel and cobalt (Schauer et al. 2008), disaccharide and polysaccharide as well as vitamin B12 uptake have been identified, their major substrate is sidereophores and heme (Hopkinson & Barbeau 2012). Recent evidence suggests that ExbBD in *Synechocystis* sp. PCC 6803 (*Synechocystis* hereafter) are also involved in inorganic Fe uptake (Jiang et al. 2015). *Trichodesmium* possesses homologues of ExbBD and TonB but does not appear to have any obvious TBDTs (Hopkinson & Morel 2009).

The expression of TonB-transporter related genes is under the control of the Fur regulator in cyanobacteria (González et al. 2010, 2012) and differential expression of components was previously identified under Fe deficient conditions (Singh et al. 2003; Stevanovic et al. 2012). Furthermore, mutants of *tonB* and *exbBD* in *Synechocystis* display reduced growth compared to the WT under Fe-limitation (Jiang et al. 2012).

Siderophores transferred to the periplasm are carried across the inner membrane through ABC transporters Fhu and Fec, responsible for hydroxamate and citrate-type siderophore transport respectively (Krewulak & Vogel 2008; Stevanovic 2015). In cyanobacteria under reduced Fe conditions, components of this system are differentially regulated and growth of their deletion mutants is compromised (Stevanovic et al. 2012; 2013). Their transcriptional regulation was recently suggested to be controlled by Fur (González et al. 2014). Of the Fec/Fhu system subunits, *Trichodesmium* possesses only one protein with homology to the periplasmic hydroxamate binding FhuD (Chappell & Webb 2010).

Table 1B: Sources of iron accessible to *Trichodesmium*.

Fe form	Accessibility	Reference
Inorganic Fe'		
Fe(II)	yes	
Fe(III)	yes	Roe et al. 2012
Organically bound		
Rhodotorullic acid (siderophore)	yes	Achilles et al. 2003
Aerobactin (siderophore)	minimal	Roe et al. 2012
Desferrioxamine B (siderophore)	no/minimal	Roe et al. 2012 Achilles et al. 2003
Protoporphyrin IX	minimal	Achilles et al. 2003
Citrate	yes	Roe et al. 2012
Dust	yes	Rubin et al. 2011 Langlois et al. 2012

For transfer of uncomplexed free Fe^{3+} across the inner membrane bacteria utilise the ferric ion binding protein (Fbp) system/ferric uptake transport system (Fut) identified in pathogenic bacteria and *Synechocystis* respectively. It is composed of a periplasmic Fe-binding component (FbpA/FutA) a transmembrane (FbpB/FutB) and an ATPase (FbpC/FutC) subunit (Katoh et al. 2001a; Krewulak & Vogel 2008) (Fig. 1.7), homologues of which are found in *Trichodesmium*. Interestingly, *Synechocystis* possesses two paralogues of the periplasmic binding protein FutA. FutA2 appears to be periplasmic and complement FutBC

in Fe transport while FutA1 was indicated to be intracellular and have a function associated with protection of PSII under Fe-deficiency induced oxidative stress (Fulda et al. 2000; Tölle et al. 2002; Waldron et al. 2007). *Trichodesmium* has only one homologue, the identity of which is examined in Chapter 4.

For reduced Fe^{2+}, internalisation occurs through the Feo uptake system, which was first characterised in *E. coli*, and is composed of the inner membrane ATP-powered transporter FeoB, the transcriptional regulator FeoC and the protein of unknown function FeoA (Kammler et al. 1993; Cartron et al. 2006; Lau et al. 2013) (Fig. 1.7). Unlike *feoA*, which is expressed simultaneously to *feoB* 89% of the time (Lau et al. 2013), *feoC* is not conserved between species. *Trichodesmium* is an example where only homologues for *feoA* and *feoB* are encountered in the genome.

Mutants of both the Feo and Fbp/Fut uptake systems in cyanobacteria have reduced growth (Katoh et al. 2001a). Their expression, which is controlled by Fe concentrations, appears to be regulated by Fur in pathogenic bacteria (Mey et al. 2005; Ho & Ellermeier 2015) and *Synechocystis* (Krynická et al. 2014).

A common pathway of Fe uptake in phytoplankton involves reduction of Fe^{3+} to Fe^{2+} prior to its uptake by means of cell derived electrons (Roe & Barbeau 2014; Kranzler et al. 2014; Lamb et al. 2014) as a way of inducing Fe dissociation from 'unpalatable' ligands (Kranzler et al. 2011). Although some siderophores can be internalised through the Fec/Fhu ABC transport systems (Fig. 1.7), other substrates like dust particles are not available for direct uptake by the cells (Rich & Morel 1990; Rueter et al. 1992).

In pathogenic bacteria, yeast and eukaryotic phytoplankton reductive Fe uptake can occur through mechanisms like the export of reactive oxygen species (ROS) (Rose & Waite 2005) or the use of a ferric reductase (FRE) (Yun et al. 2001; Kustka et al. 2007; Groussman et al. 2015) (Fig. 1.7). In some cases reduction by FRE can be followed by reoxidation using multicopper oxidase (MCO) (Stearman et al. 1996; Askwith & Kaplan 1998; Herbik et al. 2002; Paz et al. 2007a; Groussman et al. 2015) to assist transport through associated specialised Fe^{3+} transporters (Ftr1, TTf) (Stearman et al. 1996; Fisher et al. 1997, 1998; Urbanowski & Piper 1999; Paz et al. 2007b) (Fig. 1.7).

In cyanobacteria, including *Trichodesmium*, reactive oxygen species (ROS) mediated Fe reduction was previously shown (Rose & Waite 2005; Roe & Barbeau 2014; Hansel et al. 2016). Furthermore, *Synechocystis* is suggested to employ the plasma membrane located

alternative respiratory terminal oxidase (ARTO) for transfer of electrons to Fe^{3+} (Kranzler et al. 2014) (Fig. 1.7).

In addition to *Trichodesmium's* cellular Fe uptake pathways, its colonial nature is potentially key to Fe acquisition *in situ*. Fe from desert dust was previously indicated to be more accessible to environmentally collected *Trichodesmium* puff colonies (Fig. 1.5Bi) compared to free filaments. Impressive footage by the same study recorded puff colony-associated filaments to engage in coordinated motility and shuffle dust from the periphery to the colony core (Rubin et al. 2011). Differences have been also identified between puff and tuft morphotypes of *Trichodesmium* in Fe uptake (Achilles et al. 2003) and ROS (superoxide) production (Hansel et al. 2016).

The ability of filamentous *Trichodesmium* in culture to acquire Fe from desert dust and the importance of cell surface contact for this process is further examined in Chapter 5 of this work. Also transcriptomic analysis targets the study of the organism's distinct life styles when encountered with Fe deficient as opposed to Fe replete conditions.

1.4.3 Trophic life strategies- Genomic minimalism or maximalism?

There is a dichotomy between two distinct growth strategies, both concurrently employed in the ocean by different groups of microbes. Oligotrophy is characterised by stable slow growth designed to ensure persistence under nutrient deficient environments (Kirchman 2015). Maintenance of low biomass, even when encountered with increased nutrient abundance, is hypothesised to provide an advantage in avoidance of viral and grazing predation (a strategy referred to as 'cryptic escape') (Yooseph et al. 2010). Contrasting oligotrophs, copiotrophs have more flexible growth rates, that are adjusted depending on nutrient availability and can lead to blooms under improved trophic conditions (Yooseph et al. 2010).

This feast-or-famine lifestyle of the copiotrophs requires maintenance of larger genomes harbouring more genes involved in signal transduction, quorum sensing, motility and other processes associated with the organisms' interaction with their environment (Yooseph et al. 2010). Also, numerous specific nutrient transport systems can be maintained as opposed to fewer more generalised transporters in oligotrophic organisms (Lauro et al. 2009). The genomic toolkit of copiotrophs however, potentially comes at a cost (either energetic or of other resources) compared to the streamlined genome of oligotrophs (Morris et al. 2012).

1.5 Omics and Detection of stress responses

Twenty years after Francis Crick first discussed the central dogma of biology, the unidirectional flow of information within an organism from DNA to RNA to protein (Crick 1958) (Fig. 1.7), sequencing techniques enabling decoding of nucleic acids became available (Maxam & Gilbert 1977; Sanger et al. 1977). They led to the sequencing revolution which started with the first complete genome sequence of *Haemophilus influenza* (Fleischmann et al. 1995) and continued to currently reach more than 30 000 sequenced bacterial genomes (https://gold.jgi.doe.gov/, Reddy et al. 2015). Several techniques have since emerged to decode cellular transcriptomes, the DNA stored information that is expressed at a given moment in the form of messenger RNA (mRNA). Transcriptomic analysis was revolutionised with the development of the faster and cheaper next generation sequencing techniques and RNAseq in 2005 (Mardis 2011).

The snapshot of a cellular transcriptome in time is the result of a compilation of regulatory changes in transcription caused by environmental stimuli (Fig. 1.8). It involves the interaction of signalling pathways with DNA-binding transcription activators and repressors and sigma/antisigma factors regulating transcription by RNA polymerases (Wösten 1998). In addition, non-protein-coding RNA (ncRNA) modifications which can affect the nature of the transcript pool include mobile group-II introns (Ferat & Michel 1993) which interfere with transcription, and diversity generating retroelements (DGR) (Doulatov et al. 2004) introducing changes to the RNA nucleotide sequence. More recently, epigenetic regulation, where hereditary changes in the DNA physical structure, but not the nucleotide sequence, alter gene expression has also been explored (Blyn et al. 1990; Turner et al. 2009; Casadesus & Low 2013).

Transcription does not always equate to protein expression of the mRNA product since post-transcriptional controls also include RNA degradation, targeted through 5'-triphosphate removal and polyadenylation (Li et al. 2002; Kime et al. 2010) (Fig. 1.8). Although tools for the detection of the previously mentioned controls are available by RNAseq (Marguerat & Bähler 2010), modifications at the level of translation (Fig. 1.8) (Byrgazov et al. 2013; Sauert et al. 2015) are more challenging to identify through this technique and not very well characterised. The latter include controls such as ribosome, translation factor and tRNA heterogeneity which can modulate the rate of translation of different transcripts.

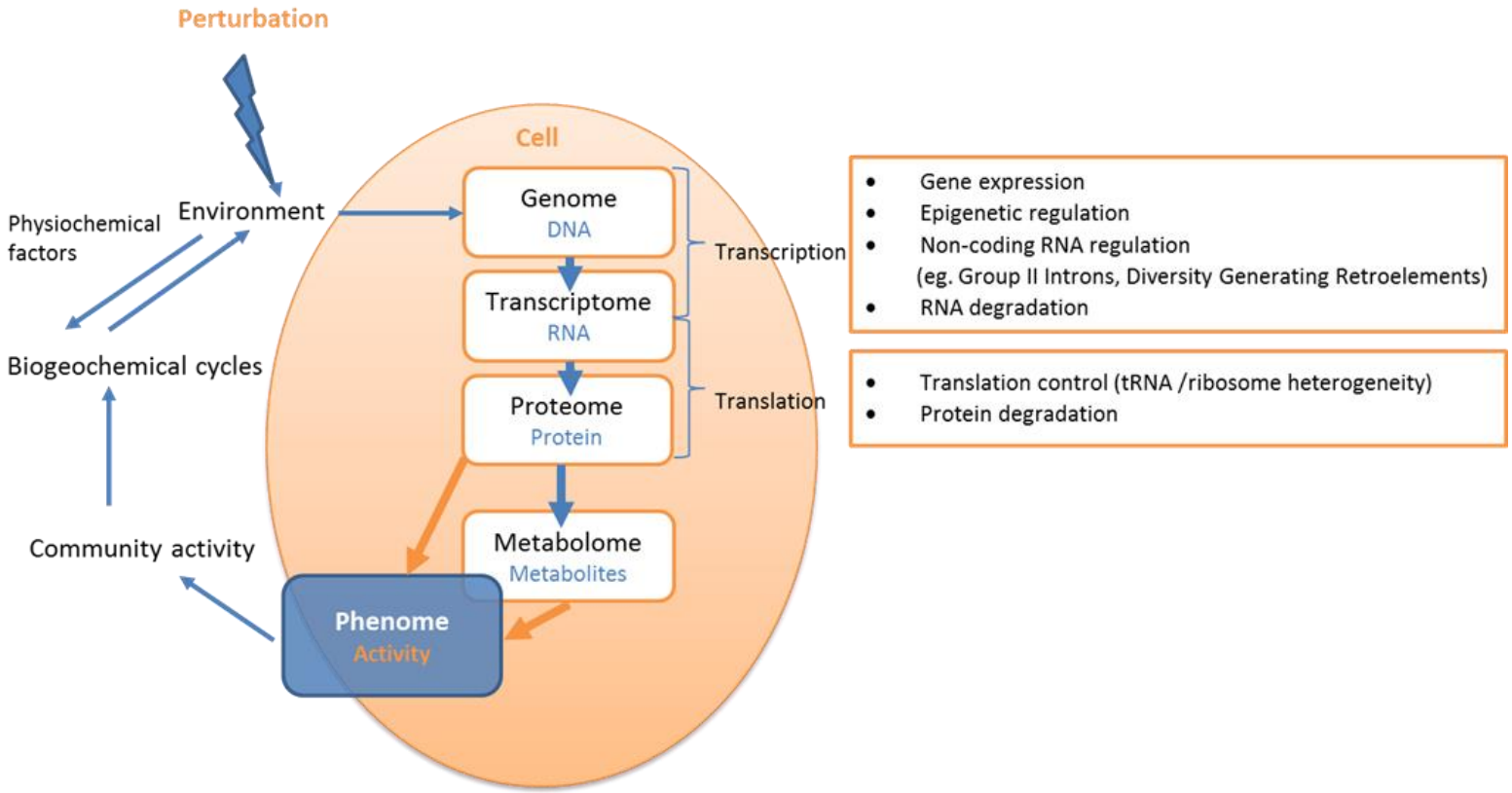

Figure 1.8: The cellular information flow and interactions with the environment. Environmental pertrubations, natural or anthropogenic, stimulate gene expression changes. The transcribed RNA will form the cells transcriptome which will be subjected to post-transcriptional modification and subsequently translated to protein. Translational controls affect the rate and nature of translation, while the resulting proteome will be further modified after its generation. Protein activity will subsequently characterise the metabolome, which provides an indication of cellular activity (the phenome). Through this pathway processes, including photosynthesis and N_2 fixation, can be adjusted as a response to the environmental changes. Combined changes at the community level will affect the functioning of biogeochemical cycles and the consequently the environment (e.g. climate).

In recent years, the availability of sequenced genomes and the improvement of mass spectrometry through novel ionisation techniques facilitated proteomic studies which assemble information translated from mRNA to proteins (reviewed in Yates 2011). Further downstream the route of DNA to activity, information at the proteomic level is generally considered a better indicator of the cell's physiological state. Although, the biggest control of protein expression still appears to be transcription itself (Li et al. 2014; Li & Biggin 2015; Jovanovic et al. 2015; Battle et al. 2015) this seems to be dependent on the stress state of the cells and the organism under investigation (Vogel & Marcotte 2012; Liu & Aebersold 2016; Cheng et al. 2016). For example, transcriptional control is suggested to be more important in organisms with copiotrophic rather than oligotrophic lifestyles (Cottrell & Kirchman 2016).

Post translational modifications including protein degradation mean that activity and protein abundance may not always correlate either, and therefore the field of metabolomics, quantitatively characterising cell produced metabolites has been developed to complement the omic analytic methods (Patti et al. 2012) (Fig. 1.8).

Trichodesmium's genome was first published in 2003 (Joint Genome Institute, http://genome.jgi.doe.gov/trier/trier.info.html). It is unusually large compared to other cyanobacteria genomes (Shih et al. 2013), being 7.75 Mbp in length and harbouring 4451 predicted genes, while it has a particularly high proportion (40%) of non-protein coding genome compared to the cyanobacterial average (15%) (Larsson et al. 2011). The recently published primary transcriptome of *Trichodesmium* (Pfreundt et al. 2014) revealed its large toolbox of regulatory DNA (Pfreundt et al. 2014; Pfreundt et al. 2015). Interestingly, *Trichodesmium's* large non-coding genome content also appears to be maintained in the environment (Walworth et al. 2015) pointing out to an important function promoting its conservation in the natural conditions encountered by the organism *in situ*. The first omic study in *Trichodesmium* was performed in 2011 looking at the response of the proteome to different nitrogen regimes (Sandh et al. 2011) and was followed by the analysis of its proteomic response to Fe and P-limitation (Snow et al. 2015; Walworth et al. 2016).

Although omic techniques are currently revolutionising the field of environmental microbiology their potential for understanding the function of characterised genes/proteins is largely limited. To this effect, targeted approaches through 'reverse genetics' can provide functional characterisation by using gene engineering coupled with physiological studies. For this, gene deletion/overexpression can provide clues towards protein function by

stimulating phenotypic alterations. Such techniques have been previously used to study the P and Fe uptake pathways of cyanobacteria (Martínez et al. 2012; Kranzler et al. 2014). Furthermore, the use of reporter genes/proteins, such as green fluorescent protein (GFP) can aid characterisation of *in vivo* protein localisation and temporal patterns of expression (Schuergers et al. 2015; Sacharz et al. 2015). The tools are not limited to biological systems as the activity and substrate binding affinity of overexpressed/purified proteins can be also examined *in vitro*, and their crystal structure elucidated, to facilitate functional characterisation. For instance the Fe^{3+} binding capacity of the *Synechocystis* FutA transporters has previously been demonstrated using this approach (Katoh 2001b; Badarau et al. 2008).

Currently, there are no established techniques to genetically modify *Trichodesmium,* therefore targeted approaches are largely limited. However, genes can be incorporated in the DNA of foreign organisms, in a process referred to as heterologous expression. Through recovery of the function of homologous deleted genes in the host organism, or generation of novel phenotypes, the targeted gene/genes can be characterised. Such a technique was previously utilised to indicate the functionality of *Trichodesmium's* transcription regulator HetR in modulating heterocyst formation in *Anabaena* sp. strain PCC 7120 when the organism's native homologue was deleted (Kim et al. 2011).

1.6 Significance of molecular data in ocean science

The expanding molecular understanding of marine microorganism metabolic processes provides the foundation for several previously unattainable applications.

For example, sensing via the use of biomarkers (Zehr et al. 2009) can identify cellular activity or stress at different oceanic locations (Saito et al. 2014), the presence/distribution of specialised populations of microorganisms such as diazotrophs (Robidart et al. 2014) and can provide an early warning system for detection of harmful species blooms (Tsaloglou et al. 2013).

In addition, a molecular understanding of cellular processes can be used to construct models of metabolism at the genome level (Genome scale metabolic network reconstructions) that are used to identify new metabolic capabilities within species (Levering et al. 2016). Gathered information about genes/proteins can be further

incorporated in models used to predict the biogeography, activity and response of organisms to environmental changes (Reed et al. 2014; Mock et al. 2016).

Finally, molecular tools can be employed to identify and utilise biotechnologically interesting proteins (Kennedy et al. 2011) such as biocatalysts (Parages et al. 2016), novel antibiotics (Eom et al. 2013) and biosurfactants (Gudiña et al. 2016) from the vast array of unstudied marine microorganism species.

1.7 Thesis plan

The work presented in this thesis employs a combination of techniques, both targeted and holistic, molecular and physiological to establish a better understanding of *Trichodesmium's* nutrient limitation responses and uptake mechanisms. We focus on the two most discussed nutrients, P and Fe, both suggested to be limiting growth and activity of this important primary producer in the ocean (Moore et al. 2009; Mills et al. 2004).

In view of recent evidence pointing towards the abundance and significance of the reduced inorganic form of P, PO_3^{3-} in the ocean (Pasek et al. 2014; Van Mooy et al. 2015), Chapter 3 is dedicated to elucidating *Trichodesmium*'s ability to utilise it for growth. The role of the organism's *ptxABCD* homologues is established through their heterologous expression in *Synechocystis* and controls on their regulation are determined.

The same technique is employed in Chapter 4 to decipher the function of the FutA homologue in *Trichodesmium*. This protein, which has previously been used as a biomarker of Fe stress in the ocean (Rivers et al. 2009; Saito et al. 2014) is equally similar to two *Synechocystis* Fe regulated homologues performing distinct functions (Tölle et al. 2002; Waldron et al. 2007; Kranzler et al. 2014). Mutants of both *Synechocystis* homologues are acquired and the *Trichodesmium* gene is introduced in their genome to identify recovered phenotypes. Additionally, the cellular localisation of the *Trichodesmium* and *Synechocystis* homologues is explored through fusion of their signal sequences to green fluorescent protein (GFP). The *Trichodesmium* protein is further studied by overexpression and purification for structural studies aimed at assessing its metal binding capacity.

Finally, in Chapter 5 the ability of *Trichodesmium* to access Fe provided as Saharan desert dust and the importance of cell surface contact for this process is established through specifically designed physiological experiments. The organism's transcriptomic response

when grown under the variable Fe regimes used during the physiological experiments is analysed to detect the effect on known *Trichodesmium* Fe metabolism coordinating genes, and identify novel ones.

Chapter 2
Materials and methods

2.1 Strains and growth conditions

Strains of *Synechocystis* sp. PCC 6803 (*Synechocystis*), *Trichodesmium erythraeum* IMS101 (*Trichodesmium*) and *Escherichia coli* (*E.coli*) generated and used throughout this work are detailed in Table 2A.

2.1.1 *E. coli*

Escherichia coli was grown at 37^{o}C in LB (Luria-Bertani) broth in 50 ml glass conical flasks or 15 ml falcon tubes (Corning Inc., NY, USA), and plates (Fisher Scientific, Loughborough, UK) set with 1% (w/v) agar, with or without 100 µg/ml ampicillin.

2.1.2 *Trichodesmium*

Trichodesmium was grown at 27 °C in modified YBC-II media (Table 2B, 2C) (Chen 1996), (referred to as mYBC-II). The molybdenum content of the media was raised to 100 nM to better match seawater concentrations (James 2005) while other metals were modified based on trace metal additions by Shi et al. (2012). The media was filter sterilised using 0.22 µm Stericup Filter units with 1 L Sterile Receiver flasks (Millipore, MA, USA). Cells were grown in 25 cm^2 sterile polystyrene cell culture flasks with 0.2 µm vent caps (Corning Inc., NY, USA) subjected to gentle orbital shaking (150 rpm) under a 12 hr/12 hr light (ca. 130 µmol photons m^{-2} s^{-1})/dark cycle.

Table 2A: Bacterial strains used for experiments. Gene insertions/deletions in *Synechocystis* were selected using antibiotic resistance to kanamycin (kan), chloramphenicol (cm) and zeocin (zn). Plasmid selection in *E. coli* was conferred using ampicillin (amp) resistance.

	Gene deletion (Ant^R µg/ml)	Gene insertion (Ant^R µg/ml)	Source	Chapter
***Synechocystis* PCC 6803**				
WT-G			Cereda et al. 2014	3,4
PtxABCD+		*Tery_0365-0368* (kan30)	This study	3
PtxABC+		*Tery_0365-0367* (kan30)	This study	3
PtxD+		*Tery_0368* (kan30)	This study	3
Δ*futA1*	*slr1295* (zeo20)		This study	4
Δ*futA2*	*slr0513* (cm25)		This study	4
Δ*futA1/futA2*	*slr1295/slr0513* (zeo20/cm25)		This study	4
Δ*futA1+3377*	*slr1295 (zeo20)*	*Tery_3377* (kan30)	This study	4
Δ*futA2+3377*	*slr0513* (cm25)	*Tery_3377* (kan30)	This study	4
FutA1ss-GFP		*slr1295ss-GFP* (cm25)	This study	4
FutA2ss-GFP		*slr0513ss-GFP* (cm25)	This study	4
3377ss-GFP		*Tery_3377ss-GFP* (cm25)	This study	4
3377ss-KK-GFP		*Tery_3377ss* (R5/6K) *GFP* (cm25)	This study	4
***Trichodesmium erythraeum* IMS101**			CCMP1985 (NCMA, Bigelow Laboratory for Ocean Sciences)	3,4,5
Escherichia coli				3,4
XL1-Blue			Agilent Technologies, Stockport, UK	3,4
BL21(DE3)			New England Biolabs Ltd, Hitchin, UK	4
DH5-alpha			New England Biolabs Ltd, Hitchin, UK	4
3377_OE		*Tery_3377* (in pET21a+) (amp100)	This study	4

Table 2B: Modified (m) YBC-II media recipe

YBC-II medium	Per L H_2O
Vitamins	
1000x Vitamin stock	1 ml
Trace metals	
1000x Iron stock	1 ml (Standard growth) 2.5 ml (Fe+ experimental cultures)
Nutrients	
1000x Phosphorus stock:	
Phosphate stock	1 ml (Standard growth)
Phosphite stock	1 ml (Chapter 3- PO_3^{3-} cultures)
Salts	
Sodium chloride	24.55 g
Potassium chloride	0.75 g
Sodium bicarbonate	0.21 g
Boric acid	0.036 g
Potassium bromide	0.116 g
Magnesium chloride	4.067 g
Calcium chloride	1.47 g
Magnesium sulphate	6.16 g
Sodium fluoride stock	1 ml
Strontium chloride stock	1 ml
Stock solutions	**Per L H_2O**
Salts	
1000x Sodium fluoride stock	2.939 g
1000x Strontium chloride stock	0.017 g
Trace metals	
1000x Trace metal stock:	
Manganese chloride	0.00396 g
Zinc Sulphate	0.00115 g
Cobalt (II) chloride	0.00059 g
Sodium molybdate	0.00266 g
Copper (II) sulphate	0.00025 g
Disodium EDTA	0.74448 g
1000x Iron stock	
Iron (III) chloride	0.0432 g
Disodium EDTA	0.0596 g
Nutrients	
1000x Phosphate stock	
Monosodium phosphate	6.899 g
1000x Phosphite stock	
Sodium phosphite	10.802 g
Vitamins	
1000x Vitamin stock:	
Thiamine	0.0998 g
Biotin	0.0005 g
Cyanocobalamin	0.0005 g

Table 2C: Modified YBC-II trace metal composition compared to standard YBC-II.

	Modified YBCII	**Standard YBC-II**
EDTA	20 µM	2 µM
Cu	8 nM	1 nM
Zn	20 nM	4 nM
Co	8 nM	2.5 nM
Mn	18 nM	20 nM
Mo	100 nM	11 nM
Ni	20 nM	-
Se	10 nM	-

Cultures were routinely grown with 160 nM iron ($FeCl_3$-EDTA). For iron (Fe)-stress growth experiments (Chapter 5) no Fe was added to Fe-deplete treatments (Fe-) compared to 400 nM of added Fe to Fe-replete treatments (Fe+).

Saharan desert dust was collected between 04°43'N, 28°55'W and 06°56'N, 28°07' using a mesh system aboard the RSS Shackleton on 01/04/1981-02/04/1981 (Murphy 1985). Equal amounds (0.25 mg ml^{-1}) were added to the media either directly or in 8 kDa MWCO dialysis tubing (DT) (BioDesign, NY, USA). Immediately before use, DT was tied on one end and boiled twice in 120 mM Na_2HCO_3 followed by another two times in 10 mM Na_2EDTA and 10 mM NaOH. After that, DT was rinsed three times in milli-Q H_2O (method adjusted from http://alta.biology.utah.edu/index.php, Horvath Lab Protocols Department of Biology, University of Utah). Clean DT was then handled with 10% HCl washed plastic tweezers and was included in all experimental treatments except form a no-DT control.

For *Trichodesmium* phosphorus (P)-stress growth experiments (Chapter 3) 50 µM phosphate ($NaH_2PO_4.H_2O$) (PO_4^{3-}) or phosphite ($Na_2HPO_3.5H_2O$) (PO_3^{3-}) were used as P sources while no P was added to control treatments.

Treatments for both, Fe (Chapter 5) and P (Chapter 3), experiments were set in triplicate cultures and inoculations were performed using cells grown to late exponential phase and pre-concentrated by filtering onto NucleoporeTM track-etched polycarbonate membranes (Whatman, Kent, UK) with a pore size of 5µm, washed with and resuspended in Fe/P free mYBC-II.

2.1.3 *Synechocystis*

Synechocystis was routinely grown in BG-11 media (Table 2D) (Rippka et al. 1979) at 30^{o}C, shaking at 150 rpm, under constant illumination of ca. 50 µmol photons m^{-2} s^{-1}. BG-11 was supplemented with 5 mM glucose and buffered to pH 8.2 with 10 mM N-17 [tris(hydroxymethyl)methyl]-2-aminoethanesulfonic acid (TES)-KOH buffer. For growth on plates, 1% agar was added. Antibiotics were used in the concentrations indicated (Table 2A).

Table 2D: BG-11 media recipe

BG-11 medium	**Per L H_2O**
100x BG-11 stock	10 ml
1000x Iron stock	1 ml
1000x Phosphate stock	1 ml
1000x Carbonate stock	1 ml
Supplementary stocks	**Per L H_2O**
Glucose stock	5 ml
TES/KOH	100 ml
Stock solutions	**Per L H_2O**
100x BG-11 stock	
Sodium nitrate	149.6 g
Magnesium sulphate	7.49 g
Calcium chloride	3.60 g
Citric acid	0.60 g
Disodium EDTA	0.56 ml of 0.5M stock pH 8.0
Trace mineral stock	100 ml
1000x Iron stock	
Ferric ammonium citrate	6 g
1000x Phosphate stock	
Dipotassium hydrophosphate	30.5 g
1000x Phosphite stock	
Sodium phosphite	37.81 g
1000x Carbonate stock	
Sodium carbonate	20 g
1000x Iron stock	
Trace mineral stock	
Boric acid	2.86 g
Magnesium sulphate	1.81 g
Zinc sulphate	0.22 g
Sodium molybdate	0.39 g
Copper sulphate	0.079 g
Cobaltous nitrate	0.049 g
1M Glucose stock	
Glucose	180 g
1M TES/KOH	
TES	229.2 g, pH 8.2

Iron-stress growth experiments (Chapter 4) were carried out in phototrophic conditions (no glucose), in triplicate cultures, using YBG-11 media (recipe described by Shcolnick et al. 2007) with 6 mM or 0.6 mM of $FeCl_3$ for Fe-replete (Fe+) and -deplete (Fe-) conditions respectively.

Ferrozine (FZ) growth experiments were carried out in Fe- (0.6 mM of $FeCl_3$) YBG-11 at a FZ final concentration of 200 µM (FZ+) or no added FZ (FZ-) (Chapter 4). Cultures were incubated at ca. 30 µmol photons m^{-2} s^{-1} of red light to minimise photoreduction of Fe (Kranzler et al. 2011).

For phosphorus (P) experiments (Chapter 3) triplicate cultures with 175 µM sodium phosphate ($NaH_2PO_4.H_2O$) (PO_4^{3-}) or the same concentration of sodium phosphite ($Na_2HPO_3.5H_2O$) (PO_3^{3-}) were compared to no P added controls.

2.2 Physiological measurements

2.2.1 Photosynthetic physiology

Photosynthetic physiology was monitored using a FASTtracka MkII Fast Repetition Rate fluorometer (FRRf) integrated with a FastActTM Laboratory system (Chelsea Technologies Group Ltd, Surrey, UK). For *Trichodesmium* measurements were made 2.5 hrs after the beginning of the photoperiod. Both *Trichodesmium* and *Synechocystis* samples were dark adapted for 20 min and consequently exposed to a background irradiance of 29 µmol photons m^{-2} s^{-1} (PAR) (Table 2E) for 2-5 min prior to measurements. This stimulates an increase in quantum yield (Richier et al. 2012).

Table 2E: Fast Repetition Rate fluorometer settings

Parameter	Setting
Sequences per acquisition	12
Sequence interval	100
Acquisition pitch (s)	2
Flashlets in sat. phase	200
Flashlet duration in sat. phase (ms)	1
Flashlets in rel. phase	30
Flashlet duration in rel. phase (ms)	49
Saturation phase duration (ms)	0.4
Relaxation phase duration (ms)	57.7
LED set	160
Background irradiance (µmol photons m^{-2} s^{-})	29

F_v/F_m was used as an estimate of the apparent PSII photochemical quantum efficiency (Kolber et al. 1998). The dark adapted state (F_o) and maximum (F_m) fluorescence were blank corrected, and the difference between them (F_v) was recalculated to manually compute an adjusted F_v/F_m ratio. The functional absorption cross-section of PSII (σ_{PSII}) was also acquired (Table 2F). Data presented is the average of three technical replicates or a single measurement (for *Trichodesmium* and *Synechocystis* respectively) for each of three independent cultures (biological replicates).

Table 2F: Description of physiological parameters recorded.

Technique	Parameter	Description
Photosynthetic physiology	F_m	The maximum fluorescence at saturation. All PSII reaction centres are 'closed'.
	F_o	Fluorescence at time=0. All PSII reaction centres are 'open'.
	F_v	The difference between the maximum fluorescence (F_m) and initial fluorescence (F_o).
	F_v/F_m	Apparent PSII photochemical quantum efficiency
	σ_{PSII} (nm^2)	Functional absorption cross-section of PSII
Growth	Cell number (*Trichodesmium*)	Equation 1: $C_N = \frac{\sum f_l}{C_l}$ C_N = cell number Σf_l = total filament length C_l = cell length
	OD (Optical Density) (*Synechocystis*)	Measured at a wavelength of 750 nm where no pigment absorption interference occurs. An OD_{750}=1 is approximately equal to 1.6×10^8 cells ml^{-1} (Pojidaeva et al. 2004)
	Growth rate	Equation 2: $\mu = \frac{\ln(cC_{t_2}/cC_{t_1})}{t_2 - t_1}$ cC_t = cell concentration (direct measurement or using OD) t = time

2.2.2 Growth

Trichodesmium growth was monitored through cell counts performed using a Sedgewick rafter counting chamber and a GX CAM-1.3 camera on an L1000A biological microscope (GT Vision Ltd, Suffolk, UK). Cell and filament lengths were identified using GX capture software (GX 14 Optical, Suffolk, UK) and ImageJ software (Schneider et al. 2012). The number of cells per ml was calculated by dividing the total filament length by the average cell length (Table 2F).

Synechocystis growth was monitored turbidimetrically by recording the optical density of the cultures at a wavelength of 750 nm (OD_{750}) using a Jenway 7315 spectrophotometer (Bibby Scientific Ltd, Staffordshire, UK). When OD_{750} exceeded that of 1, samples were diluted with filtered medium to achieve better measurement accuracy.

For both *Trichodesmium* and *Synechocystis,* growth rates were calculated from the gradient of the natural logarithm of measurements during exponential growth (Table 2F).

2.2.3 Chlorophyll *a*

Chlorophyll *a* (Chl *a*) content was assessed through extractions from 2 ml *Trichodesmium* cell culture filtered on MF 300 microfibre filters (Fisher Scientific, Loughborough, UK) or 100-200 µl *Synechocystis* culture. Cells were incubated in 90% acetone for 24-48 hrs in the dark, at 4 °C. Fluorometric measurements were recorded on a Turner TD-700 fluorometer (Turner Designs, CA, USA) as described by Welschmeyer (1994). The results were calibrated using solid secondary standards and Chl *a* concentration was calculated using a Chl *a* standard curve.

2.2.4 Statistical analysis

Statistical differences in physiological parameters were assessed using the Student's t-test (Chapter 3) or general linear model (GLM) followed by a post-hoc Tukey-test (CI=95%) (Chapters 4 and 5) (Minitab 17.3.1, Minitab Inc., Coventry, UK).

2.3 Methods for molecular analysis

2.3.1 Nucleic acid extractions and quality control

RNA extractions: RNA was extracted using the spin column based RNeasy Plant Mini Kit (Qiagen, Manchester, UK) according to the manufacturers' instructions subjected to minor alterations as follows: Cells (~ 5 x 10^6) were filtered on MF 300 microfibre filters (*Trichodesmium*) or pelleted by centrifugation (*Synechocystis*) and snap frozen in liquid nitrogen. They were subsequently stored at -80 °C for future use or processed for RNA extractions immediately. Homogenization was achieved by disruption with a pestle and resuspension in RLT lysis buffer. After removal of cell and filter-paper debris by centrifugation for 2 mins through the QIAshredder spin column, samples were loaded on the RNeasy spin column and 96-100% ethanol was used to wash the spin column twice or

until the flow through was colourless. The manufactures' protocol was followed thereafter and RNA was eluded in 30 µl nuclease free water. Extracted RNA was stored at -80 °C or DNase treated directly (Sec. 2.3.2).

DNA extractions: DNA from both *Trichodesmium* and *Synechocystis* was isolated using the DNeasy Plant Mini Kit (Qiagen, Manchester, UK) according to the manufacturers' instructions. Homogenisation was achieved as described above and the manufacturer's guidelines were followed for the subsequent extraction. Purified DNA was stored at -20 °C in buffer AE.

Nucleic acid quality control: Purity and initial quantification of 1 µl extracted DNA and RNA was determined from the 260/280 and 260/230 nm ratios measured on a NanoDrop ND-1000 UV-Vis Spectrophotometer (Thermo Scientific, DE, USA). The nucleic acid 260/280 value of ~1.8 for DNA or ~2 for RNA is generally considered a sign of purity implied by the absence of protein, phenol or other 280 nm absorbing contaminants. Equally as a secondary measure of purity a 260/230 ratio between 2.0 and 2.2 is expected. However, contaminants that absorb at 230 nm (lowering the ratio) can include guanidine thiocyanate a lysis buffer ingredient which at subnanomolar concentrations can decrease the 260/230 considerably without compromising the performance of the quantitative PCR reactions (VonAhlfen & Schlumpberger 2010). The absence of potential inhibition from any contaminants was also confirmed through linearity of quantitative Polymerase Chain Reaction (qPCR) standard curves (Sec. 2.3.3).

Integrity of RNA was determined from the electropherogram trace, RNA integrity number (RIN) and percentage of RNA fragments above 200 nucleotides (DV200) as produced by the Agilent 2100 Bioanalyzer system using the Agilent RNA 6000 Nano Kit (Agilent Technologies UK Limited, Cheshire, UK) (Table 2G).

Table 2G: RNA extracted- quality control and concentrations.

Chapter	Treatment	Sample	260/280	260/230	RIN	DV200 (%)	Concentration (ng/µl)
3	P-	1	1.97	1.35	6.6	95	32
		2	1.99	1.36	6.8	93	22
		3	2.00	1.54	6.6	94	43
	PO_3^{3-}	1	2.06	1.37	6.7	93	53
		2	2.00	0.96	6.7	90	31
		3	1.97	1.58	6.6	90	59
	PO_4^{3-}	1	2.04	1.47	5.7	91	85
		2	1.98	1.64	6.1	97	191
		3	2.03	1.43	8	97	72
4	Fe-	1	2.06	2.24	7.4	97	62
		2	1.99	1.91	7.8	99	18
		3	1.97	1.87	8	95	20
	Fe+	1	2.07	2.30	7.6	98	56
		2	2.07	2.35	7.6	99	50
		3	2.03	2.09	7.4	99	51
	[Dust]	1	2.06	2.17	7.6	99	24
		2	1.93	1.28	7.4	98	15
		3	2.00	1.57	7.5	97	15
	Dust+	1	2.04	2.09	7.4	97	45
		2	2.02	2.3	7.5	98	32
		3	2.06	2.32	7.5	99	37

2.3.2 DNase Treatment and cDNA synthesis

Since on-column DNase digestion or RNA clean-up using the RNeasy Plant Mini Kit was not effective in eliminating all identifiable traces of genomic DNA (gDNA) contaminants in trial RNA extractions, the isolated RNA was DNase treated with TURBO DNA-free DNase (Life Technologies Ltd, Paisley, UK) instead. After treatment RNA was stored at -80 °C or immediately converted to complementary DNA (cDNA) using random hexamers provided by the Tetro cDNA Synthesis Kit (Bioline Reagents Limited, London, UK). Complementary DNA (cDNA) was aliquoted to single use volumes and stored at -20 °C. Samples were tested for the absence of gDNA contamination by performing the synthesis reaction with and without Reverse Trranscriptase (RT) for each sample. Absence of visible products after 40 cycles of PCR amplification in no RT controls using reference gene primers (see below) was indicative of below the detection limit or no gDNA contamination.

2.3.3 Polymerase Chain Reaction (PCR) conditions

Primer design: Oligonucleotide primers were designed using Primer3 through the Primer-BLAST tool on the NCBI portal (http://www.ncbi.nlm.nih.gov) (Ye et al. 2012) and supplied from biomers.net GmbH (Ulm, Germany) or Integrated DNA Technologies Inc. (IA, USA). Lyophilised primers were rehydrated in 10 mM Tris-Cl, 0.1 mM EDTA, pH 8.5 to a concentration of 100 µM and stored at -20 °C.

For qPCR, 20-24 bp primers for amplification of 112-189 bp products were designed. Primer melting temperatures were chosen to be 60 ± 1 °C, the guanine (G) – cytosine (C) content between 30-80% and their last five bases at the 3' end to contain the lowest number of G/C bases possible. Primers were diluted to 250 nM final concentration immediately before use. To ensure compliance with the MIQE guidelines (Bustin et al. 2009) a dilution series (≥4 data points) of cDNA sample was constructed and all primer sets were run in triplicate at each cDNA concentration. A qPCR reaction amplification efficiency between 90 and 105% and linearity greater than r^2=0.97 was termed satisfactory for further analysis (Pfaffl et al. 2004; Bustin et al. 2009; Bustin 2010) (Table 2H). At the end of each run, melt (dissociation) curve analysis was used to confirm single product amplification by primer sets.

End point analysis: End point reverse transcription (RT)-PCR was performed on a SureCycler 8800 Thermal Cycler (Agilent Technologies UK Limited, Cheshire, UK) and MyCycler Thermal Cycler (Bio-Rad Laboratories Limited, Hertfordshire, UK) with MyTaq High Specificity Red DNA Polymerase Mix (Bioline, London, UK) or Q5 High-Fidelity Polymerase Mix (New England Biolabs Ltd, Hitchin, UK) according to the manufactures' instructions. Products were visualised using agarose gel electrophoresis (Sec. 2.3.4).

Quantitative (q) PCR: For Chapter 3 analysis was performed on an Mx3005P qPCR using Brilliant III Ultra-Fast SYBR Green qPCR Master mix (Agilent Technologies UK Limited, Cheshire, UK) at a total reaction volume of 20 µl. The PCR conditions were as follows: 1 cycle 95 °C for 180 secs (initial denaturation), 40 cycles of 95 °C for 15 secs (denaturation) followed by 60 °C for 20 secs (annealing/extension) and 1 cycle of 95 °C for 60 secs (final extension). Dissociation curves were created starting at 55 °C for 30 secs and increasing to 95°C.

For validation of transcriptomic results (Chapter 5) a ROCHE LightCycler 96 was used. Reactions were set at 20 µl with iQ SYBR Green qPCR Supermix (Bio-Rad Laboratories Limited, Hertfordshire, UK): 1 cycle 95 °C for 180 secs (initial denaturation), 45 cycles 95 °C

for 10 secs (denaturation) followed by 60°C for 30 secs (annealing/extension), 1 cycle of 95 °C for 10 secs (final extension). Dissociation curves were recorded between 55 °C and 95 °C.

For all primer sets each sample was run in triplicate (technical replicates) along with a triplicate set of no-template controls (NTC). This contained all reaction constituents apart from the sample in the place of which nuclease free water was added. For each gene analysed all samples of all treatments were included on a single plate therefore no inter-run calibrators (IRC) were required as a control of potential intra-run variation.

For Chapter 3 reference genes *rnpB* (Chappell & Webb 2010) and *rotA* (Orchard et al. 2009) were used. For Chapter 5 genes *Tery_R0021* (*rnpB*), *Tery_2660* (*GlyA*) (Chappell & Webb 2010), *Tery_2329* and *Tery_3279* (identified from transcriptomic analysis performed in the context of this work) were tested on geNorm (qBase+ software, Biogazelle, Zwijnaarde, Belgium). The best normalisation strategy predicted by the software suggested the use of *Tery_2329* and *Tery_3279* as reference genes. These produced a gene expression stability value (M) of 0.143 and a coefficient of variation on the normalized reference gene relative quantities (CV) of 0.05 well below the qBASE default thresholds of 0.5 and 0.2 respectively.

Normalised relative quantities (NRQs) in Chapter 3 were scaled using the phosphate-added (PO_4^{3-}) treatment as control, while in Chapter 5 the lowest NRQ for the specific gene analysed. They were subsequently presented as relative fold change (RFC) (qBase+ software, Biogazelle, Zwijnaarde, Belgium). The built-in statistical wizard was used to compare the means of different treatments using one-way analysis of variance (ANOVA).

2.3.4 Agarose gel electrophoresis

All PCR and cloning products were visualised through agarose gel electrophoresis. Gels were made with 30 ml TAE (tris-acetate-EDTA) buffer, 3 µl (of 10 mg/ml stock) ethidium bromide and set with 0.3 g, 0.45 g or 0.8 g of agarose for 1%, 1.5% and 3% gels (the starting concentration for the latter is lower that 3% to allow for evaporation of liquid during the heating process) respectively. Gels were run in TAE buffer (supplemented with 3 µl of 10 mg/ml ethidium bromide) for 30-45 mins at 75-90 V. Molecular weight markers HyperLadder I, II or V (Bioline, London, UK) were used for 1, 1.5 and 3% gels respectively.

Table 2H: Genes analysed by qPCR, amplicon and primer information

Chapter	Gene	Tery no.	Forward	Reverse	Size	Efficiency	R^2
3	*ptxB*	*0366*	GCGATCAAGCTTCTACTTCTAGTC	CATTGGCAACAGCAATAGCAAC	132	93.1	0.99
	ptxD	0368	CCCGACTTATTAGCAGCACC	AGCTTTTCCTAATTTTCCCATCCC	189	99.3	0.99
	rotA	0301	AAGGAGGTTGCCCAAAAGGT	GCCACCTGTATCTTTACCAGCA	125	93	0.99
	rnpB	R0021	GGAACCGGAAAAAGACCAACC	GCCACAGAAAAATACCGCCAA	168	99.4	1
5	*isiA*	1667	TTGCTTCGCTTGACCTGTTG	AGGTGGAGCAGTTGTAGACAC	145	92	0.99
	nif-like	4114	GCTGTAATGGTGGCTTTGGC	TCCGCTTCTTCCTTAGCTTGT	143	93	0.99
	cytc6	2561	TCTCCGCTGCAAACATACCA	AGTGGGAAGGGGGTATTCCA	124	97	0.99
	glyA	2660	GGCGGTCTCATCCTTACTCG	GCTTCTCCAAATGCGACTGC	125	96	1
	gvpN	2329	ACAGGGTGGTGACAATTGGA	CACTCTTTGGCGAACACTGC	134	96	1
	RNase T2	3279	AGCTGGCAACCCAGTTTTTG	TGTCAGGCCACAAACCATGTA	112	97	1
	rnpB	R0021	GGAACCGGAAAAAGACCAACC	GCCACAGAAAAATACCGCCAA	168	100.1	1

2.4 Generation of genetically modified strains

2.4.1 Approaches

For functional characterisation of proteins, *Synechocystis* was genetically engineered to generate strains with genes of interest deleted (Chapter 4) and to heterologously express *Trichodesmium* proteins of interest (Chapter 3 and 4). In addition, green fluorescent protein (GFP) fusions to protein signal sequences were constructed and their cellular localisation was examined through expression in *Synechocystis* (Chapter 4).

Deletion mutants: For the generation of *slr1295* (*futA1*) and *slr0513* (*futA2*) *Synechocystis* deletion mutants (Chapter 4), the antibiotic resistance (Ab^R) cassette for zeocin (Zeo^R) from pZEO (Invitrogen, UK) or the chloramphenicol acetyl transferase (*cat*) gene from pACYC184 (NEB, UK), amplified using the primers: zeo_F and zeo_R or cat_F and cat_R respectively (Fig. 2.1), were used. PCR products consisting of the sequence upstream of the *futA1/futA2* genes and the beginning of the open reading frame (ORF), or the end of the ORF and downstream flanking DNA, were amplified from *Synechocystis* gDNA using primers *futA1/futA2*_ P1 and P2 or P3 and P4 respectively.

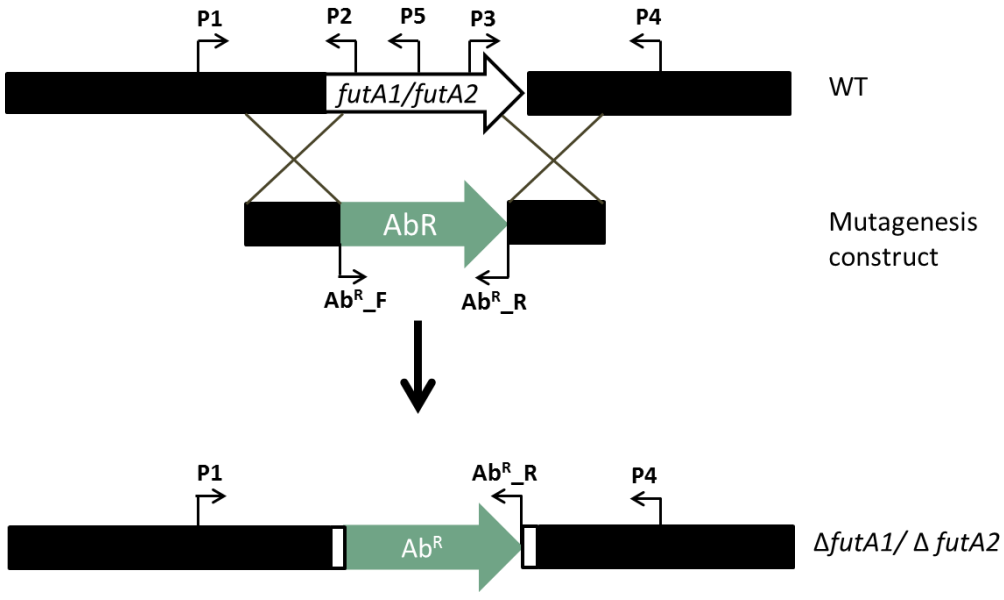

Figure 2.1: **Generation of deletion mutants.** Using overlap extension (OLE)-PCR, mutagenesis constructs with antibiotic resistance markers (Ab^R) were designed to

homologously recombine to the *futA1* or *futA2* loci of *Synechocystis* replacing the native genes in mutants Δ*futA1* and Δ*futA2*.

Overlap extension (OLE)-PCR (Se. 2.4.2) with primer pair *futA1/futA2*_ P1 and P4 was used to generate a mutagenesis construct in which the Ab^R marker (Zeo^R and cat^R for Δ*futA1* and Δ*futA2* respectively) was inserted between the upstream and downstream *futA1/futA2* PCR products (Fig. 2.1). This mutagenesis constructs were subsequently used to transform *Synechocystis* (Sec. 2.4.2). Primer *futA1/futA2*_ P5, binding internally to *futA1/futA2* was used to test segregation of each mutant.

The *ΔfutA1/A2* double mutant was generated by transforming Δ*futA1* with the *futA2* gene replacement construct.

Expression of *Trichodesmium* genes in *Synechocystis*: The function of *Trichodesmium* proteins encoded by genes *Tery_0365-0368* (Chapter 3) and *Tery_3377* (Chapter 4) was examined through expression in *Synechocystis* under the effect of the *psbA2* (*slr1311*) promoter. Gene *psbA2* encodes the D1 protein of photosystem II (PSII) and three isogenes are present in *Synechocystis*, allowing replacement of *psbA2* without any important phenotypic consequences (Mohamed & Jansson 1989).

In the case of *Tery_3377*, the gene (1050 bp) was codon optimised for *Synechocystis* as initial attempts to express the native gene were unsuccessful. The synthetic gene (Integrated DNA Technologies Inc., IA, USA), supplied in plasmid pIDTSMART-AMP, was designed with *Nde*I and *Bgl*II restriction sites at the 5' and 3' ends respectively. The lyophilised plasmid DNA was resuspended in IDTE buffer (10 mM Tris and 0.1 mM EDTA, pH 7.5-8.0) to a concentration of 50 ng/µl. Subsequently, 400 ng plasmid was digested with *Nde*I and *Bgl*II and the gene sub-cloned into the same sites of the pFLAG vector (Hollingshead et al. 2012; Canniffe et al. 2013). The pFLAG vector recombines into the *Synechocystis* genome such that the gene of interest replaces the *psbA2* gene and is therefore expressed under the control of the *psbA2* promoter. The plasmid also confers kanamycin resistance (kan^R) allowing selection of transformed cells (Fig. 2.2).

For Chapter 4 PCR products comprising the *Trichodesmium* genes *ptxABCD* (*Tery_0365-0368)*, *ptxABC* (*Tery_0365-0367*) or *ptxD* (*Tery_0368*) were amplified from *Trichodesmium* gDNA with Q5 polymerase using primers ptxABCD_F and ptxABCD_R; ptxABCD_F and ptxABC_R; or ptxD_F and ptxABCD_R respectively. All fragments were digested with restriction enzymes *Bam*H1 and *Nde*I and were ligated into the *Bgl*II and *Nde*I sites of

pFLAG. All plasmids (Table 2I) were sequence verified (Eurofins MWG Operon, Ebersberg, Germany) and used to transform *Synechocystis*.

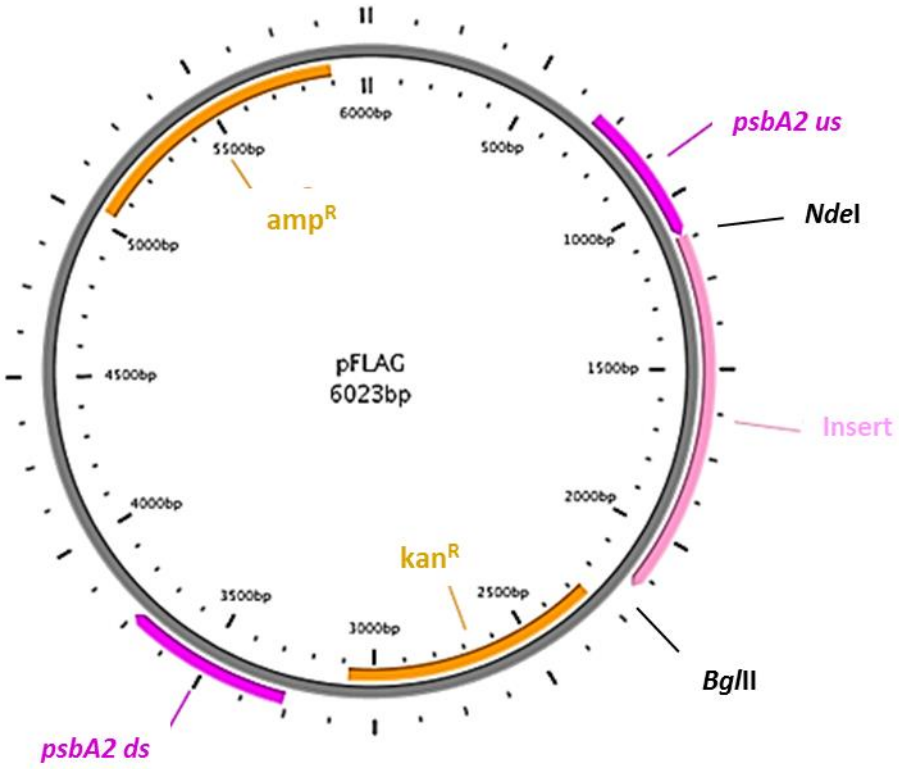

Figure 2.2: pFLAG vector map. Inserts (light pink) were incorporated between *Nde*I and *Bgl*II restriction sites adjacent, but transcribed in the opposite direction, to the kan^R resistance marker (orange). The *Synechocystis psbA2* us and ds DNA sequence (fuchsia) allows homologous recombination of the insert and kan^R at the *psbA2* locus, and sets the gene of interest under the control of the *psbA2* promoter. Plasmid selection in *E. coli* is conferred through ampicillin resistance (amp^R, orange) Plasmid annotation was performed in PlasMapper Version 2.0 (Dong et al. 2004).

Table 2I: Plasmid generated in this study

Plasmid	Gene (origin)	Antibiotic Marker	Chapter
pFLAG::*ptxABCD*	*Tery_0365-0368*	kan^R/amp^R	3
pFLAG::*ptxABC*	*Tery_0365-0367*	kan^R/amp^R	3
pFLAG::*ptxD*	*Tery_0368*	kan^R/amp^R	3
pFLAG::*3377*	*Tery_3377*	kan^R/amp^R	4
pET21a_*3377*	*Tery_3377*	amp^R	4

GFP fusions: The signal sequences of *Synechocystis* FutA1 and FutA2, *Trichodesmium* Tery_3377, and *E. coli* TorA (Chapter 4) were fused in-frame to super folded green fluorescent protein (sfGFP) by OLE-PCR while the *cat* cassette (cat^R) was included downstream of GFP to allow selection. The constructs were designed to homologously recombine into the *Synechocystis* genome exactly in place of the *psbA2* ORF (Fig. 2.3).

The DNA sequence corresponding to the predicted (in the case of *futA1*, *futA2*, *Tery_3377*) (Chapter 4, Table 4B) or known (*torA*; Thomas et al. 2001) signal sequence and first 4 amino acid residues of the mature protein (as identified by Signal P v4.1/v3.0 sensitivity and TatP v1.0 servers, Bendtsen et al. 2005; Petersen et al. 2011) was amplified from the respective organisms gDNA using the corresponding primer pair: futA1_ss_F and futA1_ss_R; futA2_ss-F and futA2_ss_R; 3377_ss_F and 3377_ss_R; or torA_ss_F and torA_ss_R. Approximately 400 bp immediately preceding the *psbA2* gene (amplified with primer pair psbA2_us_F and psbA2_us_R) was joined to each signal sequence in an OLE-PCR (Fig. 2.3) (with primers psbA2_us_F and the respective ss_R primer) such that the ATG start codon of the signal sequence replaced the ATG start codon of *psbA2*. The GFP coding sequence was isolated from plasmid pED151 (provided by A.Hitchcock) with primers GFPss_F and GFPss_R and ~400 bp of sequence immediately downstream of *psbA2* was amplified using the primer pair psbA2_ds_F/psbA2_ds_R. The cat^R marker was inserted between the GFP and downstream *psbA2* flank by OLE-PCR (Fig. 2.3) with the extreme primers GFP_F and psbA2_ds_R. Finally, each *psbA2* upstream-signal sequence fragment was joined to the GFP-cat-psbA2 downstream fragment using OLE-PCR (Fig. 2.3) with primers psbA2_us_F and psbA2_ds_R.

To create GFP fusions to the twin arginine mutated signal sequence of Tery_3377 (Tery_3377ss-KK-GFP) primer 3377_ss_F was switched for 3377-R5/6K-GFP and psbA2_us_R for psbA2-us-R2. These alternative primers were designed to align during OLE-PCR and both contained the first 18 bp of the Tery_3377 signal sequence with changed nucleotide sequence between positions 13-18 (AAA AAA in the place of AGA CGA) such that the translated sequence codes for two lysine residues in the place of the two arginine residues of the twin arginine transport (TAT) system. Following the construction of the GFP tagged signal sequence fragments and after complete segregation of each strain modified DNA segments were sent for sequencing (Eurofins MWG Operon, Ebersberg, Germany) to assure the correct sequence identity of each.

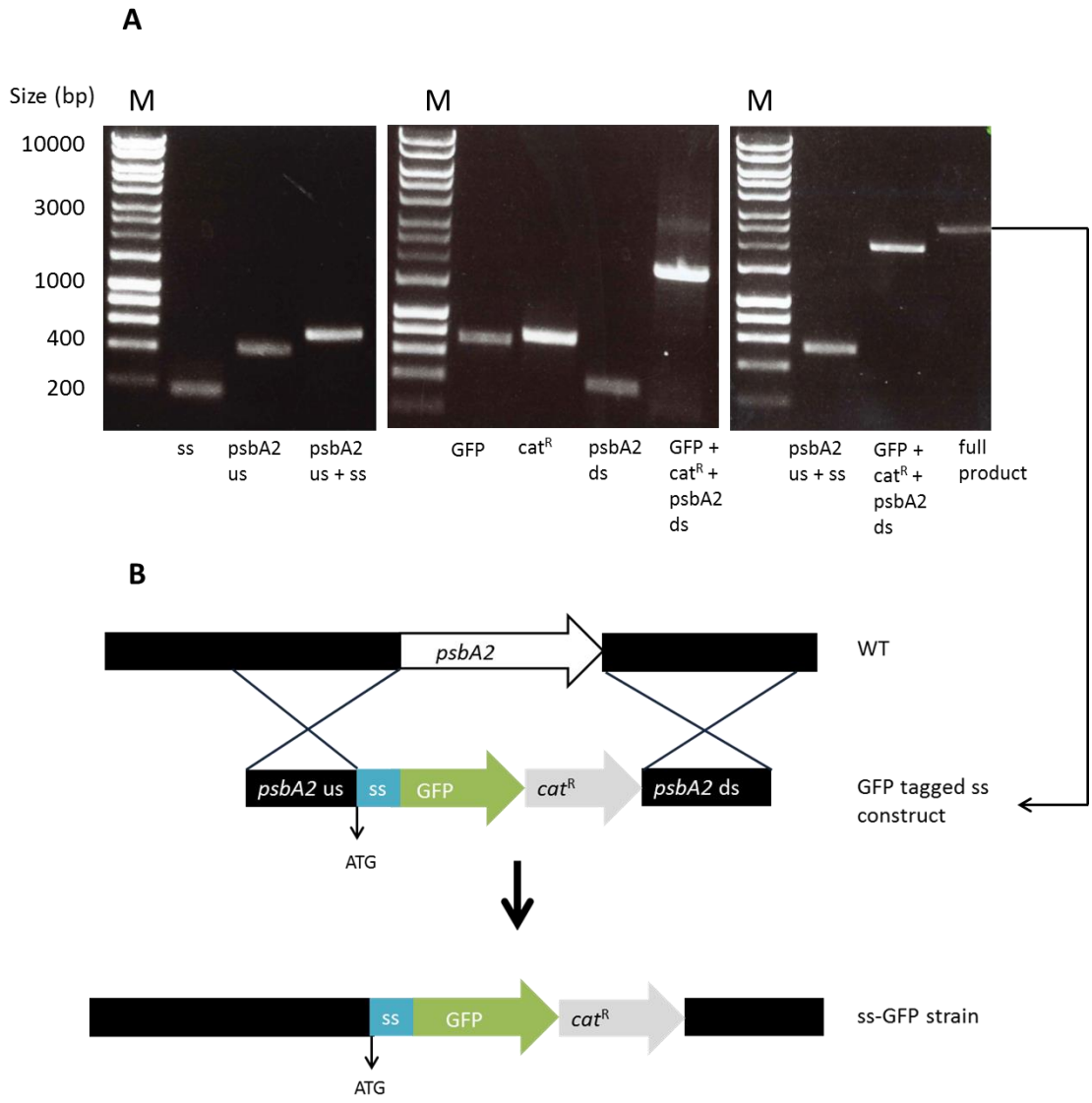

Figure 2.3: Generation of the GFP tagged signal sequence strains. (A) DNA fragments were amplified and sequentially joined through OLE-PCR to assemble the GFP tagged signal sequence (ss) constructs. **(B)** As these were bordered by the *psbA2* us and ds regions, transformations and selection on chloramphenicol (resistance conferred with *cat*^{R}) resulted in *psbA2* replacement placing the construct under the control of the *psbA2* promoter.

Protein over-expression in *E. coli:* To express C-terminally hexa histidine-tagged Tery_3377 in *E. coli*, the ORF (omitting the predicted N-terminal signal peptide and stop codon) was amplified from the *Trichodesmium* genome using primers 3377_OE_F and 3377_OE_R. The resulting PCR product was cloned into the *Nde*I/*Xho*I sites of pET21a(+) (Novagen, Madison, WI) generating the plasmid pET21a_*3377*.

2.4.2 Techniques

Overlap extension (OLE)-PCR was used to assemble fragments of amplified DNA into larger linear constructs which were used to transform *Synechocystis* in Chapter 4.

For OLE-PCRs Accuzyme Polymerase Mix (Bioline, London, UK) or Q5 High-Fidelity Polymerase Mix (New England Biolabs Ltd, Hitchin, UK) were used. Oligonucleotide primer pairs (Table A1) constructed as detailed earlier (Sec. 2.3.3) were diluted to 100 nM final, reaction concentration. They were used to amplify fragments from gDNA or plasmid DNA templates. Primers were designed to attach to ~15-25 bp of the 3' or 5' end of the fragment being amplified and generate ˜ 25bp overhangs with complementarity to the neighbouring fragments (overlapping regions).

Constructs were then assembled by connecting the fragments using flanking primers at: 98 °C for 30 secs (initial denaturation), 30 cycles of 98 °C for 10 secs (denaturation), 30 secs of annealing at 55- 60 °C, and 72 °C for the required extension time (30 secs for each 500 bp or 1000 bp for Accuzyme and Q5 polymerase respectively) and a final extension at 72 °C for 10 mins. The primers were added to the reaction after the first 5 of 30 PCR cycles.

All PCR generated fragments and constructs were visualised by gel electrophoresis (Sec. 2.3.4) to verify their correct size. Amplified fragments and constructs were purified using the QIAqucik PCR Purification Kit if a single product was identifiable or the QIAqucik Gel Extraction Kit (Qiagen, Manchester, UK) to separate the desired product from non-specific bands/plasmid template DNA.

Restriction enzyme digestions and dephosphorylation of 5'-ends: Digestions were performed with 1 µl NdeI, BglII, AfeI and MfeI restriction enzymes (Thermo Scientific, DE, USA), 0.6-1 µg vector or 0.1-0.15 µg insert according to the manufacturer's instructions. To remove the 5´ phosphoryl termini and prevent recircularization of cloning vectors they were treated with Antarctic Phosphatase (New England Biolabs Ltd, Hitchin, UK) for 30 mins at 37 °C. Restriction enzyme digested DNA and Antarctic Phosphatase reactions were QIAqucik purified (PCR Purification Kit, QIAGEN, Manchester, UK) prior to ligations.

Ligations and purifications: Digested vectors and fragments (1:3 -1:5 vector to insert ratio) were ligated by incubating with 1 µl T4 DNA Ligase (New England Biolabs Ltd, Hitchin, UK) for 2 hrs or overnight at room temperature according to the manufacture's protocol. Reactions were purified by precipitating the ligated DNA with n-butanol, removing the

supernatant (centrifugation 12 x 10^3 rpm for 10 mins) and drying the pellet (vacuum centrifuge, 2 mins at 45 °C).

Transformations:

E. coli: Plasmids were transformed into *E. coli* cloning strains through heat shock (DH5-α, BL21) or electroporation (XL1-blue).

Chemically competent DH5-α and BL21 cells (New England Biolabs Ltd, Hitchin, UK) were mixed with the ligated plasmids. The cell mixture was left on ice for 30 mins and then transferred to a 42 °C water bath for 30 secs after which it was cooled again on ice for 2 mins. Super Optimal Broth (SOC) (1 ml) was added to the cells which were incubated at 37 °C shaking at 250 rpm for 60 mins before plating 200 µl on LB-ampicillin (100 µg/ml) plates which were incubated overnight at the same temperature.

For electroporation XL1-blue competent cells were defrosted on ice, mixed with ligated plasmids and incubated on ice for 60 secs. After that, the cell/plasmid mix was transferred to a cold electroporation cuvette for electroporation. They were then immediately supplemented with 1 ml SOC and incubated at 37 °C shaking at 250 rpm for 60 mins. Cells were then centrifuged (8 x 10^3 rpm for 2 mins), resuspended in 200 µl and plated on LB-ampicillin plates to be incubated overnight at 37 °C.

Colonies were screened by colony PCR with appropriate primers and plasmids were prepped from successful clones using the QIAprep Spin Miniprep Kit (Qiagen, Manchester, UK) according to the manufacturer's instructions.

Synechocystis: Wild-type (WT) *Synechocystis* was transformed as described by Williams, (1988). Plasmid pFLAG or linear mutagenesis fragments (as described above) were incubated with 200 µl of cell culture at 30 °C for 1 hr and recovery was allowed for 24 hours on a BG-11 plate with no antibiotic. Genome copies were segregated by repeated streaking on BG-11 plates with increasing antibiotic concentration and transformants homozygous for the deletions were verified by PCR using template DNA derived from WT or transformed cells.

The correct DNA sequence in the resulting segregated strains was confirmed through automated DNA sequencing (Eurofins MWG Operon, Ebersberg, Germany).

2.5 Protein Immunoblotting and Crystallisation

2.5.1 Immunoblotting

Proteins were extracted from *Synechocystis* and *E. coli* through suspension of pelleted cells in 100 µl of 10 mM Tris-HCl pH 7.3 and heating for 5 mins at 100 °C followed by centrifugation at 13 x10^3 rpm for 5 mins at 4 °C. *Trichodesmium* protein extraction were achieved through 3, 1 min sonication cycles, the first two followed by freezing in liquid nitrogen and the third by centrifugation for 5 mins at 13 x10^3 rpm at 4 °C (Brown et al. 2008).

Protein concentrations were assessed using the Pierce™ BCA Protein Assay Kit (Thermo Scientific, DE, USA) with bovine serum albumin (BSA) standards according to the manufacturer's instructions.

Immunoblotting was performed as described by Brown et al. (2008). Samples were incubated at 80 °C for 5mins with 50 mM dithiothreitol (DTT) and run on 4–12% NuPAGE acrylamide gradient gels (Invitrogen, Paisley, UK) in MES running buffer (Invitrogen, Paisley, UK).

Primary antibodies anti-IdiA and anti-Slr0513 (generously provided by E. Pistorius) and anti-GFP (Sigma-Aldrich, St. Louis, USA) were diluted to 1:500, 1:1000 and 1:5000 respectively in 2% ECL Advance blocking reagent (GE Healthcare Little Chalfont, UK) Tris-buffered saline plus Tween (TSB-T). Dilutions of 1:10000 of horseradish peroxidase-conjugated anti-rabbit secondary antibody in 2% blocking agent TBS-T (Abcam, Cambridge, United Kingdom) were used with all primary antibodies. Primary and secondary antibody incubations were performed at room temperature for 1 hr.

For imaging a VersaDocTM CCD imager (Bio-Rad Laboratories Ltd, Hemel Hempstead, UK) was used after application of ECL Advance detection reagent (GE Healthcare, Little Chalfont, UK) as in Richier et al. (2012).

2.5.2 Purification and crystallisation

The *Trichodesmium* protein Tery_3377 (Chapter 4) was purified following over production in *E. coli* BL21(DE3) and used to set up crystal trials as a first step of resolving its three dimensional structure by X-ray crystallography.

Cells grown from a single colony on an agar plate were used to inoculate 100 ml LB-ampicillin (100 µg/ml) and were incubated at 37 °C shaking at 200 rpm overnight. The following day 10 ml was used to inoculate four 1 L batches of LB-ampicillin which were maintained at the same conditions until OD_{600} was equal to 0.6. All four flasks were then induced with Isopropyl β-D-1-thiogalactopyranoside (IPTG) at 1 mM final concentration and two were placed back at 37 °C for 3 hrs. The remaining two were left shaking at 18 °C overnight.

Cells were harvested by centrifugation at 5 x 10^3 rpm for 20 mins and the pellet was transferred to 50 ml PBS to be centrifuged again for 20 mins at 4 x 10^3 rpm. The supernatant was removed and cell pellets were either stored at -20 °C or processed directly for protein extraction. Cells were resuspended in Lysis buffer (Table 2J) and protein was extracted in an ice-water bath by sonication for a total duration of 5 mins (10/30 secs on/off cycles). The lysate was subsequently centrifuged at 45 x 10^3 rpm for 30 mins at 4 °C.

Purification of His-Tagged Tery_3377 was achieved using a Ni-column for immobilised metal affinity chromatography (IMAC) and a subsequent size exclusion chromatography (SEC) step. The Ni-column (4 ml Ni-NTA Superflow resin, Qiagen, Manchester, UK) was equilibrated with Binding Buffer (Table 2J) before applying the lysate which was previously filtered through a 2 µm filter. The lysate was run through the column 5-6 times after which the Wash buffer (Table 2J) was applied followed by the Elution buffer (Table 2J). Subsequently, the protein was concentrated to less than 1 ml with spin concentrators (Generon Ltd., Berkshire, UK) and applied to the HiLoad 16/60 Superdex 200 SEC column (GE Healthcare Life Sciences, Little Chalfont, UK) which was equilibrated with SEC Buffer (Table 2J). The fractions that contained Tery_3377 (as determined by SDS-PAGE and Coomassie-staining) were pooled together and the protein was spin concentrated to a volume of less than 100 µl and a concentration of 41.620 mg/ml.

For crystallisation trials the two 96 condition, 3D protein crystallization screens Morpheus and JBSC were set in sitting drop 96-well plates (INTELLI-PLATE) using a Gryphon liquid handling robot (ARI, CA, USA).

Table 2J: Buffers used for Tery_3377 protein extraction

Buffer	Recipe
Lysis	50 Mm Tris, pH 8.5 (1 pH below pI of Protein) 300 mM NaCl 5% Glycerol 2 mM β-Mercaptoethanol (fresh on day of use)
Binding	Same as Lysis 20 mM Imidazole
Wash	Same as Binding 50 mM Imidazole
Elution	Same as Binding 150-300 mM Imidazole
SEC	50 mM Tris, pH 8.5 150 mM NaCl

2.6 RNA sequencing

The transcriptomic response of *Trichodesmium* grown under different Fe regimes (Fe+, Fe-, [Dust] and Dust+) (as described in Chapter 5) was analysed by next generation sequencing at the National Oceanography Centre Sequencing Facility.

2.6.1 Library preparation and sequencing

Complementary (c)DNA libraries were prepared using the TruSeq Stranded mRNA Library Prep Kit (Illumina), which was modified for use with bacterial RNA samples by replacing the initial poly-A-based mRNA isolation step with probe-based depletion of ribosomal (rRNA). Subsequently, rRNA transcripts were selectively depleted from the RNA samples using a bacterial Ribo-Zero rRNA Removal Kit (Illumina INC., Ca, USA), according to the manufacturers' instructions. The precipitated RNA pellets were resuspended directly in 18 µl of Fragment-Prime-Finish mix from the TruSeq Stranded mRNA kit, and RNA fragmentation, cDNA synthesis and library construction were carried out as described in the kit protocol.

For sequencing the molarity of each library was determined from the measured concentration and average fragment size using equation 3.

Equation 3:

$$conc\ (nM) = \frac{conc\ (ng\mu l^{-1})}{average\ fragment\ size * 660\ gmol^{-1}} * 10^6$$

Libraries were then diluted to a concentration of 10 nM and pooled before denaturation to single strands. The combined sequencing library was sequenced on an Illumina MiSeq instrument using paired-end sequencing, a read length of 151 bp, and a 6 bp index read.

Image analysis, base calling and de-multiplexing of barcoded samples was carried out on-instrument (MiSeq Control Software). Raw sequencing reads were obtained in fastq format. Overall sequencing quality was assessed (FastQC version 0.11.3, Babraham Institute, http://www.bioinformatics.babraham.ac.uk/projects/fastqc/) before fastq files were processed (CutAdapt v1.8.1, http://code.google.com/p/cutadapt/) to remove TruSeq adapter sequences and low quality bases from the 3' end of reads.

The trimmed reads were mapped against the *Trichodesmium erythraeum* IMS101 reference genome assembly (Ensembl Bacteria database, accession GCA_000014265.1) using the TopHat spliced read aligner v2.0.14 (Kim et al. 2013). For each RNA sample, the number of reads mapping to each annotated gene (Ensembl Bacteria database, accession GCA_000014265.1) in IMS101 were counted (HTSeq-count script, HTSeq framework, version 0.6.0, (Anders et al. 2015)). Mapped reads were sorted by read name (Samtools version 1.2 (Li et al. 2009)), and reads mapping to each feature annotated as 'gene' were counted. Reads were processed using the -stranded=reverse option, to correctly account for strand-specific read mapping.

2.6.2 Statistical analysis

Differential gene expression analysis was carried out using the Bioconductor package DESeq2 version 1.8.2 (Love et al. 2014), running on R version 3.2.0. using an ANODEV approach implemented in the DESeq package (Anders & Huber 2010). Likelihood ratio testing was used to compare the fit of read count data against a negative binomial model in a one-factor experimental design where replicates were grouped by growth condition, against a reduced model where condition information was removed. Pairwise contrasts between conditions were calculated using a Wald test. Benjamini-Hotchberg correction for multiple testing was used and genes with a p value of < 0.05 were classed as significantly differentially expressed either for differentially expressed genes across the 4 treatments or between specific pairs of treatments (pairwise comparisons).

2.7 Bioinformatic analysis

2.7.1 Analysis of the Dust-$FeCl_3$ *Trichodesmium* transcriptome

In Chapter 5 expression of the identified differentially expressed genes from the Fe+, Fe-, [Dust] and Dust+ cultures (3 biological replicates for each) was clustered and a dendrogram was constructed (Minitab 17.3.1, Minitab Inc., Coventry, UK). Distances were calculated using correlation coefficients and amalgamated using average linkage.

Grouping and categorizing of the gene ontology (GO) classes (downloaded from CyanoBase http://genome.microbedb.jp/cyanobase/TERY) of the differentially expressed genes was performed using a generic GO Slim (GO_Slim) for which counts were accumulated (CateGOrizer, Hu et al. 2008). Enrichment of GO classes in groups of differentially expressed genes against all expressed genes identified in the transcriptome was completed using Singular Enrichment Analysis (AGRIGO, Du et al. 2010).

Further analysis of uncharacterised proteins utilised information on conserved protein domains (NCBI Conserved Domain Database, Marchler-Bauer et al. 2015), subcellular localisation or metal binding sites (UniProtKB Automatic Annotation pipeline Consortium 2015). Signal sequence prediction software Signal P v4.1 (v3.0 sensitivity) and TatP v1.0 servers (Bendtsen et al. 2005; Petersen et al. 2011) were also used.

To visualise the pattern of expression along gene clusters and unannotated or suspected miss-annotated regions, sample reads aligned against the *Trichodesmium* genome were inspected manually through visualisation in the Artemis genome browser, (Rutherford et al. 2000).

2.7.2 Investigation of omic datasets from other studies

Conservation of *Trichodesmium* phosphite utilisation genes (Chapter 4) *in situ* was examined by searching for homologues of *ptxABCD* (*Tery_0365-0368*) in three published genomic datasets, consisting of two draft genomes (*T. erythraeum* 21-75 and *T. theibautii* H9-4) and an environmental metagenome from the Atlantic Ocean (Walworth et al. 2015). Searches were performed using tBlastn (Altschul et al. 1990) with an e-value cut-off of 0.000001.

To investigate expression of genes *ptxABCD* (*Tery_0365-0368*) in transcriptomic datasets, four publically available transcriptomic datasets were searched. The datasets consisted of

two *in situ* meta-transcriptomes, one from the Amazon River Plume (Hilton et al., 2014) and one from the South Pacific Subtropical Gyre (Hewson et al. 2009), and two transcriptomes from cultured samples (Pfreundt et al., 2014; unpublished dataset: NCBI accession PRJNA237745). Illumina datasets were searched for reads aligning to *Tery_0365-0368* with > 90% sequence identity over 100% of the read length using MegaBlast (Morgulis et al. 2008), via the SRA Blast service from NCBI. 454 datasets were searched for reads encoding homologues of *Tery_0365-0368* using tBlastn with an e-value cut off of 0.000001 and a minimum percentage identity of 90%. Expression of genes *phnDCEEGHIJKLM* (*Tery_4993-5003*) in the cultured transcriptomes (Pfreundt et al., 2014; unpublished dataset, NCBI accession PRJNA237745) was assessed in a similar fashion.

2.8 Epifluorescent and confocal microscopy

GFP expressing *Synechocystis* strains were viewed using an axioscope Z plus epifluorescence microscope (Zeiss, Oberkochen, Germany) and photographed with an HRm axioCam (Zeiss, Oberkochen, Germany). Samples where excited with 400 – 490 nm light filtered with a FITC filter set.

Strains were also visualised under the Leica SP5 LSCM (Leica Microsystems, Wetzlar, Germany) confocal microscope. Cells were exposed to high light for 15 mins prior to visualisation to increase the expression of the GFP fusions from the *psbA2* promoter. As described in Aldridge et al. (2008) excitation was performed through a 488 nm laser line at which GFP emits between 510 to 530 nm while phycocyanin, used to represent pigment autofluorescence, emits between 600 and 700 nm.

2.8 Phylogenetic analysis

Maximum likelihood phylogenetic analysis of Tery_3377 homologues from *Synechocystis* and selected bacteria was performed to identify possible functional clusters (Chapter 4).

The *Trichodesmium* Tery_3377 and two *Synechocystis* proteins FutA1 and FutA2 with their closest homologues from *Lyngbya sp.* PCC 8106*, Cyanothece sp.* CCY0110 and *Phormidium willei* respectively (identified using BlastP, Altschul et al. 1990), as well as homologues from *Prochlorococcus marinus* MIT 9301, *Synechococcus elongatus* PCC 6301 and PCC 7942,

Anabaena sp. PCC 7120, *Haemophilus influenza and Neisseria meningitides* were included in the analysis (Table 2K).

Table 2K: Tery_3377 homologues included in the phylogenetic analysis

Organisms	**Protein identifier**	**Size (AA)**
Trichodesmium erythraeum IMS101	Tery_3377	349
Synechocystis PCC 6803	Slr1295 (FutA1)	360
	Slr0513 (FutA2)	346
Lyngbya sp. PCC 8106	WP_009786151.1	350
Cyanothece sp. CCY0110	WP_035799093.1	365
Phormidium willei BDU 130791	OAB59261	346
Prochlorococcus marinus	P9301_13611 (AfuA)	340
Synechococcus elongatus PCC 6301	Syc0146_c	340
	Syc1920_d	366
Synechococcus elongatus PCC 7942	Synpcc7942_1409	340
	Synpcc7942_2175	366
Anabaena sp. PCC 7120	Alr1382	336
Haemophilus influenza	FbpA	332
Neisseria meningitides	FbpA	331

The online platform Phylogeny.fr (Dereeper et al. 2008; Dereeper et al. 2010) was utilised to create an analysis pipeline whereby sequences were firstly aligned (T-coffee, v11.00.8cbe486, Notredame et al. 2000) and curated (G-blocks v0.91b, Castresana 2000). Subsequently, a maximum likelihood phylogenetic tree was reconstructed (PhyML v3.1/3.0, Guindon & Gascuel 2003) and approximate likelihood ratio test was carried out to compute branch supports (aLRT, Anisimova & Gascuel 2006). Finally, a graphical representation was produced (TreeDyn v198.3, Chevenet et al. 2006).

Chapter 3

Phosphite utilization by the globally important marine diazotroph *Trichodesmium*

Parts of this Chapter have been published in:
Polyviou, D., Hitchcock, A., Baylay, A. J., Moore, C. M. and Bibby, T. S. (2015), Phosphite utilization by the globally important marine diazotroph *Trichodesmium*. Environmental Microbiology Reports, 7: 824–830. doi:10.1111/1758-2229.12308

3.1 Introduction

Trichodesmium's growth and nitrogen (N_2) fixing activity appear to be limited by the availability of phosphorus (P) in various oceanic locations (Sañudo-Wilhelmy et al. 2001; Mills et al. 2004; Moutin et al. 2005). A better understanding of the available P sources is necessary to predict restrictions on the organism's biogeography, both presently and in the future oceans. At the same time, it is crucial to recognise the interdependence between life and the environment that surrounds it as the major marine primary producers themselves (including *Trichodesmium*) considerably affect the oceanic P cycle.

There is emerging evidence that in addition to phosphate (PO_4^{3-}), both inorganic and organically complexed, P is present in the marine environment in reduced forms including organophosphonates (Pn) and phosphite (PO_3^{3-}) (Table 3A). The concentrations of these reduced forms in the ocean are currently largely unknown (Karl 2014). Studies using ^{31}P-NMR reported Pn can comprise 25% of the dissolved organic P (DOP) pool (Clark et al. 1998; Kolowith et al. 2001). Further, a recent analysis, using high-performance liquid chromatography coupled to inductively coupled plasma mass spectrometry detection (HPLC-ICP-MS), of freshwater samples has indicated 25% of dissolved P to be in the +3 or +1 oxidation state as PO_3^{3-} and hypophosphite (PO_2^{3-}) (Pasek et al. 2014). Also, ion exchange chromatography has been previously used to identify PO_3^{3-} and PO_2^{3} in geothermal hot springs (Pech et al. 2009; 2011) and lake interstitial water (Han et al. 2013). However, no data is available regarding the concentrations of these sources of P in the ocean.

Table 3A: The different forms and oxidation states of phosphorus in the ocean. Inorganic phosphorus can be found as phosphate, phosphite and hypophosphite while organic phosphorus is encountered as organophosph(on)ates.

Complexation	**Oxidation state**	**P form**	**Enzyme for oxidation/ hydrolysis**	**In *Trichodesmium***
Inorganic				
	+5	Phosphate (PO_4^{3-})	N/A	(Orchard et al. 2003)
	+3	Phosphite (PO_3^{3-})	PtxD: NAD:phosphite oxidoreductase	Not studied
	+1	Hypophosphite (PO_2^{3-})	HtxA: hypophosphite dioxygenase	Unknown
Organic				
	+5	Ester-linked organophosphates (C-O-P bond)	APase	PO_4^{3-}regulation (Orchard et al. 2009)
	+3	Organophosphonates (Pn) (C-P bond)	C-P lyase	PO_4^{3-}regulation (Dyhrman et al. 2006)

Trichodesmium has the ability to process Pn (Dyhrman et al. 2006), and appears to have a significant role in its production (Dyhrman et al. 2009) as Pn can make up 10% of cellular particulate organic P (POP). In addition, potential uptake of PO_3^{3-} by *Trichodesmium* colonies *in situ* was recently suggested (Van Mooy et al. 2015). If PO_3^{3-} is indeed available to

Trichodesmium, and the observations are not the mere effect of uptake by other members of the *Trichodesmium* colony consortia or cell surface adsorption, a previously unrecognised pool of P could be available to fuel the organism's growth. The ability to process PO_3^{3-} could also equate to more 'bridges' interconnecting P species in a complex intracellular P redox network. Consequently, potential synthesis of PO_3^{3-} as an intermediate or end product in this network should come as no surprise (Van Mooy et al. 2015).

Although both C-P lyase (Metcalf & Wanner 1991), and APase (Yang & Metcalf 2004) (enzymes involved in Pn and organophosphate catabolism respectively) may have a secondary activity in driving the oxidation of PO_3^{3-} to PO_4^{3-} (Metcalf & Wanner 1991; Yang & Metcalf 2004), in 1998, Metcalf & Wolfe found evidence of a specific PO_3^{3-} oxidising enzyme which was later characterized as phosphite dehydrogenase (PtxD) (Costas et al. 2001). This enzyme couples PO_4^{3-} production to NADH formation. The release of NADH potentially makes PO_3^{3-} oxidation more energetically favourable and could determine PtxD as an enzyme of double functionality converting PO_3^{3-} to PO_4^{3-} and producing energy in the process. For example, for the sulphate reducing *Desulfotignum phosphitoxidans*, PO_3^{3-} oxidation provides electrons to drive the organism's energy metabolism (Schink & Friedrich 2000; Schink et al. 2002). Due to its ability to reduce NAD, PtxD has been targeted as an enzyme of interest in the regeneration of NADH (reductant) in industrial applications (Hirota et al. 2012).

Phosphite dehydrogenase (*ptxD*) was first identified to be part of a 5 gene PO_3^{3-} utilisation operon (*ptxABCDE*) in *Pseduomonas stutzeri* WM88, with *ptxABC* encoding the members of an ATP-binding cassette (ABC) transporter (an ATPase, periplasmic binding protein and permease respectively), followed by *ptxE,* which encodes a putative transcriptional regulator (Metcalf & Wolfe 1998). More recently, homologs of all the genes apart from *ptxE* were identified and characterised in the marine species *Prochlorococcus* MIT9301 (Martínez et al. 2012). The authors also indicated the presence of *ptx* gene homologs in other marine bacteria including diazotrophic *Cyanothece*, *Nodularia* and *Trichodesmium*.

This Chapter attempts to identify whether *Trichodesmium erythraeum* IMS101 in culture can be sustained with PO_3^{3-} as the only source of P. Further, the role of the putative *ptxABCD* genes and the conditions controlling their expression are described. Due to the inability to directly study the function of PtxABCD in *Trichodesmium* through deletion mutants (as molecular genetic manipulation techniques are lacking in this organism) we use heterologous expression in the model freshwater cyanobacterial species *Synechocystis* PCC

6803 to demonstrate their function in PO_3^{3-} utilisation. The environmental relevance of this work is discussed and the prevalence of the four genes/proteins in published environmental omic studies is reported.

3.2 Results and discussion

3.2.1 Phosphite as a source of P for *Trichodesmium*

To determine if PO_3^{3-} can support the growth of *Trichodesmium*, cultures of *T. erythraeum* IMS101 (*Trichodesmium*) in YBC-II media with no P additions were supplemented with 50 µM PO_3^{3-} ($Na_2HPO_3.5H_2O$) and their growth was compared to those provided with equivalent concentrations of PO_4^{3-} (50 µM $NaH_2PO_4.H_2O$) and P-deficient cultures (no P added) for 13 days (Fig. 3.1).

Maximum growth rates measured in the presence of PO_4^{3-} under our laboratory conditions (0.2 day^{-1}), were 29% higher but not significantly different to the PO_3^{3-} treatment (0.14 day^{-1}). P-starved cultures (P-) grew slower (Student's t-test, $P < 0.05$) than both of the other treatments (Fig. 3.1B) with biomass declining after day 7 of the experiment and establishing a significantly lower number of cells (Student's t-test, $P < 0.01$) from day 10 onwards (Fig. 3.1A). This indicates that the P-omitting control-treatment did reach P starvation after a few days, with survival and minimal growth during the first week possibly maintained through P carryover during inoculation of the experiment. Although the final cell concentration is lower in the PO_3^{3-} compared to the PO_4^{3-} treatment (Student's t-test, $P < 0.05$) (Fig.3.1A), a result comparable to that reported for *Prochlorococcus* MIT9301 (Martínez et al. 2012), these data clearly demonstrate that *Trichodesmium* has the capability to utilize PO_3^{3-} as its sole source of P.

The reduced growth on PO_3^{3-} compared to PO_4^{3-} possibly indicates an insufficient P supply from the former due to a lower efficiency of its uptake pathway. Another hypothesis could be that a higher PO_3^{3-} to PO_4^{3-} ratio, which can be caused by preferential PO_4^{3-} consumption/depletion, is a stimulus that downregulates cellular growth rates as part of the cells' response strategies to low P. *In situ*, maintaining a flexible growth rate is part of a trophic strategy that can confer longer lasting growth on the limited nutrient reserves of starved oceans maintaining survival until encounter with new nutrient inputs (Lauro et al. 2009; Yooseph et al. 2010; Kirchman 2015). Therefore, this strategy is potentially advantageous in fluctuating conditions such as those encountered during atmospheric

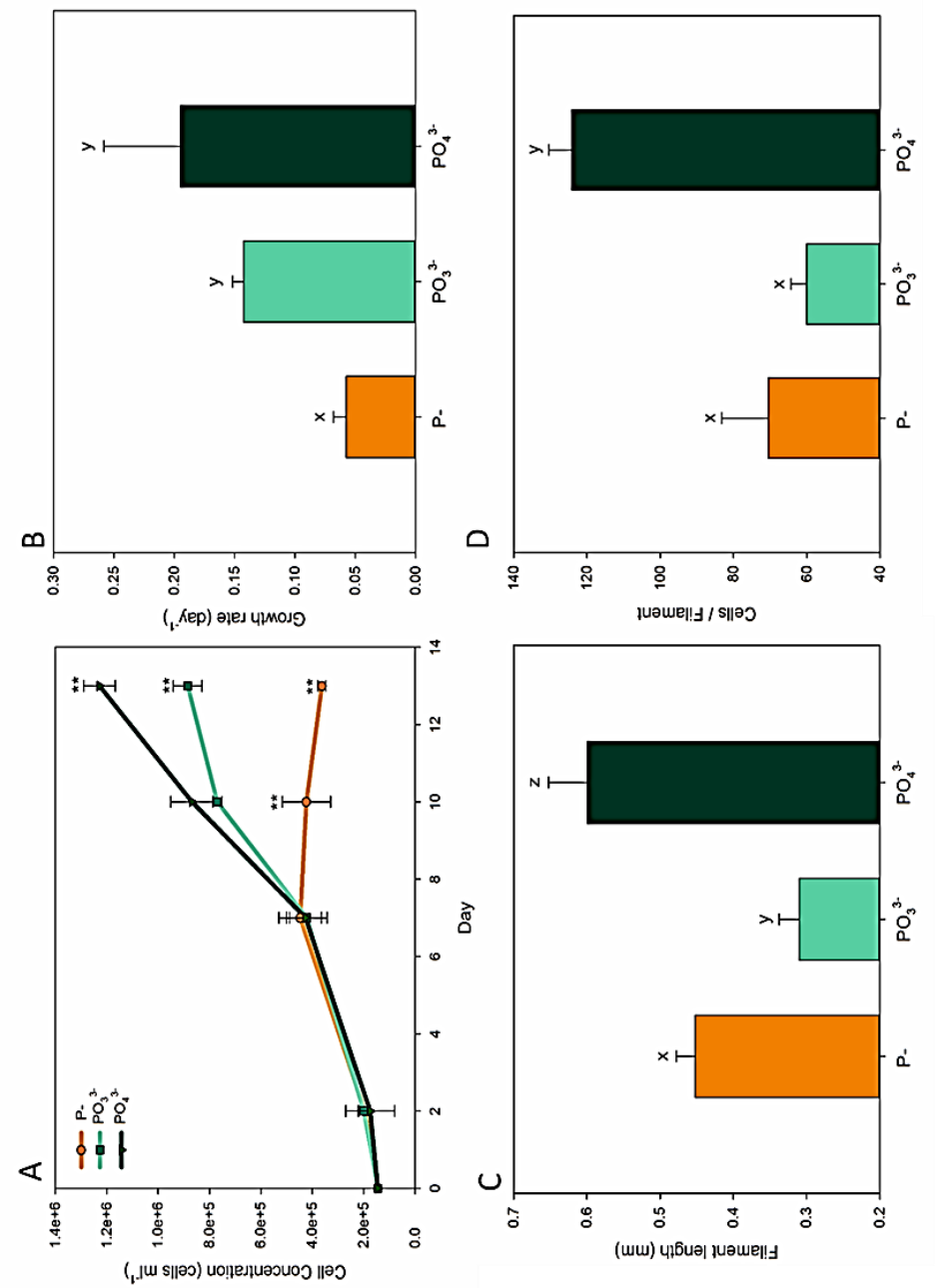

Figure 3.1: Growth and physiology of *Trichodesmium* in different P regimes. Cultures were added phosphate (PO_4^{3-}, dark blue triangles), phosphite (PO_3^{3-}, cyan squares) or no P (P-, orange circles) and cell concentrations were measured over 13 days. Asterisks (**) indicate significant difference in cell numbers (Student's t-test, $P < 0.01$) to other treatments on the same day **(A).** Growth rates were calculated for the three treatments during exponential growth **(B)** and filament length **(C)** along with the number of cells per filament **(D)** were computed for the last day of the experiment. Letter groups (x, y and z) are significantly different to one another (Student's t-test, $P < 0.05$). Error bars represent the standard deviation from the mean of three biological replicates.

deposition or upwelling events occurring in the oligotrophic oceans where *Trichodesmium* is abundant. This strategy, referred to as a 'feast or famine' lifestyle, was previously linked to marine microorganisms with larger genome sizes (Lauro et al. 2009; Yooseph et al. 2010; Kirchman 2015) as seen in *Trichodesmium*.

In the absence of PO_4^{3-} a difference in the morphology of the filaments is also observed (Fig. 3.1C/D). On the last day of the experiment, filaments growing with PO_3^{3-} were approximately half the length and comprised two times less cells (Student's t-test, $P < 0.01$) compared to those with PO_4^{3-}. Although filaments seemed to also be shorter in PO_3^{3-} compared to without P (Student's t-test, $P < 0.01$) the number of cells per filament in the two treatments is comparable due to a small difference in average cell length (not statistically significant-data not shown). The difference in filament morphology across the experimental treatments could therefore be explained by two independent factors acting in the opposite direction: (a) sensing of decreased PO_4^{3-} in the immediate environment of the cells (in PO_3^{3-} and P-) potentially stimulates a response to decrease the number of cells per filament and therefore increase the surface area to volume ratio and the uptake of P, while (b) P-stress (in P-) reduces cell division rate resulting in longer cells and longer overall filaments.

3.2.2 Description of the *Trichodesmium* putative *ptx* genes

Homologues to the *Prochlorococcus* MIT9301 PO_3^{3-} utilisation *ptxABCD* genes with similarities (64-70%) are present in the *Trichodesmium* genome (*Tery_0365-0368*). These are annotated as a Pn transporter (*Tery_0365-0367*) and an NAD binding dehydrogenase (*Tery_0368*) (Table 3B). An intragenic space of 449 bp separates *Tery_0365* from the remaining three genes (Fig. 3.2). No homologue to the transcriptional regulator *ptxE* found in *Pseduomonas stutzeri* WM88 is identified. The *Tery_0365-0368* genes will be referred to as *ptxABCD* hereafter and reasons for the reannotation are provided through this Chapter.

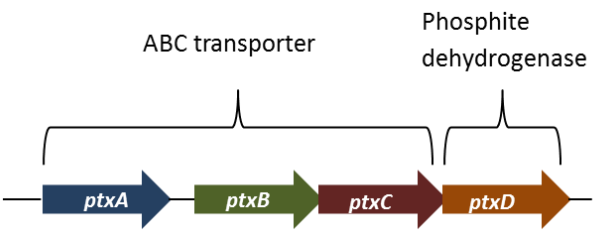

Figure 3.2: The arrangement of the *ptxABCD* genes in *Trichodesmium*. The *ptxA* (759 bp) *ptxB* (897 bp) and *ptxC* (819 bp) genes encode members of an ATP binding cassette (ABC) transporter and are located directly upstream of the NAD-dependant dehydrogenase (*ptxD*; 996 bp).

Table 3B: Details of the *ptx* homologous genes in *Trichodesmium*

Putative gene	Tery number	Annotation	Putative function	Nucleotide identity to *Prochlorococcus* str. MIT 9301
ptxA	*0365*	phosphonate ABC transporter, ATPase subunit	ATPase of ABC transporter	70%
ptxB	*0366*	phosphonate ABC transporter, periplasmic phosphonate-binding protein	Periplasmic binding protein of ABC transporter	67%
ptxC	*0367*	phosphonate ABC transporter, inner membrane subunit	Permease of ABC transporter	69%
ptxD	*0368*	D-isomer specific 2-hydroxyacid dehydrogenase, NAD-binding	Phosphite dehydrogenase	64%

3.2.3 Regulation of *ptx* gene expression in *Trichodesmium*

RNA extracted on the final day of the growth experiment (Fig. 3.1) was used for gene expression analysis by quantitative polymerase chain reaction (qPCR) to investigate whether *ptxB* (representative of the ABC-transporter) and *ptxD* were regulated in response to the nature of P source. Transcript levels were corrected using reference genes *rnpB* (Chappell & Webb 2010) and *rotA* (Orchard et al. 2009). A significant increase (one-way ANOVA, $P < 0.05$) in expression of both genes (1.5–2.0 relative fold change) was identified when growing with PO_3^{3-} or no P compared to PO_4^{3-} (Fig. 3.3). Although relatively small, the observed upregulation of genes possibly involved in PO_3^{3-} uptake and oxidation suggests PO_3^{3-} utilization to be a dynamic process responding to environmental PO_4^{3-}-limitation and/or the presence of PO_3^{3-}.

The fact that the genes are expressed under P-replete conditions at a basal level is also confirmed through identification in published (Pfreundt et al. 2014) and unpublished (NCBI accession: PRJNA237745, dataset described in Chapter 5) transcriptomes of *Trichodesmium* in culture (Table 3C). To compare, the same transcriptomic studies were also scanned for genes *phnDCEEGHIJKLM* (*Tery_4993-5003*) involved in Pn metabolism. These were previously reported to only be expressed under P-limitation in the environment (Dyhrman et al. 2006) but their expression is identified in transcriptomic studies of P-replete

Trichodesmium in culture. Therefore, although upregulation of both PO_3^{3-} and Pn metabolism genes occurs under PO_4^{3-}-limitation, a basal level of expression seems to be constantly maintained. This is consistent with the hypothesis that dynamic cycling of P between valance states occurs inside *Trichodesmium* itself, and possibly within/between members of the consortia in situ (Van Mooy et al. 2015).

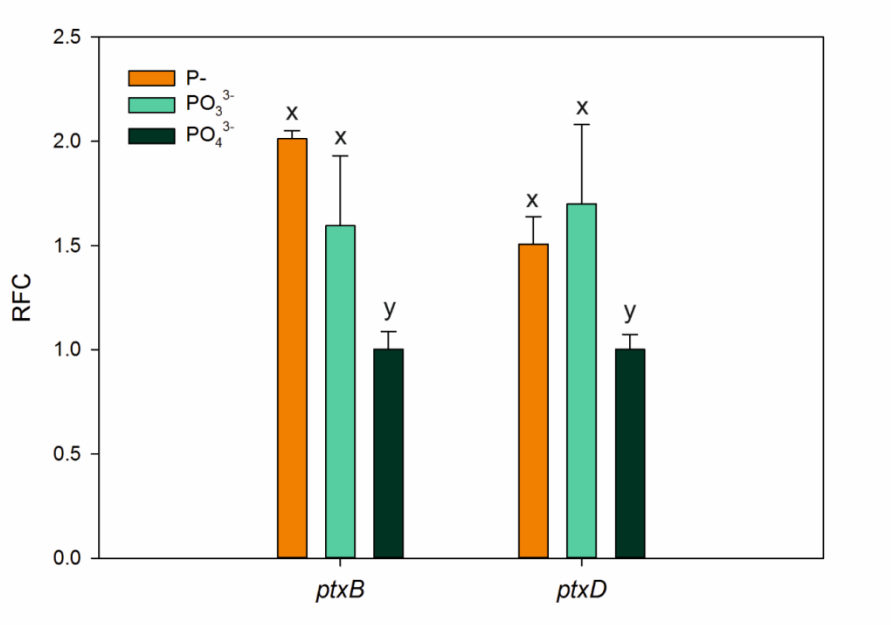

Figure 3.3: Gene expression analysis in response to P source. Expression of the periplasmic substrate-binding transporter component (*ptxB*) and phosphite dehydrogenase (*ptxD*) was quantified using qPCR and normalized against the reference genes *rnpB* and *rotA*. Expression in cultures with phosphite (PO_3^{3-}, cyan) or no P (orange) was compared to phosphate (PO_4^{3-}, dark blue) and is presented as the relative fold change (RFC). Significant differences (one-way ANOVA, $P < 0.05$) are indicated (distinct letter groups: x and y). Error bars represent standard deviation of the mean from three biological replicates

Table 3C: The expression of phosphite (*ptx*) and phosphonate (*phn*)-metabolism genes in *Trichodesmium* transcriptomes.

Experiment	***ptx* gene prevalence**	***phn* gene prevalence**	**Reference**
Primary transcriptome	*ptxABCD*	*phnDCEEGHIJKLM*	(Pfreundt et al. 2014)
Gene expression profiles from high CO_2-adapted *Trichodesmium*	*ptxABCD*	*phnDCEEGHIJKLM*	unpublished dataset NCBI accession: PRJNA237745
Transcriptomic response of *Trichodesmium* to different Fe regimes	*ptxABCD*	*phnDCEEGHIJKLM*	Chapter 5

In other bacteria the regulation of *phn* (Wackett et al. 1987) and *ptx* (White & Metcalf 2004) gene expression was demonstrated to be under the control of the Pho regulon (Santos-Beneit 2015). This is coordinated by a two-component mechanism involving the SphRS (referred to as PhoBR in *E.coli*) transduction system which orchestrates the organisms' response to low PO_4^{3-} conditions (Tommassen et al. 1982; Juntarajumnong et al. 2007). This system comprises a histidine kinase sensor on the cell membrane (SphS) and a transcriptional response regulator (SphR).

Trichodesmium is lacking the SphS component but it is suggested that SphR regulates the expression of P response operons. A putative binding site (PHO box) was identified upstream of P utilisation genes *pstS*, *sphX*, *phoX* and *phnD* (Su et al. 2007) while *phoA* is 449 bp downstream of a sequence resembling that (Orchard et al. 2009) (Table 3D). This sequence is lacking the 3 base linker sequence between conserved domains and the authors concluded that this is explained by possible heterogeneity in the *Trichodesmium* PHO box. To add to the observations by Orchard et al., (2009), a relevant short sequence directly upstream of *ptxA* is also missing the 3 bp linker. Whether this justifies SphR regulation of *ptxABCD* remains to be examined.

It is interesting to consider whether the separation of *phnD* and *ptxA*, by 862 and 449 bp respectively, from the rest of the genes in their respective 'operons' infers their distinct regulation to the rest of the cluster and/or whether more than one regulator is involved in their expression. In support of this, expression of *ptxBCD* and *phnD* seems to be independent to that of the remaining components in the unpublished transcriptome presented in Chapter 5 (Fig. 3.4). Also, anti-sense RNA appears to be expressed at the *ptxA* locus adding another potential level of control to the expression of this gene (Fig. 3.4).

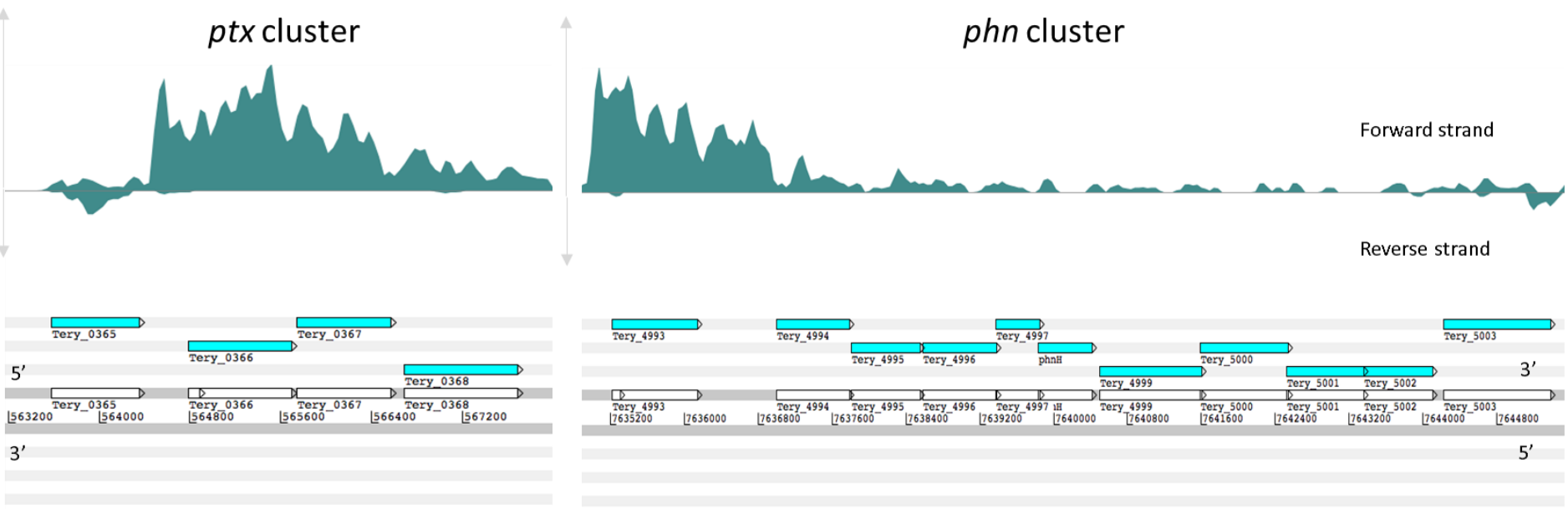

Figure 3.4: Expression of genes along the *ptx* and *phn* clusters. Genes identified from transcriptomic analysis (see Chapter 5) and visualised on ARTEMIS genome browser (Rutherford et al. 2000) are aligned along the forward DNA strand (5' to 3'). Transcription is not uniform along the clusters with expression for the first gene of each being unique to the remaining genes. For the *ptx* cluster, detection of *ptxA* (*Tery_0365*) transcripts is minimal while *ptxBCD* (*Tery_0366-0368*) expression is more distinct. The opposite is true for the *phn* cluster which is overall expressed at low levels compared to *phnD* (*Tery_4993*), the first gene of the cluster. Anti-sense RNA appears to be transcribed at the *ptxA* locus.

Table 3D: Putative Pho box promoter binding sequences associated with P-metabolism involved genes.

Tery no	Gene	Putative function	Predicted PHO box/PHO box resembling sequence	Position	Reference
3534	*sphX*	Phosphate binding	TTTGATATtttTTTAACCTgtt CTTAATCT	-164	Su et al. 2007
3537	pstS		TTTGATATtttTTTAACCTgtt CTTAATCT	-2862	Su et al. 2007
3467	*phoA*	Alkaline phosphatase	TTTAACT TTTAACT TTTAACT	-449	Orchard et al. 2009
3845	*phoX1*		TTTAACCAaagCTTAAACGa aaTTTAAACC	-173	Su et al. 2007
4993	*phnD*	Phosphonate binding	GAAAACAAgttTTTAACCTc ttCTTAAACT	-435	Su et al. 2007
0365	*ptxA*	ATPase of phosphite transporter	TTAACCA TTTAACC	-25	This study

3.2.5 Heterologous expression of *Trichodesmium ptxABCD* in *Synechocystis*.

As a stimulation of expression by PO_4^{3-} stress is not sufficient to support involvement of the *ptx* genes in PO_3^{3-} utilisation, a more direct approach was employed for their characterisation. Genetic manipulation techniques are not currently available for *Trichodesmium*, therefore to describe their function the *ptxABCD* genes were cloned into the pFLAG vector, which integrates inserted DNA in the *Synechocystis* genome so that expression is driven from the *psbA2* promoter. Homozygous strains in which all four genes (*ptxABCD*+), only the ABC-transporter genes (*ptxABC*+), or only the phosphite dehydrogenase gene (*ptxD*+) replaced *psbA2* were obtained (Fig 3.5A). The sequence of integrated DNA was verified (Eurofins MWG Operon, Ebersberg, Germany) following amplification from the transformant genome and the expected pattern of gene expression for each strain was observed by end-point reverse transcription (RT)-PCR (Fig. 3.5B).

There are no homologues of the *ptx* genes in *Synechocystis* PCC 6803 (Kaneko et al. 1996), and in contrast to *Trichodesmium*, PO_3^{3-} supplied as the sole source of P did not enhance the growth of the wild-type (WT) organism above that of a no-added P control (Fig. 3.6).

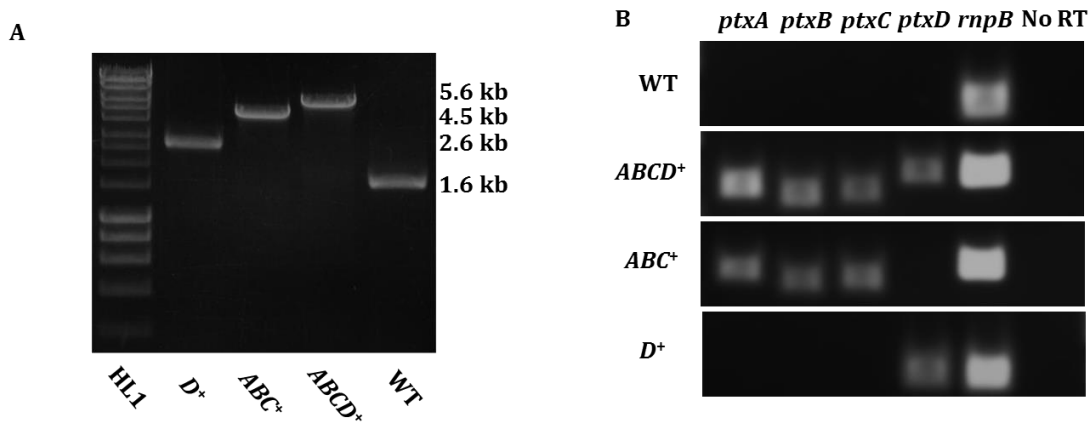

Figure 3.5: Confirmation of strain generation. **(A)** Amplification from *Synechocystis* WT and *ptxABCD+, ptxABC+, ptxD+* stains, using primers upstream and downstream of the insertion to confirm full segregation at the *psbA2* locus. In each case the correct-sized product was obtained, and no WT band was present in the modified strains. HL1 = Hyperladder™ 1 kb (Bioline Reagents Limited, London, UK). **(B)** Expression of the *ptx* genes at the RNA level was confirmed by end-point RT-PCR. For each strain, the *ptx* genes were expressed or absent as expected. The *rnpB* gene was used as a reference gene and a no reverse transcriptase (RT) control confirmed RNA was not contaminated with gDNA.

Growth of the *Synechocystis* recombinant strains and the isogenic WT on PO_3^{3-} (175 µM $Na_2HPO_3.5H_2O$) or no P was compared to that on the standard PO_4^{3-} (175 µM $NaH_2PO_4.H_2O$) containing BG11 media under phototrophic conditions (no glucose). Highest growth rates were observed on PO_4^{3-} (and were used to correct for the relative growth rate of each strain in the other treatments) (Fig. 3.6A). All strains grew poorly when P was omitted, with residual growth under this condition likely due to PO_4^{3-} carryover from the starter culture. Conversely, when PO_3^{3-} was provided as the sole added P source, growth of the *ptxABCD*+ strain expressing both the ABC-transporter and the dehydrogenase grew to a comparable extent as when supplied with PO_4^{3-} (Fig. 3.6B). However, growth of *ptxABC*+ and *ptxD*+ on PO_3^{3-} remained low (Fig. 3.6B), indicating that expression of the ABC-transporter or dehydrogenase alone is not sufficient and both components are required to utilize this form of P.

To our knowledge, this is the first simultaneous demonstration of the functionality of both the transporter and dehydrogenase modules of a PO_3^{3-} utilization system from a photosynthetic organism, and clearly demonstrates the function of PtxABCD in *Trichodesmium*.

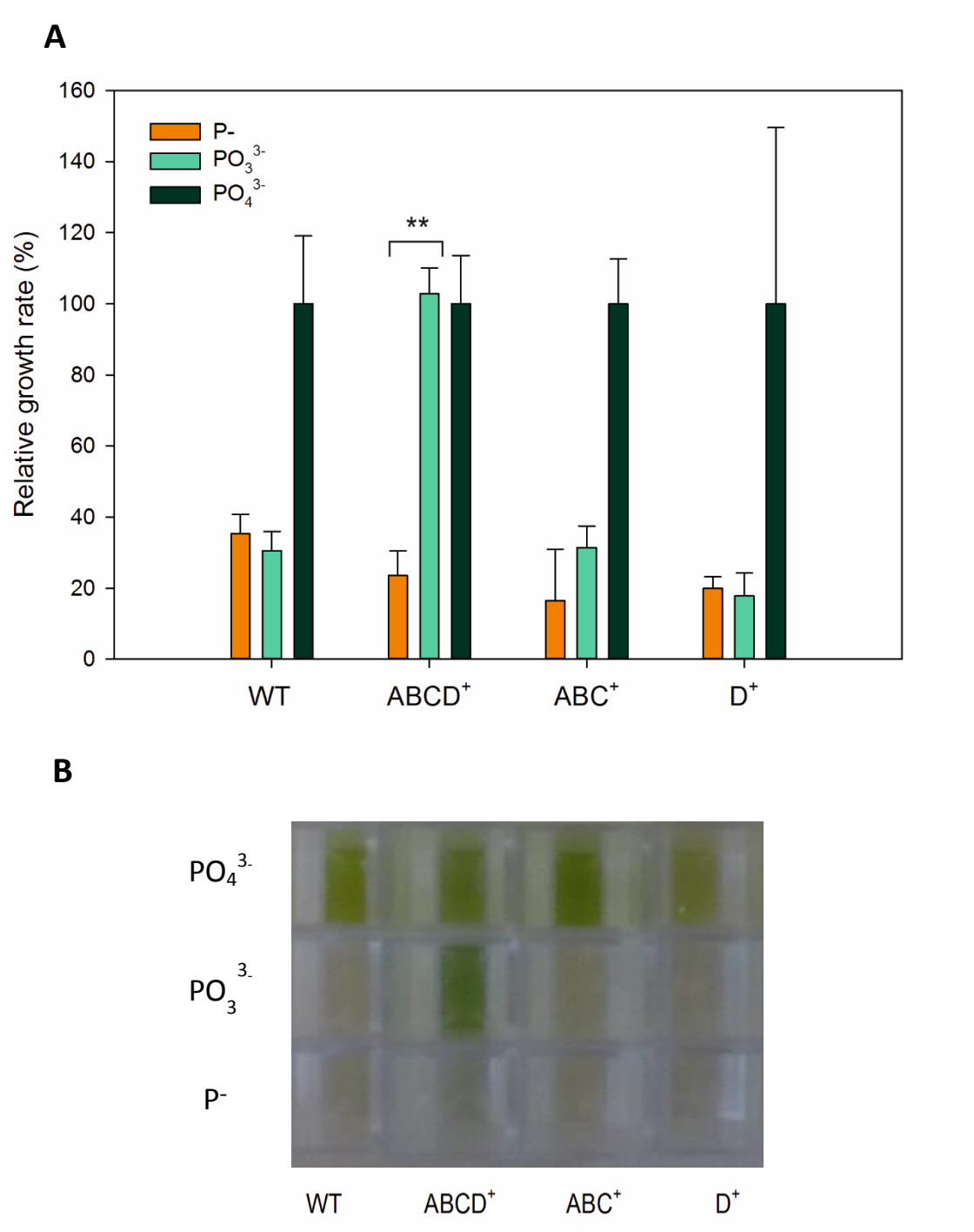

Figure 3.6: Growth of *Synechocystis* with phosphite requires all four *ptx* genes. (A) Photoautotrophic growth of strains *ptxABCD*+, *ptxABC*+ and *ptxD*+ and the isogenic parent (WT) on phosphate (PO_4^{3-}) was compared for each strain to growth on phosphite (PO_3^{3-}) and P-deplete BG11 media (relative growth rate). Error bars represent the standard deviation from the mean of three biological replicates. Asterisks (**) indicate significant differences (Student's *t*-test; $P < 0.01$) within strains. **(B)** Optical assessment of strains on the final day of the experiment after dilution 1:2.

Growth of the four strains in standard BG11 media with PO_4^{3-} was uneven, with the *ptxABCD*+ and *ptxABC*+ growing at a faster rate than the WT and *ptxD*+ ($P < 0.05$) (Fig. 3.7). These results indicate that P uptake by *Synechocystis* cells is not functioning at maximal efficiency and is therefore a limiting step during exponential growth. Therefore, the presence of a functional transporter expressed at high levels (expression controlled by *psbA2* promoter) allows faster growth rates.

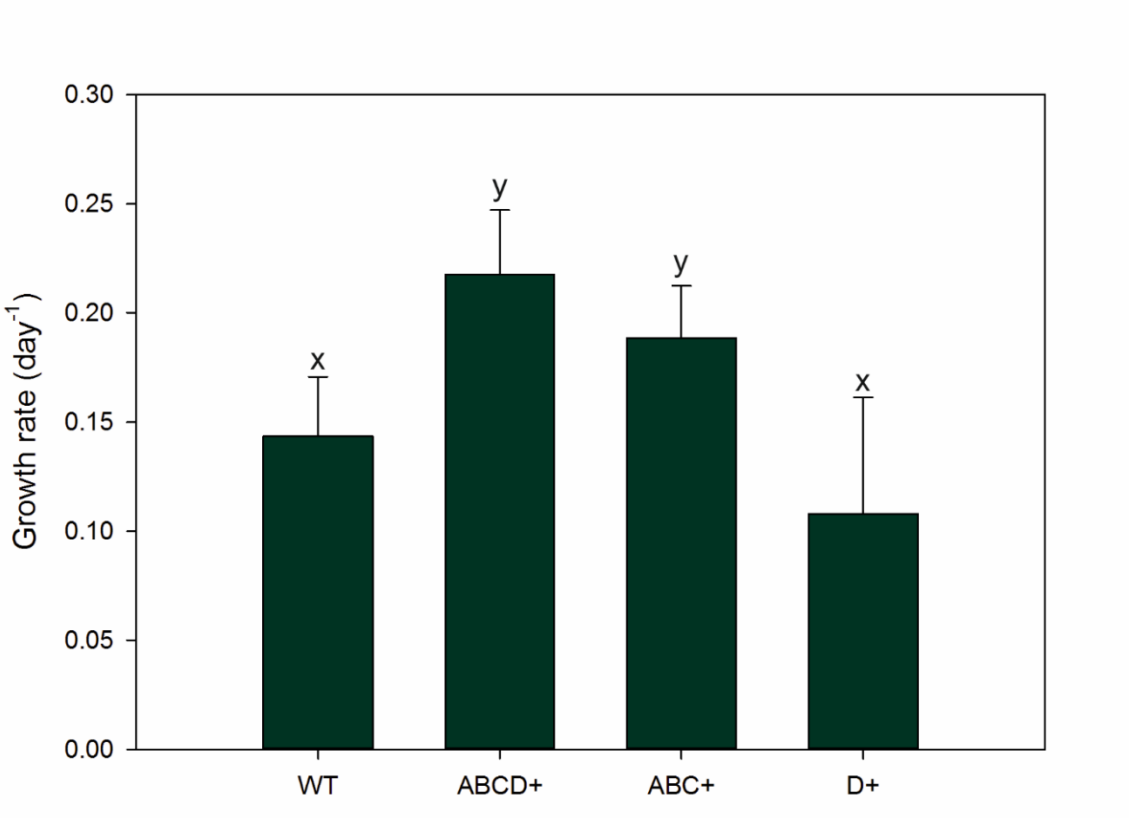

Figure 3.7: **Strains of *Synechocystis* grow unevenly on phosphate**. Growth rates of *ptxABCD*+, *ptxABC*+ and *ptxD*+ and the isogenic WT parent were compared during growth on standard, phosphate (PO_4^{3-}) containing BG11. Error bars represent the standard deviation from the mean of three biological replicates. Letter groups (x and y) are significantly different (Student's t-test, $P < 0.05$) to each other.

However, these observations can only be valid if (a) some PO_3^{3-} is present in the media, either through contamination or reduction of PO_4^{3-}, and this is taken up by the *ptxABC* transporter, and/or (b) the transporter can also take up PO_4^{3-} with lower specificity/efficiency. For the former alone to explain the observations, the cell must prepossess enzymes that can carry out oxidation of PO_3^{3-} to PO_4^{3-} as *ptxABC*+ carries the ABC transporter genes but lacks the putative phosphite dehydrogenase (*ptxD*).

As seen previously (Fig. 3.6), PO_3^{3-} cannot be efficiently used by *ptxABC*+ as a source of P therefore utilisation of PO_3^{3-} is not a possible explanation. Consequently, *ptxB* is hypothesised to also bind PO_4^{3-} and this is currently under investigation (Bisson et al., manuscript in preparation). Although the higher growth rate of *ptxABCD*+ compared to *ptxABC*+ is not statistically significant, the possibility of uptake of trace PO_3^{3-} concentrations, present in the media, by both and its subsequent utilisation by *ptxABCD*+ alone, cannot be excluded.

3.2.4 Environmental prevalence of *ptx* genes in *Trichodesmium*

To identify the environmental prevalence of *ptxABCD,* nucleotide sequences of the genes from *T. erythraeum* IMS101 were compared against all available *Trichodesmium* metagenomic and metatranscriptomic datasets (Table 3E).

A contig sequence (TCCM__contig00441) was identified in a *Trichodesmium* community metagenome assembly from the Atlantic Ocean (Walworth et al. 2015) that possessed putative open reading frames encoding homologues of *ptxA* (bit score: 401, identity: 86%), *ptxB* (bit score: 316, identity: 76%) and *ptxC* (bit score: 420, identity: 93%).

Furthermore, metatranscriptomic reads aligning to all four *ptx* genes (percentage identity > 90%) could be identified in samples from two sites in a dataset obtained from the Amazon River Plume (Hilton et al. 2015). Similarly, *ptxABC* were identified in metatranscriptome analysis from the New Caledonian Lagoon in the South West Pacific (as indicated in Spungin et al. 2016). The raw data is not yet available online to search for the presence of *ptxD*. Reads matching the *ptx* genes were not identified in a 454 metatranscriptomic dataset from the South Pacific Ocean (Hewson et al. 2009); however, the overall coverage of *Trichodesmium* coding sequences in this study was very low.

Identification of prevalence of *ptxABCD* genes in *in situ* metagenomic and metatranscriptomic datasets confirms that they are both present and expressed in diverse *Trichodesmium* species in the field, further supporting the role of PO_3^{3-} uptake in defining *Trichodesmium's* ecological niche.

Table 3E: Environmental prevalence of *ptx* genes in *Trichodesmium*

Analysis	Location	Identified	Reference
In situ metagenome	Atlantic Ocean	*ptxABC*	Walworth et al. 2015
In situ metatranscriptomes	Amazon River Plume	*ptxABCD*	Hilton et al. 2015
	South Pacific Subtropical Gyre	No	Hewson et al. 2009
	New Caledonia Lagoon	*ptxABC**	Spungin et al. 2016

* The presence of ptxD is not indicated in the paper and the raw data is not currently available for manual identification

3.3 Conclusions and further discussion

Following evidence supporting the involvement of marine organisms including *Trichodesmium* in a dynamic P redox cycle (Dyhrman et al. 2006; Martínez et al. 2012; Van Mooy et al. 2015), there is emerging interest in understanding the mechanisms involved in the biological processes responsible, and the extent that biology influences or is influenced by oceanic processes. Work developed in the context of this Chapter was aimed at deciphering whether *Trichodesmium's* physiology can support growth on reduced inorganic P and characterising the molecular mechanism underlying this.

It was established that the organism can grow on PO_3^{3-} as its sole source of P, potentially extending the oceanic locations currently considered as *Trichodesmium's* ecological niche. This possibility cannot be presently tested since no measurements of PO_3^{3-} concentrations in the ocean have been reported. The development of suitable analytic methods for the quantification of reduced P sources in the marine environment is necessary to establish its significance for the organism's lifestyle.

Using heterologous expression in *Synechocystis* PCC 6803, the putative *Trichodesmium ptxABCD* operon, which was found to be upregulated under PO_4^{3-}-limitation, is identified as the molecular system responsible for accessing PO_3^{3-} with both the transporter (*ptxABC*) and phosphite dehydrogenase (*ptxD*) required for the process. Our results highlight the power of heterologous expression for studying the function of *Trichodesmium* proteins in genetically tractable cyanobacterial species, as previously shown by HetR complementation in *Anabaena* (Kim et al. 2011).

By analogy to the heterologous expression method, it is interesting to speculate whether virally mediated lateral gene transfer, which is common in microbial communities (Lindell et al. 2005; Zeidner et al. 2005), promotes natural acquisition of *ptx* genes in the contemporary ocean, and consequently question how abundant these genes are across different species/ecotypes. The genes are identified to be present and expressed *in situ* both in *Trichodesmium* (this study) and *Prochlorococcus* (Martínez et al. 2012).

The ability to catabolise PO_3^{3-}, as demonstrated here, is also connected to the organism's ability to synthesize it (Van Mooy et al. 2015) as there would be little or no use of production of an inaccessible compound. The question of the purpose of PO_3^{3-} production remains, but there have been suggestions of possible use as an antibiotic by organisms (Karl 2014) due to its fungicide qualities (Griffith et al. 1989). In addition, if the ability to use PO_3^{3-} has, contrary to the current surge of evidence, not spread amongst marine organisms, production of PO_3^{3-} could increase the likelihood that after its release it would be reused by the same species.

To conclude, results presented in this chapter support that the PO_3^{3-} utilising ability of *Trichodesmium* is important to determining the organism's success in its natural environment, with *Trichodesmium* itself potentially a major contributor to a dynamic biological P redox cycle.

As a final note, it is interesting to discuss the potential biotechnological applications of this work. A by-product of the research conducted for purposes of this project, the PO_3^{3-} utilising *Synechocystis* PCC 6803 stain *ptxABCD*+, was observed to be particularly efficient in the use of PO_3^{3-} as its only source of P. Algae and cyanobacteria are currently beginning to be used for wastewater treatment in combination with biofuel production as the need for green energy increases (Christenson & Sims 2011; Nozzi et al. 2013; Lynch et al. 2015) with synthetic biology employed to optimise the productivity and viability of these methods (Georgianna & Mayfield 2012). Since phosphites are used as fungicides, pesticides and herbicides as well as fertilisers and could be identified in wastewater treatment water (Yu et al. 2015) the use of genetically engineered PO_3^{3-} utilising strains for wastewater treatment could be an efficient way of dealing with residual P potentially contributing to eutrophication of riverine/coastal water. In addition, the potential production of NADH during oxidation of PO_3^{3-} by the *ptxD* could drive NAD(P)H with possible applications in enhancing the activity of biophotovoltaic devices (Anderson et al. 2016).

Chapter 4

The function of Tery_3377 (IdiA) Iron transport or PSII protection?

4.1 Introduction

In addition to phosphorus (P) limitation, oceanic primary production is challenged by an insufficiency of the micronutrient iron (Fe) (Moore et al. 2013), which is necessary for construction of the cell's photosynthetic machinery (Geider & La Roche 1994). Due to its additional use as a component of the nitrogenase enzyme (Sañudo-Wilhelmy et al. 2001; Shi et al. 2007; Richier et al. 2012), Fe is essential for the prevalence of diazotrophy in the ocean (Mills et al. 2004; Moore et al. 2009; Chappell et al. 2012). Therefore, organisms have developed diverse strategies that permit survival at fluctuating or chronically depleted Fe concentrations. These include intricate Fe uptake mechanisms and protective responses against elevated production of reactive oxygen species (ROS) generated as a result of Fe-stress (Peers & Price 2004). Iron deficiency induced protein A (IdiA) homologues have been suggested to participate in both of these processes.

Proteins with similarity to IdiA are found in organisms of all domains of life from archaea (eg. *Natrialba chahannaoensis*) to eukaryotes (e.g. the polychaete *Capitella teleta* and the Tibetan antelope *Pantholops hodgsonii*), but has only been studied in a few pathogenic bacteria and cyanobacteria species.

The first homologue of IdiA, referred to as FbpA (ferric ion binding protein A), was discovered in pathogenic bacteria and was characterised as a periplasmic Fe^{3+}-binding protein, which in conjunction with transmembrane (FbpB) and ATPase (FbpC) components, forms an ATP binding cassette (ABC) transporter for transport of ferric iron (Fe^{3+}) (Krewulak & Vogel 2008). In cyanobacteria, an IdiA homologue was first identified in *Synechococcous elongatus* PCC 6301/PCC 7942 and was unexpectedly shown to be intracellular. It was associated with the thylakoid membranes and has a role in protection of photosystem II (PSII) under oxidative stress caused by Fe-deficiency (Michel et al. 1996; 1998; Exss-Sonne et al. 2000). The marked upregulation of IdiA homologues observed in several marine organisms, including *Trichodesmium*, under Fe-stress, lead to the consideration and use of IdiA as an *in vivo* marker of Fe-limitation (Rivers et al. 2009; Chappell & Webb 2010; Saito et al. 2014; Snow et al. 2015; Walworth et al. 2016)

In *Synechocystis* sp. PCC 6803 (hereafter *Synechocystis*) there are two paralogues of the protein referred to in literature as FutA1 (Slr1295) and FutA2 (Slr0513). The *futA1* and *futA2* genes as well as the permease (*futB, slr0327*) and the ATPase (*futC, sll1878*) homologues are all separately localised relative to each other in the *Synechocystis* genome. Deletion of the *futB* and *futC* components compromise the organisms growth, while the Δ*futA1/futA2* double mutant is severely Fe-limited compared to the WT (5% Fe uptake compared to the WT (Katoh et al. 2001a). Deletions of *futA1* or *futA2* independently resulted in reduced Fe uptake (37% and 84% residual activity compared to WT respectively) and impaired growth under Fe-deficiency (Katoh et al. 2001b). Contradicting the reported decrease of Fe uptake in Δ*futA1* by this study, Kranzler et al. (2014) suggest an increase compared to the WT (Table 4A).

Table 4A: Phenotypes previously reported in *Synechocystis* Δ*futA1* and Δ*futA2* mutants

Δ*futA1*	**Δ*futA2***
Low PSII activity (Tolle et al. 2002)	Plastocyanin- Cytochrome c_{553} (PC) switch not performed (Waldron et al. 2007)
Earlier progression to PSI-IsiA (Tolle et al. 2002)	Lower cytochrome c oxidase activity (Waldron et al 2007)
Fe uptake affected (reduced in Katoh et al. 2001b, increased in Kranzler et al. 2013)	Decreased Fe uptake (Katoh et al. 2001b, Kranzier et al. 2013)
Lower Fe^{3+}- FutA2 in periplasm (Badarau et al. 2007)	Pigmented supernatant (Waldron et al. 2007)

Despite one report suggesting that FutA1 and FutA2 bind Fe^{2+} (Koropatkin et al. 2007), both have been shown to bind Fe^{3+} (Katoh et al. 2001b; Waldron et al. 2007; Badarau et al. 2008). Therefore, both were initially predicted to function as semi-redundant periplasmic Fe-binding components involved in Fe^{3+} uptake in conjunction with the FutB and FutC subunits (Katoh et al. 2001b). However, further research suggested that only FutA2 is found in the periplasm, with FutA1 localised intracellularly (Fig. 4.1) (Fulda et al. 2000; Tölle et al. 2002; Waldron et al. 2007).

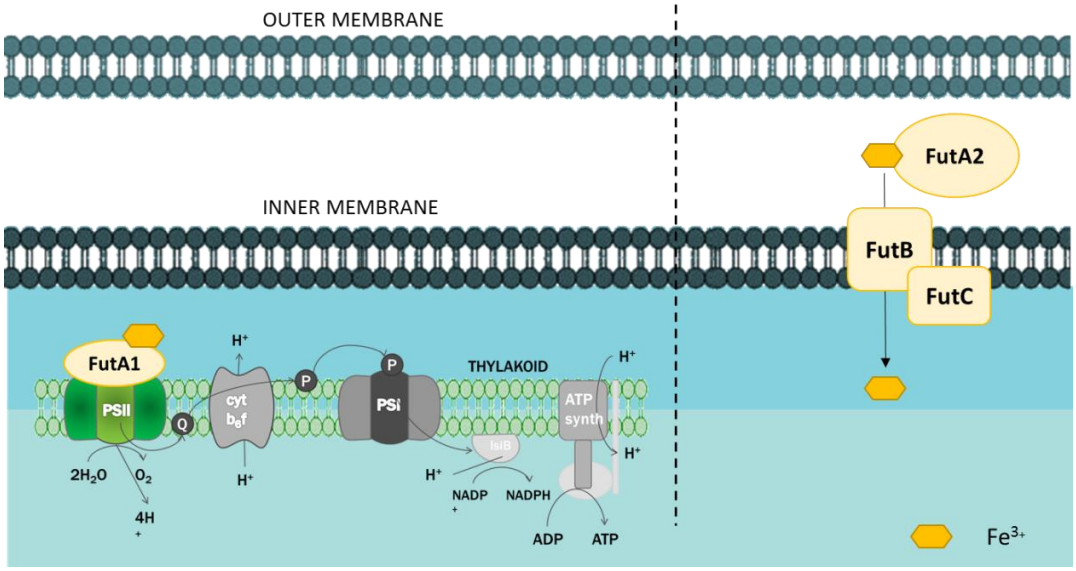

Figure 4.1: Current model of the localisation of *Synechocystis* Fut paralogues. FutA1 **(left)** is thought to be intracellular, attached to PSII at the thylakoid membranes, and have protective properties under oxidative stress caused by Fe-deficiency. FutA2 **(right)** is periplasmic and is postulated to act as the Fe^{3+} binding protein of the Fut ABC-transporter for Fe^{3+} uptake across the plasma membrane.

Functionally, FutA1 has been proposed to protect PSII under Fe-deficiency (Tölle et al. 2002), similarly to IdiA from *Synechococcus*. Indeed, PSII was more susceptible to inactivation in the Δ*futA1* mutant, which had a reduction in photosynthetic pigment content and oxygen evolution, and showed more advanced attachment of iron-stress-induced protein A (IsiA) (Fe-deficiency induced antenna) to photosystem I (PSI) under mild Fe-limitation (Table 4A) (Tölle et al. 2002). Conversely, the periplasmic FutA2 potentially interacts with FutBC to form an active Fe^{3+} transporter, and appears to have a role in preventing aberrant associations of Fe with binding sites of other metal transporters (Waldron et al. 2007). In particular, cytoplasmic copper containing enzymes are affected in the Δ*futA2* mutant, which has lower cytochrome *c* oxidase activity and uses cytochrome c_6 under conditions where the WT uses the copper-containing plastocyanin (Table 4A) (Durán et al. 2004; Waldron et al. 2007).

Unlike *Synechocystis*, *Trichodesmium erythraeum* IMS101 (hereafter *Trichodesmium*) has only one *futA* homologue in its genome, encoded by *Tery_3377* (Chappell & Webb 2010). This is the protein identified in a search for IdiA homologues by Michel & Pistorius (2004), although the authors wrongly reported it as being Tery_0244 (annotated as a hypothetical protein). Increased expression of Tery_3377 under Fe-stress has been reported at both the transcriptional (see Chapter 5 and Shi et al. 2007; Chappell & Webb 2010), and protein (Webb et al. 2001; Snow et al. 2015) levels.

This study attempts to address the question of the function of *Trichodesmium* Tery_3377 relative to the two *Synechocystis* FutA paralogues. Bioinformatic and phylogenetic analysis is first utilised to explore the similarity of the *Trichodesmium* protein to the *Synechocystis* and other bacterial homologues. Subsequently, using molecular approaches the cellular localisation and function of the protein are examined. For this, *Synechocystis* is used as a vehicle for the expression of the *Trichodesmium* protein or its signal sequence fused to green fluorescent protein (GFP).

4.2 Results and discussion

4.2.1 Bioinformatic analysis of Tery_3377

Although largely assumed to be involved in Fe transport and variably referred to as FutA or IdiA, no data is available regarding the *in vivo* function of Tery_3377. Similarly to the *Synechocystis futA* genes, *Tery_3377* is localised at an independent locus to the ABC transporter transmembrane (*Tery_3223*) and ATPase (*Tery_3222*) components in the *Trichodesmium* genome. The Tery_3377 protein has 57% identity to FutA1 and FutA2 (Table 4B).

To understand how homologues of the protein are grouped based on their sequence, maximum likelihood phylogenetic analysis was performed to include the *Trichodesmium* and the two *Synechocystis* variants along with their closest homologue (from *Lyngbya* sp. PCC 8106, *Phormidium willei* and *Cyanothece sp.* CCY 0110 for the *Trichodesmium* Tery_3377 and *Synechocystis* FutA2 and FutA1 respectively) as identified using BlastP (Altschul et al. 1990). Homologues from *Synechococcus elongatus* PCC 6301 and PCC 7942 as well as *Prochlorococcus marinus* MIT 9301 and *Anabaena* sp. PCC 7120 were also included in the analysis (Table 4B, Fig. 4.2).

Table 4B: IdiA/FutA/Fbp homologues of selected bacteria. Putative signal sequences and the first 4 amino acid residues of the mature protein as predicted from Signal P v4.1 (v3.0 sensitivity) and TatP v1.0 servers (Bendtsen et al. 2005; Petersen et al. 2011). Where relevant an alternative signal sequence end is marked (*). The likelihood that these are functional signal sequences, as assessed in each server, is also reported. Twin arginine (RR) residues, other Tat conserved amino acids, positively charged residues and putative lipobox sequence are indicated. The localisation of the protein is stated if previously studied (Michel et al. 1998; Fulda et al. 2000; Tölle et al. 2002; Waldron et al. 2007; Khambati et al. 2010). The amino acid (aa) identity of each protein to Tery_3377 was identified through BlastP (Altschul et al. 1990).

Organism	Protein	Predicted Signal Sequence	SignalP v4.1 (v3.0 sensitivity)	TatP v1.0	Putative signal sequence length (aa) (suggested alternative length)	Reported location	Identity to Tery_3377 (%)
Trichodesmium erythraeum IMS 101	Tery_3377	MTITRRVFLGTGTAIATVAIA*ELGK SNRGLAQSGA	no	no	31 (21)	unknown	100
Synechocystis sp. PCC 6803	Slr0513 (FutA2)	MTTKISRRTFFVGGTALTALVVANL PRRASAQSRT	yes	yes	31	periplasm	57
	Slr1295 (FutA1)	MVQKLSRRLFLSIGTAFTVVVGSQLL SSCGQSPDAPIADTPG	yes	no	37	intracellular	57
Synechococcus elongatus PCC 6301	Syc1920_d	MHHNLSLPSMSESMFSRRDFLLGG TALAGTLLLDSFGDWRRRAEAAEGE	no	no	45	intracellular	52
	Syc0146_c	MSCLRIWSTGLAALLLSTGLAA*CS GGDKV	yes	no	25 (22)	unknown	53
Prochlorococcus marinus MIT 9301	P9301_13 611	MQKLKKIIFSVFTCTFLLNVNIPANST EKE	yes	no	26	unknown	36
Anabaena sp. PCC 7120	Alr1382	MVSHQVRQISSAITAIVLGLGLGIAV AATPK	no	no	27	unknown	28
Haemophilus influenza	HI_0097	MQFKHFKLATLAAALAFSANSFADI TV	yes	no	23	periplasm	29

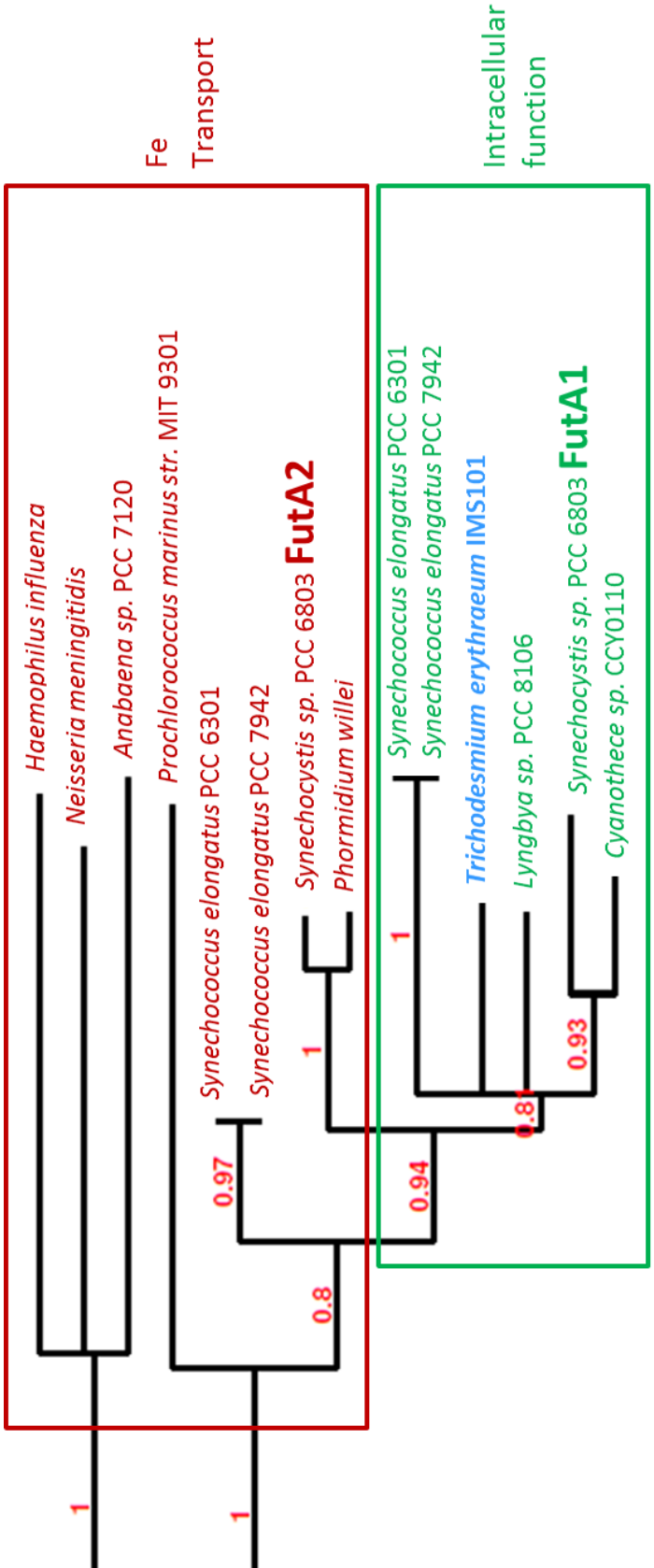

Figure 4.2: Maximum likelihood phylogenetic analysis of Tery_3377 homologues from selected bacteria. *Synechocystis* FutA1 and FutA2 proteins and the Trichodesmium Tery_3377 **(blue)** are compared. Their closest homologues identified using BlaspP (Altschul et al. 1990) as well as those from *Synechococcus elongatus* PCC 6301/7942, *Prochlorococcus marinus* MIT 9301, *Anabaena* PCC 7120 and pathogenic bacteria *Haemophilus influenza* and *Neisseria meningitides* are included in the analysis. The graphical representation was produced using TreeDyn v198.3 (Chevenet et al. 2006) and branch probabilities reported are calculated using an approximate likelihood ratio test. (aLRT, Anisimova & Gascuel 2006). The proteins form two groups: putative Fe transporters **(red)**, and those with possible intracellular function **(green)**.

Despite early studies only reporting the occurrence of a single homologue in the *Synechococcus elongatus* PCC 6301/PCC 7942 genome (Michel et al. 1996; Michel et al. 1998; Michel et al. 1999; Exss-Sonne et al. 2000; Michel & Pistorius 2004) the presence of two independent homologues was later revealed (Rivers et al. 2009; Chauvat & Cassier-Chauvat 2012). However, comparative studies for the two paralogues were not performed. The phylogenetic analysis completed here identifies that the *Synechococcus* proteins cluster closer to their corresponding *Synechocystis* homologues (FutA1 or FutA2) than to each other (Fig. 4.2). Genes encoding for the homologues that clustered with *Synechocystis* FutA2 (annotated as 'iron transport system substrate-binding protein' and 'futA2' for *S. elongatus* sp. PCC 6301 and 7942 respectively) are colocalised with other members of an ABC transporter in the *Synechococcus* genome. This is contrasting what is observed for both *Synechocystis futA* homologues and *Trichodesmium Tery_3377*, which are not colocalised with the putative partner transporter genes in their respective genomes.

The second protein homologue of the two species, annotated as 'IdiA' and previously identified to have an intracellular role in PSII protection (Michel et al., 1996, 1998; Michel and Pistorius 2004), seems to branch out of the Fe transporter group (Fig. 4.2), as does the *Synechocystis* FutA1 protein. Interestingly, the *Trichodesmium* Tery_3377 regarded as an Fe transporter is more closely related to FutA1 and IdiA compared to the Fe transporter proteins of *Synechocystis* and *Synechococcus*.

Similarly to *Trichodesmium*, and unlike *Synechococcus*, *Prochlorococcus* seems to only possess a single copy of the protein, the gene of which is not colocalised with other transporter components but is annotated and regarded (Thompson et al. 2011) as a putative Fe transporter. The phylogenetic analysis performed here indicates a closer relationship to FutA2 and other transporter homologues (Fig. 4.2) compared to FutA1 and thus supports its functional annotation. Previously identified high sequence divergence of this *Prochlorococcus* homologue and its localisation next to tRNA sequence, are indicative of potential subjection to horizontal gene transfer and loss events (Thompson et al. 2011).

Interestingly, the identified homologue of the model freshwater diazotroph *Anabaena* sp. PCC 7120 appears to be more related to the pathogenic bacteria *Hemophilus influenza* and *Neisseria meningitides* FbpA than the other cyanobacterial homologues included in the analysis. In addition, similarly to the pathogenic bacteria variant and the *Synechococcus futA2*, it is localised upstream of the ABC transporter permease and ATPase homologues, making its assignment as a transporter unambiguous.

By inspecting the predicted protein signal sequences, we can potentially draw inferences to where proteins will be directed in the cell. Export of proteins to the periplasmic space can be achieved either through the general secretory (Sec) pathway, whereby proteins fold after their transport across the inner membrane, or the twin arginine translocase (TAT) system, which transports proteins previously folded in the cytoplasm (Natale et al. 2008). The latter is distinguished through the conserved N-terminal motif SRRXFLK in which the two consecutive arginine residues (giving the TAT system its name) are almost always present (Lee et al. 2006). The *Synechocystis* FutA1 and FutA2 homologues as well as *Trichodesmium* Tery_3377 possess amino acids with similarity to this motif, and all include the conserved arginine residues (Table 4B). In addition, TAT substrate proteins commonly express AXA at the cleavage site and a positive charge of +2 or higher at the C-terminal region is thought to promote TAT specificity (Cristóbal et al. 1999; Blaudeck et al. 2003; Lee et al. 2006). This signal appears to be present for the *Synechocystis* FutA2 but not FutA1 homologue while Tery_3377 expresses AXA but no positively charged residues (Table 4B).

Signal sequence prediction server SignalP 4.1 (sensitivity of version 3.0, Petersen et al. 2011) does not positively identify a signal sequence for Tery_3377 unlike for the two *Synechocystis* FutA proteins. TAT-signal prediction server TatP 1.0 (Bendtsen et al. 2005) designed to identify proteins exported through the TAT system gives a positive result with the *Synechocystis* FutA2 protein but not FutA1 or the *Trichodesmium* Tery_3377 (Table 4B). For Tery_3377, this could be explained by either an intracellular role in PSII protection under Fe-limitation analogous to *Synechocystis* FutA1 and *Synechococcus* IdiA homologues or a divergent signal sequence for export to the periplasm. Despite both of the *Synechocystis* FutA homologues containing the twin arginine residues, the observed dissimilarity in localisation (Fulda et al. 2000; Tölle et al. 2002), also predicted by the TatP server, could be due to loss of the TAT signal sequence C-terminal peptidase recognition site required for cleavage in FutA1 (Table 4B).

The positive prediction of a Tat signal sequence for FutA2 is unique amongst the bacteria considered here and in addition to *Synechocystis* FutA1 and *Trichodesmium* Tery_3377, no other predicted signal sequences contain two arginine amino acids in the N-terminal region. Therefore, the periplasmic Fe-binding *Haemophilus influenza* FbpA (Adhikari et al. 1995; Kirby et al. 1997; Anderson et al. 2004) and potentially the *Prochlorococcus marinus* str. MIT 9301, P9301_13611, *Anabaena* PCC 7120, Alr1382, and *Synechococcus elongatus* PCC 6301 transporter homologue, Syc0146, are likely to be translocated to the periplasmic

space via the Sec pathway. Although the *Prochlorococcus marinus* str. MIT 9301 and *Synechococcus elongatus* PCC 6301 homologues, P9301_13611 and Syc0146 respectively, are positively predicted to possess a signal sequence by SignalP 4.1 (sensitivity of version 3.0 Petersen et al. 2011), Alr1382 of *Anabaena* PCC 7120 is not (Table 4B) contradicting its similarity to periplasmic FutA2-like homologues (Fig. 4.2) and colocalisation with FutBC-transporter genes in its genome (Stevanovic et al. 2012).

Bacterial lipoproteins are a large class of functionally diverse membrane associated proteins (Nakayama et al. 2012). They contain substrate binding proteins of ABC transporters but also the cyanobacterial PSII associated PsbP, PsbQ, and Psb27 (Nowaczyk et al. 2006; Fagerlund & Eaton-Rye 2011; Mizusawa & Wada 2012).Cleavage by type II (or lipoprotein) signal peptidase (Lsp) occurs at the C-terminal recognition site which commonly possess L(A/S/T)(G/A) as the last three amino acids and C always as the first residue of the mature protein (Hutchings et al. 2009). The *Synechococcus elongatus* PCC 6301 Syc0146 is the only homologue of the ones analysed which appears to possess a sequence region resembling the lipobox motif for Lsp recognition (but Lsp cleavage would result in a signal sequence shorter than the one predicted by the SignalP server) (Table 4B).

An overview: Phylogenetic analysis (Fig. 4.2) indicates that the cyanobacterial and pathogenic bacteria FutA/IdiA/FbpA homologues analysed can be grouped in FutA1-like and FutA2-like clusters. *Trichodesmium* Tery_3377 although considered an Fe transporter seems more similar to intracellular FutA1-like homologues indicating the possibility for an alternative function related to PSII protection under Fe-stress-induced oxidative stress. If this is the case, then another yet to be identified Fe^{3+} uptake mechanism must be operating in this organism.

To investigate the possible cellular localisation of proteins the signal sequences were compared (Table 4B). Using online prediction software *Trichodesmium* Tery_3377 is not identified to possess a functional signal sequence. However, the same is true for the *Anabaena* PCC 7120 homologue which phylogenetic analysis suggests to be similar to periplasmic FutA2-like proteins. Therefore, bioinformatic analysis alone is not sufficient to resolve the question of the localisation of Tery_3377.

4.2.2 Tery_3377 cellular localisation

In order to provide direct visual evidence of Tery_3377 localisation and compare it to FutA1 and FutA2 in *Synechocystis*, constructs in which each of the possible (using TatP v1.0)

longest signal peptides (Table 4B) in addition to the predicted first 4 residues of the mature protein fused to GFP were generated using overlap extension (OLE)-PCR. Selection of the construct was achieved through the chloramphenicol acetyl transferase gene (*cat*^{R}). The GFP-tagged DNA constructs were integrated at the *psbA2* (*sll1311*) locus in *Synechocystis* such that expression was under the control of the *psbA2* promoter. The *E. coli* TMAO reductase (TorA) signal sequence, previously shown to transport GFP into the periplasm in both *E. coli* (Thomas et al. 2001) and *Synechocystis* (Spence et al. 2003), was used as positive control for translocation across the cytoplasmic membrane by the TAT system. Strains expressing GFP fused signal sequences (ss-GFP) of the *Trichodesmium Tery 3377*, *Synechocystis futA1* and *futA2*, and the *E. coli* control *torA* were successfully generated (Fig. 4.3).

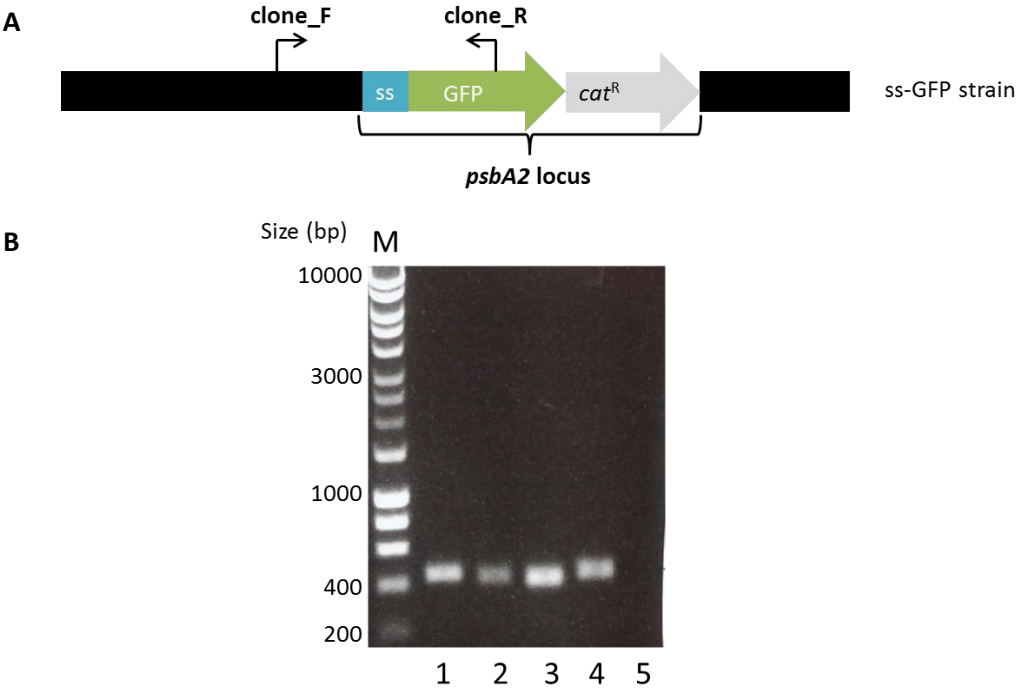

Figure 4.3: The GFP tagged-signal sequence strains. (A) Genes for GFP and *cat*^{R} were assembled next to signal sequences and the constructs replaced *psbA2* in the *Synechocystis* genome. **(B)** Signal sequences as follows: *Synechocystis futA1* (1) and *futA2* (2), *Trichodesmium Tery_3377* (3) and the *E.coli torA* (4), were amplified from each resulting strain with primers clone_F and clone_R and consequently sequenced to validate the inserted sequence. Control reactions of the WT (5) carried out with the same primers identified no product amplification as expected. Lane M = Hyperladder I (Bioline, London, UK).

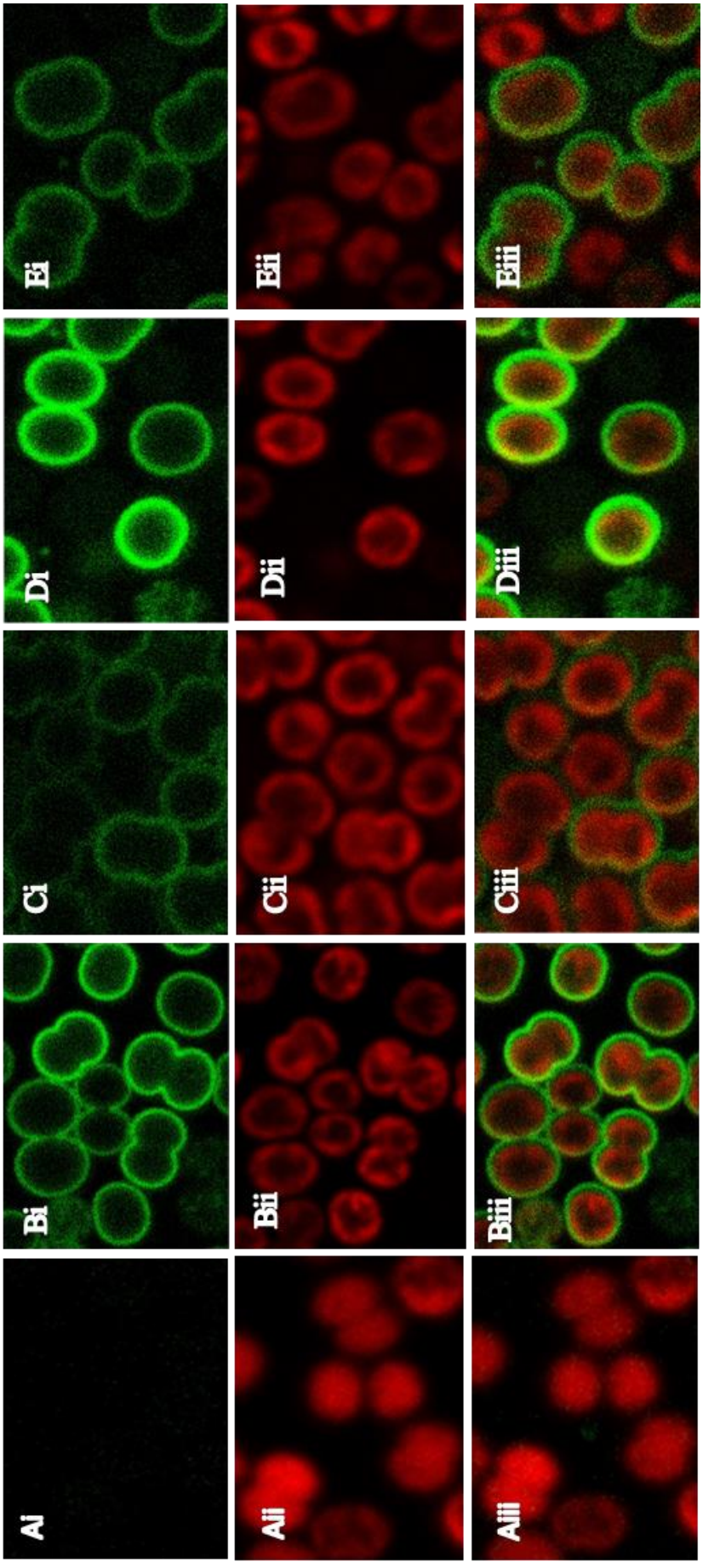

Figure 4.4: Localization of signal sequence-GFP constructs in *Synechocystis*. Using confocal microscopy the WT **(A)** and strains with GFP fused to the signal sequence of the *E.coli* control TorA **(B)**, *Synechocystis* FutA1 **(C)** and FutA2 **(D)** and *Trichodesmium* Tery_3377 **(E)** were imaged under identical settings through excitation at 488 nm where autofluorescence (represented by phycocyanin) emits at 600-700 nm **(Ai-Ei)** and GFP at 510-530 nm **(Aii-Eii).** The merged images for each strain **(Aiii-Eiii)** reveal periplasmic localisation of GFP by green fluorescent halos around the periphery of the cells in all strains (B-E) apart from the WT (A).

Confocal microscopy was used to image autofluorescence (em: 600-700 nm) and GFP fluorescence (em: 510-530 nm) simultaneously. Overlaying the two images revealed fluorescent halos in all strains except the WT, suggesting a periplasmic or cytoplasmic membrane localisation of GFP (Fig. 4.4). Our data contradict Tölle et al. (2002) that suggest the absence of any FutA1 in the periplasm. The intensity of halos differed between strains with FutA2ss-GFP, expected to be periplasmic (Fulda et al. 2000; Tölle et al. 2002; Waldron et al. 2007), being distinctly brighter than FutA1ss-GFP and closely resembling the TorAss-GFP control. The *Trichodesmium* Tery_3377ss-GFP is also prominently localised to the periplasm (Fig. 4.4). These observations can be explained as export of all ss-GFP fusions to the periplasm (possibly much less for FutA1) and provides the first direct evidence of the *Trichodesmium* Tery_3377 localisation as peripliasmic, supporting a function as an Fe transporter.

4.2.3 Mode of Tery_3377 export to the periplasm

Using site-directed mutagenesis (SDM), the twin arginine residues of Tery_3377 possibly part of a TAT signal peptide, were substituted by lysine (K) (also a large, basic and positively charged amino acid) residues. In that way, a second Tery_3377 signal sequence fusion to GFP was constructed (Tery_3377ss-KK). The double arginine to lysine substitution is known to prohibit the TAT signal sequence recognition and consequent export to the periplasm (Buchanan et al. 2001; Ize et al. 2002)

The expression of the constructs at the protein level was identified using immunoblotting with anti-GFP primary antibody (Fig. 4.5). Product size differed between strains with Tery_3377ss-GFP being smaller than the Tery_3377ss-KK-GFP. This is in agreement with cleavage of the signal sequence from GFP, occurring during translocation, when the sequence is intact (Tery_3377ss-GFP). The Tery_3377ss-KK-GFP signal sequence is potentially rendered unrecognisable to the TAT system and thus remains attached to GFP and presumably intracellular. A lower signal of GFP expression in this treatment could be indicative of intracellular degradation of non-transported substrates.

Visualisation of the ss-GFP construct expression with epifluorescence microscopy revealed loss of the fluorescent halos around the cells' periphery in the case of Tery_3377ss-KK-GFP (Fig. 4.6), compared to Tery_3377ss-GFP, confirming the immunoblot results and characterising Tery_3377 as a TAT system substrate.

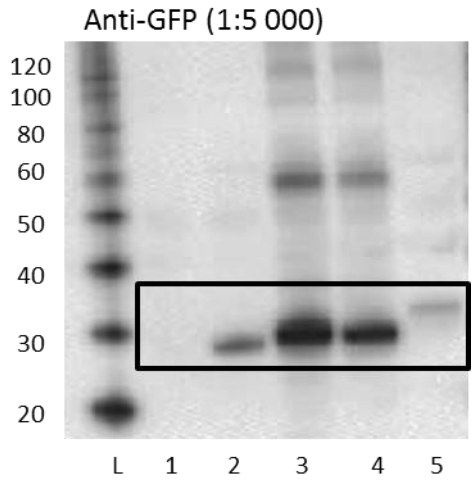

Figure 4.5: Identification of GFP expression in *Synechocystis* strains. Immunoblot analysis using primary antibody anti-GFP on protein samples extracted from WT *Synechocystis* **(1)**, strains containing GFP only **(2)**, TorAss-GFP **(3)**, Tery_3377ss-GFP **(4)** and Tery_3377ss-KK-GFP **(5).** Lane L = Ladder MagicMark™ XP (Thermo Fisher Scientific, Massachusetts, USA)

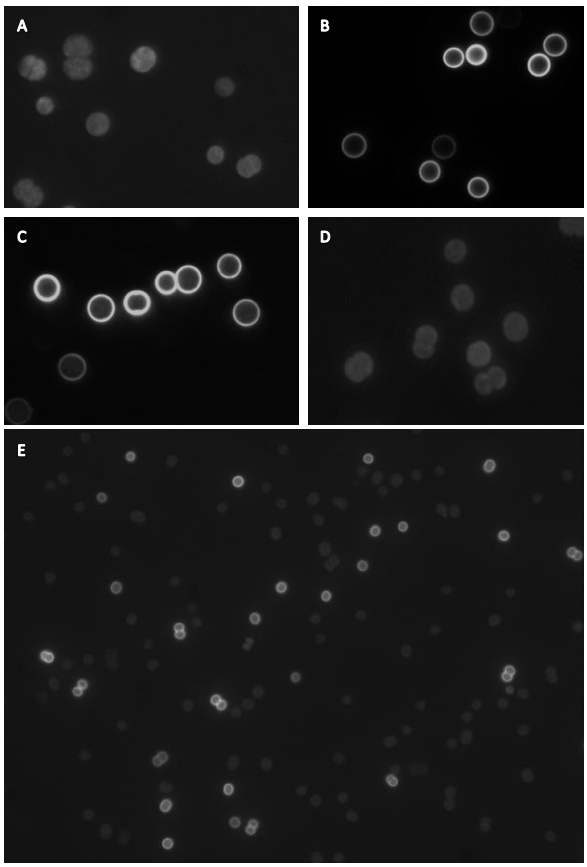

Figure 4.6: **Localization of the *Trichodesmium* Tery_3377 signal sequence-GFP constructs in *Synechocystis***. Imaged using epifluorescence microscopy WT cells **(A)** and *E.coli* TorAss-GFP fusions **(B)** are presented as a control to *Trichodesmium* Tery_3377ss-GFP **(C)** and Tery_3377ss-KK-GFP **(D).** Tery_3377ss-GFP and Tery_3377ss-KK-GFP are also visualised together for direct comparisons **(E).**

4.2.4 *Synechocystis futA* mutants generation and physiology

To study the function of Tery_3377 by relating it to that of FutA1 and FutA2, *Synechocystis futA1* and *futA2* deletion mutants (Δ*futA1* and Δ*futA2*) were generated. PCR confirmed their full segregation using a combination of flanking, gene-specific and antibiotic resistance cassette specific primers (Fig. 4.7). The Δ*futA1*/*futA2* double mutant was also constructed, and segregation was determined in a similar manner (data not shown).

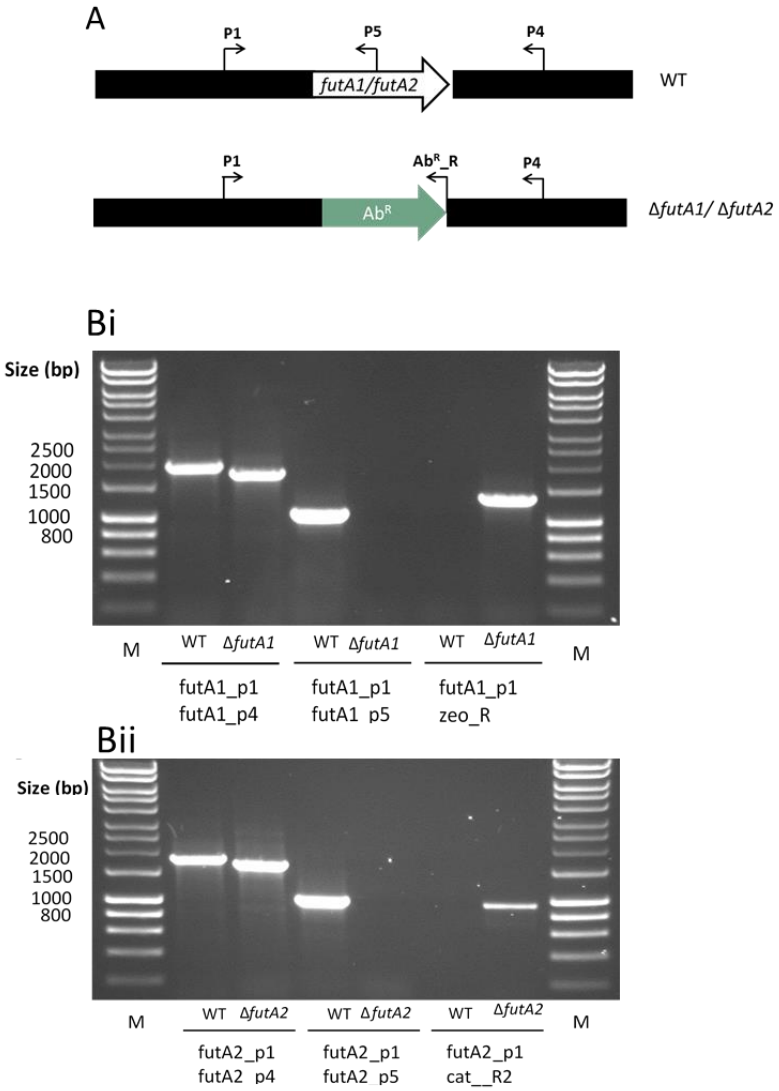

Figure 4.7: *Synechocystis* Δ*futA1* and Δ*futA2* deletion mutants were generated. (A) Representation of the *futA1/futA2* locus arrangement in WT and deletion mutants of *Synechocystis*. The position of primers used to confirm complete segregation is indicated. **(Bi)** Screening of Δ*futA1* and comparison with the WT through PCR using primers futA1_ P1, P4, P5 and zeo_R confirmed the full segregation of the mutant. **(Bii)** Similarly, Δ*futA2* and WT *Synechocystis* were screened with primers futA2_ P1, P4, P5 and cat_R2 to confirm the full segregation of the mutant. Lane M = Hyperladder I (Bioline, London, UK).

The physiology of the mutants was assessed, and similar to previous reports (Katoh et al. 2001a) it was observed that growth rate was reduced in the Δ*futA1*/*futA2* double mutant by about 50% but not in the Δ*futA1* or Δ*futA2* compared to the WT (Fig. 4.8A). Also an F_v/F_m (estimate of the apparent PSII photochemical quantum efficiency) reduction in both the Δ*futA1*/*futA2* and the Δ*futA2* mutants (60 and 25% respectively compared to the WT), as opposed to a small increase for Δ*futA1*, is reported here for the first time (Fig. 4.8B). The divergence of Δ*futA1* and Δ*futA2* F_v/F_m could be triggered by increased or decreased Fe uptake and reduction respectively compared to the WT, as previously reported by Kranzler et al. (2014).

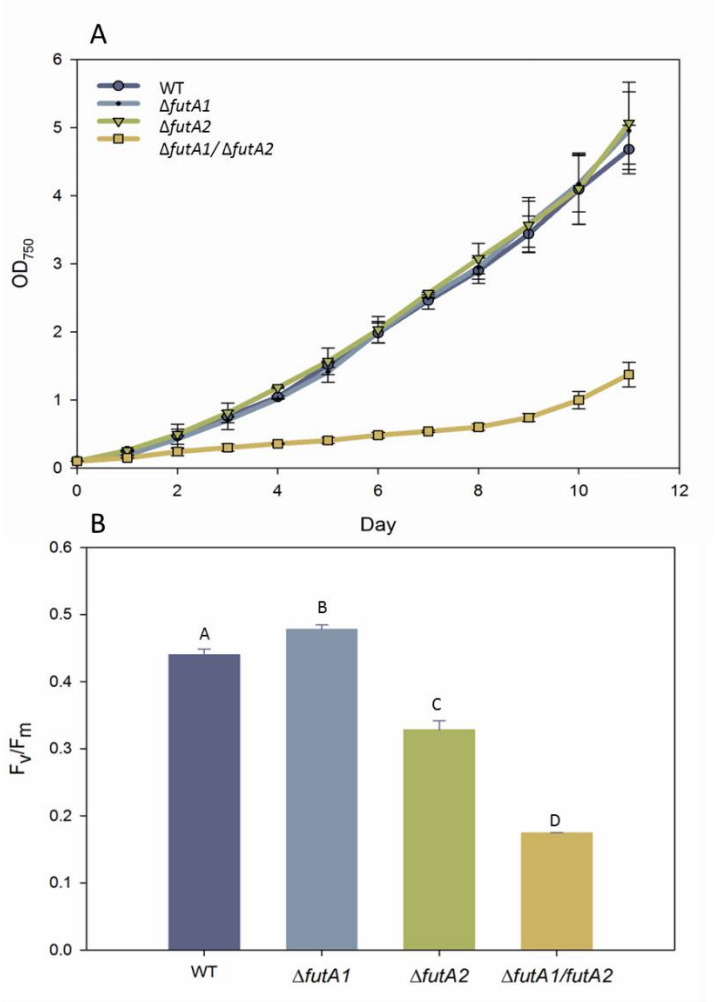

Figure 4.8: Physiology of FutA mutant strains in *Synechocystis*. (A) The growth of Δ*futA1/futA2,* measured over 11 days (OD_{750}) was severely compromised compared to that of WT, Δ*futA1* and Δ*futA2*. **(B)** The photosynthetic efficiency (F_v/F_m) of each strain differed to the others during exponential growth (day 4) (distinct letters mark significant differences between strains) (GLM and Tukey-test, CI=95%). Error bars represent standard deviations from the means of three biological replicates.

4.2.5 Expression of Tery_3377 in *Synechocystis* mutants

The codon optimised *Trichodesmium Tery_3377* gene was integrated at the *psbA2* locus in both the Δ*futA1* and Δ*futA2* mutants such that the gene's expression is under the control of the *psbA2* promoter. PCR confirmed that the strains (Δ*futA1+* and Δ*futA2+*) were homozygous for the *Trichodesmium* gene (data not shown) and sequencing (Eurofins MWG Operon, Ebersberg, Germany) confirmed no errors.

Expression of FutA1, FutA2 and Tery_3377 in the WT, mutants and complemented strains (as applicable) under normal (Fe+) and Fe-limited (Fe-) growth was determined through immunoblotting with anti-IdiA antibodies (for detection of FutA1, FutA2 and Tery_3377) or anti-Slr0513 (only cross reacts with FutA2) (Michel & Pistorius 1992; Tölle et al. 2002) (Fig. 4.9). Due to instability and poor growth of the Δ*futA1/futA2* double mutant, this and the its corresponding, Tery_3377 expressing strain, Δ*futA1/futA2+*, were omitted from subsequent analysis.

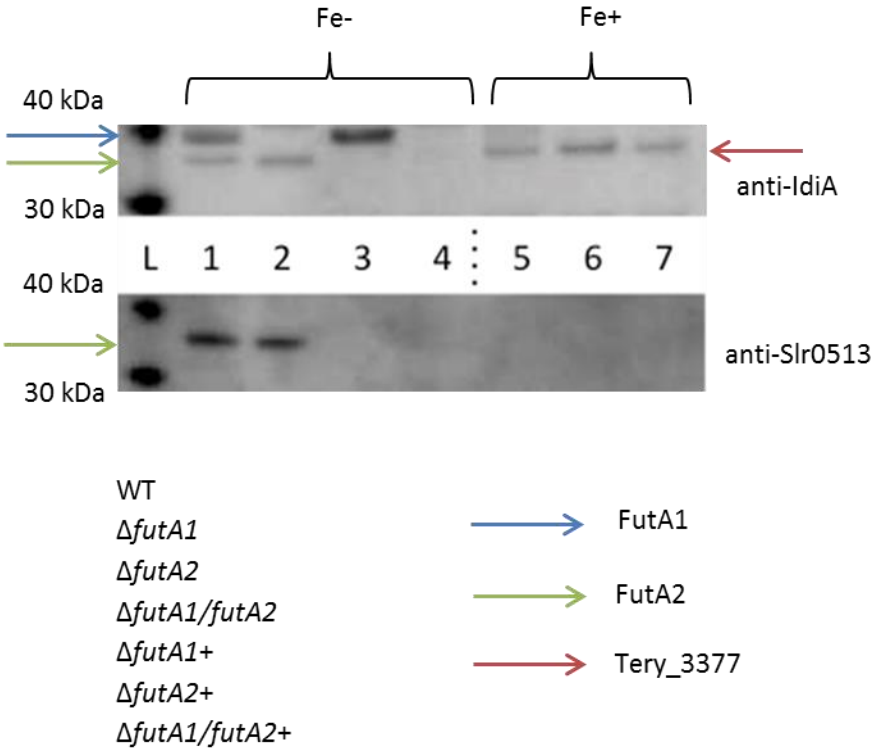

Figure 4.9: Expression of FutA1 and FutA2 in *Synechocystis* deletion and complemented mutants. Antibodies anti-IdiA (top) and anti-Slr0513 (bottom), raised against the *Synechococcus* and *Synechocystis* corresponding homologues respectively (Michel & Pistorius 1992; Tölle et al. 2002), identified the correct combination of FutA1 (blue arrow), FutA2 (green arrow) and Tery_3377 (red arrow) proteins in the WT, all constructed *futA* deletion and Tery_3377 expressing strains (1-7). Protein extracts were acquired during Fe-deplete growth for the WT and deletion mutants (1-4) and Fe-replete growth for the complemented strains (5-7).

To identify whether the periplasmic localisation of Tery_3377 (Sec.4.2.2 and 4.2.3) is associated with a function in Fe uptake, a phenotypic experiment was designed utilising the high affinity Fe^{2+} ligand ferrozine (FZ). The ligand which makes Fe^{2+} inaccessible as it cannot penetrate the cell membrane (Kustka et al. 2005; Shaked et al. 2005; Garg et al. 2007) was previously used in *Synechocystis* growth experiments to suggest that Fe reduction precedes transport across the cell membrane (Kranzler et al. 2011). Here, the ligand was hypothesised to cause an Fe-stress phenotype through reduction of *Synechocystis* Fe uptake, particularly in the case of Δ*futA2* which is presumably already compromised in Fe^{3+} uptake.

During exponential growth, Δ*futA2* experienced a reduction in F_v/F_m when FZ (200 µM) was included in BG11 media (FZ+) compared to when omitted (FZ-). This was a larger decrease (1.7 times) than the one observed between FZ-/FZ+ conditions in the WT (Fig. 4.10A). Conversely, upon addition of FZ, Δ*futA1* did not experience a significant decrease in F_v/F_m. Additionally, compared to the WT, Δ*futA1* had higher F_v/F_m both under FZ+ and FZ- conditions (Fig. 4.10A). The apparent improved F_v/F_m state of Δ*futA1* could be explained by previous observations of increased Fe reduction and uptake by Δ*futA1* compared to Δ*futA2* and WT (Kranzler et al. 2014).

Contrariwise, the Δ*futA1* functional absorption cross section of PSII (σ^{PSII}) experienced a marked increase (16%) in FZ+ compared to FZ- (Fig. 4.10B). This was larger than the observed increase in Δ*futA2* (11%) under the same conditions, while additions of FZ to the WT did not induce a statistically significant change (Fig. 4.10B). It is possible that the increase in σ^{PSII} under conditions of Fe-stress is stimulated by an accumulation of phycobilisome (Pcb) antenna complexes surrounding PSII (Bibby et al. 2003; Chen & Bibby 2005). An increase in the light harvesting efficiency of PSII could in that scenario counterbalance a potential reduction of the Fe containing photosystem. As the Δ*futA1* is hypothesised to lack PSII protection from Fe-stress generated ROS, the PSII subunits might be subjected to increased damage in this mutant. Therefore, it can be hypothesised that an increase of σ^{PSII} is caused by upregulation of Pcb stimulated to enhance the efficiency of the particularly compromised PSII subunits in Δ*futA1* under Fe-deficient conditions in FZ+. The larger overall σ^{PSII} of Δ*futA2* (Fig. 4.10B) (albeit its milder response to FZ-additions), could be indicative of a more pronounced state of cellular Fe and oxidative stress.

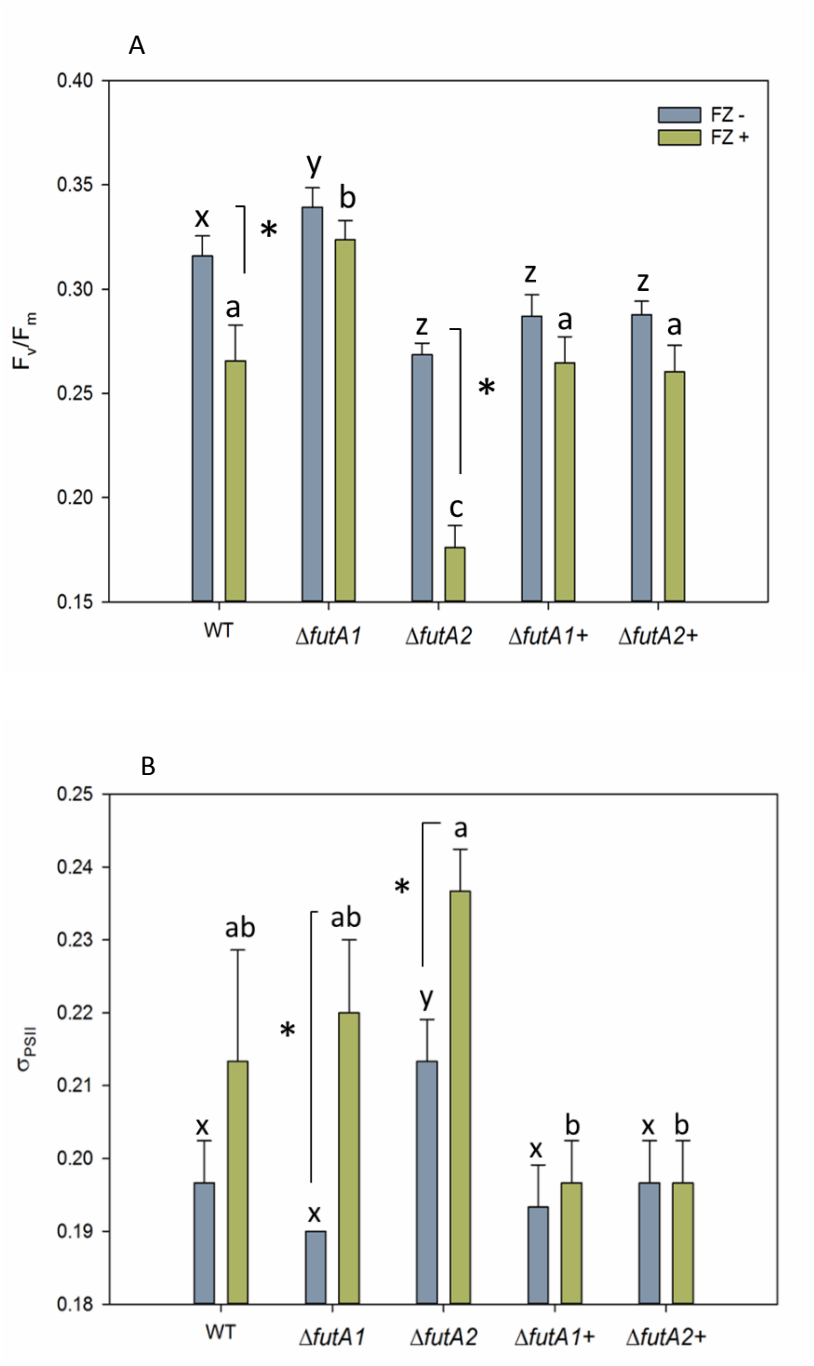

Figure 4.10: Photosynthetic physiology of strains under Fe stress. *Synechocystis futA* mutants before (Δ*futA1* and Δ*futA2*) and after (Δ*futA1*+ and Δ*futA2*+) insertions of the *Trichodesmium Tery_3377* were compared to the WT when grown in YBG11 media with (green) and without (blue) the Fe^{2+} binding ligand ferrozine (FZ). The photosynthetic physiology during exponential growth was recorded as F_v/F_m **(A)** and σ^{PSII} **(B)**. Statistical significance of differences observed was assessed using a GLM followed by a post-hoc Tukey-test (CI=95%). Between-strain (dissimilar letter group: x,y and z for Fz- and a,b and c for FZ+), and within-strain (*), differences ($P < 0.05$) are indicated. Error bars show the standard deviation from the mean of three biological replicates

In addition to photosynthetic physiology, growth rate changes also occurred. In FZ- the growth rate was lower for Δ*futA1* (0.39 day^{-1}) compared to the WT (0.45 day^{-1}) and Δ*futA2* (0.43 day^{-1}). Reductions were observed in all three strains when FZ was added to the media (Fig. 4.11). This reduction was higher (2.5 times) for Δ*futA2* than the Δ*futA1* and WT.

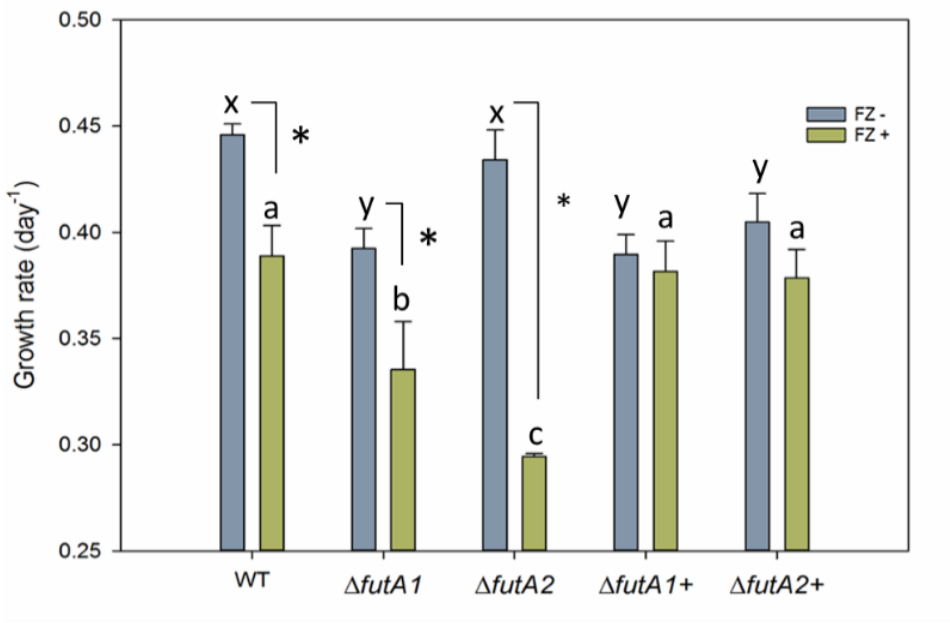

Figure 4.11: Growth rate of strains under Fe stress. Mutants Δ*futA1* and Δ*futA2* and their Tery_3377 expressing equivalents Δ*futA1*+ and Δ*futA2*+ were compared to the *Synechocystis* WT in YBG11 media with (green) and without (blue) ferrozine (FZ). Statistical significance, tested with a GLM followed by a post-hoc Tukey-test (CI=95%), is indicated between (dissimilar letter group: x,y and z for FZ- and a,b and c for FZ+) and within (*) strains.

To summarise, inclusion of FZ in the media seemed to exacerbate the Fe-stress phenotype of strains and this difference was more prominent for Δ*futA2* compared to the WT and Δ*futA1* supporting our hypothesis that stress induced by Fe^{2+} uptake inhibition is more acute in the Fe^{3+} uptake compromised Δ*futA2*. Data presented also suggests that the inferred increase in Fe uptake (Kranzler et al. 2014) could potentially enhance Δ*futA1* photosynthetic efficiency above the baseline WT levels.

Involvement of the *Trichodesmium* Tery_3377 in Fe^{3+} uptake and ability to replace FutA2 as part of a functional ABC transporter is hypothesised to cause restored growth and photosynthetic physiology in the Δ*futA2*+ strain compared to the Δ*futA2* mutant. Indeed, contrasting the phenotype of Δ*futA2*, the F_v/F_m, σ^{PSII} and growth rate of strain Δ*futA2+*, in FZ+, are no different to those of the WT. (Fig. 4.10, 4.11). In addition, the physiological changes (F_v/F_m, σ^{PSII} or growth rate) observed between FZ- and FZ+ growth conditions in

Δ*futA2* are not recoded in Δ*futA2+* indicating independence of its function to Fe^{2+} availability at the growth conditions used here (Fig. 4.10, 4.11).

The phenotype of Δ*futA1+* mimicked that of Δ*futA2+* in all parameters (F_v/F_m, σ^{PSII} and growth rate) (Fig. 4.10, 4.11), possibly indicating that a high influx of Fe^{3+} through the activity of Tery_3377 sets the function of FutA1 (protection of PSII under Fe-stress) redundant. However, it cannot be excluded that a secondary intracellular function of Tery_3377 is complementing the Δ*futA1* mutant phenotypes as well.

The small decrease in F_v/F_m and growth rate of Δ*futA1+* and Δ*futA2+* compared to the WT might be the effect of an energetic cost of Tery_3377 overexpression from the *psbA2* promoter.

4.2.6 Protein purification and crystallisation

To further confirm the Fe^{3+} binding/transporting properties of Tery_3377, the protein was hexa-histidine-tagged, over expressed in *E.coli*, extracted and purified to be analysed using crystallographic studies.

After induction with Isopropyl β-D-1-thiogalactopyranoside (IPTG), *E. coli* carrying the Tery_3377 containing pET21a_*3377* plasmid was maintained for 3 hours at 37 °C or overnight at 18° C. Both batches were subsequently processed and the protein was purified by immobilised metal affinity chromatography (IMAC) on a nickel column. SDS-PAGE and Coomassie staining indicated higher protein yields when *E.coli* was grown at 18 °C overnight compared to 3 hours at 37 °C (data not shown). Protein eluted from the IMAC column was pooled and further purified by size exclusion chromatography (SEC), the elution profile of which (Fig. 4.12) was characterised by one prominent and one secondary peak. Through SDS-PAGE of eluted samples, Tery_3377 was identified as the protein responsible for the prominent peak.

The red colouration of the purified protein (spin concentrated to 42 mg/ml) indicated the protein's Fe binding ability (Fig. 4.13). Crystal trials were set using protein before or after Fe ($FeCl_3$)-loading to acquire the apo and fully loaded structures respectively. Crystals formed after a week (Fig. 4.13) and the structure is currently being resolved (in collaboration with Moritz Machelett and Ivo Tews, Institute for Life Sciences, University of Southampton). Preliminary data indicate the Fe^{3+} binding capacity of Tery_3377 at the structural level (data not shown).

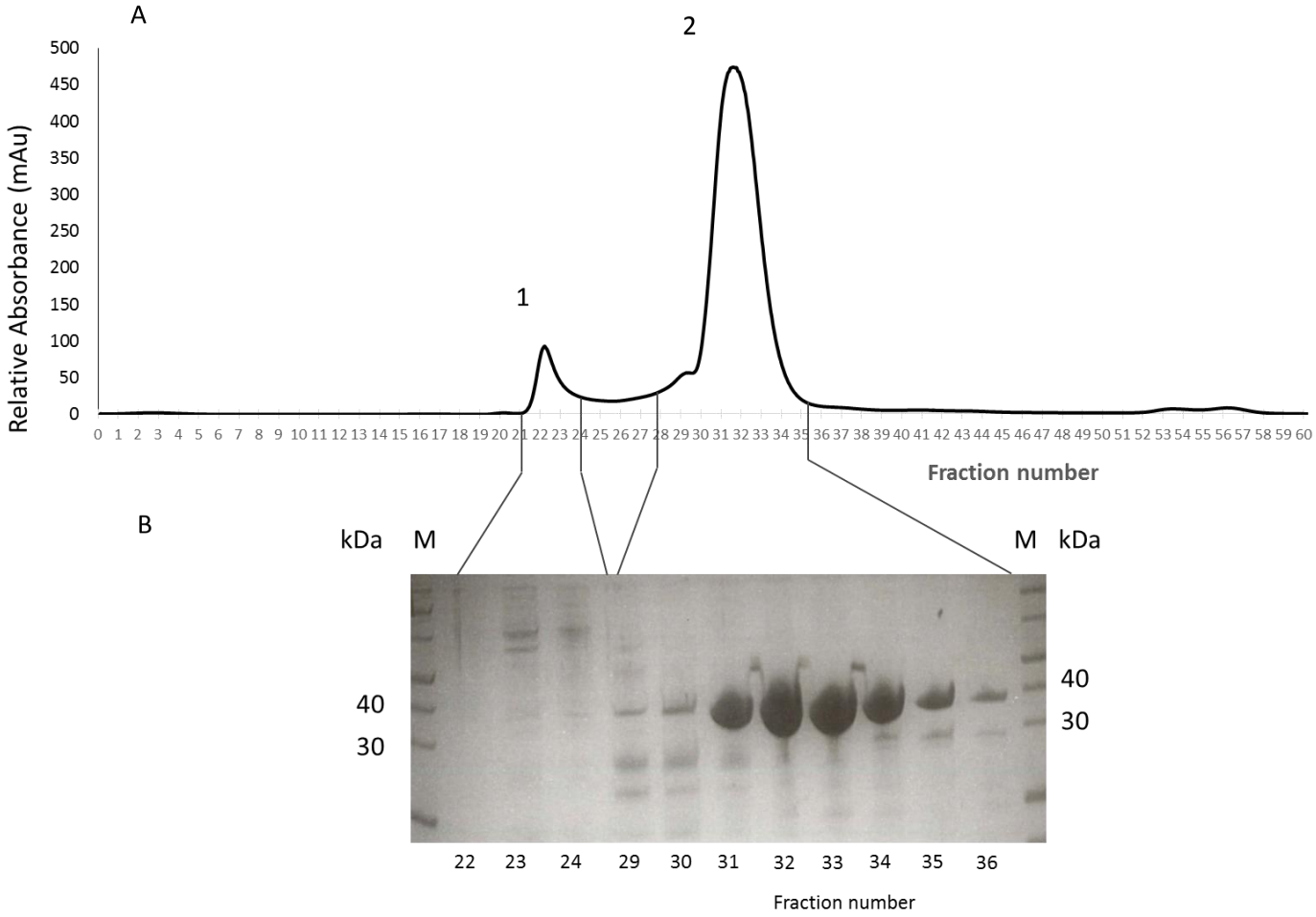

Figure 4.12: Size Exclusion Chromatography (SEC) of Tery_3377. **(A)** The purification was performed on a HiLoad 16/60 Superdex 200 size exclusion column. Fractions from peaks 1 and 2 as indicated were visualised through SDS-PAGE and Coomassie staining **(B).** Peak 2 protein samples were the correct size (36 kDa) for recombinant Tery_3377, thus fractions 31-34 were used in subsequent analysis.

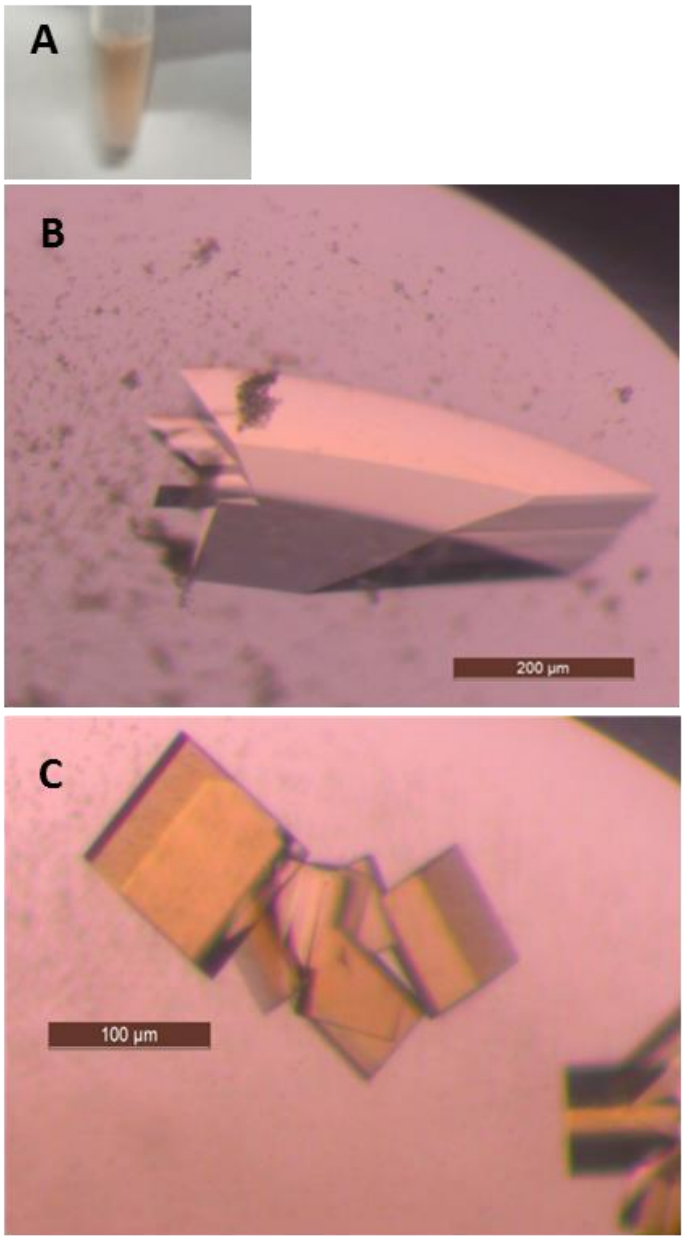

Figure 4.13: **Purification and crystallisation of Tery_3377**. The protein was overexpressed in *E.coli* which was induced with IPTG and kept for 16 hours at 18 °C. The cells were harvested and the hexa-histidine-tagged protein was extracted and subsequently purified through Ni^{2+}-affinity chromatography and size-exclusion chromatography (SEC) to give a coral-red coloured protein eluate **(A).** The protein crystallised into the apo-form **(B)** and Fe-loaded form **(C)** and the structure is currently being resolved.

4.3 Conclusions and further discussion

In an ocean of nutrient stress, primary producers have developed a plethora of adaptive strategies to survive and flourish. Two of these strategies are exemplified by the reported functions of a single protein which had been demonstrated to either contribute to Fe^{3+} uptake or protection of PSII under oxidative stress. Homologues of this protein have been differently annotated (FbpA, FutA, IdiA, AfuA, SfuA) according to their function or the organism they have been characterised in. To avoid confusion, I propose the conservation of the existing names, with FbpA assigned to the homologue of all pathogenic bacteria and the separation of cyanobacterial paralogues in FutA2 for the transporter binding protein and IdiA (FutA1) for the intracellular protein.

Bioinformatic analysis of the *Trichodesmium* homologue (Tery_3377), currently annotated as IdiA, indicates a closer similarity to FutA1 contradicting the common assumption that this protein is an Fe^{3+} transporter. However, GFP fusion to the protein signal sequence and heterologous expression in the model organism *Synechocystis* PCC 6308, indicates a clear periplasmic localisation (Sec. 4.2.2). Site directed mutagenesis (SDM) reveals that the mechanism for its export utilises the Twin Arginine Translocase (TAT) system (Sec. 4.2.3). In the periplasm Tery_3377 binds Fe (Sec. 4.2.6) and appears to contribute to cellular Fe^{3+} uptake (Sec. 4.2.5). Based on the results presented in this Chapter, Tery_3377 should be re-annotated as FutA2 instead of IdiA, as through the latter an intracellular function similar to the corresponding *Synechococcus* IdiA protein is inferred. Following these results, the cellular need for an alternative PSII protection strategy remains to be examined. The possibility of a Tery_3377 secondary intracellular role cannot be excluded (based on its complementation of the *Synechocystis futA1* mutant) (Sec. 4.2.5), and would be interesting to further address this question in the future.

A better characterisation of the two cyanobacterial variants is necessary to understanding potential secondary functions of Tery_3377. Contradicting results have previously been published regarding the two paralogues' localisation and function. Currently understood to bind Fe^{3+} (Katoh et al. 2001b; Waldron et al. 2007; Badarau et al. 2008), the two variants have previously been reported to carry Fe^{2+} (Koropatkin et al. 2007) and both have been assumed to be involved in Fe transport in early studies (Katoh et al. 2001b). FutA2 is now established as an Fe^{3+} transporter, due to the detrimental effect of its deletion to Fe uptake, and its periplasmic localisation (Fulda et al. 2000; Durán et al. 2004; Waldron et al. 2007; Badarau et al. 2008). However, it also potentially contributes to other processes such

as the reduction of Fe^{3+} during Fe uptake (Kranzler et al. 2014), or binding of periplasmic Fe to prevent obstruction of other metal transporters (e.g. copper) (Waldron et al. 2007).

The function of IdiA (FutA1) is even less well characterised than that of FutA2. In *Synechocystis*, Δ*futA1* mutants have been demonstrated either exhibit increased (Kranzler et al. 2014) or decreased (Katoh et al. 2001b) Fe uptake efficiency compared to the WT. For the former, strains of *Synechocystis* used are not derived from an isogenic parent, something that raises the risk of diverging irrelevant mutations that influence the study results. However, hypothesising that this is not the case, the observations could be explained by an upregulation of *futA2* and *feoB* expression and consequently Fe uptake (Kranzler et al. 2014) as a way of responding to the loss of FutA1 function in Δ*futA1*.

Here the presence of a valid FutA2 signal sequence acting to direct the protein to the periplasm is confirmed. Interestingly, traces of FutA1 signal sequence periplasmic expression are also observed even though we cannot exclude the case of unspecific translocation of the protein due to its potentially high levels of expression (expressed under the control of the *psbA2* promoter). From microscopic images alone this does not appear to be the case (no high intracellular pools of GFP are evident) but due to the lack of quantitative data on GFP expression we are unable to support this argument. Further study is required to identify whether FutA1 (IdiA) has an additional periplasmic role, possibly involved in Fe uptake.

To conclude, in this Chapter, the identity of Tery_3377 as an Fe^{3+} transporter is supported and its reannotation to FutA2 is suggested. However, further work is required to fully characterise the cyanobacterial FutA2 and IdiA paralogues and identify possible secondary roles of Tery_3377 in *Trichodesmium'*s Fe-stress metabolic response.

Chapter 5

Desert dust as a source of iron-

A physiological and transcriptomic study of *Trichodesmium*

5.1 Introduction

The main source of iron (Fe) to the open ocean is Aeolian dust deposition from the world deserts (Jickells et al. 2005; Ussher et al. 2013). It is expected that at circumneutral pH and oxic-conditions encountered in the surface oceans, Fe in dust (present as oxides, hydroxides and in aluminosillicate minerals) will in its majority be maintained as particulate (> 0.4 µm) or colloidal (0.02-0.4 µm) instead of soluble (< 0.02 µm). This is supported by laboratory experiments which suggest that within the dissolved fraction (< 0.2 µm) colloidal as opposed to soluble is the dominant form of dust Fe (Aguilar-Islas et al. 2010; Fitzsimmons et al. 2015). In addition, comparisons between computations of the total dust inputs and the Fe inventory of the oceans indicate solubility of dust Fe to be minimal (~1-2%) (Jickells & Spokes 2001).

The primary form of Fe utilised by phytoplankton is typically assumed to be soluble Fe and until recently it was believed that particulate/colloidal Fe is largely unavailable to these organisms. However, a growing number of studies is demonstrating the opposite (Nodwell & Price 2001; Frew et al. 2006; van der Merwe et al. 2015). Bioavailability seems to be not solely dependent on the speciation and solubility of Fe, with the identity of phytoplankton and the molecular tools in their repertoire proving critical.

Amongst their Fe acquisition strategies, phytoplankton employ siderophores, chelating agents with variable structures that are biotically produced and released in their immediate environment. There, they compete with other natural ligands and bind Fe^{3+} increasing its bioavailability (Neilands 1995). Moreover, microbially produced ligands also facilitate photolysis of Fe^{3+} to Fe^{2+} in the ocean's surface layer (Barbeau et al. 2001). The majority of known siderophores are produced by heterotrophic bacteria (Hopkinson & Morel 2009) with *Synechococcus* (Ito & Butler 2005; Boiteau & Repeta 2015) being the only marine cyanobacteria that have been identified to produce such ligands. However, other microorganisms (Poole et al. 1990; Guan et al. 2001) and amongst them *Trichodesmium* (Achilles et al. 2003; Roe et al. 2012), possess the ability to engage in a form of 'siderophore piracy' and benefit through the uptake of exogenous siderophores.

Uptake of organically complexed Fe can be direct or involve an extracellular reduction step and consequent release from its ligands before transport. In addition to organically complexed Fe species, reductive mechanisms possibly also target particulate and colloidal inorganic Fe (Rubin et al. 2011). Studies using the ligand ferrozine (which strongly binds Fe^{2+} and renders it unavailable for uptake) indicate a requirement for Fe reduction prior to its uptake by various phytoplankton species including eukaryotes as well as cyanobacteria such as *Synechocystis* and *Trichodesmium* (Shaked et al. 2005; Lis & Shaked 2009; Kranzler et al. 2011; Roe & Barbeau 2014).

Eukaryotic phytoplankton possess transmembrane ferric reductases (FRE) which transfer electrons to complexed Fe^{3+} and reduce it to Fe^{2+} facilitating its dissolution (Kustka et al. 2007). Consequently, the elevated Fe^{2+} concentrations surrounding the cell create potential for its uptake through divalent transporters including ZIP and NRAMPs (Kustka et al. 2007; Allen et al. 2008; Blaby-Haas & Merchant 2012). Further, multi-copper oxidases (MCO) (with similarity to the yeast multicopper oxidase, FET), can reoxidise Fe^{2+} to Fe^{3+} before uptake through associated Fe^{3+} permeases (FTR) (Herbik et al. 2002; Boukhalfa & Crumbliss 2002; Maldonado et al. 2006; Y. Paz et al. 2007a). Recently, a copper oxidase-independent Fe^{3+} uptake system was also identified to function in eukaryotic phytoplankton through the membrane protein ISIP2a (Morrissey et al. 2015).

Reduction and uptake of Fe by cyanobacterial cells is less well understood and the components involved are yet to be fully elucidated. In *Synechocystis* PCC 6803 *Synechocystis* hereafter), the transfer of electrons to Fe^{3+} was suggested to be mediated through the plasma-membrane-located alternative respiratory terminal oxidase (ARTO),

with the knockout mutant displaying impaired Fe reduction and uptake (Kranzler et al. 2014). Also, deletions of pili (Lamb et al. 2014), structures known to be electrically conductive (Reguera et al. 2005; Gorby et al. 2006) inhibit the organism's growth on Fe oxides.

Moreover, the export of reactive oxygen species (ROS) has been proposed to contribute to reductive Fe uptake in both eukaryotic and prokaryotic phytoplankton. Several species including *Trichodesmium* were previously shown to produce ROS (Henry & Vignais 1980; Yamasaki et al. 2004; Marshall et al. 2005; Rose et al. 2005; Godrant et al. 2009; Roe & Barbeau 2014; Hansel et al. 2016) and evidence suggests that superoxide can contribute to inorganic Fe (but not to ferric citrate) uptake in *Trichodesmium* (Roe & Barbeau 2014).

Once reduced, Fe can very quickly revert to its original oxidised state, therefore binding of Fe^{2+} and microbial adaptations that increase its stability, as well as its efficient transport, are necessary. The puff colony morphotype of *Trichodesmium* was hypothesised to increase uptake of Fe from dust by maintaining an anoxic colony core environment, favourable in keeping Fe^{2+} reduced (Hall & Pearl 2011; Rubin et al. 2011). Environmentally collected *Trichodesmium* puff colonies attach to desert dust particles and coordinate in an incredible example of cooperative multicellularity to centralise dust to the colony cores (Rubin et al. 2011). Previous experiments have also recorded dust-stimulated colony formation by *Trichodesmium erythraeum* IMS101 in culture (Langlois et al. 2012).

Although processes associated with the *Trichodesmium* cell surface have been suggested to enhance dissolution of Fe from desert dust and ferrihydrite, Rubin et al. 2011 only observe this to be the case for *Trichodesmium* puff colonies and not filamentous *Trichodesmium* in culture. The latter could enhance dissolution from ferrihydrite, approximately 13 x less efficiently than puffs. Nevertheless, filamentous laboratory grown *Trichodesmium* is able to access desert dust-bound Fe for growth (Langlois et al. 2012).

The contribution of the cell surface to Fe dissolution was previously supported (Rubin et al. 2011) through comparisons of Fe uptake from free ^{55}Fe ferrihydrite to that trapped within the fibres of a glass fibre filter. The possibility that this entrapment blocks dissociation of free inorganic Fe (Fe') from ferrihydrite particles was not addressed. Also EDTA was not included in the experimental media and therefore re-precipitation of Fe' following its dissolution is possible when binding by the cells is prevented (Rubin et al. 2011). Therefore, although evidence seems to support that the cellular processes promote dissolution of Fe

from colloidal ferrihydrate, the importance of cell-to-substrate contact for this process is yet to be fully determined.

Using *Trichodesmium erythraeum* IMS101 cultures (hereafter *Trichodesmium*) we attempt to better characterise the Fe uptake strategies involved in accessing Saharan desert dust Fe. Through the development of a simple experimental design, we evaluate the significance of cell surface contact for this process. Furthermore, the organism's response to dust and Fe-stress are compared at the transcriptomic level by RNA sequencing analysis with the aim of describing the molecular pathways coordinating them.

5.2 Experimental design

The importance of cell-to-substrate contact for acquisition of Fe from Saharan desert dust by *Trichodesmium*, was assessed by separating the cells from dust added to the media (mYBC-II), using dialysis tubing ([Dust]). This was compared to cultures in which dust was included in the direct vicinity of the cells (Dust+) and no- dust treatments with (Fe+) or without (Fe-) the addition of 400 nM $FeCl_3$-EDTA. All cultures contained dialysis tubing to keep experimental conditions identical across treatments and a no-dialysis tubing control (no DT) was used to assess potential Fe contamination as a result its inclusion (Fig. 5.1). The experiment was run in triplicate and was maintained for 17 days during which the physiology of *Trichodesmium* was monitored.

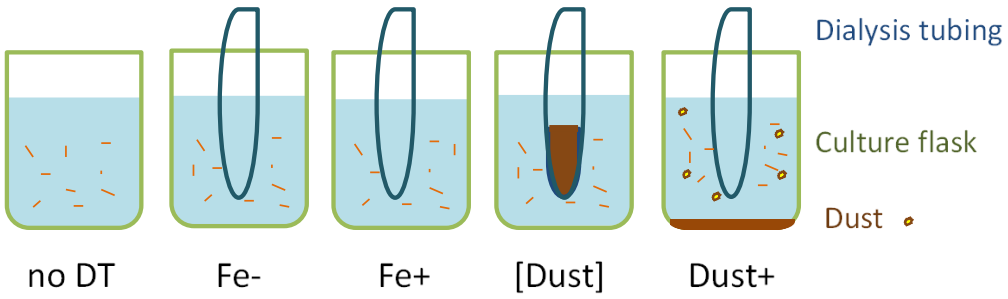

Figure 5.1: The experimental design. Dust was provided to cultures with mYBC-II and equal concentrations of *Trichodesmium* cells either separated by a dialysis membrane such that leachate but not dust comes in contact with cells ([Dust]) or in the direct vicinity of cells (Dust+) permitting their interaction. Set in the same way cultures with (Fe+) or without (Fe) added $FeCl_3$-EDTA were used for comparison. Dialysis tubing, was included in all treatments to correct for any possible effects, and no-dialysis tubing cultures (no DT) were maintained as a control.

To test whether nutrients from dust dissolved preferentially when dust was free in the culture vessels, compared to when enclosed in dialysis tubing *Trichodesmium*'s physiological response was monitored in a separate control experiment. This involved the incubation of experimental treatments, identical to the ones set in the abovementioned experiment, but without *Trichodesmium* cells, for a period of 14 days before filtration in clean culture flasks and subsequent inoculation with equal concentrations of cells (Fig. 5.2). The growth of cultures was monitored for a period of 9 days thereafter.

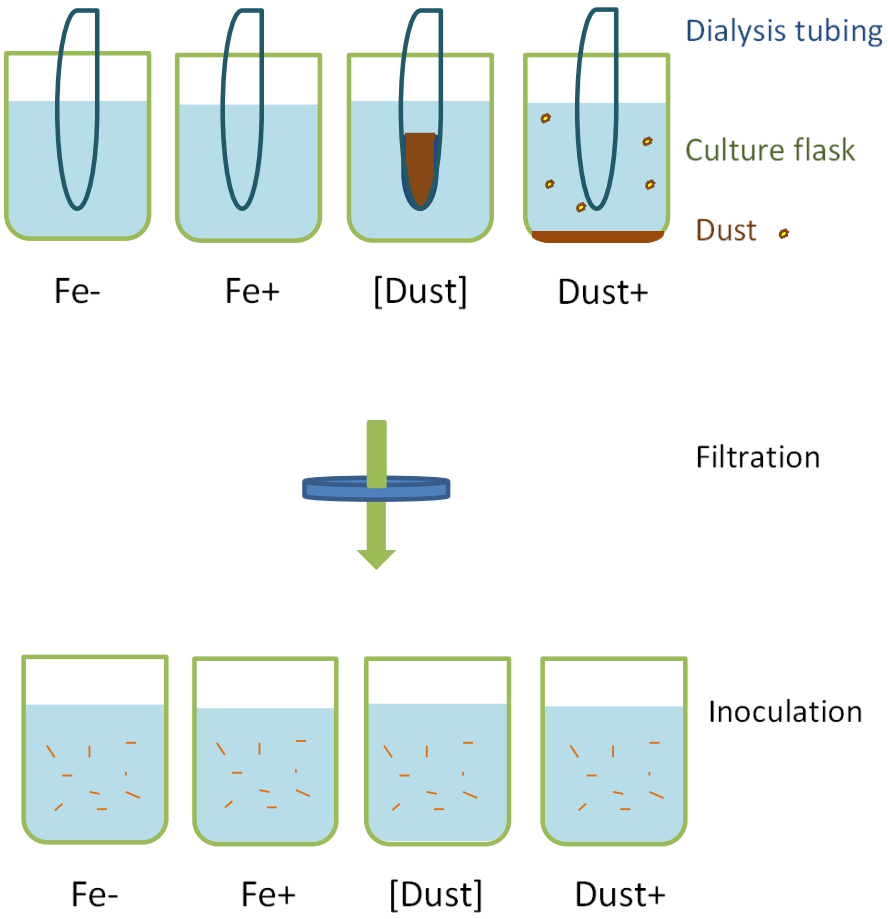

Figure 5.2: Experimental design to assess possible differential dissolution of nutrients from dust enclosed or not enclosed in dialysis tubing. Conditions used were identical to the previous experiment but *Trichodesmium* cells were omitted. Following a period of 14 days all conditions were filtered through 0.22 µm sterile filters (Millipore, Watford, UK) and mYBC-II was inoculated with equal concentrations of *Trichodesmium* cells.

5.3 Results and discussion

5.3.1 Experimental controls

Using a control treatment, the effect of washed dialysis tubing (DT) to Fe deficient media was examined. Comparison between the Fe deficient treatment with (Fe-) and without (no DT) DT revealed no statistical differences in F_V/F_m (estimate of the apparent photosystem II photochemical quantum efficiency) and σ^{PSII} (functional absorption cross section of photosystem II) or growth rates and filament lengths indicating no/insignificant trace metal contamination during installation of the DT (Fig. 5.3).

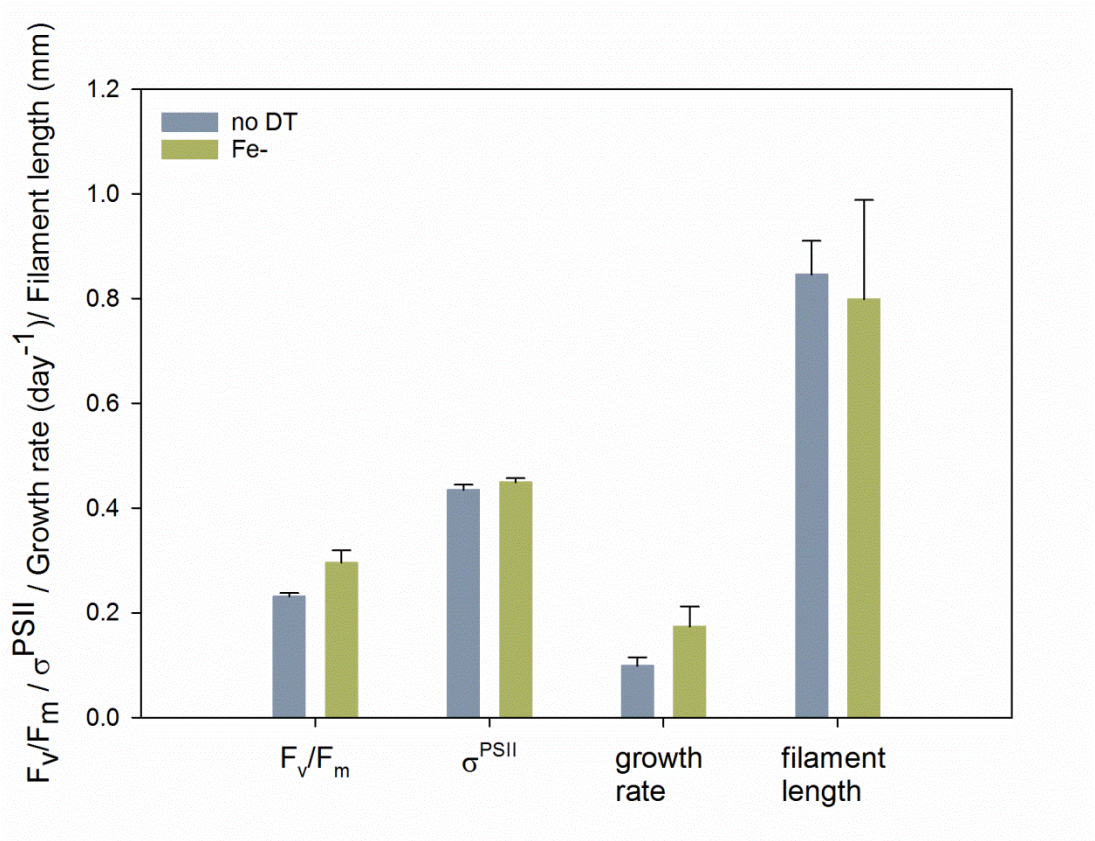

Figure 5.3: Assessment of potential dialysis tubing effects when included in the experiment. Comparison of the no dialysis tubing (no DT) control treatment to the equivalent Fe- treatment with DT included (Fe-) indicates that growth rate during exponential growth, as well as filament lengths and photosynthetic physiology parameters (F_v/F_m and σ^{PSII}) measured on the final day of the experiment, did not differ significantly between the two treatments. Error bars represent standard deviations from the mean of three biological replicates.

The second control experiment was aimed at investigating whether the experimental set up alone promoted differential release of dust-associated chemicals affecting *Trichodesmium* between [Dust] and Dust+ treatments. No statistically different growth was identified in media preincubated with dust inside or outside the DT and growth rates in both cases did not exceed those of the Fe- cultures. On the contrary, in Fe+ media growth rates were significantly (GLM and Tukey test, $P < 0.05$) faster (25-35%) compared to all other treatments (Fig. 5.4).

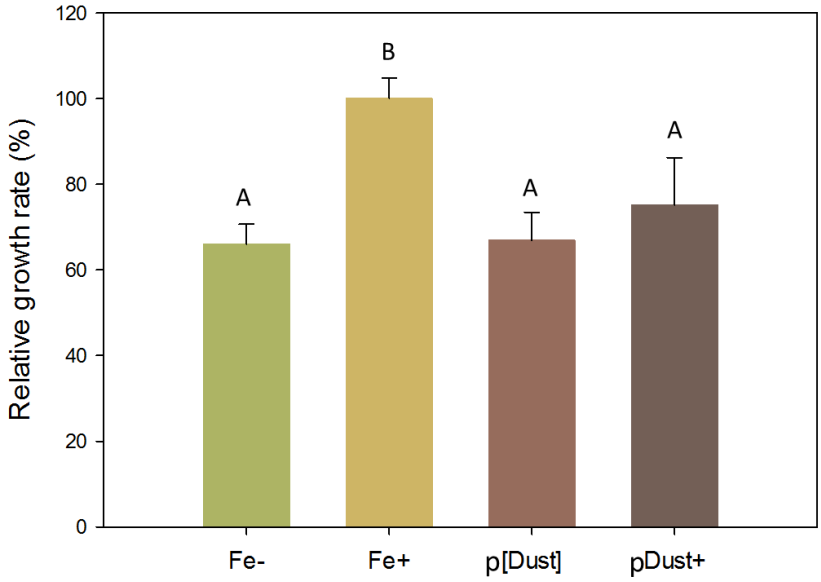

Figure 5.4: Assessment of potential inhibitory effect of the dialysis tubing on abiotic dust-chemical dissolution. Similar growth rate of *Trichodesmium* in preincubated (p) Dust+ and [Dust] treatments indicates that differential dissolution of nutrients from dust is not affecting the experimental results. The growth rate is represented as the percentage of the highest (recorded in the Fe+ treatment). Distinct letter groups (A and B) mark significant differences (GLM and Tukey test, $P < 0.05$) between Fe+ and the remaining treatments. Error bars are standard deviations of the mean of triplicate cultures.

5.3.2 Dust as a source of iron- the role of cell surface contact

As the experimental design was tested through control experiments and the results excluded major interference and bias by the DT, the set up was justified as a valid approach to address our scientific questions. Therefore, the effect of Saharan desert dust to *Trichodesmium* physiology when in contact (Dust+) or separated ([Dust]) from the cells was compared to Fe- and Fe+ treatments to investigate the potential contribution of cell surface processes to Fe acquisition.

During the course of the experiment growth of *Trichodesmium* was significantly (GLM and Tukey test, $P < 0.05$) faster in Fe+ (0.35 day^{-1}) and Dust+ (0.31 day^{-1}) compared to Fe- (0.17 day^{-1}) and [Dust] (0.22 day^{-1}) for which growth rate was 1.8-2 and 1.4-1.6 times reduced respectively (Fig. 5.5). This indicates the preferential growth in the presence of $FeCl_3$, but also when dust is added to the direct environment of *Trichodesmium* cells. The same does not apply when dust is separated from the cells (significantly slower growth in [Dust] compared to both Dust+ and Fe+).

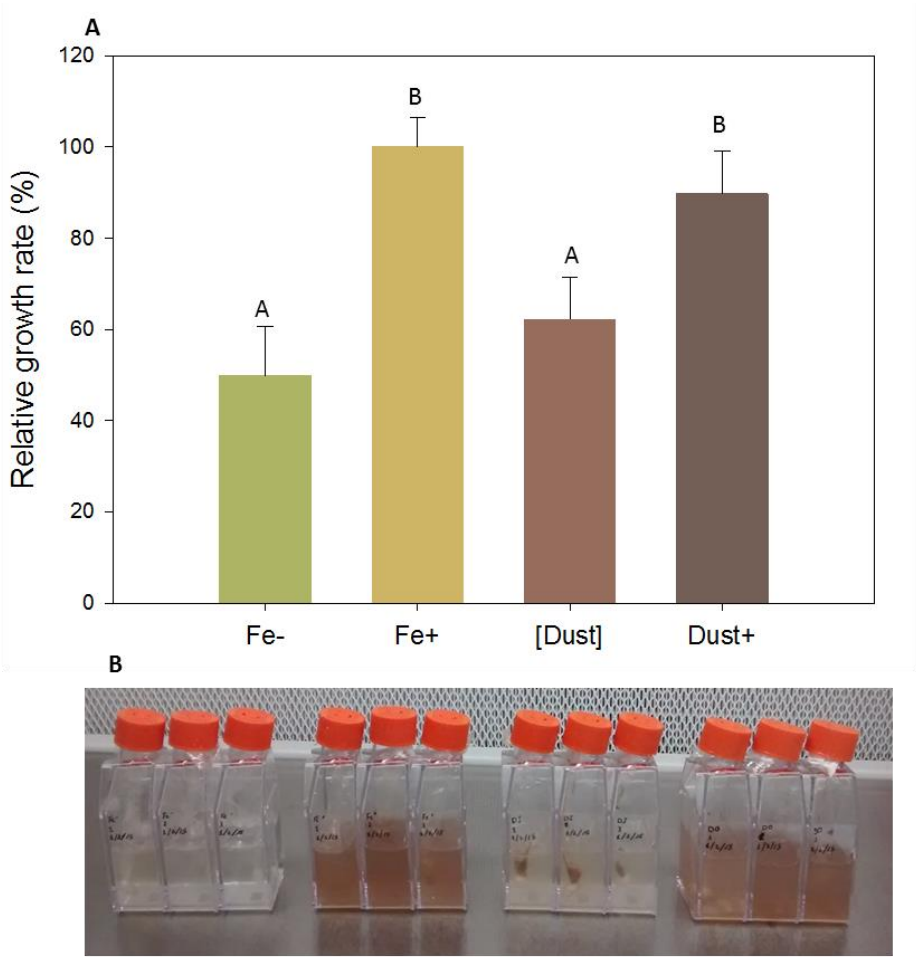

Figure 5.5: Growth of *Trichodesmium* under different Fe regimes. Cell concentration in dust added (Dust+, dark brown), dust separated ([Dust], light brown), $FeCl_3$-EDTA added (Fe+, yellow) or Fe deficient (Fe-, green) cultures was monitored over 17 days and **(A)** growth rates were calculated during late exponential phase. Growth rates presented are scaled relative to the maximum (Fe+) and statistically significant differences (GLM and Tukey test; $P < 0.05$) between treatments are indicated with dissimilar letter groups (A, B). Error bars represent standard deviations of three biological replicates. **(B)** Visual assessment of the cultures reveals different pigment concentration across treatments on the last day of the experiment (day 17).

Furthermore, on the last day of the experiment filaments were on average shorter in Fe+ (0.45 mm) compared to Fe- (0.80 mm) and Dust+ (0.76 mm) cultures (GLM and Tukey test, $P < 0.05$). The filament length of [Dust] cultures (0.72 mm) was not significantly dissimilar to any of the other treatments (Fig. 5.6). Deviation in *Trichodesmium* filament lengths between Fe+ and Fe- conditions was previously described in literature, but this has not always been consistent with some studies reporting longer filaments in Fe+ compared to Fe- (Küpper et al. 2008) and some in Fe- compared to Fe+ (Roe et al. 2012). Iron limitation experiments conducted under our laboratory conditions have consistently supported the results presented here (Snow et al. 2015).

Although the shorter size of Fe+ filaments could be the result of faster growth rate in this treatment, this explanation cannot justify the similarity between Fe- and Dust+. We suggest that a different process might be stimulating persistence of longer filaments in the Dust+ and [Dust] treatments. It can be hypothesised that stimuli from dust-leached minerals trigger this physiology and the possibility that longer filaments are favourable to more efficiently access particulate or colloidal Fe requires further study. Multicellularity has been previously linked to dust processing (Rubin et al. 2011) and studies indicated induction of colony formation by dust in *Trichodesmium* filamentous cultures (Langlois et al. 2012).

The growth rate dissimilarity between treatments is paralleled by difference in photosynthetic efficiency (F_v/F_m). In Fe- and [Dust] treatments F_v/F_m declined from day 6 to day 17 by 0.15 and 0.16 respectively while Fe+ cultures established a significantly (GLM and Tukey test, $P < 0.05$) higher F_v/F_m compared to the rest of the treatments from day 6 onwards (F_v/F_m on day 6= 0.53). Dust+ cultures experienced an initial drop on day 6 (0.42) with recovery by day 8 (0.5) and remained significantly (GLM and Tukey test, $P < 0.05$) higher than Fe- and [Dust] cultures until the end of the experiment (Fig. 5.7). The differences in F_v/F_m, if used as an indication of cellular photosynthetic activity, provide justification to the distinct growth rates observed between treatments.

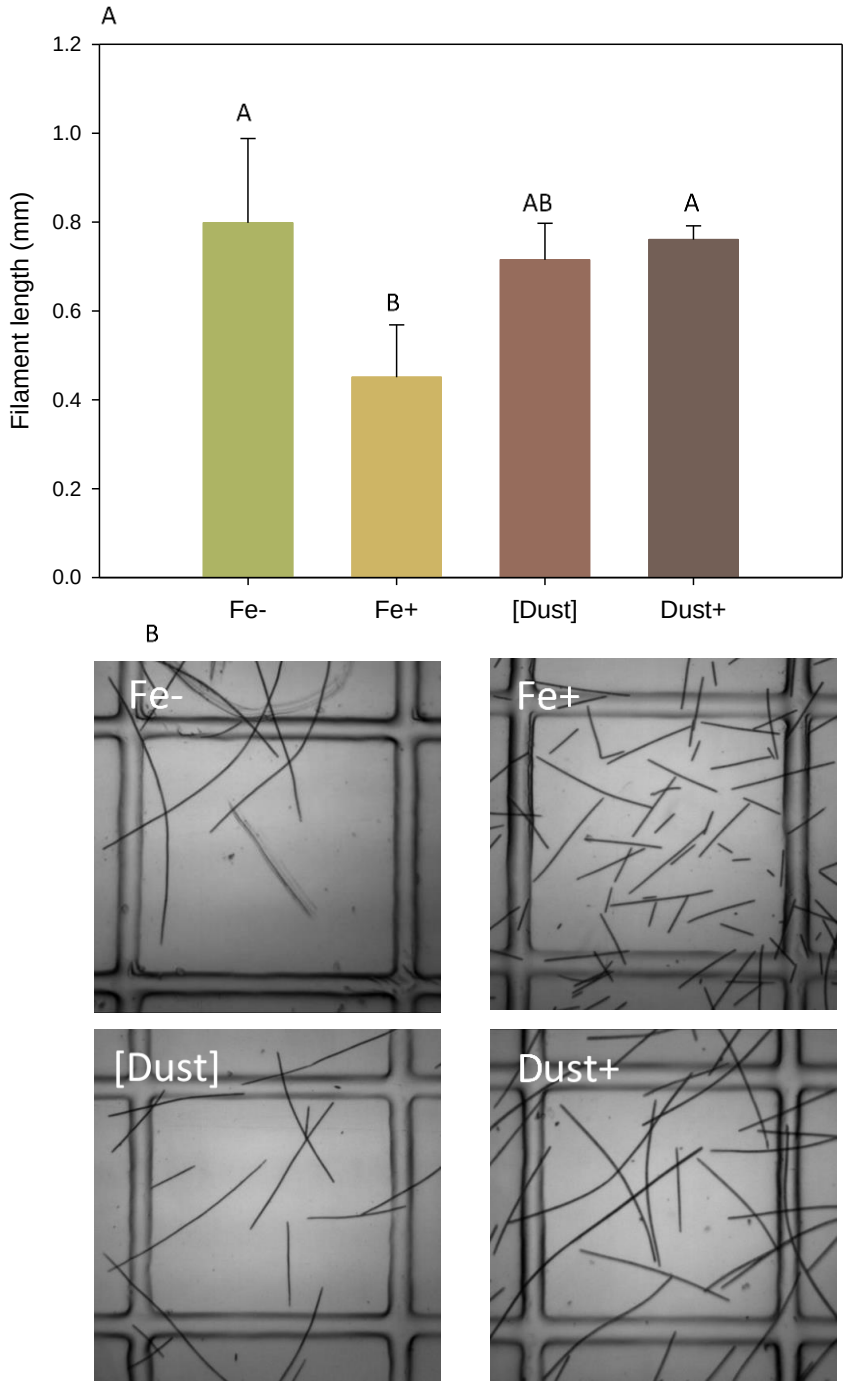

Figure 5.6: *Trichodesmium* filament physiology under different Fe regimes. $FeCl_3$-EDTA added (Fe+) cultures (A: yellow, B: top right) had significantly (GLM and Tukey test; $P < 0.05$) shorter filaments compared to Fe deficient (Fe-) (A: green, B: top left) and dust added (Dust+) cultures (A: dark brown, B: bottom right). In the dust separated ([Dust]) treatment (A: light brown, B: bottom left) filaments were not different in size to any other treatment. Statistically different filament lengths are indicated by distinct letter groups (A, B). Error bars are standard deviations of triplicates.

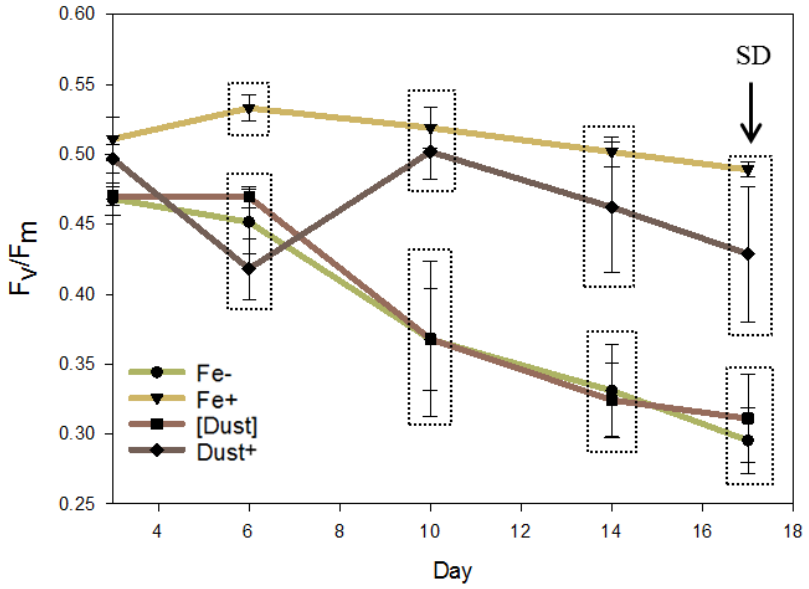

Figure 5.7: *Trichodesmium* photosynthetic efficiency (F_v/F_m) under different Fe regimes. Samples from Fe+ (yellow), Dust+ (dark brown), Fe-(green) and [Dust] (light brown) cultures were taken after 2-2:30 hrs of light during a 12 hr: 12 hr light: dark cycle for 17 days of growth. Statistically different groupings (GLM and Tukey test; $P < 0.05$) between treatments for each day are marked (dashed squares) until the end of the experiment (sampling day, SD). Error bars are standard deviations of the means of three biological replicates for each treatment.

The functional absorption cross section of PSII (PSII), σ^{PSII}, had a more varied response over time and between treatments compared to F_v/F_m. The Fe+ treatment had lower values (0.40-0.42 $Å^2$ $quantum^{-1}$) than the rest (0.42-0.50 $Å^2$ $quantum^{-1}$) between days 6 to 14 and this difference was on some occasions significant (GLM and Tukey test, $P < 0.05$) (Fig. 5.8). By day 17 of the experiment σ^{PSII} of all treatments converges around 0.45 $Å^2$ $quantum^{-1}$ except for the Dust+ cultures which maintain high values (0.49 $Å^2$ $quantum^{-1}$). Iron stress conditions are known to stimulate an increase of σ^{PSII} possibly as a result of accumulating antennae complexes (Küpper et al. 2008). This physiological behaviour, currently not fully understood, is thought to perhaps allow a reduction in the number of the Fe expensive photosystem II (PSII) units as does the iron stress induced protein A, IsiA (Bibby et al. 2001) for photosystem I (PSI). Although this could justify the lower σ^{PSII} recorded in the Fe+ compared to the Fe- treatment the same relationship is not identifiable in Dust+ compared to [Dust]. Instead Dust+ σ^{PSII} is maintained at a significantly (GLM and Tukey test, $P < 0.05$) higher level compare to that of Fe+ cultures (day 6 -17). Shading or reflection of light by dust particles has to be considered as a possible driver for bigger antenna size requirements in Dust+.

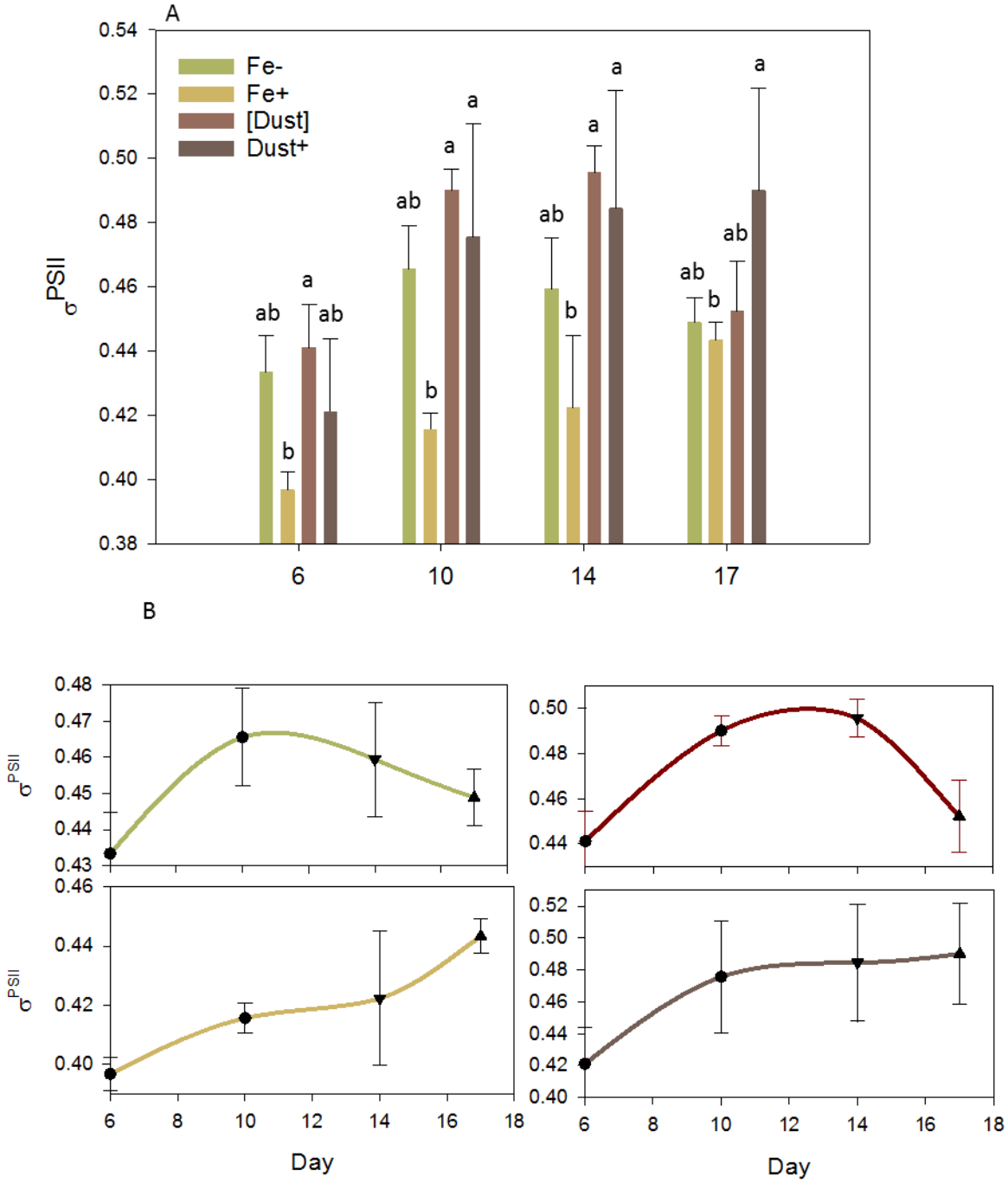

Figure 5.8: *Trichodesmium* functional absorption cross section of PSII (σ^{PSII}) during growth under different Fe regimes. (A) The treatments Fe+ (yellow), Dust+ (dark brown), Fe- (green) and [Dust] (light brown) are compared to each other on different days of the experiment and **(B)** changes in their σ^{PSII} are assessed over time. Statistical significant differences in A (GLM and Tukey test; $P < 0.05$) is indicated by a distinct letter group (a, b). Error bars are the standard deviations from the mean of three replicate cultures.

Looking at the evolution of the σ^{PSII} response in each treatment over time allows the identification of two distinct patterns of behaviour amongst the four treatments (Fig. 5.8B). The first is observed in the [Dust] and Fe- treatments as an elevated σ^{PSII} on days 10 and 14 compared to days 6 and 17 creating an inverted U-shape pattern. The late reduction of the photosystem antennae on day 17 could be due to an extreme exhaustion of Fe resources beyond the threshold at which an increase would be beneficial to the cells. The second behaviour is observed in the Fe+ and Dust+ treatments and involves the steady increase or maintenance of σ^{PSII} over time (day 6-17). It is possible that this describes the fine tuning of the antennae as light or Fe concentrations in the media are decreasing in the Fe+ and Dust+ treatments over time.

The deviation of physiological parameters, including growth rate and F_v/F_m as well as the σ^{PSII}, between Dust+ and [Dust] treatments, indicates an advantage when dust particles are in direct physical contact with cells. These differences resemble those measured between Fe- and Fe+ suggesting differential Fe uptake efficiency in the two dust treatments. The observations provide the first direct evidence for a link between cell growth and photosynthetic physiology to cell surface contact with dust.

5.3.3 RNA sequencing results- An overview

To determine the underlying mechanisms resulting in the physiological differences between Dust+ and [Dust] and compare them to those between Fe+ and Fe-, samples from all conditions were acquired on the last day of the experiment (day 17) at 5 hrs through the light period (12 hr: 12 hr light: dark cycle) and RNA was extracted and sequenced.

Reads were aligned against the *Trichodesmium erythraeum* IMS101 genome which is composed of 4451 annotated genes only ~54% of which are annotated with a Gene Ontology (GO) classification number (GO annotated) (Fig. 5.9). Expression of the majority of *Trichodesmium* genes (4342 genes) was identified in at least one treatment and 4076 were identified in all 4 treatments. Of these 3257 genes had read counts above the statistical threshold required for inclusion in differential gene expression analysis, as determined by the DESeq2 Bioconductor package (Love et al. 2014). Expression of approximately one third of those genes (1050) was significantly affected by growth condition ($P < 0.05$, DESeq ANODEV) (Fig. 5.9). It can also be observed that greater statistical power for detection leads to a higher identification of differentially expressed genes at increased expression intensities (aligned read counts) (Fig. 5.10).

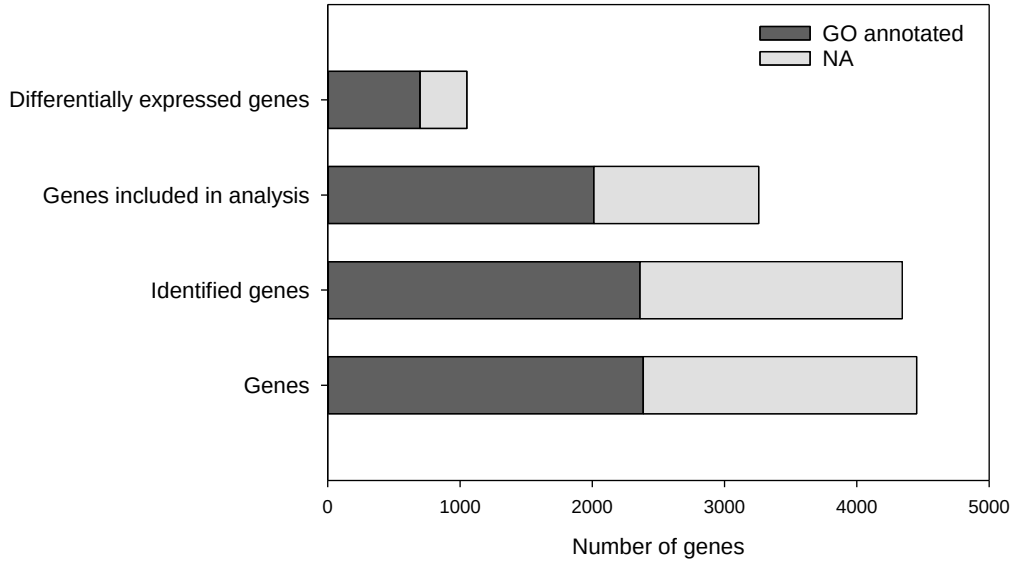

Figure 5.9: Gene numbers and GO annotation coverage. The majority of *Trichodesmium* genes (Genes) are identified in at least one condition of the experiment (Identified genes). Genes for which expression is recorded in all treatments above threshold quantities (Genes included in analysis) are analysed to identify differential expression (differentially expressed genes). A large proportion of the *Trichodesmium* genome is not GO annotated (NA, light grey).

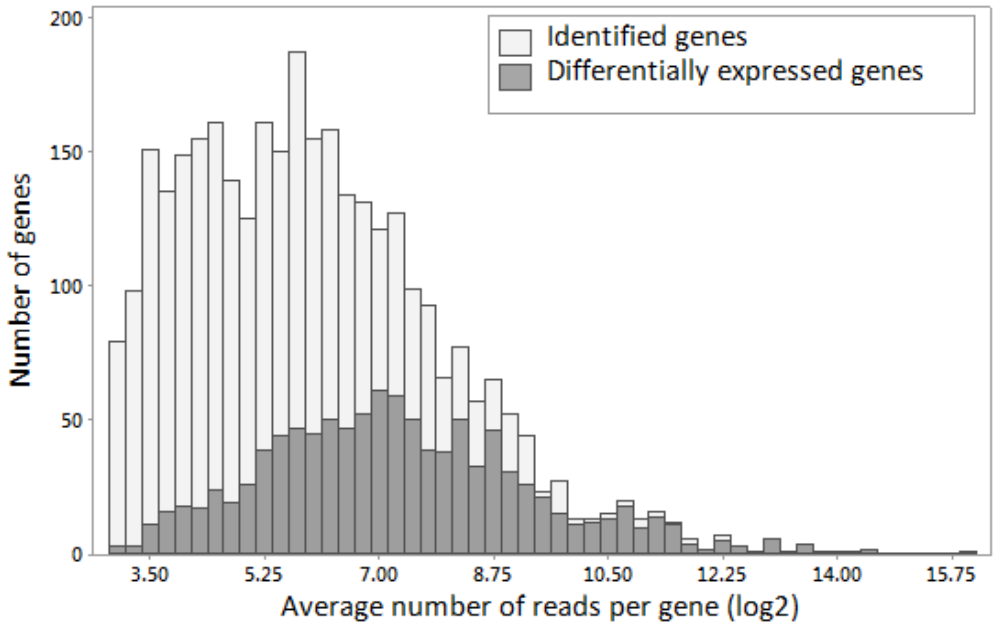

Figure 5.10: Distribution of the number of genes expressed across different levels of reads/gene. The distribution of the number of genes identified in the analysis (light grey) is compared to the distribution of the number of differentially expressed genes (dark grey). Detection of differential expression is skewed towards highly expressed genes.

The validity of replicates within each treatment was confirmed through clustering analysis which showed closer intra-treatment to inter-treatment similarities. Treatments clustered in two distinct sets with closer similarity between [Dust] and Fe- cultures and between Fe+ and Dust+ (Fig. 5.11). This indicates that the growth conditions stimulate related gene expression phenotypes between those groups in support of growth and photosynthetic physiological responses observed (Sec. 5.3.2).

In addition, comparisons of the numbers of genes differentially expressed in treatments Dust+, [Dust] and Fe- relative to Fe+ is presented in Figure 5.12. The highest dissimilarity to Fe+ was identified in [Dust] samples (797 genes), while 419 genes are differentially expressed compared to Dust+, and 438 genes compared to Fe-. Increased changes in gene expression between of Fe+ and [Dust] is perhaps the result of no access to Fe in this treatment (compared to Dust+) but at the same time dissolution of dust-bound chemicals, altering the chemical composition of the media (as opposed to Fe-).

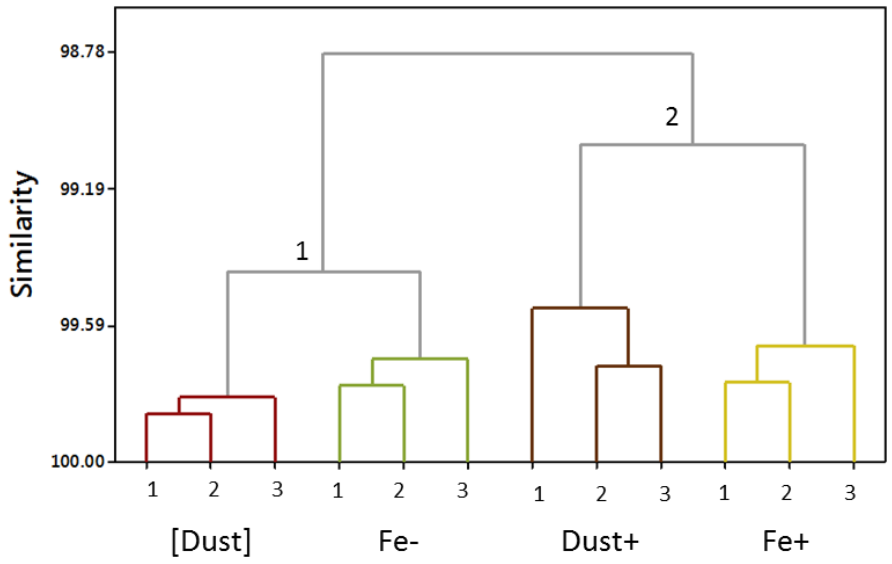

Figure 5.11: Gene expression clustering across treatments and replicates. Dendrogram from average linkage clustering of treatments [Dust], Fe-, Dust+ and Fe+ indicates that replicates of each treatment are grouped together while two main clusters (1, 2) describe closer expression relationships between treatments [Dust] and Fe- (1). and Dust+ with Fe+ (2).

When compared to gene expression in Fe+ conditions, Dust+ and [Dust] treatments share 125 genes expressed similarly, [Dust] and Fe- 179 genes, while Fe- and Dust+ only 16 genes This observation suggests the presence of two main drivers shaping the transcriptomic responses identified in this experiment: (A) the availability of Fe and (B) the presumed

presence of dust-leached chemical stimuli. As identified in the clustering analysis (Fig. 5.11), the former appears to be the overriding driver (Fe+ and Dust+ are more similar than Fe+ and Fe-).

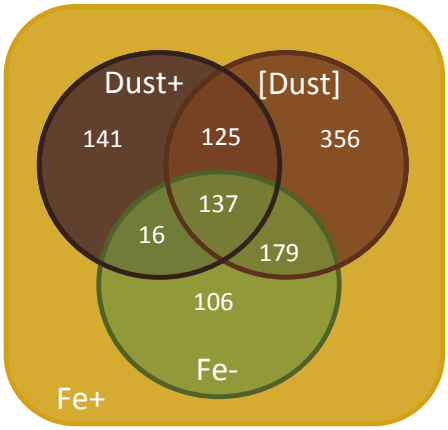

Figure 5.12: Comparison of differential expression across the experimental treatments. The number of genes differentially expressed uniquely and in combination in the Fe- (green), Dust+ (dark brown) and [Dust] (light brown) treatments is compared to the Fe+ (yellow) treatment.

To visualise the array of expression patterns across the experimental treatments (Fig. A.1) and characterise the drivers shaping these, the differentially expressed genes were grouped in 10 clusters based on their expression profile across the four experimental conditions (Fig. 5.13, Table 5A). The Dust+ stimulated genes are observed to group together in Cluster 3 (n=86) while dust leached chemical stimuli seem to affect the expression of genes in Clusters 1 (upregulation in [Dust] and Dust+ compared to Fe+ and Fe-, n=71) and 8 (downregulation in [Dust] and Dust+ compared to Fe+ and Fe-, n=74). The majority of genes fall in Clusters 10 (n=259) and 2 (n=185) in which Fe+ and Dust+ treatments are either experiencing higher (Cluster 2) or lower (Cluster 10) expression levels relative to Fe- and [Dust]. The third (Cluster 6, n=135) and fourth (Cluster 4, n=109) largest clusters represent the bidirectional gene regulation of Fe+ distinctly to Fe-, Dust+ and [Dust] treatments.

These clustering results indicate that the majority of genes follow a linked response in Fe+ and Dust+ compared to [Dust] and Fe- but also a considerable number of genes in Fe+ but not Dust+ is uniquely different to the Fe deficient [Dust] and Fe-. These results are interesting as they point to a response specific to either (1) increased available Fe/higher Fe concentrations, (2) higher presence of Fe as dissolved inorganic Fe' as opposed to bound in particulate/colloidal dust or (3) dissimilar nutrient composition of the media when Fe is provided alone (Fe+) compared to when provided as dust (Dust+).

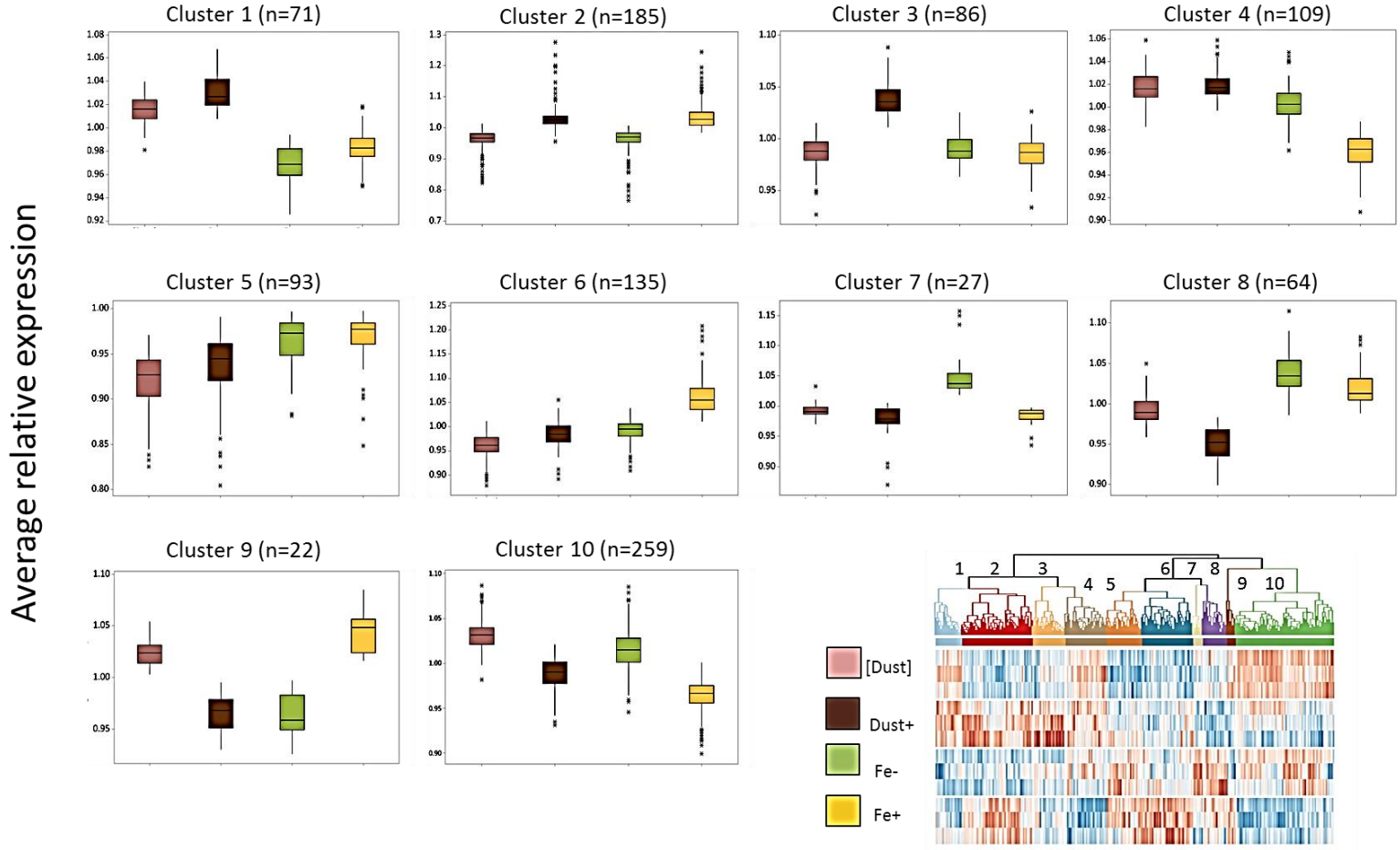

Figure 5.13: Clustering demonstrates patters of differential expression across all genes and treatments. Ten clusters of different expression profiles across the [Dust] (light brown), Dust+ (dark brown), Fe- (green) and Fe+ (yellow) treatments were generated (Pearson product moment correlation coefficient between each pair of differentially expressed genes and WPGMA). For plots Cluster 1-10 the average expression for each treatment is corrected to the average across all treatments. A dendrogram of the clusters details the expression across all differentially expressed genes in a heatmap.

Table 5A: Clustering of differentially expressed genes in 10 distinct patterns across experimental treatments.

Cluster	Number of genes	Description	Gene examples
1	71	Upregulation in [Dust] and Dust+ compared to Fe- and $FeCl_3$	*psbH (Tery_2868)* *psbJ (Tery_3507)* 50S ribosomal protein L25 *(Tery_3283)*
2	185	Upregulation in $FeCl_3$ and Dust+ compared to [Dust] and Fe-	cytochrome c (*Tery_2561*) hemolysin-type calcium-binding (*Tery_0419*) cell surface protein (*Tery_0849*)
3	86	Upregulation in Dust+ compared to $FeCl_3$ [Dust] and Fe-	F0F1 ATP synthase subunit C (*Tery_2203*) phycobilisome protein (*Tery_0983*) phycocyanin, alpha subunit (*Tery_5048*)
4	109	Downregulation in $FeCl_3$compared to Dust+, [Dust] and Fe-	photosystem q(b) protein (*Tery_4763*) fructose-bisphosphate aldolase (*Tery_1687*) photosystem antenna protein-like (*Tery_1667*)
5	93	Upregulation in Fe- and $FeCl_3$ compared to Dust+ and [Dust]	ATPase AAA-2 (*Tery_2437*) peptidyl-prolyl cis-trans isomerase, cyclophilin type (*Tery_2705*) UDP-glucose 6-dehydrogenase (*Tery_2477*)
6	135	Upregulation in $FeCl_3$compared to Dust+, [Dust] and Fe-	hemolysin-type calcium-binding (*Tery_3467*) tetratricopeptide TPR_2 (*Tery_2560*) ATPase (*Tery_2501*)
7	27	Upregulation in Fe- compared to Dust+, [Dust] and $FeCl_3$	ferredoxin-nitrite reductase (*Tery_1068*) OpcA protein (*Tery_0685*) 6-phosphogluconate dehydrogenase (*Tery_1834*)
8	64	Downregulation in Dust+ and [Dust] (more intensely in the former) compared to Fe- and $FeCl_3$	cytochrome-c oxidase (*Tery_0277*) peptidoglycan glycosyltransferase (*Tery_2090*) fructose-1,6-bisphosphatase (*Tery_0682*)
9	22	Upregulation in [Dust] and $FeCl_3$compared to Dust+ and Fe-	signal transduction protein (*Tery_2045*) ribonuclease III (*Tery_2839*) Chk2 histidine kinase (*Tery_3912*)
10	259	Downregulation in $FeCl_3$ and Dust+ compared to [Dust] and Fe-	plastocyanin (*Tery_2563*) hemolysin-type calcium-binding region (*Tery_2055*) Mo-dependent nitrogenase-like (*Tery_4114*)

5.3.4 RNA sequencing technique validation

The results of the RNA sequencing (RNAseq) analysis were validated via quantitative reverse transcription (RT) Polymerase Chain Reaction (qPCR) using three of the identified differently expressed genes (*Tery_2561, Tery_1667, Tery_4114*) The cytochrome c_{553} gene (*cyt* c_{553}*, Tery_2561*) was upregulated in Fe+ and Dust+ compared to Fe- and [Dust], iron-stressed-induced protein-A gene (*isiA, Tery_1667*) downregulated in Fe+ compared to the rest of the treatments and the Mo-dependent nitrogenase-like-protein gene (*nif-like*, *Tery_4114*) upregulated in the [Dust] and Fe- compared to Dust+ and Fe+ treatments.

For qPCR normalisation, candidate reference genes *rnpB* (*Tery_R0021*) and *glyA* (*Tery_2660*), previously used to correct gene expression in Fe-stress experiments (Chappell & Webb 2010), and genes for the gas vesicle protein (*gvpN*, *Tery_2329*) and ribonuclease T2 (*Tery_3279*) selected from stably expressed genes across the experimental treatments (as identified from this RNAseq analysis), were tested. The latter pair was the most stable combination (geNorm, qBase, Biogazelle, Belgium) and was consequently chosen for normalisation of qPCR derived expression values.:

Following normalisation, the results were compared to the RNAseq expression of the chosen genes. Patterns of expression from the two methods closely resembled each other and regression analysis indicated a good correlation (R^2 = 99%) (Fig. 5.14).

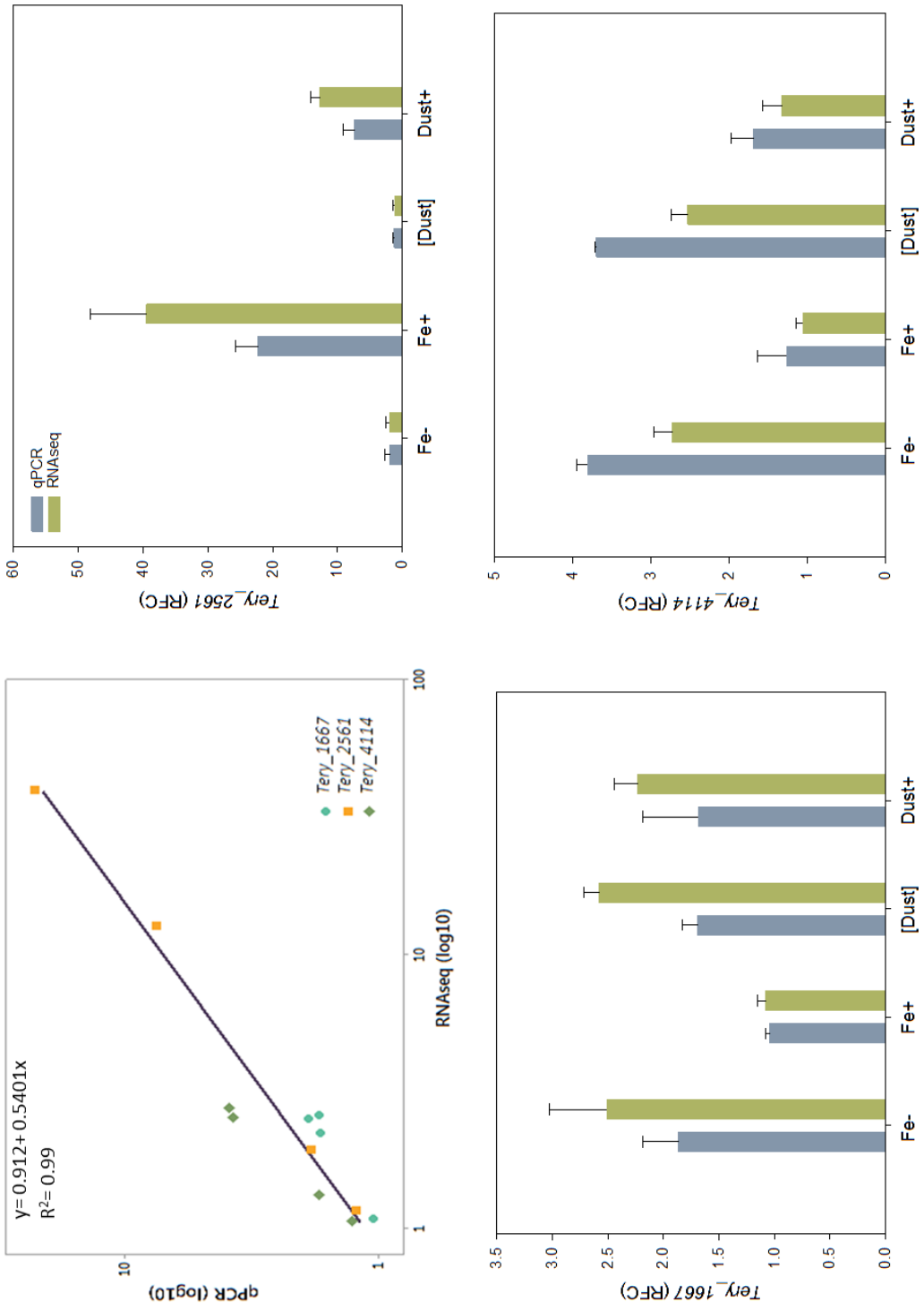

Figure 5.14: Validation of the RNAseq results using quantitative RT-PCR (qPCR). (A) Regression analysis indicated a correspondence of calculated relative fold changes (RFC) in expression between RNAseq analysis (green) and qPCR (blue) for genes: **(B)** *Tery_2561*, **(C)** *Tery_1667*, and **(D)** *Tery_4114*. RFC is calculated by normalisation to the lowest expression across the four treatments (Fe-, Fe+, [Dust], Dust+).

5.3.5 Differentially regulated processes and genes

As a first step to identifying the nature of changes observed in the transcriptome, gene ontology (GO) classification was utilised. GO classifications stem under the domains of Cellular component, Molecular function and Biological process. However, a large proportion of *Trichodesmium* genes are not GO annotated with 46% of the differentially expressed genes not belonging to any GO category (Fig. 5.9) and therefore, it is possible that processes and genes less well characterised are missed in the descriptions that follow.

To identify significantly overrepresented GO categories within the differentially regulated genes, singular enrichment analysis (SEA) was performed (AGRIGO, Du et al. 2010) (Fig. 5.15). In the domain of Biological Processes, photosynthesis, including both electron transport and the light reaction of photosynthesis, is overrepresented. Confirming this, genes related to the thylakoid membranes belonging to categories including the light harvesting complex, photosystems I and II, as well as the ATP synthase complex are overrepresented for the Cellular Component domain. Amongst the top 20 differentially expressed genes (Table 5B, Table A2), are those encoding for the oxidoreductases plastocyanin and cytochrome c_{553} proteins (1st and 3rd most differentially expressed respectively) which have an important function in photosynthetic electron transport. In addition, *psbA3* (*Tery_4763*) encoding for the Fe-binding PSII core protein D1 is the 15th most differentially expressed gene.

What is more, the Molecular Function domain is enriched in genes coding for calcium-ion-binding-proteins which also appear to be heavily represented in the top 20 differentially expressed genes. The function of such proteins in cyanobacteria is currently not clearly characterised (Sec 5.3.8).

Other highly differentially expressed genes encode for the potentially Fe binding *Tery_4114* (Mo-dependent nitrogenase-like) and the heme binding *nirA* (nitrite reductase, *Tery_1068*) (14th and 19th differentially expressed genes respectively) with the former hypothesised- and the latter known- to be involved in *Trichodesmium's* nitrogen metabolism.

Also worth mentioning, *Tery_1687*, encoding for the glycolytic enzyme fructose-bisphosphate aldolase class I, is the 20th most differentially expressed gene. The protein was previously observed to substitute the Fe containing class II fructose-bisphosphate aldolase in diatoms (Allen et al. 2012; Lommer et al. 2012) and *Trichodesmium* (Snow et al. 2015) under Fe-stress.

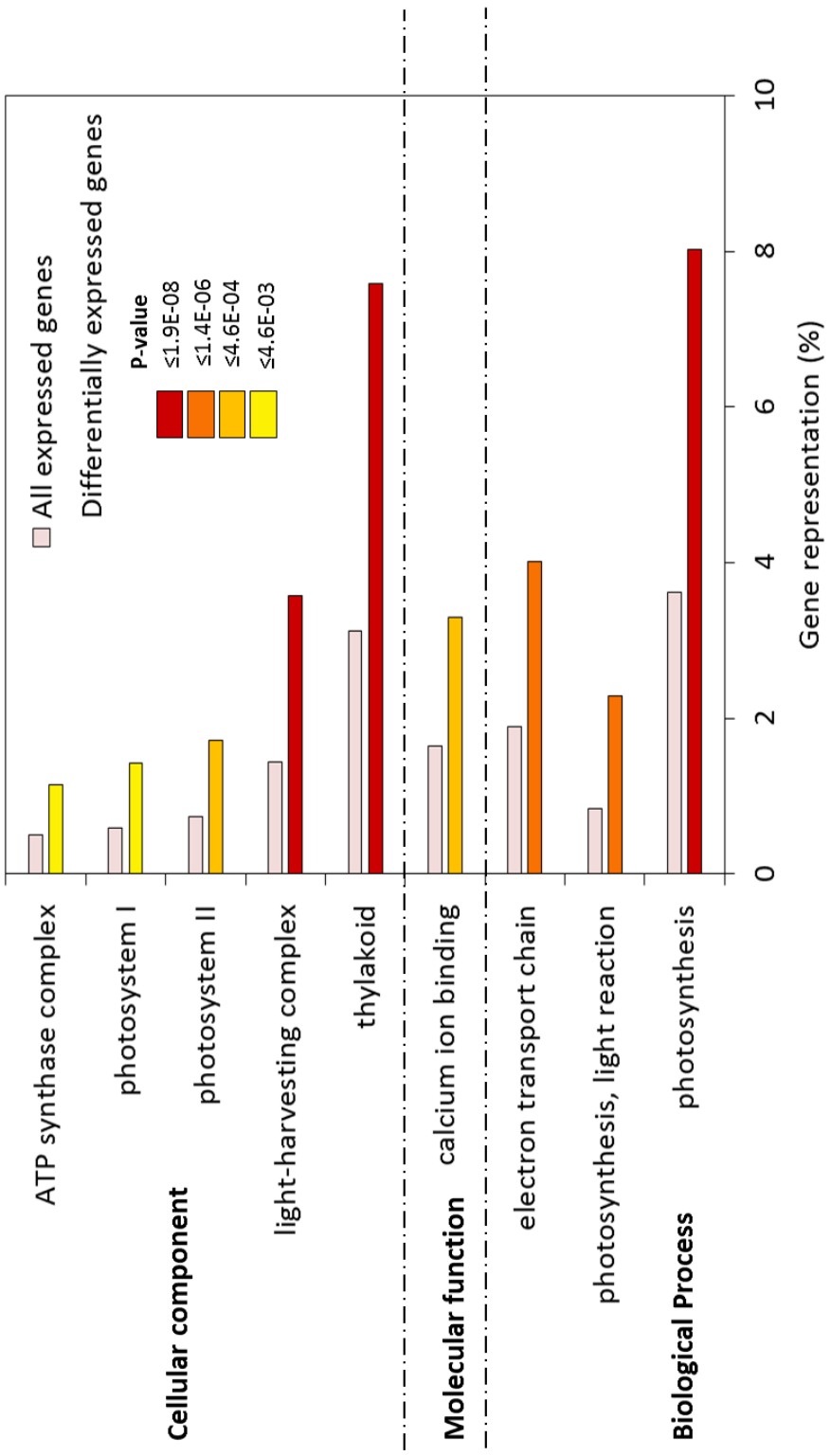

Figure 5.15: GO enrichment in differentially expressed genes. Select enriched GO categories as identified through singular enrichment analysis (SEA- AGRIGO) classified within the domains of cellular component, molecular function and biological process are presented for the differentially expressed genes (yellow- red bars) compared to the background of all the identified genes included in the analysis (salmon bars).

A large number of *Trichodesmium* genes are not yet annotated with several annotated as 'hypothetical proteins'. An example is members of the Tery_08xx operon (discussed later) which is heavily represented (5 genes) in the top 20 differentially expressed genes. The second most differentially expressed gene identified in the experiment is also annotated as a hypothetical protein. This gene was previously identified as one of two *phoX1* alkaline phosphatase homologues in *Trichodesmium* (Orchard et al. 2009). Interestingly, it was recently reported that PhoX requires both calcium and Fe for its production (Yong et al. 2014) and that its activity is influenced by phosphate but also desert dust and zinc (Mahaffey et al. 2014).

Table 5B: The top 20 differentially expressed genes presented is descending order of statistical significance (P-value).

Gene	Annotation	Cluster	P-value
Tery_2561	cytochrome c, class I (*petJ*)	2	1.09E-118
Tery_3845	hypothetical protein (*phoX1*)	6	1.85E-51
Tery_2563	plastocyanin	10	1.76E-48
Tery_0419	hemolysin-type calcium-binding region	2	1.25E-39
Tery_2055	hemolysin-type calcium-binding region	10	4.28E-38
Tery_0424	hemolysin-type calcium-binding region	2	4.91E-37
Tery_0850	hypothetical protein	2	1.00E-33
Tery_3467	hemolysin-type calcium-binding region	6	2.54E-28
Tery_1500	hypothetical protein	6	2.14E-25
Tery_0845	TENA/THI-4 protein	2	1.14E-22
Tery_3659	hypothetical protein	5	5.00E-22
Tery_3376	phosphoglycerate kinase (*pgk*)	5	1.35E-21
Tery_0846	hypothetical protein	2	2.48E-21
Tery_4114	Mo-dependent nitrogenase-like	10	5.20E-21
Tery_4763	photosystem q(b) protein	4	8.77E-21
Tery_0849	cell surface protein	2	1.96E-20
Tery_2976	caffeoyl-CoA O-methyltransferase	2	1.96E-20
Tery_0847	5-methyltetrahydropteroyltriglutamate-- homocysteine methyltransferase (*metE*)	2	1.11E-19
Tery_1068	ferredoxin-nitrite reductase (*nirA*)	7	6.28E-19
Tery_1687	fructose-bisphosphate aldolase	4	1.57E-18

5.3.6 Responses to $FeCl_3$ and dust-additions- Pairwise comparisons

Varied expression profiles across the four treatments Fe+, Fe-, Dust+ and [Dust] were previously recognised (Fig. 5.13). Four main drivers shaping these include:

A. **Iron**: Both in the form of $FeCl_3$-EDTA (Fe+) and Sahara Desert dust (Dust+)
B. **$FeCl_3$-EDTA ($FeCl_3$):** Response stimulated either due to higher concentrations of Fe provided overall in Fe+, or due to increased levels of Fe' provided compared to particulate/colloidal dust-bound Fe.
C. **Dust**: Induced through contact of the cells with dust (Dust+)
D. **Other chemical stimuli** leached from Dust: Independently or in combination with Fe

To better describe the changes induced by iron, dust and $FeCl_3$ the similarities and differences between the pairwise comparisons: Fe+ vs Fe- and Dust+ vs [Dust] are examined. We identify 376 genes regulated by dust and 438 genes by $FeCl_3$ from which 138 are coregulated by both drivers.

The response to contact with dust is biased towards upregulation in all of all three GO domains of Cellular Component, Molecular Function and Biological Process (Fig. 5.16). In contrast, $FeCl_3$ causes a more balanced response of upregulation: downregulation as do other stimuli from dust (comparison of [Dust] and Dust+ against Fe+ and Fe-). GO enrichment analysis for genes uniquely changed by contact with dust, $FeCl_3$ or co-influenced by both, indicated that dust alone has an effect on translation-related genes (Fig. 5.17). This possibly suggests that dust-related stimuli (only effective upon contact of cells with dust) trigger protein production in *Trichodesmium* and an increase of metabolic activity. The expected increase in transcription in such a scenario (to facilitate faster translation) would explain the large bias towards upregulation compared to downregulation of dust-affected genes.

It has previously been noted that the process of translation is downregulated as a response to stress related conditions (López-Maury et al. 2008; Singh et al. 2010) in order for energy reserves to be directed towards cell protection instead. Here, having an abundance of nutrients provided by dust might act as a trigger to boost *Trichodesmium* activity. Nevertheless, we cannot exclude a possibility that the more slow growing (compared to Fe+) Dust+ cultures are sampled at an earlier exponential phase when protein production is increased.

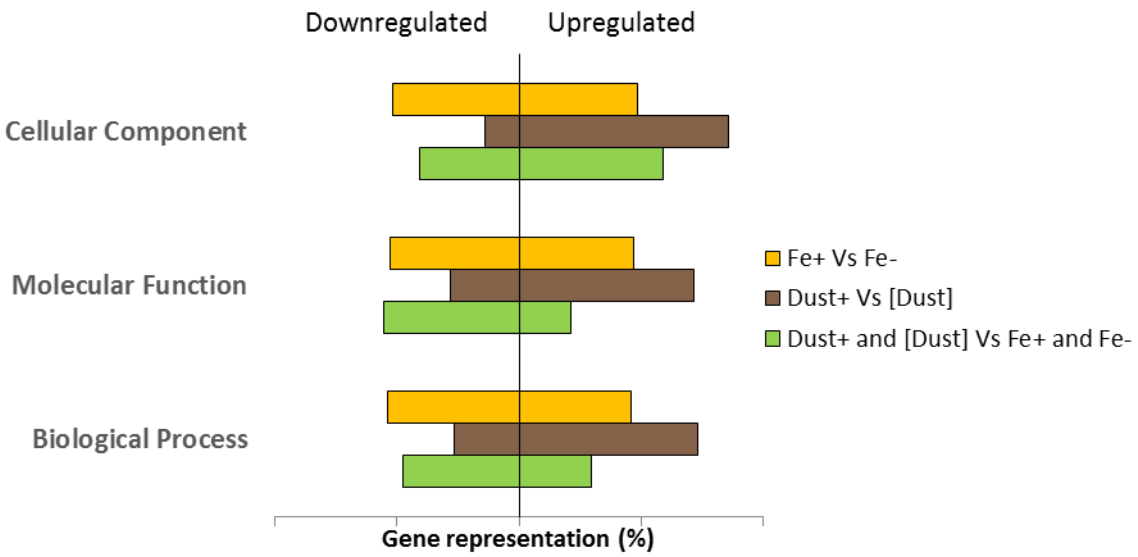

Figure 5.16: The balance of positive and negative changes in gene expression. The percentage of genes downregulated and upregulated by contact with dust (brown), $FeCl_3$ (yellow) or other dust-stimuli (green), calculated for each GO domain (cellular component, molecular function and biological process).

Iron in general (both as $FeCl_3$ and dust) induced processes such as photosynthesis, ATP synthesis, electron transport, phycobilisome proteins and Fe binding proteins. This is expected due to the large Fe demand of photosynthetic processes (Raven et al. 1999; Shi et al. 2007). At the same time, a different suit of phycobilisome proteins is upregulated only in response to dust while $FeCl_3$ alone is identified to significantly stimulate the light reaction of photosynthesis. The latter, involves the Fe demanding PSI and PSII requiring 12 and 3 atoms respectively (Shi et al. 2007), and includes the process of cyclic flow of electrons around PSI (which does not involve PSII). Protein components involved in cyclic electron transport were previously identified to be affected by Fe-limitation at the proteomic level in *Trichodesmium* (Snow et al. 2015). Changes in expression of genes involved in photosynthetic processes are reviewed in more detail later in this report.

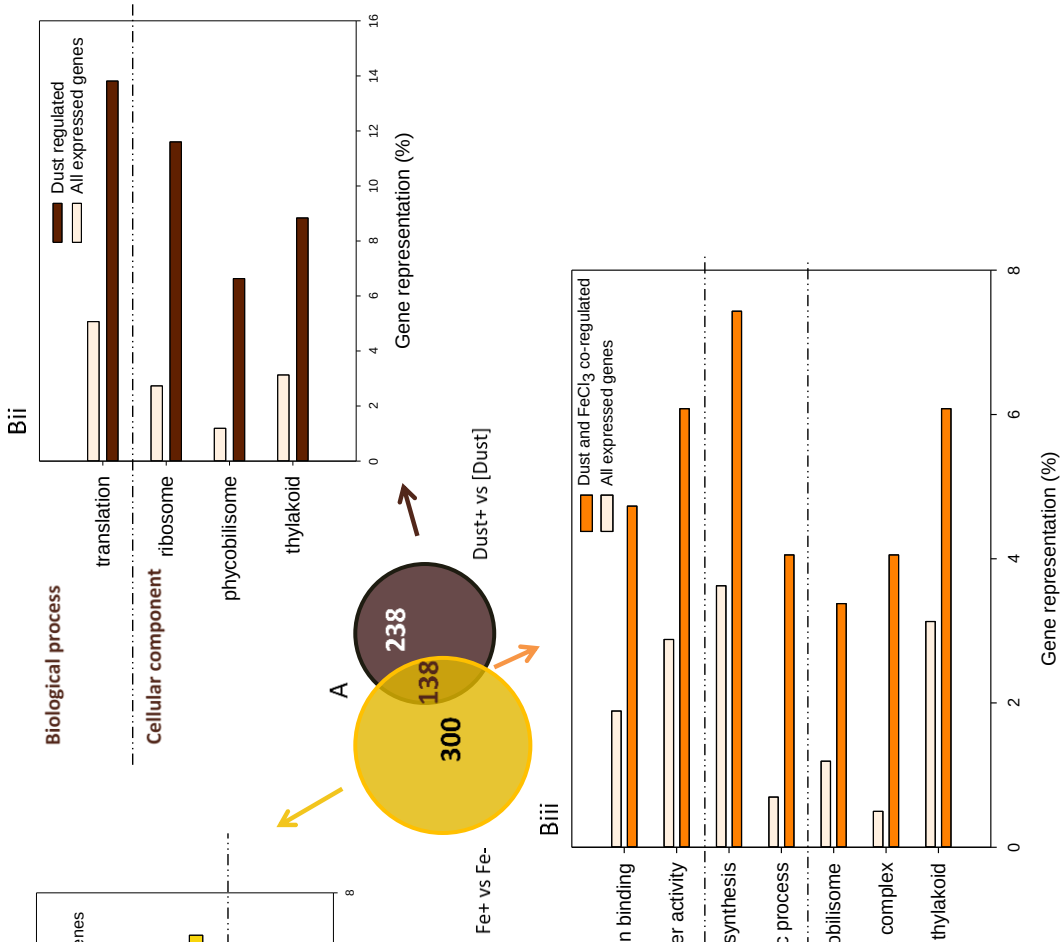

Figure 5.17: Comparisons of transcriptomic changes due to additions of Dust and $FeCl_3$. (A). The number of genes affected in the Fe+ (yellow) and Dust+ (brown) treatments, with Fe- and [Dust] as background controls respectively, are presented in relation to each other to reveal genes regulated by both Fe sources **(Bi-iii)** Singular enrichment analysis of GO annotated genes is performed for the $FeCl_3$ (i), Dust (ii) and commonly Fe regulated genes (iii).

5.3.7 Markers of iron limitation. Confirmation of the cellular Fe state

From a set of 12 genes known to be regulated by Fe and previously used as markers to indicate its limitation, we identify that 5 are shaped by Fe both when provided as $FeCl_3$ and dust (*fld2*, *petE*, *petJ*, *fur1* and *fur2*) while an additional 3 are controlled solely by $FeCl_3$ (*fbaB*, *isiA* and *isiB*) (Table 5C).

The ferric uptake regulator genes 1 and 2 (*fur1, fur2*) (but not *fur3*) are differentially expressed in response to both Fe sources, with upregulation in Fe- and [Dust] compared to Fe+ and Dust+. Recent data demonstrate Fur's role as both a repressor and activator of genes involved in Fe metabolism and regulator of the cellular redox status (González, M Teresa Bes, et al. 2012; González et al. 2016).

The 5 genes regulated by both Fe sources also include the electron transporters cytochrome c_{553} (*petJ*), binding heme, and plastocyanin (*petE*), binding copper, mentioned previously to be the first and third most affected genes respectively. These interchangeable oxidoreductases are known to engage in a behaviour referred to as the plastocyanin-cytochrome switch regulated by copper and Fe concentrations (Wood 1978; De la Cerda et al. 2007). Here, in agreement to their characterised behaviour in other microbes, expression of *petJ* is increased while that of *petE* is reduced in Fe+ and Dust+ compared to Fe- and [Dust] treatments.

Another electron transporter that is switched for an alternative, Fe-cheaper protein, is ferredoxin. Under Fe limiting conditions this is known to be replaced by the flavin-containing, flavodoxin (LaRoche et al. 1996). Different expression patterns are observed here for the two *Trichodesmium* homologues of flavodoxin, with *fld2* upregulated in Fe- and [Dust] relative to Fe+ and Dust+, while expression of *fld1* (*isiB*) is upregulated in all conditions except Fe+. The latter is colocalised with the, similarly expressed, *isiA* gene in the *Trichodesmium* genome. IsiA proteins form an antennae surrounding the Fe demanding PSI complexes and thus enable a higher light trapping efficiency by fewer PSI units as a way of conserving Fe resources (Bibby et al. 2001). IsiA and IsiB proteins were also identified to differ at the protein level in a previous similar study (Snow et al. 2015).

Table 5C: Expression of suggested biomarkers of iron limitation. The regulation of genes by $FeCl_3$ only (yellow) or in combination with dust (orange) is compared to previously identified differential regulation at the protein level (blue, Snow et al 2015). No dust only changes were observed in this group of genes

Category	gene	Tery number	RNA changes	Protein changes
Photosynthesis	Iron stress induced protein A (isiA)	1667		
Elecron transport	Flavodoxin (isiB/fld1)	1666		
	Flavodoxin (fld2)	2559		
	Plastocyanin	2563		
	Cytochrome c_{553}	2561		
Storage	Bacterioferritin	2787		
	Ferritin	4282		
Regulation	Ferric uptake regulator1	1958		
	Ferric uptake regulator2	3404		
	Ferric uptake regulator3	1953		
Nitrogen fixation	NifH	4136		
Glycolysis	Fructose bisphosphate aldolase (Class I)	1687		

Similarly to *isiB* and *isiA*, expression of the class I fructose-bisphosphate aldolase gene (*fbaB*) is suppressed only by additions of $FeCl_3$ and not dust. This protein is switched with class II fructose bisphosphate aldolase when Fe is abundant (Snow et al. 2015), a change not identified here at the transcriptomic level.

Regulation by $FeCl_3$ but not dust indicates that some genes considered as good Fe-limitation biomarkers (*isiA, isiB and fbaB*) are either not sensitive to particulate/colloidal Fe or that the concentration acquired from the latter is not sufficient to suppress the expression of these stress related genes. This is the first time the transcriptomic response of these genes to dust is assessed in culture and indicates that caution should be applied before their use as markers in the field.

5.3.8 Transcriptomic response of major processes across the experimental treatments.

The effect of desert dust and $FeCl_3$ to processes expected, or previously indicated to be affected by Fe-limitation, including Fe transport, photosynthesis, energy production and nitrogen metabolism is discussed below. In addition, putative outer membrane components potentially involved in the Fe-limitation response of *Trichodesmium* are identified.

5.3.8.1 Iron transport

Iron is carried across the cyanobacterial membranes through various pathways depending on its speciation and complexation. Expression of the *Trichodesmium* genes involved in these pathways, as inferred by homology, is reviewed below.

The ferrous iron uptake system Feo, first characterised in *E.coli*, is composed of three proteins (Kammler et al. 1993): FeoA which is suggested to interact with a conserved transmembrane domain of the inner membrane ATP powered transporter, FeoB, and FeoC a transcriptional regulator (Cartron et al. 2006; Lau et al. 2013). In the model cyanobacterium *Synechocystis feoB* is upregulated under Fe-stress while its mutant shows reduced Fe^{2+} uptake compared to the WT (Katoh et al. 2001b; Kranzler et al. 2014). Kranzler et al. (2014) suggest that the FeoAB is the major Fe transport system in this organism as minimal uptake is observed in the Δ*feoB* mutant. *Trichodesmium* possess *feoAB* homologues and *feoB* transcription was shown to be upregulated under Fe-limitation (Chappell & Webb 2010). This observation is supported in the present transcriptome as expression in $FeCl_3$ added cultures is lower than that of the other treatments although the

difference is not statistically significant (Fig. 5.19). Contrariwise, *feoA* expression is low compared to *feoB* and its level is stable across all treatments.

Oxidised Fe' (Fe^{3+}) is transferred across the inner membrane using the ferric ion binding protein (Fbp) system first described in pathogenic bacteria (Krewulak & Vogel 2008). It is composed of a periplasmic iron-binding component (FbpA), a transmembrane protein (FbpB), and an ATPase (FbpC) subunit which in *Synechocystis* are referred to as FutABC. Deletion of *futBC* in this species causes reduced growth (Katoh et al. 2001a), while deletion of the two *futA* homologues interferes with Fe uptake and reduction (Kranzler et al. 2014). Further information regarding *Synechocystis futA1* and *futA2* is provided in Chapter 4. The expression of the *Trichodesmium futA* but not *futBC* is significantly lower in the presence of $FeCl_3$ compared to other treatments (Fig. 5.18, 5.19).

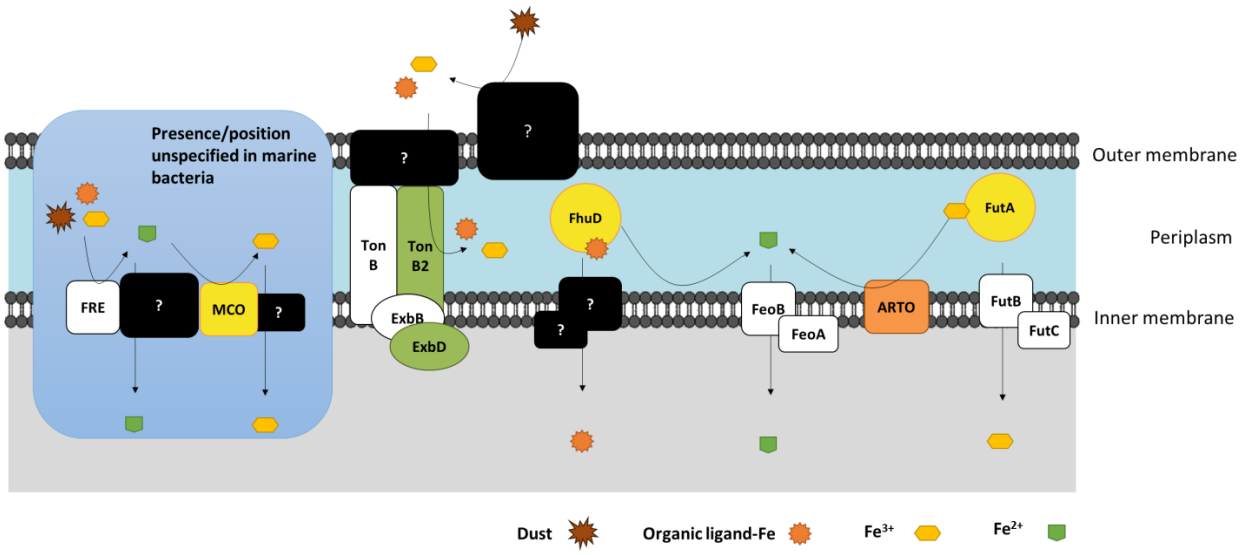

Figure 5.18: Iron uptake across the inner and outer cell membranes. Representation of *Trichodesmium* putative Fe transporters and related proteins as identified by homology to studied pathways of other organisms. Shading indicates changes at the RNA level in response to $FeCl_3$ both uniquely (yellow) and in combination with dust (orange). No changes specific to contact with dust are identified in the expression of genes for this set of proteins. Differences between the Dust+ and [Dust] cultures relative to Fe- and Fe+ (green) potentially indicate changes in transcription stimulated by dust-released chemicals.

Both the abovementioned uptake systems are involved in transfer of Fe' through the cyanobacterial inner membrane. Although small molecules are able to pass through porins of the outer membrane (Nikaido 2003), molecules bigger than 600 Da are actively transported to the periplasmic space by TonB- dependent transporters (TBDTs). TBDTs involved in nickel and cobalt (Schauer et al. 2008), disaccharide and polysaccharide as well as vitamin B12 uptake have been identified, but siderophores and heme are considered their major substrates (Hopkinson & Barbeau 2012). These transporters are powered by

energy transferred through the periplasm-spanning TonB anchored on the plasma membrane. For this energy transduction the auxiliary proteins ExbB and ExbD located in the plasma membrane are also required (Ollis et al. 2009). Recent evidence suggest that in addition to siderophore uptake *Synechocystis* ExbBD are also involved in inorganic Fe uptake (Jiang et al. 2015).

Under Fe starvation, differential expression of *tonB* and *exbBD* has been reported for the model diazotroph *Anabaena* sp. PCC 7120 (*Anabaena*) (Stevanovic et al. 2012) and of *exbBD* for *Synechocystis* (Singh et al. 2003; Jiang et al. 2015). Under the same conditions, mutants of *tonB* and *exbBD* in *Synechocystis* display reduced growth compared to the WT. In addition, the four *Synechocystis* TBDTs are upregulation under Fe-limitation (Katoh et al. 2001a; Jiang et al. 2012). *Anabaena* has 22 TBDTs which have been shown to be differentially expressed under variable copper/Fe and nitrogen concentrations (Mirus et al. 2009; Stevanovic et al. 2013). The function of only some of these TBDTs has been researched, including SchT involved in schizokinen/aerobactin uptake, IutA2 involved in schizokinen uptake as well as IacT which takes up Fe and copper (Cu) (Nicolaisen et al. 2008; Nicolaisen et al. 2010; Rudolf et al. 2016).

Trichodesmium on the other hand, possesses homologues of ExbBD and TonB but does not appear to have any obvious TBDTs (Hopkinson & Morel 2009). Expression of *exbD* but not *exbB* is upregulated in the Fe+ and Fe- treatments compared to the [Dust] and Dust treatments here. The two *tonB* homologues also show a similar expression profile but only *tonB2* is significantly increased in Fe- and Fe+ compared to [Dust] and Dust+ (Fig. 5.18, 5.19). The results suggest that in *Trichodesmium* this transport system might be associated with a soluble substrate released from the desert dust.

Adjacent to *tonB1* but transcribed from the opposite DNA strand, *Tery_1561* annotated as a hypothetical protein, has suppressed expression in response to Fe as both $FeCl_3$ and dust. compared to the Fe-deficient Fe- and [Dust] treatments. The protein appears to contain an alpha/beta hydrolase fold (NCBI Conserved Domain Database, Marchler-Bauer et al. 2015) which if linked to Fe uptake could be speculated to contribute to extraction of Fe from ligands prior to uptake through TBDTs. In addition, the adjacent *Tery_1562* is homologous to a copper translocating P-type ATPase. This is more highly expressed in Fe- compared to Fe+ and it remains at low levels in both the Dust+ and [Dust] treatments. A possible association of this proteins to TonB and any involvement to Fe transport remains to be examined.

Furthermore, transcription of heme oxygenase (*Tery_0335*), catalysing the degradation of heme, is decreased in Fe- compared to Fe+ as well as the dust treatments Dust+ and [Dust] although the former is not statistically different. The increased expression in Fe+ compared to Fe- is also shown at the protein level (Snow et al. 2015). Additionally, the same study identifies proteins Tery_3823-3826 as potentially involved in siderophore production and uptake and indicates differential expression between Fe+/Fe-. Here, increased expression at the transcriptomic level is identified in Fe+ and Dust+ compared to Fe- and [Dust] for *Tery_3824*, and in Fe+ compared to Fe- for *Tery_3825-3826* reinforcing the author's suggestions.

Once inside the periplasm, siderophores that are taken up by bacterial TBDTs can be carried across the inner membrane through specialised ABC transporters. The Fhu system, best characterised in proteobacteria, involves binding of hydroxamate siderophores by the periplasmic FhuD protein and their transport across the inner membrane FhuB. The process is powered by the ATP binding FhuC. In a similar way, citrate-type siderophores are transferred by the Fec system (Krewulak & Vogel 2008).

In *Anabaena*, which possesses both of the abovementioned systems, *fhu* genes are upregulated under Fe-deficient conditions and in mutants of the siderophore secretion and uptake pathways. Also, deletions of the Fhu uptake system components cause reduced growth compared to the WT under Fe-limitation (Stevanovic et al. 2012). Furthermore, three Fec systems have been identified so far in this organism (Nicolaisen et al. 2008; Mirus et al. 2009; Stevanovic et al. 2012) and components were shown to be affected by Fe, copper and nitrogen concentrations (Stevanovic et al. 2012; Stevanovic et al. 2013). In *Synechocystis* members of the Fec system were also identified but there was no obvious upregulation under Fe-limitation (Katoh et al. 2001a).

Contrary to *Anabaena* and *Synechocystis*, *Trichodesmium* does not appear to possess members of these two pathways except from a homologue to the periplasmic hydroxamate binding FhuD (Chappell & Webb 2010). This could be either due to the existence of a distinct, yet to be discovered, siderophore uptake transport pathway in this organism, or the dissociation of Fe from ligands prior to uptake through the inner membrane. In the presented analysis expression of *fhuD* is increased in Fe- and [Dust] compared to Fe+ and Dust+ conditions (only Fe- compared to Fe+ are significantly different) (Fig. 5.18, 5.19).

Independently or in synergy to the previously described systems, Fe can be reduced either before or after its transfer through the outer membrane. Reduction pathways in eukaryotic phytoplankton include the use of cell surface ferric reductase (FRE) similar to that of *Saccharomyces cerevisiae* (Yun et al. 2001; Kustka et al. 2007; Groussman et al. 2015). A ferric-reductase-like gene (*Tery_2227*) identified in the *Trichodesmium* genome shows no differential expression under any condition (Fig.5.18).

Moreover, in yeast and eukaryotic phytoplankton like *T.pseudonana* and *C.reinhardtii*, after reduction by FRE and consequent release from organic ligands, Fe can be reoxidised to Fe^{3+} by multicopper oxidases (MCO) to be transported through Fe^{3+} specific transporters. An MCO with Fe^{3+} oxidising function has not yet been characterised in cyanobacteria. Here, a gene homologue to multicopper oxidases (*Tery_0359*) in *Trichodesmium* demonstrates increased expression in Fe- compared to Fe+ (Fig. 5.18, Fig. 5.19). However, prediction software (Signal P, Petersen et al. 2011) does not identify a likely a signal sequence to this protein, either indicating an intracellular function or a divergent sequence for export from the cytoplasm.

Ferric (Fe^{3+}) transporters associated with MCO include permeases (Ftr1) (Stearman et al. 1996; Askwith & Kaplan 1998; Urbanowski & Piper 1999; Wang & Dei 2003; Bonaccorsi di Patti et al. 2005) and transferrins (TTf) (Fisher et al. 1997; Fisher et al. 1998; Paz et al. 2007b). No homologues of such proteins are identified in the *Trichodesmium* genome. However, immediately downstream of multicopper oxidase- like *Tery_0359*, *Tery_0360* is indicated as a transmembrane protein (contains the Tmemb_14 domain of transmembrane uncharacterised proteins). Similarly to *Tery_0359*, this gene is upregulated in Fe- compared to Fe+. Further evidence is required to identify the function of this protein and whether in association with the putative MCO they constitute a *Trichodesmium* Fe uptake system.

Although similarly to *Lyngbya majuscula* (Rose & Waite 2005) the use of electron donating reactive oxygen species (ROS) in the form of superoxide has been suggested for *Trichodesmium* (Roe & Barbeau 2014; Hansel et al. 2016), the pathway of this process is not characterised and thus could not be investigated using the molecular data collected in the context of this work.

A different hypothesised mechanism for reduction involves transfer of electrons to Fe^{3+} through the plasma membrane-located alternative respiratory terminal oxidase (ARTO). Evidence for this was the observation that the *Synechocystis* ARTO mutant displays.

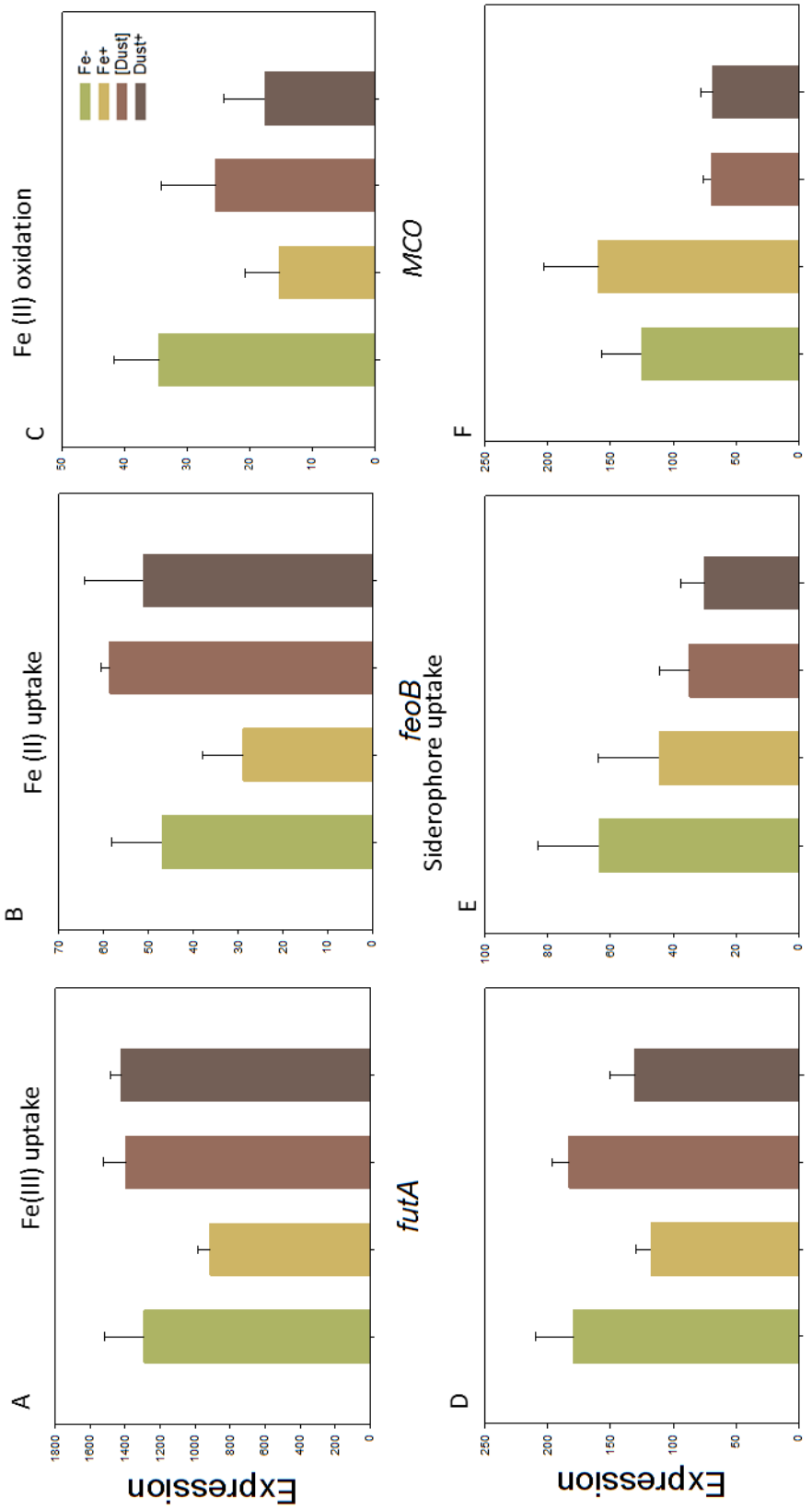

Figure 5.19: Gene expression of various components of putative Fe uptake pathways in *Trichodesmium*. Expression of genes possibly involved in transport of Fe either as **(A)** Fe^{3+} or **(B)** Fe^{2+} across the inner cell membrane, **(C)** Fe^{2+} oxidation prior to uptake and **(D-F)** siderophore uptake, is presented across the experimental treatments [Dust] (light brown), Dust + (dark brown), Fe- (green) and Fe+ (yellow). Error bars represent standard deviation of the means of three biological replicates.

impaired Fe reduction and uptake (Kranzler et al. 2014). Possibly suggesting a similar function in *Trichodesmium*, the ARTO genes (*Tery_0276-0278*) are upregulated in Fe- and [Dust] compared to Fe+ and Dust+ (Fig. 5.18).

5.3.8.2 Photosynthetic Electron Transport Chain

Genes involved in the process of photosynthesis are amongst the most highly expressed (Table A3) and enrichment analysis suggests that it is one of the most heavily affected processes across the experimental treatments, with the response of different components depending on the form of Fe provided (Fig. 5.17). Although Fe as both dust and $FeCl_3$ have common effects on a group of photosynthesis related genes, dust additions exclusively cause differential expression in thylakoid and phycobilisome genes while $FeCl_3$ causes GO enrichment in the categories of the photosynthetic light reaction and electron transport. Below the responses of genes encoding for each component of the photosynthetic electron transport chain are reviewed separately.

PSII**:** This protein-pigment complex, comprised of around 30 proteins, utilises solar energy to oxidise water and reduce plastoquinone (PQ) starting a chain of electron transfer that will ultimately result in reduction of NADP to NADPH (Vinyard et al. 2013). Subunits cytochrome c_{550} and c_{559} bind heme and the D1/D2 core proteins bind non-heme Fe, resulting in a requirement of 3 Fe atoms per PSII monomer (Shi et al. 2007).

Genes *psbV* (*psbV1* and *psbV2*) and *psbE/psbF* for the heme containing cytochrome c_{550} and b_{559} respectively are upregulated in Fe+ and Dust+ compared to Fe- and [Dust] (Fig. 5.20). For the cytochrome b_{559} beta subunit gene *psbF* these differences are not statistically significant. In contrast to the cytochrome subunits, genes *psbA1-3* and *psbD* for the non-heme Fe-binding D1/D2 are downregulated in Fe+ compared to Fe- (Fig. 5.20) and their levels remain high in the Dust+ and [Dust] treatments. Contradicting the expression pattern of *psbD* observed here, upregulation in Fe+ compared to Fe- was previously reported (Shi et al. 2007). At the proteomic level PsbD levels were suggested to remain stable in comparable conditions (Snow et al. 2015).

Genes *psbB* and *psbC1* forming intrinsic transmembrane CP43 and CP47 antennae proteins of PSII are upregulated in Dust+ compared to [Dust] while they remain at lower levels in both Fe+ and Fe (Fig. 5.20)-. Homologs *psbC2* and *psbC3* of the CP47 gene have reduced transcription in Fe+ relative to Fe- (Fig. 5.20) while the Dust+ and [Dust] expression levels remain high. Upregulation in Fe- compared to Fe+ is also observed for the *psbW* (*psb28)*

gene (Fig. 5.20), forming a subunit of the oxygen evolving complex with functions in biogenesis, assembly and stabilisation of PSII (García-Cerdán et al. 2011).

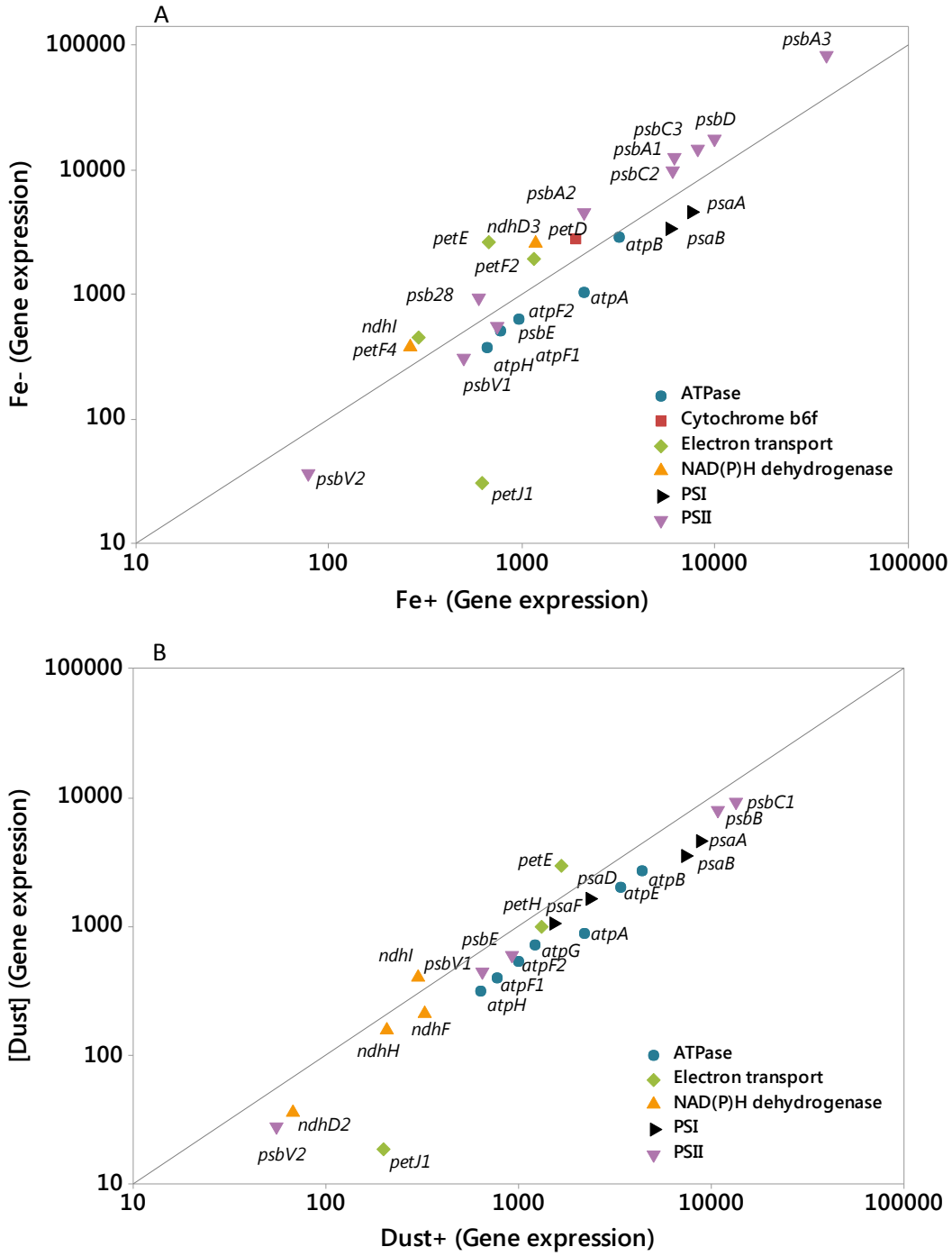

Figure 5.20: Changes in transcription of genes involved in the process of photosynthesis. The differential expression of genes from pairwise comparisons between **(A)** Fe- to Fe+ and **(B)** [Dust] to Dust+ involved in electron transport (green) or encoding for subunits of F_1F_O ATPase (blue), NADPH dehydrogenase (orange), PSI (black) and PSII (purple) is plotted in log scale. The line y=x separates upregulated (below) from downregulated (above) of genes upon additions of $FeCl_3$ (A) and Dust (B).

Results also suggest that possible release of dust-leached chemicals influences transcription of PSII subunit genes. This is indicated by an upregulation of PSII genes for accessory subunits PsbHIJKLNOTUZ27 and one of the PsbA isoforms, in Dust+ and [Dust] compared to the Fe- and Fe+ treatments.

Cytochrome b_6f: This thylakoid membrane located enzyme catalyses the transfer of electrons from plastoquinol to plastocyanin/cytochrome c_{553} and generates a proton gradient by pumping H^+ through the thylakoid membranes into the lumen (Kurisu et al. 2003).

The cytochrome b_6f complex is made of 4 core subunits two of which, PetB (2 Fe, cytochrome b_6) and PetD (subunit IV), are membrane intrinsic, and two, PetA (1 Fe, cytochrome *f*) and PetC (2 Fe, Rieske Fe-S protein), are membrane extrinsic (Kurisu et al. 2003). The genes for each set are colocalised in the *Trichodesmium* genome.

The two clusters appear to be under distinct regulatory control. Genes *petB* and *petD* are upregulated under Fe- compared to Fe+ conditions (statistical significance only for *petD)* while genes *petA* and *petC* are more highly expressed in the dust treatments, Dust+ and [Dust], compared to Fe- and Fe+. Gene *petG* potentially involved in assembly and stability of cytochrome b_6f (Schneider et al. 2007) is also upregulated in Dust+ and [Dust] treatments.

Our results contradict those of previous studies reporting a downregulation of cytochrome b_6f in Fe- conditions in *Trichodesmium* (Shi et al. 2007; Snow et al. 2015), the diatom *T.oceanica* (Lommer et al. 2012) and *Prochlorococcus* (Thompson et al. 2011) indicating possible dependency on the growth phase or other unknown factors.

PSI**:** The second light- absorbing protein complex of photosynthesis, PSI, mediates transfer of electrons from plastocyanin/cytochrome c_{553} to ferredoxin which will in turn reduce ferredoxin-NADP+ reductase (FNR) the protein generating NADPH from NADP (Jordan et al. 2001). PSI is composed of multiple subunits (around 15) and is more Fe demanding compared to PSII, binding 12 Fe atoms per monomer (Shi et al. 2007). These are associated with the 4Fe-4S iron-sulphur centres F_X, F_A and F_B (Jordan et al. 2001).

The PSI PsaA and PsaB subunits form heterodimers that bind the 4Fe-4S iron-sulphur centre F_X. They also interact with the electron donor P700 (primary electron donor of PSI) and the acceptors A_0, A_1 (Jordan et al. 2001). Genes *psaA* and *psaB* are downregulated in Fe- and

[Dust] conditions compared to Fe+ and Dust+ (Fig. 5.20) as also observed at the protein level between Fe- and Fe+ (Snow et al. 2015).

The F_A and F_B 4Fe-4S centres are bound to PsaC (Jordan et al. 2001), previously identified to be upregulated in response to $FeCl_3$ (Snow et al. 2015). Gene *psaC* is not differentially expressed here under similar conditions, and although expression is lower in [Dust] compared to Dust+ this change is not statistically significant. However, similarly to genes *psaIJ* (encoding for subunits PsaI and PsaJ), a secondary controlling factor stimulates increased expression of *psaC* in the [Dust] and Dust+ treatments compared to Fe- and Fe+.

Furthermore, genes for PsaD, which can form complexes with the electron transporter ferredoxin, and PsaF the plastocyanin-docking protein important in electron transfer from plastocyanin to P700 (Jordan et al. 2001) are upregulated in Dust+ compared to [Dust] (Fig. 5.20).

PSI/PSII expression comparison**:** It is interesting to note that the PSI or PSII genes affected by $FeCl_3$ have an opposite response to each other. PSII genes (apart from the heme containing *psbE* and *psbV*) are upregulated in Fe- compared to Fe+ while the PSI genes that are significantly changed (*psaAB*) are downregulated (Fig 5.20, 5.21). It is possible that this reflects the shift of PSI: PSII ratio to reduce the more Fe demanding PSI compared to PSII under Fe deficient conditions (Snow et al. 2015). The plasticity of the PSI: PSII ratio was also previously documented in comparisons between coastal and open ocean phytoplankton growing under Fe-deficiency (Strzepek & Harrison 2004).

However, the lower PSI:PSII potentially negatively impacts cyclic electron transport (CET) (Berman-Frank et al. 2001; Snow et al. 2015). Through CET, NADPH generated by FNR can be reoxidised and the electrons released, recirculated through cytochrome b_6f and PSI to fuel additional ATP production without the accumulation of NADPH normally occurring during linear electron transport (LET) (Lea-Smith et al. 2016). Also, the reduction of CET can potentially lead to increased oxygen evolution and ROS production and is expected to affect N_2 fixation through oxygen deactivation of its key enzyme, nitrogenase (Milligan et al. 2007).

Electron transport: The *petE* and *petJ* genes encoding for the electron transporters plastocyanin and cytochrome c_{553} respectively are regulated inversely to each other both in response to $FeCl_3$ and dust as the Fe containing cytochrome c_{553} is replaced by plastocyanin in Fe-deficient conditions (Fig. 5.20, 5.21) (Wood 1978; De la Cerda et al. 2007).

Another known Fe-stress response involves switching of the Fe containing electron transporter ferredoxin to flavodoxin (La Roche et al. 1996). The non-Fe containing flavodoxin genes *fld1* and *fld2* are upregulated in Fe- compared to Fe+. Gene expression of *fld2* is also stimulated in [Dust] compared to Dust+ (Fig. 5.20, 5.21). However, from the 5 ferredoxin encoding *petF* homologues found in the *Trichodesmium* genome, 2 are upregulated in Fe- compared to Fe+ treatments (Fig. 5.20, 5.21) and are kept at high levels in Dust+ and [Dust] while the remaining 3 are not significantly changed.

Finally, the ferredoxin NADP+ reductase (FNR) encoding, *petH*, is upregulated in Dust+ and Fe+ compared to [Dust] and Fe- treatments with the difference being significant only in response to dust (Fig. 5.20, 5.21).

F_1F_o ATP synthase: The proton gradient generated from photolysis of water by PSII and shuttling of H+ by cytochrome b_6f stimulates H^+ transport down the electrochemical gradient through the F_o proton porin of the ATP synthase. The F_1 motor consequently catalyses the formation of ATP from ADP and Pi (Berg et al. 2002).

Components alpha, gamma, delta of F_1 and b of F_O are upregulated in Fe+ and Dust+ compared to Fe- and [Dust] treatments whereas subunits a and c of F_O are only upregulated in response to dust but not $FeCl_3$ (Fig. 5.20, 5.21).

NAD(P)H dehydrogenase**:** NAD(P)H dehydrogenase I (Ndh-1), is an enzyme composed of around 15 subunits which can be involved in PSI CET as well as respiration and CO_2 uptake (Ohkawa et al. 2000b; Battchikova et al. 2011; Lea-Smith et al. 2016). Although most subunits are shared between Ndh-1 performing different functions, NdhD and NdhF seem to specialise according to the activity: Gene deletions in *Synechocystis* reveal involvement of *ndhD1-2* in PSI CET and *ndh3-4* in CO_2 uptake (Ohkawa et al. 2000a; 2000b; Shibata et al. 2001; 2002; Maeda et al. 2002; Battchikova et al. 2011).

Trichodesmium has 3 *ndhD* paralogues with homology to the *Synechocystis ndhD1, ndhD2* and *ndhD3/4* genes Gene *ndhD2* is stimulated in Fe- compared to Fe+ while *ndhD1* in Dust+ compared to [Dust] (Fig. 5.20). Upregulation of *ndhD2* in Fe- conditions (as well as P, N, CO_2 and S-limitation and high light) was also previously identified in *Synechococcus* PCC 7002 (Ludwig & Bryant 2011; Ludwig & Bryant 2012). The function was associated with balancing the ratio of protons translocated across the membrane to that of electrons in Fe- conditions when the availability of reducing equivalents is lower.

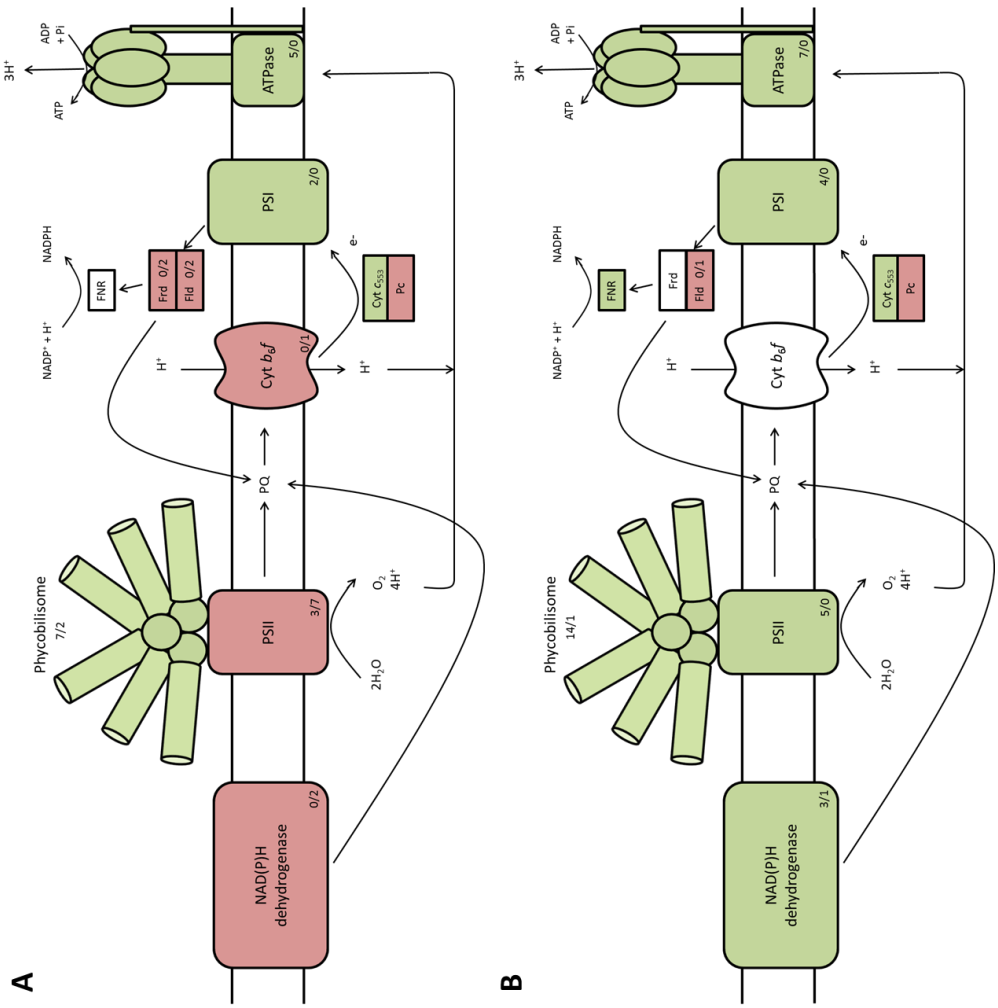

Figure 5.21: Transcriptomic response of subunits involved in the photosynthetic electron transport chain. Positive (green) or negative (red) changes caused by **(A)** $FeCl_3$ and **(B)** Dust-additions (relative to Fe- and [Dust] respectively) are compared. Positive/negative changes indicated are based on the direction of changes of the majority of genes for each subunit. The number of upregulated genes/downregulated genes is presented for each component (bottom right).

Similarly to *ndhD1*, genes *ndhH* and *ndhF1* are upregulated in Dust+ compared to [Dust] (Fig. 5.20). The former is also more highly expressed in both of the Dust+ and [Dust] treatments compared to Fe- and Fe+.

Subunit NdhI which is responsible for the transfer of electrons from an electron donor to NdhK and eventually plastoquinone, harbours two iron-sulphur clusters (N6a, N6b) (Battchikova et al. 2011). In the presented transcriptome gene *ndhI* is upregulated in Fe- and [Dust] compared to Fe+ and Dust+.

Light-harvesting antennae: The phycobilisome antennae made of the phycobiliproteins allophycocyanin (core), phycocyanin/phycoerythrocyanin (linker) and phycoerythrin (rods) are known to attach and transfer light energy mainly to PSII but also to PSI. Their synthesis has high Fe requirements (Grossman et al. 1993). In the presented transcriptome, genes for most of these components are upregulated in Dust+ and Fe+ compared to Fe- and [Dust]. This was also previously observed for *Synechococcus* sp. PCC 7942 and *Synechocystis* (Sandström et al. 2002; Schrader et al. 2011).

Although the structure of the PSII phycobilisome antennae has been well studied the PSI antenna is less well understood. Recent evidence indicates that subunit CpcG3 of *Anabaena* sp. PCC 7120 (Watanabe et al. 2014) and CpcG2 of *Synechococcus* PCC 7002 (Deng et al. 2012) have an important function in the organisation of the PSI phycobilisome antenna. Upregulation of *cpcG2* in [Dust] and Fe-, opposite to the remaining phycobilisome genes, could be indicative of an increase in PSI antennae to enhance the light harvesting efficiency. and ameliorate the impact of a reduction in PSI subunits.

Finally, similarly to what is observed for various PSI and PSII subunit genes, *apcD, apcF, cpcA, cpeC* and *cpeE3* are upregulated in Dust+ and [Dust] compared to Fe- and Fe+ treatments.

An overview: Changes of gene expression are observed in all the major electron transport chain components (Fig. 5.20). Dust+ stimulates expression of the majority of genes in all components except ferredoxin and cytochrome b_6f whose transcript levels remain unaffected, and the electron transporters flavodoxin and plastocyanin which are expressed at reduced levels compared to the [Dust] treatment. Flavodoxin and plastocyanin are known to replace ferredoxin and cytochrome c_{553} under Fe-deficiency (Wood 1978; LaRoche et al. 1996) and this is also confirmed in the comparison between Fe+ and Fe-gene expression, as observed here (Fig. 5.20).

On the other hand, upregulation of genes (the majority of the genes whose expression is altered) encoding NAD(P) dehydrogenase, PSII and cytochrome b_6f is observed in Fe- compared to Fe+ (Fig. 5.20). It is possible that this is a cellular attempt to compensate for a reduction of the Fe-expensive PSI subunits and phycobilisome antennae under Fe-stress.

Another hypothesis is that the rapidly growing Fe+ cultures deplete reserves of a nutrient that by contrast is not limiting in Dust+ and therefore permit upregulation of PSII and NAD(P) dehydrogenase in the latter (compared to [Dust]). This could also justify the general upregulation in dust cultures, ([Dust] and Dust+) compared to Fe+ and Fe- observed across the photosynthetic components.

It is important to recognise that these hypotheses cannot be strongly supported with transcriptomic data as changes in one, or several genes, encoding for a protein complex are not indicative of its expression and assembly at the protein level. However, they can serve to signify potentially interesting targets for further analysis.

5.3.8.3 Oxidative phosphorylation

In cyanobacteria oxidative phosphorylation utilises both the thylakoid and plasma membranes while members of the photosynthetic and respiratory electron transport chain plastoquinone, plastocyanin/cytochrome c_{553}, cytochrome b_6f and NADH dehydrogenase are shared (Lea-Smith et al. 2016). Additional components in the respiratory electron transport chain are cytochrome oxidase (COX) and alternative respiratory terminal oxidase (ARTO) which reduce oxygen to water and pump H^+ across the thylakoid and cell membranes to power ATP production (through ATP synthase) (Hart et al. 2005; Lea-Smith et al. 2016).

Genes encoding for subunits of ARTO (*ctaCDE*) are upregulated in Fe- and [Dust] compared to Fe+ and Dust+ respectively. Also, genes *Tery_0279* and *Tery_0280* for transmembrane 'hypothetical proteins' upstream of the ARTO genes are expressed in a similar fashion. These were previously shown to be co-transcribed with ARTO in *Anabaena* but their function is not characterised (Valladares et al. 2003). The potential importance of ARTO in Fe reduction prior to its uptake (Kranzler et al. 2014) needs to also be considered.

Similarly, to the ARTO genes, cytochrome c oxidase assembly genes *cox15* and *cyoE* are regulated by Fe but only differences between [Dust] and Dust+ are statistically significant. The COX genes are not differentially expressed in response to Fe.

However, expression of *coxA*, whose protein binds heme *a* and a heme a_3-Cu_B centre (Alge et al. 1994), as well as the ARTO *ctaCD,* are lower in the dust treatments [Dust] and Dust+ compared to Fe- and Fe+. This indicates an additional effect of putative dust derived chemicals to the process of oxidative phosphorylation.

5.3.8.4 Nitrogen metabolism

Nitrogen (N_2) fixation is negatively affected by photosynthetic oxygen evolution and therefore strategies have evolved to separate the two processes. In *Trichodesmium* the peak N_2 fixation activity occurs at midday and coincides with a depression of photosynthetic activity (Berman-Frank et al. 2001). Samples from our experiment were acquired at 5 hrs through the 12 hr light period.

Contrary to previous reports (Shi et al. 2007; Snow et al. 2015) the genes encoding for the nitrogenase structural proteins NifD, NifH and NifK (*nifDHK*) were not differentially expressed. However, gene *nifZ*, involved in the maturation of the Mo-Fe protein P-cluster site containing a [4Fe-4S], and *fdxH*, encoding for the ferredoxin protein of nitrogenase are upregulated in Fe- relative to Fe+. In addition, *nifB* (involved in the biosynthesis of the Mo-Fe cofactor of nitrogenase) and *cysE* (involved in biosynthesis of cystein required for Fe-S cluster construction) are upregulated in Dust+ compared to [Dust].

The nitrate/nitrite utilisation genes *nirA* (nitrite reductase), *narB* (nitrate reductase) and *napA* (nitrate permease) are upregulated in Fe- and [Dust] cultures compared to Fe+ and Dust+ indicating the potentially N limited state of the cells in the former. A similar response in the expression of genes involved in nitrate/nitrite reduction and transport was observed under Fe-deficiency of *Synechocystis* (Hernández-Prieto et al. 2012). It should be mentioned that nitrate and nitrite reductase enzymes both have [4Fe-4S] cluster cofactors and therefore require Fe for their production (Luque et al. 1993; Rubio et al. 2002; Jepsoni et al. 2004).

Furthermore, upregulation of gene *gdhA* for the GdhA subunit of glutamate dehydrogenase in Fe+ compared to Fe- could be linked to an increased production of fixed nitrogen in Fe+, which is consequently processed through this enzyme to generate glutamate. Finally, regulatory genes of nitrate assimilation, *ntcA* and *ntcB* are not differentially expressed in the experimental treatments.

5.3.8.5 Outer membrane proteins

Haemolysin-type calcium binding (HTCaB) region domain**:** Growth of *Trichodesmium* on $FeCl_3$ and dust stimulates gene expression changes for proteins with HTCaB domains. The GO analysis identifies calcium-ion binding as an enriched category and 4 such genes are in the top 10 most differentially expressed genes identified in the transcriptome.

Calcium (Ca) has an important structural role in bacteria as part of the lipopolysaccharide layer and cell wall (Smith 1995, pp.83–133) and is involved in the cellular signalling system. A close link between the Ca and ROS signalling systems (Gordeeva et al. 2003; Brookes et al. 2004; Yan et al. 2006; Singh & Mishra 2015) denotes that changes in the former can be caused as an effect to stimulated ROS production under stress conditions. Such stress conditions are assumed to be encountered here in the Fe deficient, Fe- and [Dust].

Calcium binding domains in bacteria include HTCaB and EF-hand domains. HTCaB occur in tandem repeats in proteins that can form a parallel β roll structure (Baumann et al. 1993; Lilie et al. 2000) and are exported from the cell to function as haemolysin, cyclolysin, leukotoxin and metallopeptidases (Duong et al. 1992; Boehm et al. 1990; Rose et al. 1995). Adhesive properties (Sánchez-Magraner et al. 2007) and roles in motility (Brahamsha & Haselkorn 1996; Hoiczyk & Baumeister 1997; Pitta et al. 1997) have also been demonstrated.

Trichodesmium's HTCaB proteins have not been previously studied but the presented transcriptomic analysis suggests an important role. Ten out of the 15 HTCaB genes in the *Trichodesmium* genome are differentially expressed with variable profiles across the 4 experimental treatments (Fig. 5.22A). Three of these have characteristic Fe+ to Fe- and Dust+ to [Dust] differences (*Tery_0419, Tery_0424 and Tery_2055*) and bioinformatic analysis indicates that their sequence includes multiple CHRD domains (identified in chordin). These domains are expected to have an immunoglobulin-like β-barrel structure based on some similarity to superoxide dismutases, enzymes with protective function against oxidative stress, but their function is currently unknown (Hyvönen et al. 2003). Also annotated as HTCaB, and upregulated under Fe+, *Tery_3467* was previously identified as the alkaline phosphatase (APase) gene *phoA* (Orchard et al. 2003). Although the involvement of Fe in assembly and regulation of the APase PhoX has been previously mentioned (Yong et al. 2014, Mahaffey et al. 2014), PhoA is thought to require zinc and magnesium (Coleman 1992, Jakuba et al. 2008). Results presented here show Fe regulation of PhoA suggesting possible Fe binding properties.

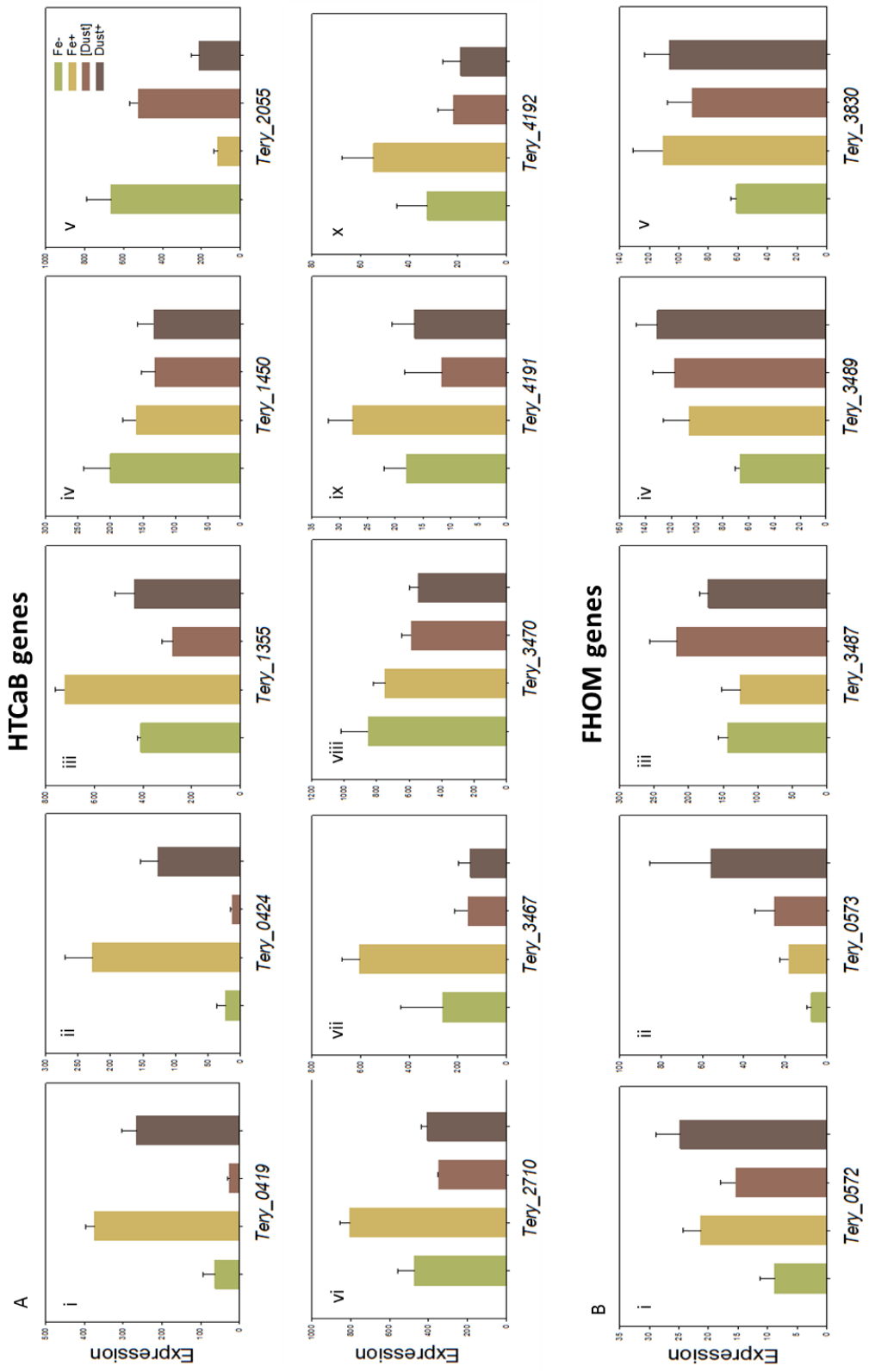

Figure 5.22: Gene expression of putative outer membrane proteins. Expression of genes with haemolysin-type calcium binding domains (HTCaB) (Ai-x) and filamentous hemagglutinin outer membrane domains (FHOM) (i-v) in the Fe- (green), Fe+ (yellow), [Dust] (light brown) and Dust+ (dark brown) treatments. Error bars are the standard deviations from the calculated means of triplicate cultures.

Filamentous hemagglutinin outer membrane (FHOM) domain proteins with similarity to the filamentous hemagglutinin family (containing the FhaB domain) consists of 10 large proteins in *Trichodesmium*, 5 of which are differentially expressed (Fig. 5.22) in the presented transcriptome. In pathogenic microorganisms such as *Bordetella pertussis* filamentous hemagglutinin forms adhesive molecules produced as virulence factors (Melvin et al. 2015). FhaB is the pre-pro protein that will be processed during export from the cell to form a long rod-shaped outer membrane product. Its translocation utilises the plasma membrane SEC export system and the two-partner secretion (Tps) pathway with the assistance of FhaC in the outer membrane. It is also interesting to note that Tps-system transported proteins have been associated with heme binding and utilisation functions (Zambolin et al. 2016).

The FhaC domain is identified in the differentially expressed *Trichodesmium* FHOM genes *Tery_3489, Tery_3487* (Fig. 5.22) and the non-differentially expressed *Tery_3266.* All three genes also contain the polypeptide-transport-associated (POTRA) domain. Gene *Tery_1533* (annotated as 'polypeptide-transport-associated' and not 'filamentous hemagglutinin outer membrane protein') also contains the POTRA and FhaC domains and is identified as differentially expressed in the transcriptome.

The 5 genes have mixed expression profiles across the 4 treatments indicating a response to different Fe cues either from dust, $FeCl_3$ or both (Fig. 5.22). Whether these genes might be involved in adhesion, Fe acquisition, or both, they seem to be significant and require further investigation.

The Tery_08xx gene cluster spans 8 genes (*Tery_0843-Tery_0850*) (Table 5D) all of which are differentially expressed in response to $FeCl_3$ and Dust (Fig. 5.23), with 5 being amongst the top 20 most differentially expressed genes identified in the presented analysis.

Tery_0848 and Tery_0849 are annotated as cell surface proteins while Tery_0843 is recognised by the UniProtKB Automatic Annotation pipeline as a membrane protein. In addition, Tery_0844 is predicted to contain an iron-sulphur binding site and Tery_0845 belongs to the heme oxygenase superfamily. Therefore, some of these properties indicate a possible association with cell membrane systems and/or the Fe metabolism of *Trichodesmium* but there is no sufficient evidence to suggest an involvement in Fe acquisition. Further investigation is required to characterise the function of these proteins.

Surprisingly, the fifth gene in this cluster (*Tery_0847*) encodes for MetE (5-methyltetrahydropteroyltriglutamate/homocysteine S-methyltransferase) which catalyses the transfer of a methyl group to and form methionine. This vitamin B12- independent methionine synthase was previously identified to be inactivated under oxidative stress in *E. coli* (Hondorp & Matthews 2004). In addition, MetE functions as a replacement to MetH (B12-dependent methionine synthase) under vitamin B12-limitation but requires higher zinc and nitrogen concentrations in diatoms (Bertrand et al. 2013). *Trichodesmium* possesses two *metH* genes (*Tery 1073, Tery_2492*) which are downregulated in Fe+ compared to Fe- (opposite regulation to *metE*) but these are not significantly different between [Dust] and Dust+.

It is difficult to suggest whether expression of the *metE* gene is regulated by the cell oxidation state, a dust-associated stimulus or a different cue associated with cellular contact to desert dust. Further understanding the controls on its expression, and the metal requirements for the protein's production in *Trichodesmium*, is required to investigate its potential as a biomarker of dust-Fe availability *in situ.*

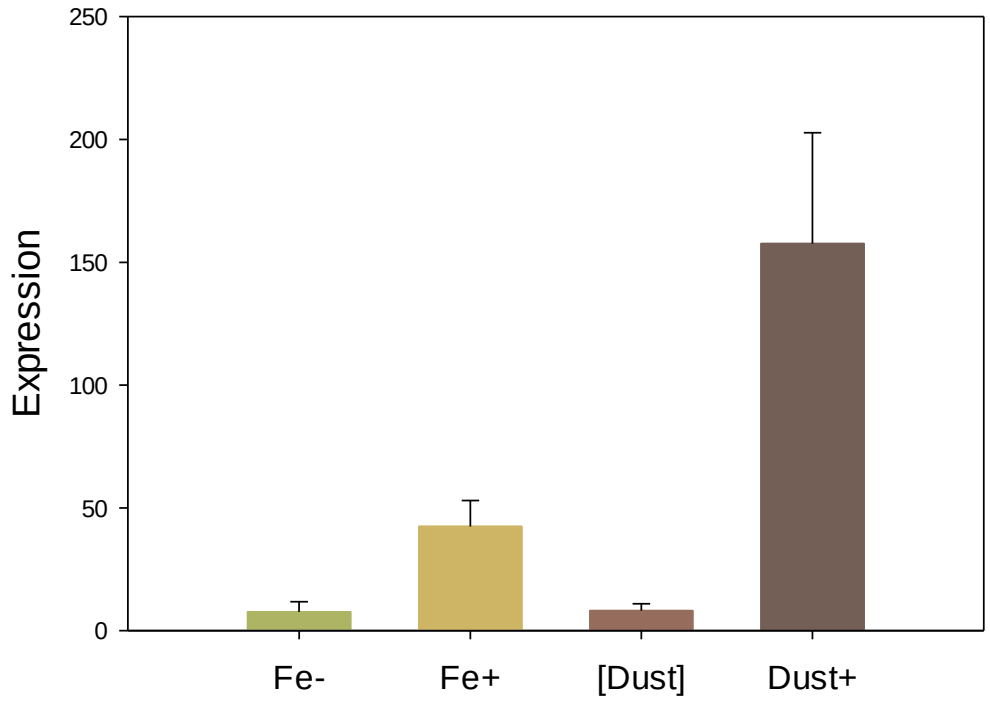

Figure 5.23: Representative expression across the *Tery_08xx* cluster. The expression of *Tery_0843* is higher in the Dust+ (dark brown) and Fe+ (yellow) treatments compared to [Dust] (light brown) and Fe- (green) respectively. Error bars represent standard deviations from the mean of 3 biological replicates.

Table 5D: The *Trichodesmium Tery_08xx* operon components. Features of interest indicate predicted conserved domains, subcellular localisation or metal binding sites (UniProtKB Automatic Annotation pipeline).

Gene	Annotation	Size (bp)	Features of interest
Tery_0843	hypothetical protein	609	5 alpha-helical transmembrane regions
Tery_0844	putative iron-sulfur cluster-binding protein	876	[2Fe-2S] cluster binding site
Tery_0845	TENA/THI-4 protein	705	Heme oxidase superfamily
Tery_0846	hypothetical protein	459	-
Tery_0847	5-methyltetrahydropteroyltriglutamate/homocysteine S-methyltransferase	2235	methionine synthesis 3 zinc-binding regions
Tery_0848	cell surface protein	183	-
Tery_0849	cell surface protein	573	-
Tery_0850	hypothetical protein	141	-

5.3.9 Regulatory DNA

Trichodesmium with 40% of its genome comprised of non-protein-coding DNA both in culture and in natural populations, is unique amongst cyanobacteria which as a group have an average of 15% (Larsson et al. 2011; Pfreundt et al. 2014; Walworth et al. 2015). Non-coding RNA that makes up about 80% of it (Walworth et al. 2015) could have an important regulatory role that provides *Trichodesmium* with an advantage in the fluctuating nutrient conditions of its natural environment.

Group II Introns function as ribozymes (catalytic RNA) and mobile genetic elements capable of self-splicing and inserting themselves in the DNA, resulting in interruption of their host genes. Most possess an intron encoded protein (IEP) that forms maturases, to aid splicing, and reverse transcriptases (RT). Open reading frame (ORF)-less group-II introns also occur and their splicing potentially requires the function of trans-encoded maturases (Meng et al. 2005).

Trichodesmium harbours 17 group-II introns which interrupt 11 genes, the highest number known to date for bacteria. Only 25% of bacterial genomes are known to contain at least 1 such element. In addition, despite their rarity amongst bacteria, 10 out of the 17 group II introns found in *Trichodesmium* are ORF-less (Pfreundt et al. 2014).

Here, we identify that 7 of the 11 group II intron host genes are differentially expressed across our experimental treatments. We suggest that the importance of these genes in the Fe response of *Trichodesmium* could be vital to provide necessary increased regulatory complexity in a fluctuating environment with ephemeral Fe supplies. The possibility that differential splicing of these introns occurs has to be addressed through further analysis.

Twintron**:** One of the elements mentioned above forms a twintron, an arrangement where one intron resides within another intron. This is yet another rare genetic phenomenon found in *Trichodesmium's* rich regulatory toolkit. It interrupts gene *Tery_4732* which is annotated as RNase HI but the mature/spliced mRNA product appears to be a member of a conserved hypothetical protein domain seemingly linked to a function in RNA metabolism (Pfreundt et al. 2015). Annotated gene *Tery_4730* is located within the host intron and *Tery_4731* within the inner intron (Fig. 5.24).

In the RNAseq analysis performed here we observe that the twintron host is differentially expressed across the experimental treatments (Fig. 5.25). Expression of the first part of the host gene before the 5' splice site of the host intron is increased in the Fe+ and Dust+ treatments compared to Fe- and [Dust] with a higher difference stimulated by additions of dust (2.3 times increase) compared to $FeCl_3$ (1.4 times increase). The same pattern is true for the host and inner intron. The second part of the host gene is expressed at much higher levels than the rest of the twintron region (5-13 times than the first part of the host gene) and expression is increased in the Dust+ and [Dust] cultures compared to Fe+ and Fe-. Unequal expression levels are also observed between the two parts of the host intron (5' side has 4-7 times higher reads).

Variability in splice site spanning reads is also observed. An increased number of reads covers the 5' host gene-host intron splice sites in the Dust+ and Fe+ compared to the [Dust] and Fe- (only the former is statistically significant). Similarly, to the unequal transcription profiles between the upstream and downstream regions of the host gene the splice site spanning regions vary in coverage. The 3' host gene-host intron splice site is spanned by a higher level of reads (1.3- 3 times) compared to the 5' splice site and the expression varies between treatments so that Dust+ and [Dust] have increased coverage compared to Fe- and Fe+. There are no statistically significant differences in the read coverage of the host intron-inner intron splice sites but there is significantly reduced (2.7-7 times) coverage in 3' compared to the 5' site.

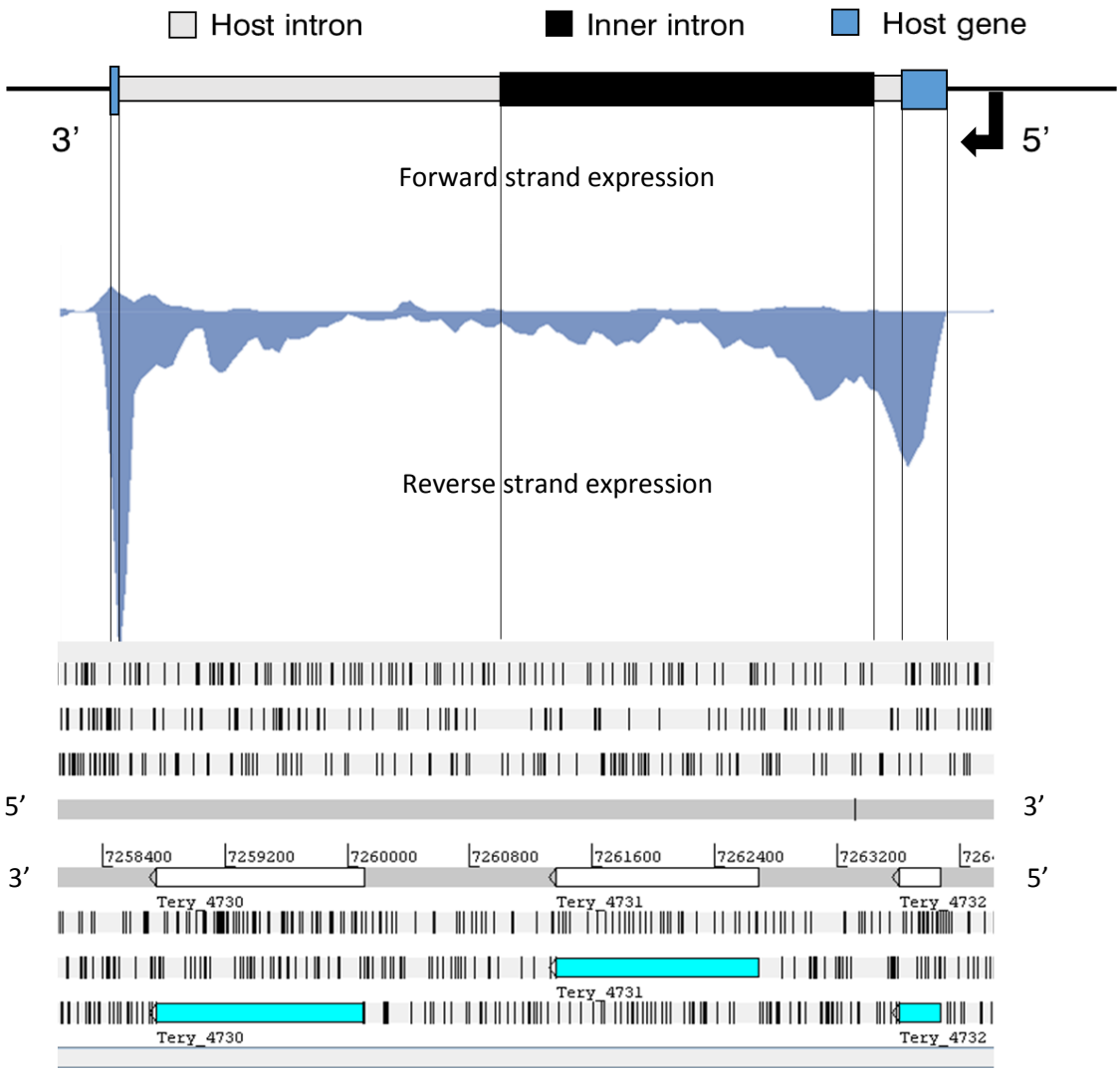

Figure 5.24: Representative expression profile along the *Trichodesmium* twintron arrangement. Read coverage from treatment Fe+ across the forward and reverse DNA strand is presented mapped against the annotated *Trichodesmium* genome (ARTEMIS genome browser) The inner intron (black), host intron (grey) and host gene (blue) are indicated along the expression profile.

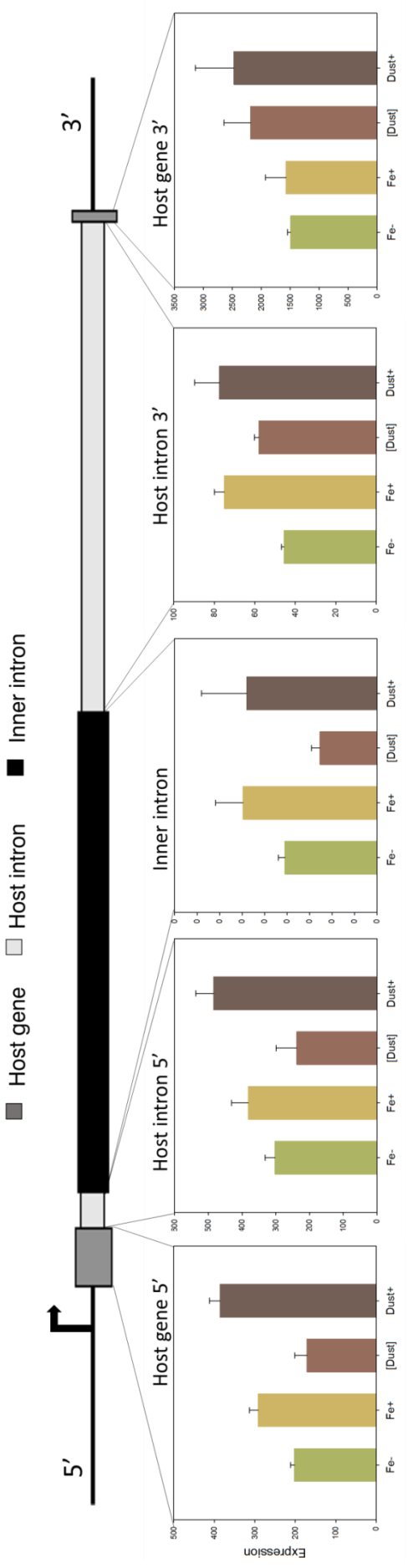

Figure 5.25: Expression of the *Trichodesmium* twintron across the experimental treatments. The expression of the inner intron (black), the host intron (light grey) and host gene (dark grey) differs between the experimental treatments: Fe- (green), Fe+ (yellow), [Dust] (light brown) and Dust+ (dark brown), and along the length of the DNA arrangement. Error bars represent the standard deviations of three biological replicates.

Diversity generating retroelement: A highly abundant 265 nt diversity generating retroelement functioning by mutagenic homing was previously identified in the non-coding fraction of the *Trichodesmium* genome (Pfreundt et al. 2014). Its analysis revealed 12 genes targets (Pfreundt et al. 2014) of which all, with one exception, are not differentially expressed in our sequencing results. The genes are expressed at low levels and no consistent SNPs appear compared to the *Trichodesmium* genome. The differentially expressed gene *Tery_1727* has higher expression of its 5' region in the Dust+ treatment, similar to an unannotated region preceding this gene.

The 265 bp retroelement itself (2632789r- 2632524r) is also more highly expressed in Dust+ (Fig. 5.26). We suggest that expression of the retroelement might not be controlled by the same factors as expression of its target genes. A combination of stimuli could be responsible for co-expression and diversity generation through this mechanism.

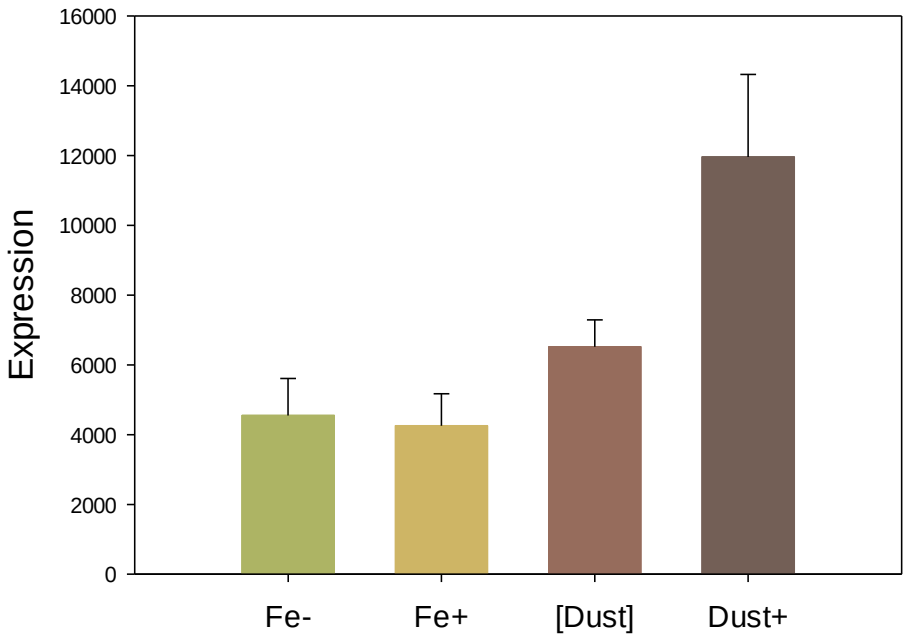

Figure 5.26: Expression of the *Trichodesmium* diversity generating retroelement. This 265 bp fragment is differentially regulated across the Fe- (green)-, Fe+ (yellow), [Dust] (light brown) and Dust+ (dark brown) treatments with high expression level indicated in the latter compared to the other conditions. Error bars represent standard deviations of the means of three biological replicates.

An overview: Although the analysis of non-coding/regulatory RNA was beyond the scope of this study the results indicated its central role in *Trichodesmium's* Fe-stress/dust-encounter response. Group II intron host genes, the *Trichodesmium* twintron region and the previously identified diversity generating retroelement (Pfreundt et al. 2014; Pfreundt et al. 2015) were all differentially expressed across the four growth conditions. A more extended analysis is required to indicate the specific nature of non-coding RNA controls on the transcription of genes involved in *Trichodesmium's* Fe metabolism.

5.3.10 Other metals

As mentioned previously, in addition to gene expression differences stimulated by Fe, as both Dust and $FeCl_3$, certain genes demonstrate an expression profile where in both the Dust+ and [Dust] cultures expression levels are higher than in Fe+ and Fe-. This is likely stimulated by soluble (i.e. capable of passing through the dialysis tubing) chemicals from dust, potentially including trace metals such as manganese, cobalt and zinc. These metals could be presenting secondary nutrient limitation challenges to growing *Trichodesmium* cells in no-dust added treatments. To identify effects of manganese, zinc or cobalt to the *Trichodesmium* molecular response across the experimental treatments the expression of genes involved in their uptake is reviewed.

Manganese: Adjacent to the Fe transporter *futBC* (*Tery_3222- Tery_3223*) genes, *Tery_3218* and *Tery_3219* are homologous to the *Anabaena all3575-alr3576* which are regulated by manganese (Huang & Wu 2004) and the manganese transporter MntAC (*sll1599-sll1598*) of *Synechocystis* (Bartsevich & Pakrasi 1996). The *mntA* homologue encoding for the ATP binding component of the transporter is differentially expressed with increased transcription in the non-dust (Fe-, Fe+) compared to dust (Dust+, [Dust]) treatments. This suggests that manganese might be released from dust and affect the expression of genes and processes differentially to that of the Fe- and Fe+ treatments.

Zinc: Homologues for the zinc transporter *znuAB* of *Anabaena* (*all0833-all0832*) are encoded by *Tery_4951-Tery_4952*, forming the putative periplasmic zinc binding protein, and ATPase respectively. The neighbouring *Tery_4953* is related to an ABC-transporter permease. None of these genes show differential expression in the conditions tested here.

Cobalt: Genes *Tery_2781-2782* encode for the cobalt transporting system, composed of the CbiQ inner membrane permease and the cobalt binding CbiM (homologues of *Anabaena alr3945-alr3943*). The ATP binding subunit CbiO is not annotated in the *Trichodesmium*

genome but downstream of the *cbiQ/cbiM* genes, *Tery_2780* is homologous to the Anabaena CbiO gene, *alr3949*. None of these genes are differentially expressed in the presented transcriptome. A fourth gene annotated as 'cobalt transport protein' *Tery_4901* is not identified as differentially expressed either.

5.4 Conclusions and further discussion

Despite *Trichodesmium's* role in the global biogeochemical cycles, little is known about its nutrient acquisition strategies. In particular, mechanisms employed by this organism in handling environmentally relevant nutrient sources, i.e. desert dust, have only recently started to be considered (Rubin et al. 2011). It has been demonstrated that environmentally collected *Trichodesmium* puff colonies handle dust as a unit exhibiting traits of multicellularity, and that their contact with dust particles is potentially important for Fe acquisition. With the aim to better characterise *Trichodesmium's* ability to extract Fe from Saharan desert dust we used controlled laboratory conditions to grow *Trichodesmium erythraeum* IMS101 in its presence, either when physically separated or by allowing direct contact. We compare the differences observed to those stimulated by additions of the conventional culture study Fe source $FeCl_3$-EDTA to a no added Fe background. Results indicate an advantage in utilising Fe to cells permitted to come in contact with dust. Therefore, Fe acquisition from particles likely exploits an as yet unspecified cell surface process.

To further investigate the Fe utilisation tools available to *Trichodesmium* the transcriptomic response of cells grown in contact or separated from dust, with $FeCl_3$-EDTA ($FeCl_3$) or under Fe-deficient conditions was analysed. Dust-added cultures were found to be transcriptomically more similar to $FeCl_3$-added than Fe-stressed cultures which share expression features with the dust-separated cultures. Several patterns of gene expression were identified, including coordinated and unique changes by dust and $FeCl_3$-additions (compared to the dust-separated and Fe deficient conditions respectively).

Previously recognised Fe-limitation marker genes are either affected by both dust and $FeCl_3$ or only the latter. This might be the result of increased available Fe concentrations, the provision of uncomplexed rather than particulate Fe, or the absence of additional nutrients which are available in dust, in the Fe+ treatment. Regardless of which are the underlying factors, results raise the need to apply caution when using these biomarkers in the field

where Fe concentrations are low and the major Fe source is Aeolian desert dust deposition. Based on the presented analysis, the *petE-petJ* genes of the plastocyanin- cytochrome c_{553} switch are the most well suited for use as biomarkers of the cellular Fe state.

To summarise the results of the transcriptomic analysis, gene ontology (GO) annotations were used to investigate the involvement of differentially expressed genes in various processes. Processes like photosynthesis, N_2 fixation, oxidative phosphorylation and Fe transport were reviewed in detail.

The process of photosynthesis was significantly affected and changes were observed in response to both Fe sources- dust and $FeCl_3$- simultaneously as well as by each addition separately. An effect on photosynthesis is to be expected as components including photosystems, electron transporters and photosynthetic pigments require Fe to be assembled and correctly function. In addition, when comparing the general response of genes for PSI/PSII subunits in Fe+ to Fe- cultures, a general upregulation of PSII and downregulation of PSI genes is observed during Fe-deficiency. This conservation strategy previously identified to occur at the protein level minimises utilisation of the Fe expensive PSI (Snow et al. 2015) whose light harvesting efficiency is increased by upregulation of *isiA* (Bibby et al. 2001). Interestingly, *cpcG2* which encodes for the CpcG phycobilisome paralogue that associates with PSI preferentially to PSII (as opposed to *cpcG1*) (Kondo et al. 2007; Deng et al. 2012) is also upregulated in Fe- compares to Fe+. We suggest that for the same reason as IsiA this functions to maximise efficiency of numerically decreased PSI complexes.

Although nitrogenase encoding genes, do not appear to be downregulated under Fe depleted conditions, as expected based on previous studies (Snow et al. 2015; Shi et al. 2007), expression of genes for enzymes nitrate/nitrite reductase and glutamate dehydrogenase involved in the organism's nitrogen metabolism are affected. This could be the result of the N-limited state of cells under Fe-deficiency due to lower nitrogenase activity or the enzymes' Fe content.

Furthermore, amongst the hypothesised Fe transport genes, the periplasmic binding proteins of the Fe^{3+} and siderophore uptake systems *futA* and *fhuD*, are $FeCl_3$ regulated. Although *Trichodesmium* also possesses homologues to the other members of the Fut transporter (*futB, futC*) it does not appear to encode homologues of the Fhu permease (*fhuB*) and ATPase (*fhuC*) components. This could be the result of divergent protein

components to complement FhuD in *Trichodesmium* or reduction and dissociation of Fe from hydroxamate siderophores once in the cell periplasm with subsequent transport across the plasma membrane through a different uptake system (e.g. FeoAB or FutABC).

The reductive mechanisms involved are also uncharacterised but possibly involve the previously suggested superoxide-mediated reduction of Fe (Roe & Barbeau 2014; Hansel et al. 2016). In addition, *Synechocystis* has been suggested to utilise electrons exported by the terminal oxidase ARTO (Kranzler et al. 2014). Based on the presented differential regulation of this membrane complex at the transcriptomic level, we suggest that reduction of Fe by ARTO-exported electrons could also be employed by *Trichodesmium*

Despite Fe being reduced prior to its uptake by several microorganisms, oxidation to Fe^{3+} by multicopper oxidases (MCO) and uptake through specialised Fe^{3+} transporters also occurs. We show the presence of an MCO-like gene in the *Trichodesmium* genome that is differentially expressed in response to $FeCl_3$ and could potentially be involved in *Trichodesmium's* Fe uptake pathway.

Most of the information currently available about *Trichodesmium's* Fe uptake system, as inferred by homology to proteins of other organisms, describe transport of Fe through the inner membrane. Interestingly, despite the presence of homologues to the TonB machinery (TonB, ExbBD) involved in siderophore uptake, *Trichodesmium* lacks known outer membrane TonB-dependent transporters (TBDT). It is possible that in this organism TBDTs are divergent to the known proteins of other cyanobacteria.

We identify an array of differentially expressed genes predicted to form large, calcium-binding proteins (annotated as Haemolysins-type calcium binding region domain proteins-HTCaB) likely to be localised at the cell outer membrane. These proteins have peptidase-like domains but could also be involved in adhesion and motility. Considering the involvement of superoxide in Fe uptake (Roe & Barbeau 2014), the interconnection of the ROS and Calcium cellular signalling systems (Gordeeva et al. 2003; Brookes et al. 2004; Yan et al. 2006; Singh & Mishra 2015) is also an interesting point to consider during further study of the HTCaB proteins. In addition, another set of possibly extracellular proteins that might be involved in adhesion and heme utilisation, annotated as filamentous hemagglutinin outer membrane domain proteins, has gene members displaying strong differential regulation across the experimental treatments. Lastly, the *Tery_08xx* cluster is a

novel set of genes with an apparent key role in *Trichodesmium's* Fe-deficiency response and includes members predicted to be localised at the cell surface.

Despite the lack of information regarding *Trichodesmium* outer cell membranes, it is potentially a key cellular component playing a critical role in the organism's life style. The *Trichodesmium* cells interact not only with nutrient substrates, but also with each other to form filaments and colonies in the environment, and with a diverse community of epibionts. Each of these features is significant to *Trichodesmium's* success in the world oceans. Therefore, further study of the putative extracellular proteins identified is necessary.

The absence of an established system for genetic manipulation of *Trichodesmium* limits greatly the tools available for further study of proteins and genes. It would be beneficial for future research to attempt an optimisation of growth conditions and explore possible options for genetic engineering of the organism. Additionally, proteins can be heterologously expressed in other organisms (Chapters 3 and 4) to assist their functional characterisation.

In this study, changes in gene transcription have been used to better characterise the organism's response to different Fe regimes. It is important to recognize that in addition to transcription several other controls mediate cellular activity. For example, pre-translation processes also include the interference of non-coding RNA. This appears to be particularly important for *Trichodesmium* whose non-coding genome proportion far exceeds the bacterial average (Larsson et al. 2011; Pfreundt et al. 2014). Indeed, we observe differential expression of the majority of group II intron hosts and the recently discovered twintron arrangement found in its genome (Pfreundt et al. 2014; Pfreundt et al. 2015). Finally, a diversity generating retroelement is stimulated by dust despite the fact that its target genes are expressed at low levels and are stable across the experimental treatments. We speculate, that its high non-coding genome content provides *Trichodesmium* with an additional regulatory capacity and flexibility, which is advantageous in a highly variable environment where nutrients fluctuate over time and space.

With a large fraction of *Trichodemium* genes being miss- or unannotated it is likely that a wealth of information regarding its physiological adaptations to a nutrient deficient niche are disregarded. This information could provide a window to understanding the evolution of adaptive strategies to a broader range of marine primary producers and assist in the

development of tools for detection and prediction of nutrient limitation in the ocean. Therefore, future efforts will be directed to a better characterisation of the *Trichodesmium* genome primarily though bioinformatic but also using analytic targeted techniques of gene/protein function in order to accommodate a more thorough understanding of the increasing pool of omic-technique derived data.

Chapter 6
Synthesis

6.1 Introduction

The research presented in the previous chapters aimed to better characterise *Trichodesmium* iron (Fe) and phosphorus (P) utilisation mechanisms and to provide a better understanding of the nutrient stress responses of this organism using a series of laboratory studies, involving both targeted and holistic molecular approaches.

In Chapter 3, the ability of *Trichodesmium* to grow on the reduced inorganic source of P, phosphite (PO_3^{3-}) was assessed. A gene cluster with homology to the PO_3^{3-} utilisation operon, *ptxABCD*, of pathogenic bacteria and *Prochlorococcus marinus* str. MIT 9301 was examined. Heterologous expression in *Synechocystis* sp. PCC 6803 (*Synechocystis* hereafter) was used to characterise its function, and its regulation by different P regimes was studied by quantitative RT-PCR (qPCR).

The technique of heterologous expression was also used in Chapter 4 to address the ambiguous function of protein Tery_3377, also referred to as IdiA. Although the protein is assumed to be involved in Fe transport it is equally similar to the *Synechocystis* FutA1 and FutA2 paralogues which are differentially localised and perform dissimilar functions.

Finally, acquisition of Fe from Saharan desert dust by *Trichodesmium* and the role of cell surface contact for this process was assessed through a physiological experiment. Transcriptomic changes stimulated by Fe-limitation or provision of dust were analysed in an attempt to explore the organism's adaptive strategies to environmentally relevant Fe fluctuations.

6.2 Main findings and concluding remarks

6.2.1 Better characterisation of nutrient uptake systems

Trichodesmium's niche spans vast nutrient limited areas of the low latitude ocean (Sohm et al. 2011), therefore the organism is hypothesised to possess efficient Fe and P utilisation systems that target several forms of these nutrients (Fig. 6.1). As *Trichodesmium* is currently not genetically tractable, most of what is presently known about the molecular control of such pathways is inferred from homology to characterised proteins of other organisms.

Work performed in the context of Chapters 3 and 4 demonstrated the efficacy of heterologous gene expression as a technique for characterising the function of *Trichodesmium* proteins. The action of two nutrient uptake/utilisation pathways of this organism was elucidated: The Fut system for uptake of Fe^{3+} across the plasma membrane and the Ptx system for uptake and utilisation of PO_3^{3-} (Fig. 6.1). These constitute the first direct evidence for the functioning of nutrient uptake pathways in this organism.

Phosphite, an unlikely source of P in the ocean

As described in Chapter 3 the *Trichodesmium ptxABCD* cluster is responsible for uptake and utilisation of PO_3^{3-} for growth. Essential for this pathway are both the ABC transporter (*ptxABC*) and the enzyme phosphite dehydrogenase (*ptxD*). These genes are also identifiable in published metagenomic and metatranscriptomic datasets from the North Atlantic and West Pacific (Fig. 6.2). Their prevalence and expression *in situ* indicates that their role stretches beyond that displayed in the controlled environment of laboratory cultures

The new data presented adds to recent evidence which suggest that oceanic P exists in more than just its fully oxidised +5 valence state in the marine environment, and that valence state +3 P is available to marine cyanobacteria both as organic phosphonates (Pn) and inorganic PO_3^{3-} (Martínez et al. 2012; Dyhrman et al. 2006; Van Mooy et al. 2015). One source of Pn to the ocean appears to be microorganisms themselves (Dyhrman et al. 2009; Pasek et al. 2014; Van Mooy et al. 2015). This could also be true for PO_3^{3-} as Van Mooy et al. (2015) showed its production^{-} by water column sample incubations and *Trichodesmium* colonies as well release of the majority of P reduced by the latter.

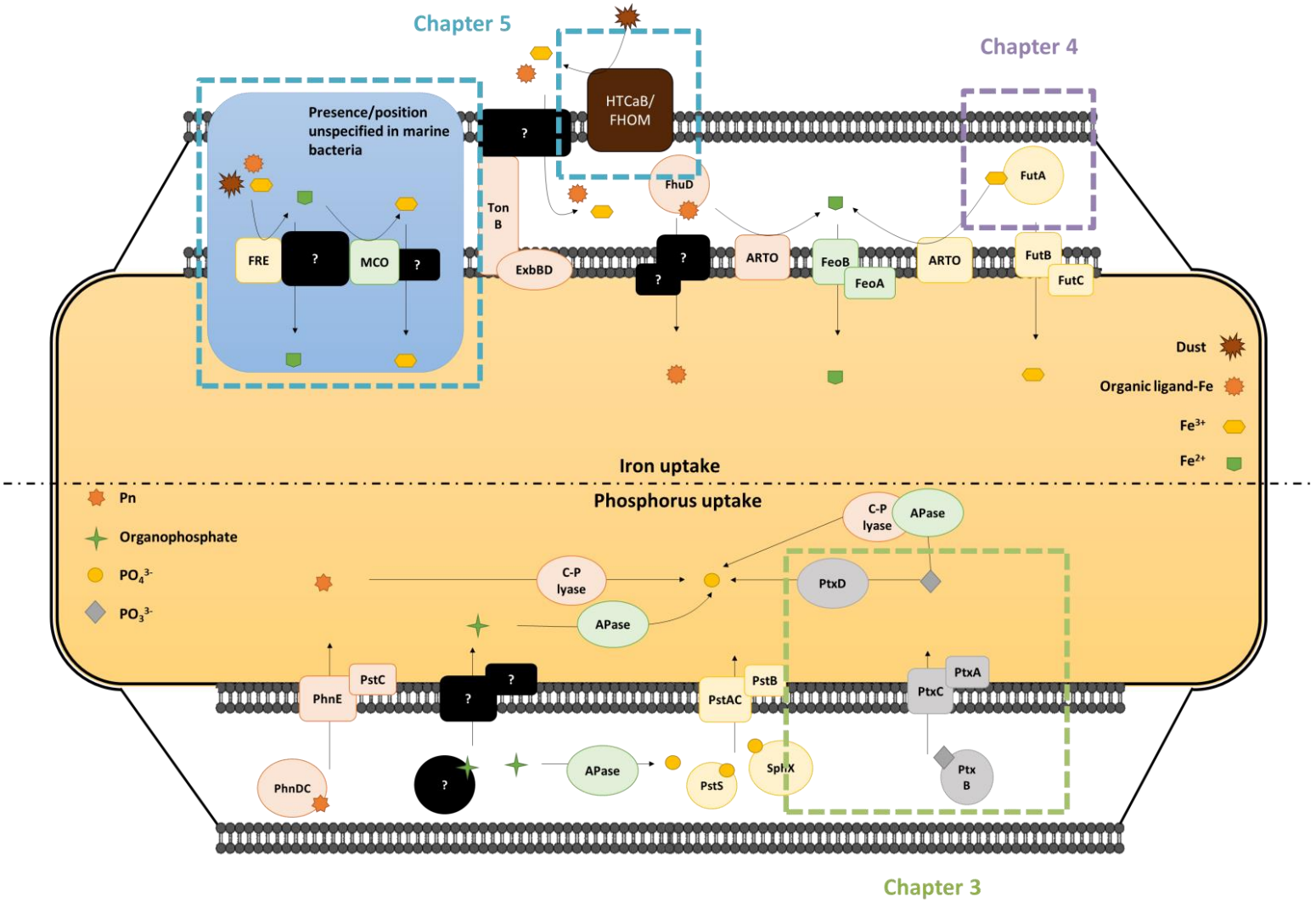

Figure 6.1: Iron and Phosphorus uptake by *Trichodesmium*. Subunits with homology to known Fe (top) and P (bottom) uptake systems are indicated. The P uptake pathways include the Phn organophosphonate (Pn) transporter and C-P lyase (orange), the APase for catalysis of organophosphates (green), the high affinity phosphate (PO_4^{3-}) transporter Pst (yellow) and the Ptx transporter shown to be responsible for PO_3^{3-} utilisation in Chapter 3(grey). Subunits involved in utilisation of Fe include organic ligand-Fe transporters of the TonB/ExbBD system and periplasmic component FhuD (orange). We hypothesise a role of ARTO in reduction of organic ligand bound Fe (orange). Fe^{3+}might be transported directly through the Fut system which includes the Fe-binding, periplasmic protein, FutA (Chapter 4) (yellow) or reduced by ARTO/FRE (Chapter 5)(yellow). Similarly, Fe^{2+} might be taken up by the Feo system (green) or oxidised by a MCO protein before uptake (Chapter 5) (green). Possible outer membrane HTCaB and FHOM

Although the purpose of biological PO_3^{3-} production is unknown, it could simply be an intermediate product of cellular Pn production and degradation pathways (Pasek et al. 2014). Based on the compound's antifungal qualities (Griffith et al. 1989; Karl 2014), possible use of PO_3^{3-} as an antibiotic defence by its producers is also suggested. In the case of *Trichodesmium* this could extend to protection of the entire colony consortia and/or keeping a balanced epibiont community. Additionally, if the genetic toolkit for accessing this source of P is not universal in the ocean, the specificity of nutrient exchange between *Trichodesmium* and specialist PO_3^{3-} utilising epibiont species could benefit the symbiotic relationship.

Regardless of the reasons behind biological PO_3^{3-} production, its presence in the ocean renders the existence of specialised uptake pathways (PtxABC transporter) beneficial for marine organisms. Intracellularly, although C-P lyases or APases, used for catalysis of Pn and organophosphate respectively, are also capable of driving the oxidation of PO_3^{3-} to PO_4^{3-} (Metcalf & Wanner 1991; Yang & Metcalf 2004) (Fig.6.1), NADPH/NADH formation (Costas et al. 2001) during PtxD activity makes this reaction energetically favourable. Therefore, the latter is more likely to be the preferred pathway for transforming PO_3^{3-} to PO_4^{3-} which will be consequently used for the cells' metabolic reactions.

A better characterisation of the Fe regulated IdiA

The ability of *Trichodesmium* to take up Fe^{3+} has not been clearly established in previous studies. Although reduction prior to Fe uptake is a major step of Fe acquisition by this organism, evidence indicates that free Fe^{3+} is also directly available (Roe & Barbeau 2014). However, the pathways involved have not been described at the molecular level.

Protein Tery_3377 is considered a periplasmic Fe^{3+} binding protein, part of an ABC uptake transporter, but is confusingly annotated after the *Synechococcus* sp. PCC 6301/PCC 7942, intracellular IdiA, involved in protection of PSII from oxidative stress (Michel et al. 1996; Michel et al. 1998; Exss-Sonne et al. 2000), due to their homology. They are both similar to the pathogenic bacteria Fe-binding FbpA part of the Fbp ABC-transporter for transport of Fe^{3+} (Krewulak & Vogel 2008). *Synechocystis* has two paralogues of this protein termed FutA1 and FutA2 which appear to be differentially localised, performing dissimilar functions one potentially similar to the pathogenic bacteria transporter FbpA (FutA2) and the other to the *Synechococcus* PSII-associated IdiA (FutA1).

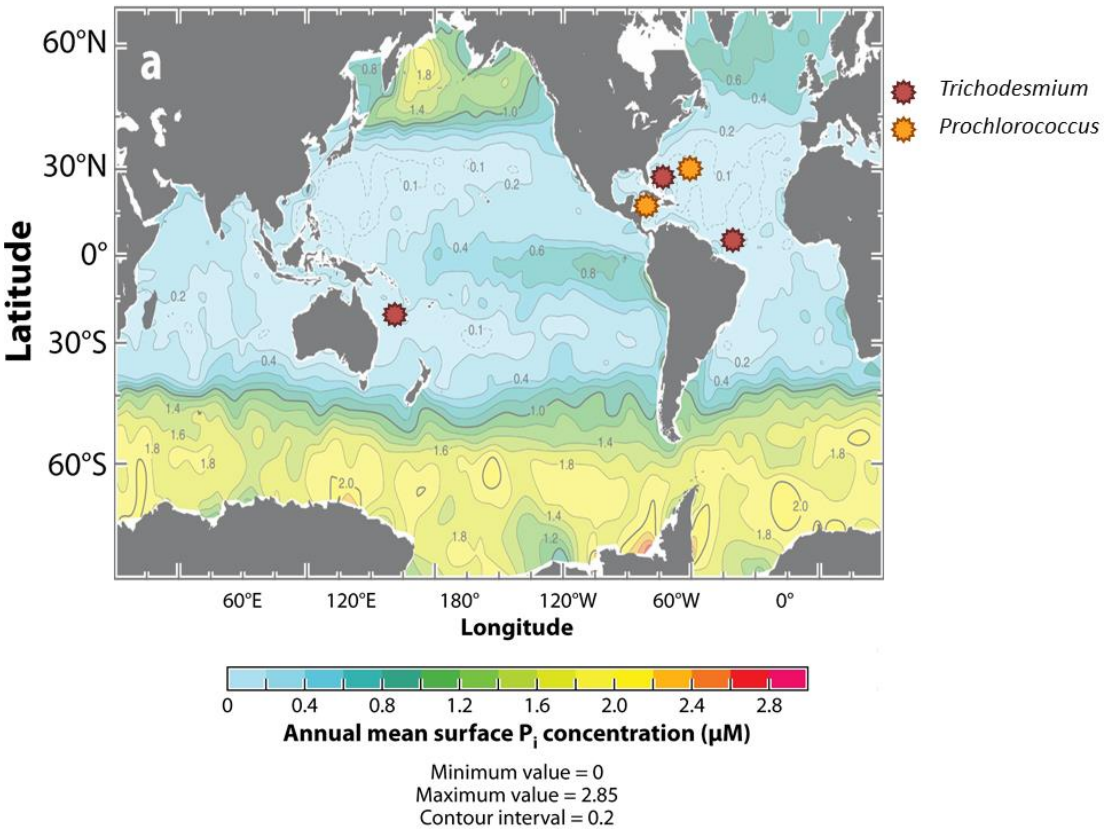

Figure 6.2: The prevalence /expression of the *ptx* gene cluster in marine cyanobacteria *Trichodesmium* and *Prochlorococcus*. Identified members of the cluster in published metagenomes and metatranscriptomes of *Trichodesmium* (summarised in Polyviou et al. 2015) (red) and *Prochlorococcus* (Martínez et al. 2012) (orange) mapped over the global distribution of PO_4^{3-} in the ocean (Karl 2014).

In Chapter 4, data to support the role of *Trichodesmium* Tery_3377 as an Fe^{3+} transporter is presented (Fig. 6.1). The protein possesses a signal sequence that directs it to the periplasmic space through the twin argenine transporter (TAT) system. The purified protein binds Fe^{3+} with high affinity and the protein structure bound to Fe^{3+} is retrieved (Polyviou et al, manuscript in preparation). Finally, heterologous expression in *Synechocystis futA2* mutants appears to relieve the compromised physiology (generated when Fe^{2+} is bound to the strong ligand ferrozine). We therefore propose the reannotation of Tery_3377 as FutA2 (referred to it as Tery_3377 for the purpose of this discussion to avoid confusion).

Despite the identified function of *Trichodesmium* Tery_3377 as an Fe^{3+} transporter, the collected results raise questions about the exact function of the two *Synechocystis* paralogues. Disproportional growth reduction of the double mutant Δ*futA1*/Δ*futA2* compared to the pooled decrease of Δ*futA1* and Δ*futA2* growth, could be the result of accumulated pressures above the level at which they can be internally managed by the

organism, when two rather than one Fe-stress response proteins are deleted. However, this disproportional growth reduction could also be an indication of a complementary FutA1 and FutA2 function, in which case at least one of the two will be required for efficient growth under Fe-stress. Traces of GFP in the periphery of cells when fused to the FutA1 signal sequence is possible evidence towards a more intricate function of FutA1, with a hypothesised additional role in Fe uptake. This theory is also supported by the growth/photosynthetic physiology improvement of the Tery_3377 expressing Δ*futA1+* compared to Δ*futA1*. Other justifications for this recovered physiology of Δ*futA1+* include a putative secondary function of Tery_3377 similar to that of the intracellular FutA1, or 'boosting' of Fe uptake (resulting from regulation of its expression by a constitutive promoter) favouring the Δ*futA1* independently.

These questions remain to be elucidated in more in-depth studies focusing on the functional characterisation of the *Synechocystis* paralogues. An interesting approach could be to *in vivo* track FutA1/FutA2 localisation, during the diel cycle and *Synechocystis* growth phase stages, both under Fe-replete and deplete conditions.

Cell Surface- The importance for utilisation of dust-Fe

The involvement of cell surface/outer membrane processes in Fe uptake is not currently well characterised in marine cyanobacteria. *Trichodesmium* is capable of utilising siderophores and dust for which passive diffusion through the cell membranes is unlikely (Achilles et al. 2003; Langlois et al. 2012; Rubin et al. 2011, Chapter 5). The dissolution and acquisition of Fe from dust and ferrihydrite appears to occur extracellularly and it is suggested that processes at the cell surface involving substrate adsorption on the cells is a necessary prerequisite for this process (Rubin et al. 2011). The latter was indicated through inhibition of Fe dissolution by entrapment of ferrihydrite within glass fiber filters. There are pitfalls to this technique as it is not possible to demonstrate whether dissociation of Fe is prevented because of the way that ferrihydrite is attached to the filters. Also the media used does not include any ligands such as EDTA to prevent re-precipitation of Fe immediately after its potential dissolution.

Knowledge of pathways for extracellular, cell surface-associated, Fe reduction/dissolution from ligands in marine cyanobacteria is limited. *Synechocystis* pili appear to facilitate electron export for Fe reduction (Lamb et al. 2014) while in *Trichodesmium* cell derived superoxide might be involved in the process (Roe & Barbeau 2014; Hansel et al. 2016). In addition, other than TonB dependent transporters (TBDTs) (Hopkinson & Morel 2009), no

known proteins facilitating cell surface adsorption/uptake of Fe/Fe ligands are characterised in marine cyanobacteria. In *Trichodesmium*, although periplasmic and inner membrane components the TBDT pathway (TonB and ExbBD) have been identified (Fig. 6.2), no obvious homologues of the outer membrane components are encoded in the genome.

In Chapter 5 the question of the role of cell surface processes to extracting Fe from dust was addressed in a simple and direct experimental set-up. Dust was either released within the culture flasks in contact with cells (Dust+), or separated by means of a dialysis membrane ([Dust]). The growth and photosynthetic physiology was compared to no Fe (Fe-) and $FeCl_3$-EDTA added (Fe+) cultures. The results revealed that when direct contact with dust is prevented, Fe limits *Trichodesmium* growth and photosynthetic efficiency.

The treatments were analysed using RNA sequencing (RNAseq) to look deeper into the molecular pathways underlying the growth and photosynthetic physiology response of the cultures to the different Fe regimes. Uncharacterised genes encoding for proteins possibly associated with the cell/outer membranes were identified based on conserved protein domains. Protein groups annotated after the 'Haemolysins-type calcium binding region domain' (HTCaB) and 'Filamentous hemagglutinin outer membrane domain' (FHOM) as well as an eight gene cluster (Tery_08xx) included some of the most significantly differentially expressed genes between the experimental treatments.

Proteins of the HTCaB group have recognised similarity to COG2931 (Ca^{2+}-binding protein) and Peptidase_M10_C (Peptidase M10 serralysin C terminal) conserved domains. These domains are encountered in extracellular metallopeptidases involved in proteo/hemo-lyic activity of pathogenic bacteria (Miyata et al. 1970; Boehm et al. 1990; Duong et al. 1992; Rose et al. 1995; Kuhnert et al. 2000; Christie-Oleza & Armengaud 2010; Massaoud et al. 2011). Roles in adhesion and motility have also been suggested (Brahamsha & Haselkorn 1996; Hoiczyk & Baumeister 1997; Pitta et al. 1997; Sánchez-Magraner et al. 2007). To our knowledge the role of these domains has not been previously discussed in cyanobacteria. The properties of adhesion, motility and lysis of extracellular substrates could be beneficial qualities for particulate Fe utilisation by *Trichodesmium*.

The same is true for the FHOM protein group which is also associated with virulence of pathogenic bacteria trough adhesive properties (Melvin et al. 2015). Such proteins are extracellular, exported from the cell through the two-partner secretion (TPS) system

(Hodak et al. 2006). It is worth mentioning that TPS translocated proteins can also be non FHOM containing such as the *Haemophilus influenzae* HxuA. Interestingly, this protein has a role in heamopexin utilisation by extracting its heme group which is then available for transport through the TonB-dependent transporter (TBDT) protein HxuC. It can be hypothesised that the FHOM proteins in *Trichodesmium* have evolved to perform similar functions.

It is interesting to speculate whether in association with TonB a diversified outer membrane-linked protease has evolved to perform both functions of extraction and translocation of Fe from ligands. Possible involvement of HTCaB and FHOM proteins remains to be examined.

Another group of uncharacterised genes with strong differential expression in the transcriptomic analysis, contains 8 genes (*Tery_0843- Tery_0850*) sequentially localised in the *Trichodesmium* genome. Two are annotated as cell surface proteins and one is predicted to be membrane associated but further analysis is required to identify possible association with extracellular processes.

Based on the transcriptomic results (as presented in Chapter 5), it appears that processes occurring at the *Trichodesmium* cell surface are fundamental in coordinating its response to desert dust additions, and further investigation is required to characterise the function of identified genes with potential relevance to this. Heterologous expression, as demonstrated in Chapters 3 and 4, could be used as an approach for their localisation and functional characterisation, while the metal binding capacity of proteins can be tested *in vitro*.

The skeleton-frame of *Trichodesmium's* Fe uptake system

Through research performed in the context of this thesis, progress is made in elucidating *Trichodesmium's* Fe uptake system. We suggest a working model (Fig. 6.1) through which putative outer membrane HTCaB and FHOM proteins act through lytic/adhesive properties to extract Fe from dust. Additionally, either in combination or independently to these processes, Fe dissolution via reduction by cell derived ROS (Roe & Barbeau 2014; Hansel et al. 2016) might be involved. However, no information regarding the molecular pathways behind this process is currently available.

Released Fe^{2+} and Fe^{3+}, uncomplexed or bound to organic ligands, is subsequently transported across the outer membrane through unidentified TBDTs. In the periplasm, FhuD binds ligand-associated Fe and either leads it to an as yet unidentified inner

membrane permease (related to FhuB) or an electron source such as ARTO for its reduction to Fe^{2+} (Fig. 6.1). Likewise, FutA2 binds $Fe^{3+}$and either facilitates its transport across the inner membrane in combination with FutBC or releases it after its reduction (Fig. 6.1). Reduced Fe released in the periplasm will be subsequently transported by the FeoAB system.

Putative ferric reductase (FRE) and multicopper oxidase (MCO) subunits potentially confer redox activity contributing to Fe transformations either intracellularly, or at the exterior of the cell prior to its uptake, complementing processes of the hypothesised model.

6.2.2 Dust/$FeCl_3$ effects on photosynthesis

The most prominent changes identified to be coordinated by $FeCl_3$ and dust are related to photosynthesis. This could, to a large extent, be due to the better characterisation of photosynthesis compared to other cellular processes. Changes in response to one or more of the experimental treatments are identified for all the major photosynthetic electron transport chain components (Fig. 6.3).

Similar responses are induced by $FeCl_3$ and desert dust in genes of: the cytochrome subunits of PSII, cytochrome c_{550} and b_{559}, the PSI subunits PsaA and PsaB binding the F_X Fe-S centre, several phycobilisome proteins, the electron transporters plastocyanin and cytochrome c_{553}, one flavodoxin protein, the NADPH dehydrogenase NdhI binding the Fe–S clusters N6a and N6b, and components of the F_1F_o ATP synthase complex.

Genes for several subunits of the phycobilisome antenna are commonly upregulated in the presence of dust and $FeCl_3$, as expected from the high Fe requirements of phycobilisome synthesis. However, interestingly, the opposite behaviour (upregulation in Fe-/[Dust]) is displayed by the gene encoding CpcG2 for which there is evidence indicating an involvement in organisation of a PSI phycobilisome antenna (Deng et al. 2012; Watanabe et al. 2014). Although the attachment of the phycobilisome antennae to PSII is generally well described, a justification for the nature of phycobilisome-PSI interaction was only recently published (Watanabe et al. 2014). It appears to involve a supercomplex of a double-dimeric (tetrameric) PSI complex which is associated with one to three rods of two hexameric phycocyanin units. As CpcG2 is mostly found in daytime fixing diazotrophs compared to species like *Crocosphaera* that fix N_2 in the dark, and the concentrations are elevated in heterocysts rather than vegetative cells, the authors suggest an important function related to N_2 fixation. The tetrameric PSI- phycobilisome supercomplex could be enhancing cyclic

electron transport (CET) as a way of reducing oxygen (detrimental to nitrogenase) evolution by PSII (Fig. 6.3). Our results can be explained by an N-depleted state of Fe- and dust-separated cultures stimulating upregulation of the supercomplex to allow more efficient N_2 fixation. It can be also suggested that formation of the supercomplex is an Fe-stress response strategy facilitating an increased light harvesting efficiency by the fewer PSI subunits (reduced due to their high Fe requirements relative to PSII) in a similar way as IsiA antennae proteins.

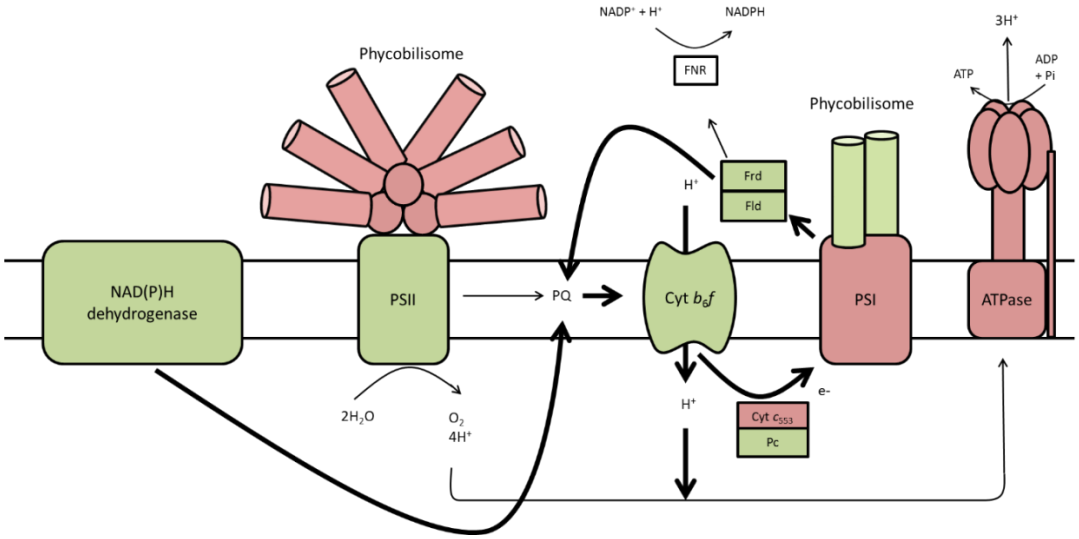

Figure 6.3: The hypothesised response of the photosynthetic electron transport (PET) chain to Fe limitation in *Trichodesmium*. Based on the direction of the expression change of the majority of genes for each subunit as identified in Chapter 5 of this thesis (Fe- vs Fe+ comparison). Photosystem I (PSI), PSII-phycobilisome, cytochrome c_{553} (Cyt c_{553}) and F_oF_1 ATPase (ATPase) are downregulated under Fe-stress (red). Conversely, NAD(P)H dehydrogenase, photosystem II (PSII), cytochrome b_6f (Cyt b_6f), plastocyanin (PC) flavodoxin (Flvd) and ferredoxin (Frd) appear to be upregulated (green) under the same conditions. The PSI phycobilisome is hypothesised to be upregulated (green) based on increased expression of the *cpcG2* gene important for its organisation. Cyclic electron flow (CEF) around PSI is enhanced under low Fe (bold arrows).

Despite the similarities mentioned there are also differences between gene expression responses of *Trichodesmium* to $FeCl_3$ compared to dust. Genes that are only differentially expressed in response to contact with dust encode for the PSII transmembrane CP43 and CP47, additional subunits of the phycobilisome antenna, F_1F_o ATP-synthase, NADPH dehydrogenase and the ferredoxin NADP+ reductase. Genes only regulated by $FeCl_3$ include the D1/D2 of PSII, the membrane intrinsic subunits of cytochrome b6f, an additional flavodoxin, two ferredoxin proteins, and an additional component of NADPH

dehydrogenase. These differences might either be associated with the nature/quantity of Fe available in the two treatments or the presence of other chemical stimuli from dust. A general upregulation of the photosynthetic components in both the dust-separated and dust-added cultures compared to Fe- and Fe+ is also observed. It is difficult to indicate the stimuli responsible for these differences based on the provided data alone. Elevated concentrations of specific nutrients from dust (e.g. Manganese -See Sec. 5.3.10) could be responsible if limiting in the non-dust cultures. As discussed below, alterations of the general ratio of resources in the dust containing media could also be important.

6.2.3 Is it more than just the concentration of nutrients? The problem with biomarkers of iron limitation

Phosphorus and Fe colimitation has been identified both in field and laboratory studies (Mills et al. 2004; Walworth et al. 2016; Garcia et al. 2015). Garcia et al. 2015 has shown that in P-deficient conditions *Trichodesmium* and *Crocosphaera* that are Fe-challenged grow and fix N_2 faster than when provided with an abundance of Fe and attributed this to a decrease of cell size upon colimitation. The hypothesis ('Nutrient-Balance' hypothesis hereafter) is that marine life has adapted to colimitations and combination additions of nutrients and will thus have more effective strategies to deal with such scenarios. This could result in inaccurate results from several field and laboratory studies attempting to elucidate the response of organisms to single nutrient deficiencies/additions.

This 'Nutrient-Balance' hypothesis is critical to the arguments presented in Chapter 5 regarding the *in situ* use of nutrient limitation biomarkers identified in laboratory stress experiments. Culture experiments almost exclusively utilise nutrient forms that are of little relevance to the natural sources introduced to the ocean system, and the resources are provided in excess. This sets the interpretation of results more manageable but less representative of the natural word. Therefore, the differential expression of molecular Fe-limitation biomarkers identified in culture experiments could be indicative of the nutrient's limitation/abundance but also:

- The nutrient-balance
- Regulation by a specific form of nutrient provided in the experiment
- The presence of a large excess of that nutrient

The former two can set the biomarkers environmentally irrelevant. For example, although the usual supplement in *Trichodesmium* Fe+ cultures in laboratory Fe-stress experiments is Fe' from $FeCl_3$-EDTA, desert dust is the primary source of Fe to the open ocean and will also

deliver other nutrients such as P, zinc, cobalt, nickel, manganese, and copper (Duce et al. 1991; Okin et al. 2004). In addition, the provision of a large excess of the nutrient in cultures can result in identification of biomarkers that will lack the sensitivity often required for detection of milder nutrient fluctuations often encountered *in situ*. In Chapter 5 *Trichodesmium* cultures were supplied with either $FeCl_3$-EDTA or Saharan desert dust as a source of Fe. Several common gene expression responses were recognised for the two sources but differences were also obvious.

Furthermore, the expression levels of a gene are often highly growth-phase dependent. This can be monitored through the expression profile of a gene/protein in parallel to the growth curve of laboratory cultures and also the expression during the development of phytoplankton bloom events (Shi et al. 2007; Spungin et al. 2016). It is also worth remembering that a biomarker chosen and tested based on the physiology of one organism will not necessarily be representative of its behaviour in other members of the community. For example, although *Trichodesmium*'s abundance/distribution was repeatedly shown to follow dust deposition (Langlois et al. 2012; Langlois et al. 2008; Lenes et al. 2008; Moore et al. 2009; Fernández et al. 2010) the response of *Synechococcus* and *Prochlorococcus* to dust can be variable with negative/toxic effects indicated in some occasions (Langlois et al. 2012; Paytan et al. 2009).

The arguments stressed above can, depending on the experimental approaches, either present limitations to the use of molecular biomarkers as detectors of nutrient stress, or provide a platform for novel applications of these tools. It is theoretically possible, using biomarkers, to detect bioavailability of different nutrient sources- the nutrient status- and the progression stage of a bloom event in-time. The Nutrient-Balance disturbance of natural/anthropogenic events could also be followed after suitable tool optimisation.

We suggest the following pipeline to be followed from the identification to the utilisation of marine gene/protein expression biomarkers of nutrient limitation: (1) Transcriptomic/ proteomic analysis with a gradient of environmentally relevant nutrient forms to identify potential biomarker targets. (2) Characterisation of the targets' differential expression development over time through quantitative RT-PCR (qPCR). (3) *In situ* testing. Sampling and expression-detection sensors (currently under development) have the capability of monitoring expression of the identified biomarkers over the course of bloom events. (4) Use of biomarkers to detect nutrient-stress in the field. Finally, multiplicity of biomarkers

targeting concurrent identification of various nutrient stressors can provide a more comprehensive picture (Saito et al. 2014).

In Chapter 5 we identified that some commonly used biomarkers of Fe-limitation were not differentially regulated by dust at the time of sampling while expression differences were strong in response to $FeCl_3$-additions. These include genes for the PSI antenna IsiA, the flavodoxin protein IsiB and the Fe transporter Tery_3377 (FutA2). Commonly differentially expressed genes between the two Fe sources include the interchangeable electron transporters plastocyanin and cytochrome c_{553} (3^{rd} and 1^{st} most differentially expressed genes respectively). The copper containing plastocyanin is known to replace the Fe containing cytochrome c_{553} under conditions of Fe-stress in a behaviour referred to as the plastocyanin-cytochrome (P-C) switch (Wood 1978; De la Cerda et al. 2007). We suggest further testing of the P-C switch, for its application as a biomarker of Fe-limitation. Due to the copper dependent nature of plastocyanin, the simultaneous use of an associated copper-status biomarker and/or seawater copper concentration measurements may be necessary.

6.2.4 Non-coding RNA- A role in the response of *Trichodesmium* to dust

Data presented in Chapter 5 indicate a significant involvement of non-protein coding DNA in the Fe-limitation/Dust-addition response of *Trichodesmium*. The unexpectedly high proportion of non-coding genome in *Trichodesmium* (40%), far exceeding the average for other cyanobacteria (15%), has been recently discussed after the characterisation of its primary transcriptome (Pfreundt et al. 2014) which indicated the highest number of non-coding DNA transcription start sites (TSS) compared of all bacterial species currently analysed. Unusual non-coding RNA properties, including a bacterial record breaking number of 17 group II introns targeting 10 host genes, a group II twintron arrangement (the only known bacterial twintron to interrupt a protein coding gene), as well as a diversity generating retroelement (DGR) targeting 11 different genes, have been identified (Pfreundt et al. 2014; Pfreundt et al. 2015). These, properties are added to the previously identified high number of transposable elements in this organism (Larsson et al. 2011; Lin et al. 2011; Mikheeva et al. 2013). The non-protein coding fraction of the genome seems to also be maintained in the environment (Walworth et al. 2015). This finding leads to the conclusion that regulatory RNA is linked to the organisms' lifestyle, possibly its cohabitation with other microorganisms and the nutrient fluctuating conditions it encounters.

In the transcriptome presented, 7 out of the 11 group II intron host gene regions are identified to be differentially expressed with the twintronic region displaying a very high positive response when dust is in contact with *Trichodesmium* cells. In addition, although no major differences in expression of the 12 DGR gene targets between treatments are obvious, the retroelement itself is again upregulated in response to contact of cells with dust. We suggest that *Trichodesmium's* unusual genome features may be linked to episodic desert dust influx events in the environment, and potentially its success in the ocean.

6.3 Final discussions

The study of biology at the systems level through omic approaches is expanding rapidly and provides a wealth of new information. As demonstrated, it can be useful in identifying key genes, both studied and uncharacterised, involved in organismal metabolic processes. In addition, the tools currently available enable the decryption of environmental metagenomes and metatranscriptoms *en masse* in projects like the Global Ocean Sampling (GOS) and TARA Oceans project while sequencing of single cells is opening a whole new suit of possibilities for marine research.

However, data generation currently far exceeds our analytic capabilities and is, in my opinion, the limiting step to a better characterisation of biological systems and processes. Taking *Trichodesmium* as an example, the function of the majority of the genome is unresolved with several unannotated, and a high incidence of miss-annotated, proteins often setting the generated results incomprehensible. Future efforts will need to be directed towards better bioinformatic and targeted gene characterisation of this species.

This characterisation, as demonstrated, can utilise state of the art genetic modification techniques even in a genetically intractable species such as *Trichodesmium*. This organism has an unusually large 'deck of genes' identification of which is not only important to understanding its possible response options in the future of ocean changes, but also to discover biotechnologically interesting potentials. As an example, the *Synechocystis* PtxABCD+ mutant able to grow on reduced inorganic P (Chapter 3, Polyviou et al. 2015), is currently under optimisation for use in bioreactors. Specialised growth on PO_3^{3-} can promote culturing specificity and inhibit growth of contaminating species.

In the meanwhile, the presence and expression of this gene cluster in the environment is strong evidence for significant PO_3^{3-} availability in the ocean, something that has not yet been demonstrated, with environmental concentrations and quantified fluxes of reduced P

(both organic and inorganic) currently lacking. The detection limits of analytical chemistry techniques for P but also for Fe may lead to misguided interpretations of nutrient availability to primary producers. The biological approach for identifying the presence of available nutrient pools through the use of biomarkers comes with its own limitations. Coupling of chemical measurements with biomarker detection through the development of integrated biochemical sensors is an approach with high potential, able to combine the advantages of both methods and deliver a more representative picture of the presence/availability of nutrients as well as their interaction with phytoplankton. Monitoring changes in the nutrient/production status of the world oceans, through autonomous *in situ* marine sensors, can indicate disturbances in the system over space and time and facilitate the prediction of biogeochemical cycle functioning and associated climatic changes.

Appendix

Table A1: Primer sequences used for genetic modification.

Chapter	Purpose	Method	Construct	Primer	Sequence
3	Heterologous expression of Trichodesmium ptx genes in Synechocystis	pFLAG	ptxABCD	F	ATGCCATATGATCTCTCTAAATAAACTGGGTGTGAC
				R	ATGCGGATCCTTATAGCTTGTTAACAGCTCCTTGA
			ptxABC	R	ATGCGGATCCTTAAATAAACTTTTGACGCAAATAGTTAC
			ptxD	F	ATGCCATATGGATAAAAAAACCATTAGTTGTTATTACC
4	Generation of Synechocystis knockout mutants	OLE-PCR	futA1	P1	CCAACCTCCAGTTCCACTGAC
				P2	ACATTAATTGCGTTGCGCTCACTGCGACGGGATAACTTTTGGACC
				P3	CAACTTAATCGCCTTGCAGCACATAGGTCCATTGGCAATGGTTG
				P4	GCCATTACGAAGGGGTGGACG
				P5	CGGCATTTTTCAGCCGGTGC
				P6	GGGCTGTGTCATTGCCCTGG
				zeo_F	GCAGTGAGCGCAACGCAATTAATGT
				zeo_R	ATGTGCTGCAAGGCGATTAAGTTG
		OLE-PCR	futA2	P1	AAGGCAGTGGTAAGGGCAAG
				P2	AAAGTTGGCCCAGGGCTTCCCGGTATACCACTAGGGCAGTGAGGG
				P3	CGATGAGTGGCAGGGCGGGGCGTAACCGATTCAGCTCGTTTAATG
				P4	GGGATTTCTTTGGCGGAGGT
				P5	AGCGTATCCAAAGTGAAGGGG
				P6	CGTGTCATTACCCTCCGGTT
				cm_F	TACCGGGAAGCCCTGGGCCAACTTT
				cm_R	TTACGCCCCGCCCTGCCACTCATCG
	GFP-protein signal sequence co-expression in Synechocystis	OLE-PCR	futA1ss-GFP	F	CAAATACATAAGGAATTATAACCAAATGGTCCAAAAGTTATCCCGTC
				R	TGAACAGCTCTTCGCCTTTACGCATCCCTGGTGTGTCGGCGAT
			futA2ss-GFP	F	CAAATACATAAGGAATTATAACCAAATGACAACTAAGATTTCCCGGCG
				R	TGAACAGCTCTTCGCCTTTACGCATCGTGCGGGACTGGGCA
			3377ss-GFP	F	CAAATACATAAGGAATTATAACCAAATGACAATTACTAGACGAGTATTTC
				R	TGAACAGCTCTTCGCCTTTACGCATTGCACCGCTTTGAGCTAAT
			torAss-GFP	F	CAAATACATAAGGAATTATAACCAAATGAACAATAACGATCTCTTTCAGG
				R	TGAACAGCTCTTCGCCTTTACGCATCGCCGCTTGCGCCGCA
			psbA2us	F	GGTATATGGATCATAATTGTATGCC

				R	TTGGTTATAATTCCTTATGTATTTGTCGATG
			psbA2ds	F	CGATGAGTGGCAGGGCGGGGCGTAAATTCCTTGGTGTAATGCCAACTG
				R	CTGGTGGAAGCCCTGCGG
			kan	F	TACCGGGAAGCCCTGGGCCAACTTT
				R	TTACGCCCCGCCCTGCCACTCATCG
			GFPss	F	ATGCGTAAAGGCGAAGAGCT
				R	AAAGTTGGCCCAGGGCTTCCCGGTATCATTTGTACAGTTCATCCATACC
			3377ss-R5/6K-GFP		ATGACAATTACTAAAAAAGTATTTCTAGGA
			psbA2-us-R2		ACTTTTTTAGTAATTGTCATTTGGTTATAATTCCTTATGTATTTG
	GFP-whole protein co-expression in Synechocystis	Gibson	G_futA1	P1	GTCGACTCTAGAGGATCCCCCCAACCTCCAGTTCCACTGAC
				P2	CTTTACGCATCTTCCAGCCTGCTTCGTTC
				P3	AGGCTGGAAGATGCGTAAAGGCGAAGAGCTGTTCAC
				P4	CCTTGGAATCTTACGCCCCGCCCTGCCA
				P5	CGGGGCGTAAGATTCCAAGGTCCATTGGCAATG
				P6	CGAATTCGAGCTCGGTACCCGCCATTACGAAGGGGTGG
			G_futA2	P1	GTCGACTCTAGAGGATCCCCAAGGCAGTGGTAAGGGCAAG
				P2	GTTTAATGAATGAAGTTGGCTGGCAGATGCGTAAAG
				P3	ATGCGTAAAGGCGAAGAGCTGTTCAC
				P4	AATTTTTTTTGCATTACGCCCCGCCCTGCCA
				P5	CGGGGCGTAATGCAAAAAAAATTGGACAATTGCCGG
				P6	CGAATTCGAGCTCGGTACCCTTGGGGGGATTTCTTTGGCG
			futA1-GFP	F	AGTCCATATGGTCCAAAAGTTATCCCGTCG
				R	TCGAAGCGCTCTTCCAGCCTGCTTCGTTCA
			futA2-GFP	F	AGTCCATATGACAACTAAGATTTCCCGGCG
				R	TCGAAGCGCTCTGCCAGCCAACTTCATTCA
			GFP	F	AGTCCATATGCGTAAAGGCGAAGAGCTGTTC
				R	TCGAAGATCTTCATTTGTACAGTTCATCCATACC
	Tery_3377 Overexpression in E.Coli	pet_21a	3377_OE	F	CATATGCAAAGCGGTGCAATTAATCTCTATT
				R	TCAGTGGTGGTGGTGGTGGTGCTCGAGCTTCCAGCCTACACGATCCA

Table A2: The 50 top differentially expressed genes in the transcriptomic analysis. Presented are each treatment's average normalised read counts of the 50 most significantly differentially expressed genes in descending significance (P-value).

Tery no.	Annotation	[Dust]	Dust+	Fe-	Fe+	P-Value
2561	cytochrome c, class I	18	195	30	608	1.1E-118
3845	hypothetical protein	176	106	263	1831	1.9E-51
2563	plastocyanin	2875	1654	2567	664	1.8E-48
0419	hemolysin-type calcium-binding protein	26	266	63	374	1.2E-39
2055	hemolysin-type calcium-binding protein	524	212	664	114	4.3E-38
0424	hemolysin-type calcium-binding protein	13	127	23	228	4.9E-37
0850	hypothetical protein	22	216	9	122	1.0E-33
3467	hemolysin-type calcium-binding protein	158	148	263	603	2.5E-28
1500	hypothetical protein	32	35	25	160	2.1E-25
0845	TENA/THI-4 protein	270	1514	132	677	1.1E-22
3659	hypothetical protein	64	180	143	337	5.0E-22
3376	phosphoglycerate kinase	230	475	372	706	1.3E-21
0846	hypothetical protein	4	57	1	38	2.5E-21
4114	Mo-dependent nitrogenase-like	651	342	702	272	5.2E-21
4763	photosystem q(b) protein	88774	80535	82336	37588	8.8E-21
0849	cell surface protein	40	542	5	229	2.0E-20
2976	caffeoyl-CoA O-methyltransferase	64	170	71	262	2.0E-20
0847	5-methyltetrahydropteroyltriglutamate/homocysteine S-methyltransferase	99	2579	31	1347	1.1E-19
1068	ferredoxin-nitrite reductase	78	16	163	39	6.3E-19
1687	fructose-bisphosphate aldolase	24590	24346	28958	10777	1.6E-18
2560	hypothetical protein	46	37	51	144	2.2E-18

1047	AAA ATPase	8491	6707	11000	5830	2.4E-18
1070	assimilatory nitrate reductase	51	19	132	30	3.1E-18
0803	hypothetical protein	199	328	283	574	3.4E-18
2500	hypothetical protein	10	16	17	77	5.4E-18
2501	BadF/BadG/BcrA/BcrD type ATPase	108	260	112	642	1.3E-17
0844	putative iron-sulfur cluster-binding protein	25	158	23	87	4.7E-17
0685	OpcA protein	747	433	1259	566	1.4E-16
4209	phosphoenolpyruvate synthase	23	42	35	143	4.0E-16
2710	hemolysin-type calcium-binding protein	348	405	474	804	5.0E-16
1380	triosephosphate isomerase	289	448	210	176	1.9E-15
2902	two component transcriptional regulator	79	42	88	229	2.6E-15
2437	ATPase	348	451	753	763	5.7E-15
1667	photosystem antenna protein-like protein	18035	15593	17542	7566	7.9E-15
1048	hypothetical protein	6858	4970	7448	3866	1.1E-14
0677	glutaredoxin-like protein	650	440	578	313	2.3E-14
1355	hemolysin-type calcium-binding protein	277	435	409	722	4.1E-14
0672	hypothetical protein	340	205	344	120	6.7E-14
0843	hypothetical protein	8	79	8	42	2.2E-13
4280	hypothetical protein	3771	2474	3960	2205	8.4E-13
4617	cobalamin synthesis protein, P47K	2992	1623	1810	1006	1.3E-12
3320	acyl-[acyl-carrier-protein]--UDP-N-acetylglucosamine O-acyltransferase	13	26	31	80	1.3E-12
0489	undecaprenyl-phosphate galactosephosphotransferase	184	281	106	161	2.1E-12
1230	photosystem II D2 protein (photosystem q(a) protein)	18551	18196	17655	9876	2.2E-12
2486	phycobilisome linker polypeptide	1099	750	1135	445	2.2E-12

4616	GTP cyclohydrolase I	4047	2966	3129	1574	4.1E-12
1959	peptidoglycan binding domain-containing protein	298	472	253	644	8.1E-12
4355	cysteine desulfurase activator complex subunit SufB	449	328	640	304	1.0E-11
0684	glucose-6-phosphate 1-dehydrogenase	1114	626	1782	790	1.8E-11
2820	hypothetical protein	947	439	962	201	1.9E-11

Table A3: The 50 most highly expressed genes in the transcriptomic analysis. Expression intensity (normalised read counts) is calculated as the average of all treatments and is presented in descending order for the 50 most highly expressed genes. Significantly differentially expressed genes are indicated (bold).

Tery no.	Annotation	[Dust]	Dust+	Fe-	Fe+	Average	P-Value
4763	photosystem q(b) protein	88774	80535	82336	37588	72309	**9E-21**
1046	hypothetical protein	33533	20360	36591	14093	26144	**2E-10**
2325	gas vesicle synthesis protein GvpA	35190	25545	19344	16305	24096	**5E-07**
1687	fructose-bisphosphate aldolase	24590	24346	28958	10777	22168	**2E-18**
1230	photosystem II D2 protein (photosystem q(a) protein)	18551	18196	17655	9876	16069	**2E-12**
1667	photosystem antenna protein-like protein	18035	15593	17542	7566	14684	**8E-15**
0182	photosystem q(b) protein	16909	14842	12277	6044	12518	**3E-05**
2483	photosystem antenna protein-like protein	12310	13415	15273	8443	12360	**3E-07**
2485	photosystem antenna protein-like protein	10292	13482	14280	8041	11524	**6E-04**
0513	photosystem II 44 kDa subunit reaction center protein	9227	13496	10681	11817	11305	**1E-04**
2623	S-adenosyl-L-homocysteine hydrolase	12603	10288	11877	7263	10508	**3E-06**
3815	hypothetical protein	12847	8300	8012	6414	8893	**2E-05**
4666	photosystem antenna protein-like protein	7972	10742	8456	7541	8678	**2E-02**

1666	flavodoxin FldA	7753	9020	9475	6166	8104	**9E-03**
1047	AAA ATPase	8491	6707	11000	5830	8007	**2E-18**
3826	dimethylaniline monooxygenase	9681	8151	8955	4944	7933	**4E-06**
2484	photosystem antenna protein-like protein	7079	8319	9810	5956	7791	**6E-03**
2324	gas vesicle synthesis protein GvpA	9545	6622	7223	6208	7399	2E-01
4669	photosystem I P700 chlorophyll a apoprotein A1	4496	8663	4401	7450	6252	**9E-07**
4367	hypothetical protein	7409	5057	7104	3578	5787	**4E-09**
1048	hypothetical protein	6858	4970	7448	3866	5785	**1E-14**
3372	beta-Ig-H3/fasciclin	8555	4009	7139	3023	5682	**1E-07**
4136	nitrogenase iron protein subunit NifH	3315	5025	5708	7087	5284	**3E-02**
4099	fructose-1,6-bisphosphate aldolase	4804	5856	5567	4436	5166	6E-02
4137	nitrogenase molybdenum-iron protein subunit alpha	3019	4567	5781	6661	5007	2E-01
4410	ribulose bisophosphate carboxylase	3296	7294	4267	4835	4923	**8E-05**
4668	photosystem I P700 chlorophyll a apoprotein A2	3410	7244	3295	5696	4912	**4E-08**
0397	phage tail Collar	4017	6691	4330	4445	4871	**2E-02**
0183	photosystem q(b) protein	6927	4833	4437	2066	4566	**3E-07**
2559	flavodoxin	5124	3238	5397	3482	4310	**8E-05**
1776	type 12 methyltransferase	2622	4036	2867	4685	3552	**1E-05**
4138	nitrogenase molybdenum-iron protein subunit beta	2317	2986	3955	4288	3386	6E-02
0600	hypothetical protein	2226	2913	3982	4352	3368	3E-01
1137	cytochrome b6	3720	3294	3411	2676	3275	**3E-02**
1798	apocytochrome f	3456	4218	2754	2570	3250	**2E-06**
2204	F0F1 ATP synthase subunit A	2668	4335	2781	3182	3241	**8E-06**
3819	beta-ketoacyl synthase	2862	3197	3620	3132	3203	4E-01
0997	phycobilisome protein	2313	5254	2359	2654	3145	**1E-05**

4280	hypothetical protein	3771	2474	3960	2205	3103	**8E-13**
4661	S-adenosylmethionine synthetase	2374	3796	2465	3562	3049	**1E-05**
5048	phycocyanin subunit alpha	2768	4528	2373	2293	2991	**2E-06**
4327	chaperonin GroEL	2068	3801	3174	2871	2979	**1E-04**
4616	GTP cyclohydrolase I	4047	2966	3129	1574	2929	**4E-12**
0996	phycobilisome protein	2125	5052	1945	2278	2850	**4E-06**
1834	6-phosphogluconate dehydrogenase	2349	2099	4345	2500	2823	**2E-05**
0998	phycobilisome protein	2272	4688	1950	2245	2789	**1E-06**
2900	hypothetical protein	2846	1844	3973	2452	2779	**9E-07**
5049	phycocyanin subunit beta	2390	4118	2370	2226	2776	**6E-05**
0117	peptidase S8/S53 subtilisin kexin sedolisin	1977	2660	2789	3538	2741	**1E-06**
4030	glyceraldehyde-3-phosphate dehydrogenase	2345	3114	2567	2801	2707	**2E-02**

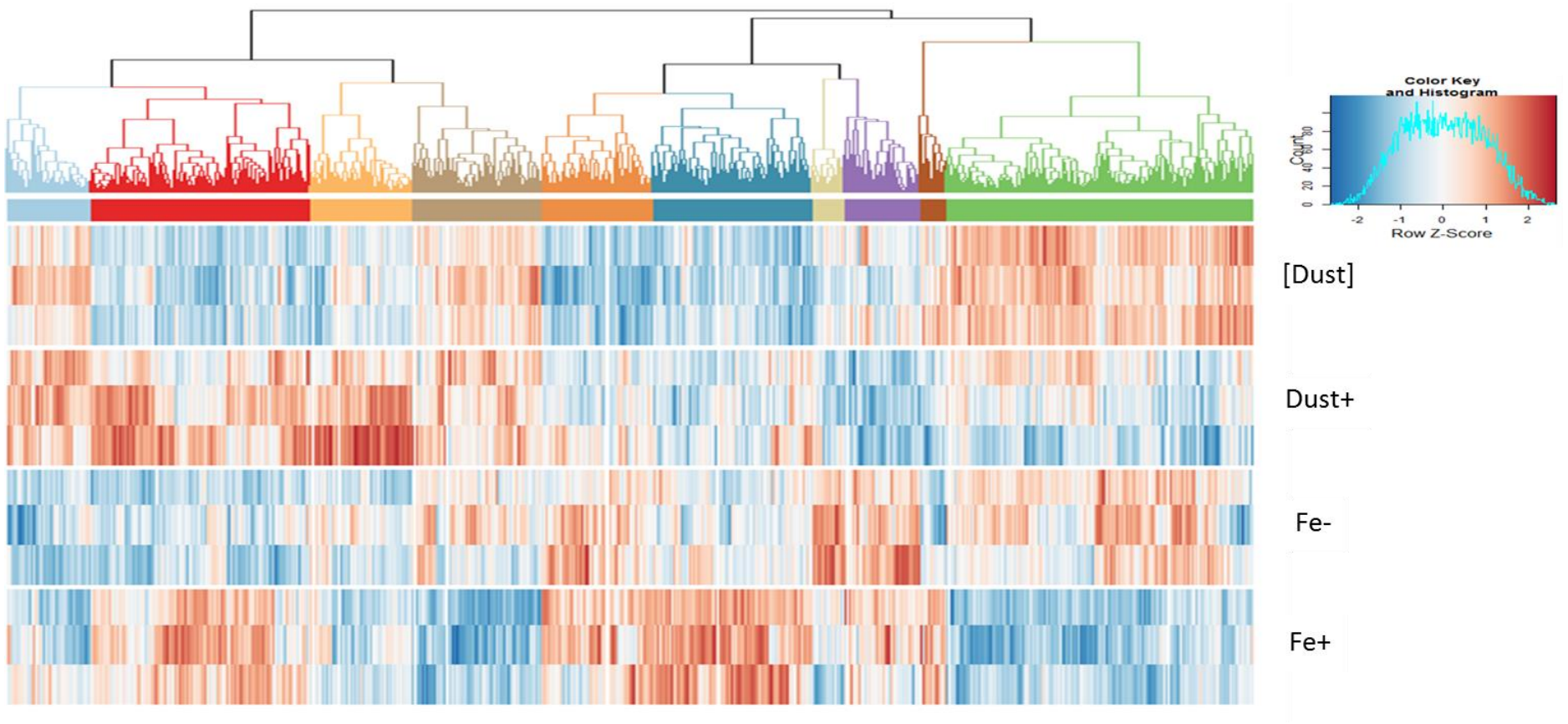

Figure A.1: Clustered expression patterns across the four experimental treatments. Pearson product moment correlation coefficient between each pair of differentially expressed genes and WPGMA was used to cluster expression profiles across the three replicate cultures of each of the 4 experimental treatments: [Dust], Dust+, Fe- and Fe+, in 10 groups.

Bibliography

Achilles, K. M., Church, T. M., Wilhelm, S. W., Luther, G. W., & Hutchins, D. A. (2003). Bioavailability of iron to *Trichodesmium* colonies in the western subtropical Atlantic Ocean. *Limnology and Oceanography,* 48(6), 2250–2255.

Adhikari, P., Kirby, S. D., Nowalk, A. J., Veraldi, K. L., Schryvers, A. B., & Mietzner, T. A. (1995). Biochemical characterization of a *Haemophilus influenzae* periplasmic iron transport operon. *Journal of Biological Chemistry*, 270(42), 25142–25149.

Aguilar-Islas, A. M., Wu, J., Rember, R., Johansen, A. M., & Shank, L. M. (2010). Dissolution of aerosol-derived iron in seawater: Leach solution chemistry, aerosol type, and colloidal iron fraction. *Marine Chemistry*, 120(1–4), 25–33.

Aldridge, C., Spence, E., Kirkilionis, M. A., Frigerio, L., & Robinson, C. (2008). Tat-dependent targeting of Rieske iron-sulphur proteins to both the plasma and thylakoid membranes in the cyanobacterium *Synechocystis* PCC6803*. Molecular Microbiology*, 70(1), 140–150.

Alge, D., Schmetterer, G., & Peschek, G. A. (1994). The gene encoding cytochrome-c oxidase subunit I from *Synechocystis* PCC6803. *Gene*, 138(1–2), 127–132.

Allen, A. E., LaRoche, J., Maheswari, U., Lommer, M., Schauer, N., Lopez, P. J., Giovanni, F., Fernie, A. R., Bowler, C. (2008). Whole-cell response of the pennate diatom *Phaeodactylum tricornutum* to iron starvation. *Proceedings of the National Academy of Sciences of the United States of America*, 105(30), 10438–10443.

Allen, A. E., Moustafa, A., Montsant, A., Eckert, A., Kroth, P. G., & Bowler, C. (2012). Evolution and functional diversification of fructose bisphosphate aldolase genes in photosynthetic marine diatoms. *Molecular Biology and Evolution*, 29(1), 367–379.

Altschul, S. F., Gish, W., Miller, W., Myers, E. W., & Lipman, D. J. (1990). Basic local alignment search tool. *Journal of Molecular Biology*, 215(3), 403–10.

Anders, S., & Huber, W. (2010). Differential expression analysis for sequence count data. *Genome Biology*, 11(10), R106.

Anders, S., Pyl, P. T., & Huber, W. (2015). HTSeq-A Python framework to work with high-throughput sequencing data. *Bioinformatics*, 31(2), 166–169.

Anderson, D. S., Adhikari, P., Nowalk, A. J., Chen, C. Y., & Mietzner, T. A. (2004). The hFbpABC transporter from *Haemophilus influenzae* functions as a binding-protein-dependent ABC transporter with high specificity and affinity for ferric iron. *Journal of Bacteriology*, 186(18), 6220–6229.

Anderson, A., Laohavisit, A., Blaby, I. K., Bombelli, P., Howe, C. J., Merchant, S. S., Davies, J. M. & Smith, A. G. (2016). Exploiting algal NADPH oxidase for biophotovoltaic energy. *Plant Biotechnology Journal*, 14(1), 22–28.

Andrews, S. C. (1998). Iron Storage in Bacteria. *Advances in Microbial Physiology*, 40, 281–351.

Andrews, S. C. (2010). The Ferritin-like superfamily: Evolution of the biological iron storeman from a rubrerythrin-like ancestor. *Biochimica et Biophysica Acta - General Subjects*. 1800(8), pp.691-705

Anisimova, M., & Gascuel, O. (2006). Approximate Likelihood-Ratio Test for Branches: A Fast, Accurate, and Powerful Alternative. *Systematic Biology* , 55(4), 539–552.

Askwith, C. C., & Kaplan, J. (1998). Site-directed mutagenesis of the yeast multicopper oxidase Fet3p. *Journal of Biological Chemistry*, 273(35), 22415–22419.

Ault-Riché, D., Fraley, C. D., Tzeng, C. M., & Kornberg, A. (1998). Novel assay reveals multiple pathways regulating stress-induced accumulations of inorganic polyphosphate in *Escherichia coli. Journal of Bacteriology*, 180(7), 1841–7.

Badarau, A., Firbank, S. J., Waldron, K. J., Yanagisawa, S., Robinson, N. J., Banfield, M. J., & Dennison, C. (2008). FutA2 Is a Ferric Binding Protein from Synechocystis PCC 6803. *Journal of Biological Chemistry* , 283(18), 12520–12527.

Bagg, A., & Neilands, J. B. (1987a). Ferric uptake regulation protein acts as a repressor,

employing iron (II) as a cofactor to bind the operator of an iron transport operon in *Escherichia coli*. *Biochemistry*, 26(17), 5471–7.

Bagg, A., & Neilands, J. B. (1987b). Molecular mechanism of regulation of siderophore-mediated iron assimilation. *Microbiological Reviews*, 51(4), 509–18.

Baker, A. R., & Croot, P. L. (2010). Atmospheric and marine controls on aerosol iron solubility in seawater. *Marine Chemistry*, 120(1–4), 4–13.

Banks, J. (1770). The Endeavour Journal of Sir Joseph Banks.

Bar-Zeev, E., Avishay, I., Bidle, K. D., & Berman-Frank, I. (2013). Programmed cell death in the marine cyanobacterium *Trichodesmium* mediates carbon and nitrogen export. *The ISME Journal*, 7(12), 2340–2348.

Barbeau, K., Rue, E. L., Bruland, K. W., & Butler, A. (2001). Photochemical cycling of iron in the surface ocean mediated by microbial iron(iii)-binding ligands. *Nature*, 413(6854), 409–413.

Bartsevich, V. V, & Pakrasi, H. B. (1996). Manganese Transport in the cyanobacterium *Synechocystis* sp. PCC 6803. *Journal of Biological Chemistry*, 271(42), 26057–26061.

Battchikova, N., Eisenhut, M., & Aro, E.-M. (2011). Cyanobacterial NDH-1 complexes: Novel insights and remaining puzzles. *Biochimica et Biophysica Acta (BBA) - Bioenergetics*, 1807(8), 935–944.

Battle, A., Khan, Z., Wang, S. H., Mitrano, A., Ford, M. J., Pritchard, J. K., & Gilad, Y. (2015). Impact of regulatory variation from RNA to protein. *Science*, 347(6222), 664–667.

Baumann, U., Wu, S., Flaherty, K. M., & McKay, D. B. (1993). Three-dimensional structure of the alkaline protease of *Pseudomonas aeruginosa*: a two-domain protein with a calcium binding parallel beta roll motif. *The EMBO Journal,* 12(9), 3357–64.

Bendtsen, J. D., Nielsen, H., Widdick, D., Palmer, T., & Brunak, S. (2005). Prediction of twin-arginine signal peptides. *BMC Bioinformatics*, 6(1), 167.

Berg, J. M., Tymoczko, J. L., & Stryer, L. (2002). A proton gradient powers the synthesis of ATP. In *Biochemistry* (5th editio, p. Section 18.4). W H Freeman.

Bergman, B., Sandh, G., Lin, S., Larsson, J., & Carpenter, E. J. (2013). *Trichodesmium*--a widespread marine cyanobacterium with unusual nitrogen fixation properties. *FEMS Microbiology Reviews*, 37(3), 286–302.

Berman-Frank, I., Lundgren, P., Chen, Y. B., Küpper, H., Kolber, Z., Bergman, B., & Falkowski, P. (2001). Segregation of nitrogen fixation and oxygenic photosynthesis in the marine cyanobacterium *Trichodesmium*. *Science*, 294(5546), 1534–7.

Berman-Frank, I., Lundgren, P., & Falkowski, P. (2003). Nitrogen fixation and photosynthetic oxygen evolution in cyanobacteria. *Research in Microbiology*, 154, 157–164.

Berman-Frank, I., Bidle, K. D., Haramaty, L., & Falkowski, P. G. (2004). The demise of the marine cyanobacterium, *Trichodesmium* spp., via an autocatalyzed cell death pathway. *Limnology and Oceanography*, 49(4), 997–1005.

Berman-Frank, I., Rosenberg, G., Levitan, O., Haramaty, L., & Mari, X. (2007). Coupling between autocatalytic cell death and transparent exopolymeric particle production in the marine cyanobacterium *Trichodesmium. Environmental Microbiology*, 9(6), 1415–1422.

Berthelot, H., Bonnet, S., Camps, M., Grosso, O., & Moutin, T. (2015). Assessment of the dinitrogen released as ammonium and dissolved organic nitrogen by unicellular and filamentous marine diazotrophic cyanobacteria grown in culture. *Frontiers in Marine Science*, 2, 80.

Bertrand, E. M., Moran, D. M., McIlvin, M. R., Hoffman, J. M., Allen, A. E., & Saito, M. A. (2013). Methionine synthase interreplacement in diatom cultures and communities: Implications for the persistence of B12 use by eukaryotic phytoplankton. *Limnology and Oceanography*, 58(4), 1431–1450.

Bibby, T., Nield, J., & Barber, J. (2001). Iron deficiency induces the formation of an antenna

ring around trimeric photosystem I in cyanobacteria. *Nature*, 412, 743–745.

Bibby, T. S., Mary, I., Nield, J., Partensky, F., & Barber, J. (2003). Low-light-adapted *Prochlorococcus* species possess specific antennae for each photosystem. *Nature*, 424(6952), 1051–1054.

Blaby-Haas, C. E., & Merchant, S. S. (2012). The ins and outs of algal metal transport. B*iochimica et Biophysica Acta (BBA) - Molecular Cell Research*, 1823(9), 1531–1552.

Blackman, F. F. (1903). Optima and Limiting Factors on JSTOR. Retrieved August 11, 2016, from http://aob.oxfordjournals.org/

Blain, S., Quéguiner, B., Armand, L., Belviso, S., Bombled, B., Bopp, L.Bowie, A.,Brunet, C., Brussaard, C., Carlotti, F., Christaki, U., Corbière, A., Durand, I., Ebersbach, F. Fuda, J.-L., Garcia, N., Gerringa, L., Griffiths, B., Guigue, C., Guillerm, C., Jacquet, S., Jeandel, C., Laan, P., Lefèvre, D., Lo Monaco, C., Malits, A., Mosseri, J., Obernosterer, I., Park, Y.-H., Picheral, M., Pondaven, P., Remenyi, T., Sandroni, V., Sarthou, G., Savoye, N., Scouarnec, L., Souhaut, M., Thuiller, D., Timmermans, K., Trull, T., Uitz, J., van Beek, P., Veldhuis, M., Vincent, D., Viollier, E., Vong, L., Wagener, T. (2007). Effect of natural iron fertilization on carbon sequestration in the Southern Ocean. *Nature*, 446(7139), 1070–1074.

Blanchard, J. L., Jennings, S., Holmes, R., Harle, J., Merino, G., Allen, J. I., Holt, J., Dulvy, N. K., Barange, M. (2012). Potential consequences of climate change for primary production and fish production in large marine ecosystems. *Philosophical Transactions of the Royal Society B: Biological Sciences*, 367(1605), 2979–2989.

Blaudeck, N., Kreutzenbeck, P., Freudl, R., & Sprenger, G. A. (2003). Genetic analysis of pathway specificity during posttranslational protein translocation across the *Escherichia coli* plasma membrane. *Journal of Bacteriology*, 185(9), 2811–2819.

Blyn, L. B., Braaten, B. A., & Low, D. A. (1990). Regulation of pap pilin phase variation by a mechanism involving differential Dam methylation states. *The EMBO Journal*, 9(12), 4045–4054.

Boehm, D. F., Welch, R. A., & Snyder, I. S. (1990). Calcium is required for binding of *Escherichia coli* hemolysin (HlyA) to erythrocyte membranes. *Infection and Immunity*, 58(6), 1951–1958.

Boiteau, R. M., & Repeta, D. J. (2015). An extended siderophore suite from *Synechococcus* sp. PCC 7002 revealed by LC-ICPMS-ESIMS. *Metallomics*, 7(5), 877–884.

Bombar, D., Heller, P., Sanchez-Baracaldo, P., Carter, B. J., & Zehr, J. P. (2014). Comparative genomics reveals surprising divergence of two closely related strains of uncultivated UCYN-A cyanobacteria. *The ISME Journal*, 8(12), 2530–2542.

Bonaccorsi di Patti, M. C., Felice, M. R., De Domenico, I., Lania, A., Alaleona, F., & Musci, G. (2005). Specific aspartate residues in FET3 control high-affinity iron transport in *Saccharomyces cerevisiae*. *Yeast*, 22(9), 677–687.

Bonnet, S., Berthelot, H., Turk-Kubo, K., Cornet-Bartaux, V., Fawcett, S. E., Berman-Frank, I., Barani, A., Dekaezemacker, J., Benavides, M., Charriere B., & Capone, D. G. (2015). Diazotroph derived nitrogen supports diatoms growth in the South West Pacific: a quantitative study using nanoSIMS. *Limnology and Oceanography*, in rev.

Bonnet, S., Baklouti, M., Gimenez, A & Berthelot, H. (2016). Biogeochemical and biological impacts of diazotroph blooms in a Low Nutrient Low Chlorophyll ecosystem: 2 synthesis from the VAHINE mesocosm experiment . New. *Biogeosciences*, 13(10), 3131–3145.

Botebol, H., Lesuisse, E., Šuták, R., Six, C., Lozano, J.-C., Schatt, P., Vergé, V., Kirilovsky, A., Morrissey, J., Léger, T., Camadro, J.-M., Gueneugues, A., Bowler, C., Blain, S. & Bouget, F.-Y. (2015). Central role for ferritin in the day/night regulation of iron homeostasis in marine phytoplankton. *Proceedings of the National Academy of Sciences*, 112(47), 14652–14657.

Boukhalfa, H., & Crumbliss, A. L. (2002). Chemical aspects of siderophore mediated iron transport. *Biometals*, 15(4), 325–339.

Boyd, P. W., Watson, a J., Law, C. S., Abraham, E. R., Trull, T., Murdoch, R., Chang, H., Charette, M., Croot, P., Downing, K., Frew, R., Gall, M., Hadfield, M.,Hall, J., Harvey, M., Jameson, G., LaRoche, J., Liddicoat, M., Ling, R., Maldonado, M T., McKay, R M., Nodder, S., Pickmere, S., Pridmore, R., Rintoul, S., Safi, K., Sutton, P., Strzepek, R., Tanneberger, K., Turner, S., Waite, A., Zeldis, J. (2000). A mesoscale phytoplankton bloom in the polar Southern Ocean stimulated by iron fertilization. *Nature*, 407(6805), 695–702.

Boyd, P. W., Jickells, T., Law, C. S., Blain, S., Boyle, E. A., Buesseler, K. O., Coale, K H., Cullen, J J., de Baar, H J W., Follows, M., Harvey, M., Lancelot, C., Levasseur, M., Owens, N P J., Pollard, R., Rivkin, R B., Sarmiento, J., Schoemann, V., Smetacek, V., Takeda, S., Tsuda, A., Turner, S., Watson, A. J. (2007). Mesoscale iron enrichment experiments 1993-2005: synthesis and future directions. *Science*, 315(5812), 612–7.

Brahamsha, B., & Haselkorn, R. (1996). An abundant cell-surface polypeptide is required for swimming by the nonflagellated marine cyanobacterium *Synechococcus*. *Microbiology*, 93, 6504–6509.

Brinkman, K. K., & Larsen, R. A. (2008). Interactions of the Energy Transducer TonB with Noncognate Energy-Harvesting Complexes. *Journal of Bacteriology*, 190(1), 421–427.

Brookes, P. S., Yoon, Y., Robotham, J. L., Anders, M. W., & Sheu, S.-S. (2004). Calcium, ATP, and ROS: a mitochondrial love-hate triangle. *American Journal of Physiology. Cell Physiology*, 287(4), C817-33.

Brown, C. M., MacKinnon, J. D., Cockshutt, A. M., Villareal, T. A., & Campbell, D. A. (2008). Flux capacities and acclimation costs in *Trichodesmium* from the Gulf of Mexico. *Marine Biology,* 154(3), 413–422.

Brzoska, P., & Boos, W. (1988). Characteristics of a ugp-encoded and *phoB*-dependent glycerophosphoryl diester phosphodiesterase which is physically dependent on the ugp transport system of *Escherichia coli*. *Journal of Bacteriology,* 170(9), 4125–35.

Buchanan, G., Sargent, F., Berks, B. C., & Palmer, T. (2001). A genetic screen for suppressors of *Escherichia coli* Tat signal peptide mutations establishes a critical role for the second arginine within the twin-arginine motif. *Archives of Microbiology*, 177(1), 107–112.

Buesseler, K. O., Andrews, J. E., Pike, S. M., & Charette, M. A. (2004). The effects of iron fertilization on carbon sequestration in the Southern Ocean. *Science* 304(5669), 414–7.

Bustin, S., Benes, V., Garson, J., Hellemans, J., Huggett, J., Kubista, M., Mueller, R., Nolan, T., Pfaffl, M. W., Shipley, G. L., Vandesompele, J. & Wittwer, C. (2009). The MIQE guidelines: minimum information for publication of quantitative real-time PCR experiments. *Clinical Chemistry*, 55(4), 611–622.

Bustin, S. A. (2010). Why the need for qPCR publication guidelines?—The case for MIQE. *Methods*, 50(4), 217–226.

Byrgazov, K., Vesper, O., & Moll, I. (2013). Ribosome heterogeneity: Another level of complexity in bacterial translation regulation. *Current Opinion in Microbiology.* 16(2), 133-139

Canniffe, D. P., Jackson, P. J., Hollingshead, S., Dickman, M. J., & Hunter, C. N. (2013). Identification of an 8-vinyl reductase involved in bacteriochlorophyll biosynthesis in *Rhodobacter sphaeroides* and evidence for the existence of a third distinct class of the enzyme. *The Biochemical Journal*, 450(2), 397–405.

Capone, D. G., Zehr, J. P., Paerl, H. W., Bergman, B., & Carpenter, E. J. (1997). *Trichodesmium*, a globally significant marine cyanobacterium. *Science*, 276(May), 1221–1229.

Carpenter, E. J., Capone, D. G., & Rueter, J. G. (1992). Marine pelagic cyanobacteria: *Trichodesmium* and other diazotrophs. (D. G. C. E.J. Carpenter, Ed.) NATO ASI series. Springer Science & Business Media, 2013.

Carpenter, E., O'Neil, J., Dawson, R., Capone, D., Siddiqui, P., Roenneberg, T., & Bergman, B. (1993). The tropical diazotrophic phytoplankter *Trichodesmium*: biological characteristics of two common species. *Marine Ecology*, 95, 295–304.

Carpenter, E. J., & Janson, S. (2000). Intracellular cyanobacterial symbionts in the marine diatom *Climacodium frauenfeldianum* (*Bacillariophyceae*). *Journal of Phycology*, 36, 540–544.

Cartron, M. L., Maddocks, S., Gillingham, P., Craven, C. J., & Andrews, S. C. (2006). Feo--transport of ferrous iron into bacteria. *Biometals*, 19(2), 143–57.

Casadesus, J., & Low, D. A. (2013). Programmed heterogeneity: epigenetic mechanisms in bacteria. *Journal of Biological Chemistry*, 288(20), 13929–13935.

Castresana, J. (2000). Selection of conserved blocks from multiple alignments for their use in phylogenetic analysis. *Molecular Biology and Evolution*, 17(4), 540–552.

Castruita, M., Saito, M., Schottel, P. C., Elmegreen, L. A., Myneni, S., Stiefel, E. I., & Morel, F. M. M. (2006). Overexpression and characterization of an iron storage and DNA-binding Dps protein from *Trichodesmium erythraeum*. *Applied and Environmental Microbiology*, 72(4), 2918–2924.

Cereda, A., Hitchcock, A., Symes, M. D., Cronin, L., Bibby, T. S., & Jones, A. K. (2014). A bioelectrochemical approach to characterize extracellular electron transfer by *Synechocystis* sp. PCC6803. *PloS One*, 9(3), e91484.

Chappell, P. D., & Webb, E. (2010). A molecular assessment of the iron stress response in the two phylogenetic clades of *Trichodesmium. Environmental Microbiology*, 12(1), 13–27.

Chappell, P. D., Moffett, J. W., Hynes, A. M., & Webb, E. A. (2012). Molecular evidence of iron limitation and availability in the global diazotroph *Trichodesmium*. *The ISME Journal*, 1–12.

Chauvat, F., & Cassier-Chauvat, C. (2012). *Genomics of Cyanobacteria*. Elsevier Science.

Chen, Y. (1996). Growth and nitrogen fixation of the diazotrophic filamentous non heterocystous cyanobacterioum *Trichodesmium* sp. IMS 101 in defined media: evidence for a circadian rhythm. *Journal of Phycology*, 32, 916–923.

Chen, Y., Chen, H., & Lin, Y. (2003). Distribution and downward flux of *Trichodesmium* in the South China Sea as influenced by the transport from the Kuroshio Curren. *Marine Ecology Progress Series,* 259, 47–57.

Chen, M., & Bibby, T. S. (2005). Photosynthetic apparatus of antenna-reaction centres supercomplexes in oxyphotobacteria: insight through significance of Pcb/IsiA proteins. *Photosynthesis Research*, 86(1–2), 165–173.

Cheng, Z., Teo, G., Krueger, S., Rock, T. M., Koh, H. W. L., Choi, H., & Vogel, C. (2016). Differential dynamics of the mammalian mRNA and protein expression response to misfolding stress. *Molecular Systems Biology*, 12(1), 855.

Chevenet, F., Brun, C., Bañuls, A.-L., Jacq, B., & Christen, R. (2006). TreeDyn: towards dynamic graphics and annotations for analyses of trees*. BMC Bioinformatics*, 7, 439.

Christenson, L., & Sims, R. (2011). Production and harvesting of microalgae for wastewater treatment, biofuels, and bioproducts. *Biotechnology Advances*, 29(6), 686–702.

Christie-Oleza, J. A., & Armengaud, J. (2010). In-depth analysis of exoproteomes from marine bacteria by shotgun liquid chromatography-tandem mass spectrometry: the *Ruegeria pomeroyi* DSS-3 case-study. *Marine Drugs*, 8(8), 2223–39.

Clark, L. L., Ingall, E. D., & Benner, R. (1998). Marine phosphorus is selectively remineralized. *Nature*, 393(6684), 426.

Coleman, J. E. (1992). Structure and mechanism of alkaline phosphatase. *Annual Review of*

Biophysics and Biomolecular Structure, 21(1), 441–483.

Compton, J., Mallinson, D., Glenn, C. R., Filippelli, G., Föllmi, K., Shields, G., & Zanin, Y. (2000). Variations in the global phosphorus cycle. *Marine Authigenesis: From Global to Microbial*, 66(66), 21–33.

Consortium, T. U. (2015). UniProt: a hub for protein information. *Nucleic Acids Research* , 43(D1), D204–D212

Cornejo-Castillo, F. M., Cabello, A. M., Salazar, G., Sánchez-Baracaldo, P., Lima-Mendez, G., Hingamp, P., Alberti, A., Sunagawa, S., Bork, P., de Vargas, C., Raes, J., Bowler, C., Wincker, P., Zehr, J. P., Gasol, J. M., Massana, R. & Acinas, S. G. (2016). Cyanobacterial symbionts diverged in the late Cretaceous towards lineage-specific nitrogen fixation factories in single-celled phytoplankton. *Nature Communications*, 7, 11071.

Costas, A. M. G., White, A. K., & Metcalf, W. W. (2001). Purification and characterization of a novel phosphorus-oxidizing enzyme *from Pseudomonas stutzeri* WM88 . *Journal of Biological Chemistry ,* 276(20), 17429–17436.

Cottrell, M., & Kirchman, D. (2016). Transcriptional control in marine copiotrophic and oligotrophic bacteria with streamlined genomes. *Applied and Environmental*. 82(19), 6010-6018.

Crick, F. H. C. (1958). On protein synthesis. *In Symp Soc Exp Biol* (Vol. 12, p. 8).

Cristóbal, S., de Gier, J., Nielsen, H., & von Heijne, G. (1999). Competition between Sec-and TAT-dependent protein translocation in *Escherichia coli*. *The EMBO Journal*, 18(11), 2982–2990.

Darwin, C. (1909). The Voyage of the Beagle. Chapter I. New York: P.F. Collier & Son Company.

de Baar, H. J. W. (1994). von Liebig's law of the minimum and plankton ecology (1899–1991). *Progress in Oceanography*, 33(4), 347–386.

De la Cerda, B., Castielli, O., Durán, R. V, Navarro, J. A., Hervás, M., & De la Rosa, M. A. (2007). A proteomic approach to iron and copper homeostasis in cyanobacteria. Briefings in Functional Genomics & Proteomics, 6(4), 322–9.

Delany, I., Spohn, G., Rappuoli, R., & Scarlato, V. (2002). The Fur repressor controls transcription of iron-activated and -repressed genes in *Helicobacter pylori. Molecular Microbiology*, 42(5), 1297–1309.

Deng, G., Liu, F., Liu, X., & Zhao, J. (2012). Significant energy transfer from CpcG2-phycobilisomes to photosystem i in the cyanobacterium *Synechococcus* sp. PCC 7002 in the absence of ApcD-dependent state transitions. *FEBS Letters*, 586(16), 2342–2345.

Deng, Z., Wang, Q., Liu, Z., Zhang, M., Machado, A.C.D., Chiu, T.P., Feng, C., Zhang, Q., Yu, L., Qi, L. & Zheng, J. (2015). Mechanistic insights into metal ion activation and operator recognition by the ferric uptake regulator. *Nature Communications*, 6, 7642.

Dereeper, A., Guignon, V., Blanc, G., Audic, S., Buffet, S., Chevenet, F., Dufayard, J.F., Guindon, S., Lefort, V., Lescot, M. & Claverie, J.M. (2008). Phylogeny.fr: robust phylogenetic analysis for the non-specialist. *Nucleic Acids Research*, 36(Web Server issue), W465–W469.

Dereeper, A., Audic, S., Claverie, J.-M., & Blanc, G. (2010). BLAST-EXPLORER helps you building datasets for phylogenetic analysis. *BMC Evolutionary Biology*, 10, 8.

Dong, X., Stothard, P., Forsythe, I. J., & Wishart, D. S. (2004). PlasMapper: a web server for drawing and auto-annotating plasmid maps. *Nucleic Acids Research*, 32(Web Server issue), W660–W664.

Doulatov, S., Hodes, A., Dai, L., Mandhana, N., Liu, M., Deora, R., Simons, R.W., Zimmerly, S. & Miller, J.F. (2004). Tropism switching in *Bordetella* bacteriophage defines a family of diversity-generating retroelements. *Nature*, 431(7007), 476–81.

Du, Z., Zhou, X., Ling, Y., Zhang, Z., & Su, Z. (2010). agriGO: a GO analysis toolkit for the

agricultural community. *Nucleic Acids Research*, gkq310.

Duarte, C. M. (2009). Marine Ecology: EOLSS Publications, 2009.

Duce, R.A., Liss, P.S., Merrill, J.T., Atlas, E.L., Buat-Menard, P., Hicks, B.B., Miller, J.M., Prospero, J.M., Arimoto, R.C.T.M., Church, T.M. & Ellis, W. (1991). The atmospheric input of trace species to the world ocean. *Global Biogeochemical Cycles*, 5(3), 193–259.

Duong, F., Lazdunski, A., Carni, B., & Murgier, M. (1992). Sequence of a cluster of genes controlling synthesis and secretion of alkaline protease in *Pseudomonas aeruginosa*: relationships to other secretory pathways. *Gene*, 121(1), 47–54.

Durán, R. V, Hervás, M., Miguel, A., & Navarro, J. A. (2004). The efficient functioning of photosynthesis and respiration in *Synechocystis* sp. PCC 6803 strictly requires the presence of either cytochrome c6 or plastocyanin. *Journal of Biological Chemistry*, 279(8), 7229–7233.

Dyhrman, S. T., Webb, E. A., Anderson, D. M., Moffett, J. W., & Waterbury, J. B. (2002). Cell-specific detection of phosphorus stress in *Trichodesmium* from the Western North Atlantic. *Limnology and Oceanography*, 47(6), 1832–1836.

Dyhrman, S. T., Chappell, P. D., Haley, S. T., Moffett, J. W., Orchard, E. D., Waterbury, J. B., & Webb, E. A. (2006). Phosphonate utilization by the globally important marine diazotroph *Trichodesmium*. *Nature*, 439(7072), 68–71.

Dyhrman, S. T., & Ruttenberg, K. C. (2006). Presence and regulation of alkaline phosphatase activity in eukaryotic phytoplankton from the coastal ocean: Implications for dissolved organic phosphorus remineralization. *Limnology and Oceanography*, 51(3), 1381–1390.

Dyhrman, S. T., Benitez-Nelson, C. R., Orchard, E. D., Haley, S. T., & Pellechia, P. J. (2009). A microbial source of phosphonates in oligotrophic marine systems. *Nature Geosci*, 2(10), 696–699.

Ehrenberg, C. G. (1830). Neue beobachtungen uber bluartige erbscheinungen in Aegypten, Arabien, and Siberien nebst einer uebersicht und kritik der fruher bekannten, *Ann. Ann. Phys. Chem*, (18), 477–514.

Eom, S.-H., Kim, Y.-M., & Kim, S.-K. (2013). Marine bacteria: potential sources for compounds to overcome antibiotic resistance. *Applied Microbiology and Biotechnology*, 97(11), 4763–4773.

Eppley, R. W., Holm-Harisen, O., & Strickland, J. D. H. (1968). Some observations on the vertical migration of dinoflagellates. *Journal of Phycology*, 4(4), 333–340.

Erdner, D. L., & Anderson, D. M. (1999). Ferredoxin and flavodoxin as biochemical indicators of iron limitation during open-ocean iron enrichment. *Limnology and Oceanography*, 44(7), 1609–1615.

Exss-Sonne, P., Tölle, J., Bader, K. P., Pistorius, E. K., & Michel, K.-P. (2000). The IdiA protein of *Synechococcus* sp. PCC 7942 functions in protecting the acceptor side of photosystem II under oxidative stress. *Photosynthesis Research*, 63(2), 145–157.

Fagerlund, R. D., & Eaton-Rye, J. J. (2011). The lipoproteins of cyanobacterial photosystem II. *Journal of Photochemistry and Photobiology B: Biology*, 104(1–2), 191–203.

Falcon, L. I., Carpenter, E. J., Cipriano, F., Bergman, B., & Capone, D. G. (2004). N_2 Fixation by unicellular bacterioplankton from the Atlantic and Pacific Oceans: Phylogeny and in situ rates. *Applied and Environmental Microbiology*, 70(2), 765–770.

Falkowski, P. G. (1997). Evolution of the nitrogen cycle and its influence on the biological sequestration of CO_2 in the ocean. *Nature*, 387(6630), 272–275. http://doi.org/10.1038/387272a0

Falkowski, Barber, & Smetacek. (1998). Biogeochemical controls and feedbacks on ocean primary production. *Science*, 281(5374), 200–7.

Falkowski, P. G., Katz, M. E., Knoll, A. H., Quigg, A., Raven, J. a, Schofield, O., & Taylor, F. J. R.

(2004). The evolution of modern eukaryotic phytoplankton. *Science*, 305(5682), 354–60.

Farnelid, H., Andersson, A.F., Bertilsson, S., Al-Soud, W.A., Hansen, L.H., Sørensen, S., Steward, G.F., Hagström, Å. & Riemann, L. (2011). Nitrogenase gene amplicons from global marine surface waters are dominated by genes of non-cyanobacteria. *PLoS ONE*, 6(4), e19223.

Farnelid, H., Bentzon-Tilia, M., Andersson, A.F., Bertilsson, S., Jost, G., Labrenz, M., Jürgens, K. & Riemann, L. (2013). Active nitrogen-fixing heterotrophic bacteria at and below the chemocline of the central Baltic Sea. *The ISME Journal*, 7(7), 1413–1423.

Ferat, J. L., & Michel, F. (1993). Group II self-splicing introns in bacteria. *Nature*, 364(6435), 358–61.

Fernández, A., Mour No-Carballido, B., Bode, A., Varela, M., Marã Nón, E., & Marañón, E. (2010). Latitudinal distribution of *Trichodesmium* spp. and N_2 fixation in the Atlantic Ocean. *Biogeosciences*, 7, 3167–3176.

Fernandez, C., Farías, L., & Ulloa, O. (2011). Nitrogen fixation in denitrified marine waters. *PLoS One*, 6(6), e20539.

Field, C. B., Behrenfeld, M. J., Randerson, J. T., & Falkowski, P. (1998). Primary production of the biosphere: Integrating terrestrial and oceanic components. *Science*, 281(5374), 237–240.

Fisher, M., Gokhman, I., Pick, U., & Zamir, A. (1997). A structurally novel transferrin-like protein accumulates in the plasma membrane of the unicellular green alga *Dunaliella salina* grown in high salinities. *The Journal of Biological Chemistry*, 272(3), 1565–70.

Fisher, M., Zamir, A., & Pick, U. (1998). Iron uptake by the halotolerant alga *Dunaliella* is mediated by a plasma membrane transferrin. *The Journal of Biological Chemistry*, 273(28), 17553–8.

Fitzsimmons, J.N., Carrasco, G.G., Wu, J., Roshan, S., Hatta, M., Measures, C.I., Conway, T.M., John, S.G. & Boyle, E.A. (2015). Partitioning of dissolved iron and iron isotopes into soluble and colloidal phases along the GA03 GEOTRACES North Atlantic Transect. Deep Sea Research Part II: *Topical Studies in Oceanography*, 116, 130–151.

Fleischmann, R.D., Adams, M.D., White, O. & Clayton, R.A. (1995). Whole-genome random sequencing and assembly of *Haemophilus influenzae* Rd. *Science,* 269(5223), 496–512.

Foster, R. A., & Zehr, J. P. (2006). Characterization of diatom–cyanobacteria symbioses on the basis of nifH, hetR and 16S rRNA sequences. *Environmental Microbiology*, 8(11), 1913–1925.

Foster, R. A., Goebel, N. L., & Zehr, J. P. (2010). Isolation of *Calothrix rhizosoleniae* (cyanobacteria) strain SC01 from *Chaetoceros* (bacillariophyta) spp. diatoms of the subtropical North Pacific Ocean. *Journal of Phycology*, 46(5), 1028–1037.

Foster, R. A., Kuypers, M. M. M., Vagner, T., Paerl, R. W., Musat, N., & Zehr, J. P. (2011). Nitrogen fixation and transfer in open ocean diatom–cyanobacterial symbioses. *The ISME Journal*, 5(9), 1484–1493.

Foster, R. A., Sztejrenszus, S., & Kuypers, M. M. M. (2013). Measuring carbon and N_2 fixation in field populations of colonial and free-living unicellular cyanobacteria using nanometer-scale secondary ion mass spectrometry 1. *Journal of Phycology*, 49(3), 502–516.

Fraser, J. M., Tulk, S. E., Jeans, J. A., Campbell, D. A., Bibby, T. S., & Cockshutt, A. M. (2013). Photophysiological and photosynthetic complex changes during iron starvation in *Synechocystis* sp. PCC 6803 and *Synechococcus elongatus* PCC 7942. *PLoS ONE*, 8(3), e59861.

Frew, R.D., Hutchins, D.A., Nodder, S., Sanudo-Wilhelmy, S., Tovar-Sanchez, A., Leblanc, K., Hare, C.E. & Boyd, P.W. (2006). Particulate iron dynamics during FeCycle in subantarctic waters southeast of New Zealand. *Global Biogeochemical Cycles*, 20(1),

Fulda, S., Huang, F., Nilsson, F., Hagemann, M., & Norling, B. (2000). Proteomics of *Synechocystis* sp. strain PCC 6803. *European Journal of Biochemistry*, 267(19), 5900–5907.

Garcia, N. S., Fu, F., Sedwick, P. N., & Hutchins, D. A. (2015). Iron deficiency increases growth and nitrogen-fixation rates of phosphorus-deficient marine cyanobacteria. *The ISME Journal*, 9(1), 238–45.

García-Cerdán, J.G., Kovács, L., Tóth, T., Kereïche, S., Aseeva, E., Boekema, E.J., Mamedov, F., Funk, C. & Schröder, W.P. (2011). The PsbW protein stabilizes the supramolecular organization of photosystem II in higher plants. *The Plant Journal : For Cell and Molecular Biology*, 65(3), 368–81.

Garg, S., Rose, A. L., Godrant, A., & Waite, T. D. (2007). Iron uptake by the ichthyotoxic *Chattonella marina* (Raphidophyceae): impact of superoxide generation1. *Journal of Phycology*, 43(5), 978–991.

Geider, R. J., & La Roche, J. (1994). The role of iron in phytoplankton photosynthesis, and the potential for iron-limitation of primary productivity in the sea. *Photosynthesis Research*, 39(3), 275–301.

Georgianna, D. R., & Mayfield, S. P. (2012). Exploiting diversity and synthetic biology for the production of algal biofuels. *Nature*, 488(7411), 329–335.

Gledhill, M., & Berg, C. van den. (1994). Determination of complexation of iron (III) with natural organic complexing ligands in seawater using cathodic stripping voltammetry. *Marine Chemistry*. 47(1), pp.41-54.

Gledhill, M., & Buck, K. N. (2012). The organic complexation of iron in the marine environment: a review. *Frontiers in Microbiology,* 3(February), 69.

Godrant, A., Rose, A. L., Sarthou, G., & Waite, T. D. (2009). New method for the determination of extracellular production of superoxide by marine phytoplankton using the chemiluminescence probes MCLA and red-CLA. *Limnology and Oceanography*: *Methods*, 7, 682–692.

Goebel, N. L., Edwards, C. A., Church, M. J., & Zehr, J. P. (2007). Modeled contributions of three types of diazotrophs to nitrogen fixation at Station ALOHA. *The ISME Journal*, 1(7), 606–619.

Gomez, F., Furuya, K., & Takeda, S. (2005). Distribution of the cyanobacterium *Richelia intracellularis* as an epiphyte of the diatom *Chaetoceros compressus* in the western Pacific Ocean. *Journal of Plankton Research*, 27(4), 323–330.

González, A., Bes, M. T., Barja, F., Peleato, M. L. & Fillat, M. F. (2010). Overexpression of FurA in *Anabaena* sp. PCC 7120 reveals new targets for this regulator involved in photosynthesis, iron uptake and cellular morphology. *Plant & Cell Physiology*, 51(11), 1900–14.

González, A., Bes, M. T., Valladares, A., Peleato, M. L. & Fillat, M. F. (2012). FurA is the master regulator of iron homeostasis and modulates the expression of tetrapyrrole biosynthesis genes in Anabaena sp. PCC 7120. *Environmental Microbiology*, 14(12), 3175–3187.

González, A., Angarica, V. E., Sancho, J., & Fillat, M. F. (2014). The FurA regulon in *Anabaena* sp. PCC 7120: in silico prediction and experimental validation of novel target genes. *Nucleic Acids Research,* 42(8), 4833–46.

González, A., Bes, M.T., Peleato, M.L. & Fillat, M.F. (2016). Expanding the role of FurA as essential global regulator in cyanobacteria. *PLOS ONE,* 11(3), e0151384.

Gorby, Y.A., Yanina, S., McLean, J.S., Rosso, K.M., Moyles, D., Dohnalkova, A., Beveridge, T.J., Chang, I.S., Kim, B.H., Kim, K.S. & Culley, D.E. (2006). Electrically conductive bacterial nanowires produced by *Shewanella oneidensis* strain MR-1 and other microorganisms. *Proceedings of the National Academy of Sciences*, 103(30), 11358–11363.

Gordeeva, A. V., Zvyagilskaya, R. A., & Labas, Y. A. (2003). Cross-talk between reactive oxygen species and calcium in living cells. *Biochemistry (Moscow),* 68(10), 1077–1080.

Griffith, J. M., Smillie, R. H., Niere, J. O., & Grant, B. R. (1989). Effect of phosphate on the toxicity of phosphite in *Phytophthora palmivora*. *Archives of Microbiology*, 152(5), 425–429.

Grossman, A. R., Schaefer, M. R., Chiang, G. G., & Collier, J. L. (1993). The phycobilisome, a light-harvesting complex responsive to environmental conditions. *Microbiological Reviews*, 57(3), 725–49.

Groussman, R. D., Parker, M. S., & Armbrust, E. V. (2015). Diversity and evolutionary history of iron metabolism genes in diatoms. *PloS One*, 10(6), e0129081.

Guan, L. L., Kanoh, K., & Kamino, K. (2001). Effect of exogenous siderophores on iron uptake activity of marine bacteria under iron-limited conditions. *Applied and Environmental Microbiology* , 67(4), 1710–1717.

Gudiña, J. E., Teixeira, A. J., & Rodrigues, R. L. (2016). Biosurfactants produced by marine microorganisms with therapeutic applications. *Marine Drugs.,* 14 (2).

Guindon, S., & Gascuel, O. (2003). A simple, fast, and accurate algorithm to estimate large phylogenies by maximum likelihood. *Systematic Biology* , 52(5), 696–704.

Hagino, K., Onuma, R., Kawachi, M. & Horiguchi, T. (2013). Discovery of an endosymbiotic nitrogen-fixing cyanobacterium UCYN-A in *Braarudosphaera bigelowii* (Prymnesiophyceae). *PLoS ONE*, 8(12), e81749.

Hall, N., & Pearl, H. (2011). Vertical migration patterns of phytoflagellates in relation to light and nutrient availability in a shallow microtidal estuary. *Marine Ecology Progress Series*, 425, 1–19.

Halm, H., Musat, N., Lam, P., Langlois, R., Musat, F., Peduzzi, S., Lavik, G., Schubert, C.J., Singha, B., LaRoche, J. & Kuypers, M.M. (2009). Co-occurrence of denitrification and nitrogen fixation in a meromictic lake, Lake Cadagno (Switzerland). *Environmental Microbiology*, 11(8), 1945–1958.

Han, C., Geng, J., Ren, H., Gao, S., Xie, X., & Wang, X. (2013). Phosphite in sedimentary interstitial water of Lake Taihu, a large eutrophic shallow lake in China. *Environmental Science & Technology*, 47(11), 5679–5685.

Hansel, C. M., Buchwald, C., Diaz J. M., A., Ossolinski, J. E., Dyhrman, S. T., Van Mooy, B. A. S., & Polyviou, D. (2016). Dynamics of extracellular superoxide production by *Trichodesmium* colonies from the Sargasso Sea. *Limnology and Oceanography*, 61(4), 1188–1200.

Hantke, K. (1981). Regulation of ferric iron transport in *Escherichia coli* K12: isolation of a constitutive mutant. *Molecular & General Genetics :* MGG, 182(2), 288–92.

Hart, S. E., Schlarb-Ridley, B. G., Bendall, D. S., & Howe, C. J. (2005). Terminal oxidases of cyanobacteria. *Biochemical Society Transactions,* 33(Pt 4), 832–5.

Henry, M.-F., & Vignais, P. M. (1980). Production of superoxide anions in *Paracoccus denitrificans*. *Archives of Biochemistry and Biophysics*, 203(1), 365–371.

Herbik, A., Bölling, C., & Buckhout, T. J. (2002). The Involvement of a multicopper oxidase in iron uptake by the green algae *Chlamydomonas reinhardtii*. *Plant Physiology,* 130(4), 2039–2048.

Hernández-Prieto, M. a, Schön, V., Georg, J., Barreira, L., Varela, J., Hess, W. R., & Futschik, M. E. (2012). Iron deprivation in *Synechocystis*: Inference of pathways, non-coding RNAs, and regulatory elements from comprehensive expression profiling. G3 (Bethesda, Md.), 2(12), 1475–95.

Herndl, G. J., & Reinthaler, T. (2013). Microbial control of the dark end of the biological pump. *Nature Geoscience*, 6(9), 718–724.

Hewson, I., Govil, S., Capone, D., Carpenter, E., & Fuhrman, J. (2004). Evidence of *Trichodesmium* viral lysis and potential significance for biogeochemical cycling in the

oligotrophic ocean. Aquatic *Microbial Ecology*, 36(1), 1–8.

Hewson, I., Poretsky, R.S., Dyhrman, S.T., Zielinski, B., White, A.E., Tripp, H.J., Montoya, J.P. & Zehr, J.P.. (2009). Microbial community gene expression within colonies of the diazotroph, *Trichodesmium*, from the Southwest Pacific Ocean. *The ISME Journal*, 3(11), 1286–1300.

Hilton, J. A., Foster, R. A., James Tripp, H., Carter, B. J., Zehr, J. P., & Villareal, T. A. (2013). Genomic deletions disrupt nitrogen metabolism pathways of a cyanobacterial diatom symbiont. *Nature Communications*, 4, 1767.

Hilton, J. A., Satinsky, B. M., Doherty, M., Zielinski, B., & Zehr, J. P. (2015). Metatranscriptomics of N_2-fixing cyanobacteria in the Amazon River plume. *The ISME Journal*, 9(7), 1557–1569.

Hirota, R., Yamane, S., Fujibuchi, T., Motomura, K., Ishida, T., Ikeda, T., & Kuroda, A. (2012). Isolation and characterization of a soluble and thermostable phosphite dehydrogenase from *Ralstonia* sp. strain 4506. *Journal of Bioscience and Bioengineering*, 113(4), 445–450. 027

Hmelo, L., Van Mooy, B., & Mincer, T. (2012). Characterization of bacterial epibionts on the cyanobacterium *Trichodesmium*. Aquatic Microbial Ecology, 67(1), 1–14.

Ho, T. D., & Ellermeier, C. D. (2015). Ferric uptake regulator Fur control of putative iron acquisition systems in *Clostridium difficile*. *Journal of Bacteriology*, 197(18), 2930–2940.

Hodak, H., Clantin, B., Willery, E., Villeret, V., Locht, C., & Jacob-Dubuisson, F. (2006). Secretion signal of the filamentous haemagglutinin, a model two-partner secretion substrate. *Molecular Microbiology*, 61(2), 368–382.

Hoiczyk, E., & Baumeister, W. (1997). Oscillin, an extracellular, Ca^{2+} -binding glycoprotein essential for the gliding motility of cyanobacteria. *Molecular Microbiology*, 26(4), 699–708.

Hollingshead, S., Kopečná, J., Jackson, P.J., Canniffe, D.P., Davison, P.A., Dickman, M.J., Sobotka, R. & Hunter, C.N. (2012). Conserved chloroplast open-reading frame ycf54 is required for activity of the magnesium protoporphyrin monomethylester oxidative cyclase in Synechocystis PCC 6803. *Journal of Biological Chemistry,* 287(33), pp.27823-27833.

Hondorp, E. R., & Matthews, R. G. (2004). Oxidative stress inactivates cobalamin-independent methionine synthase (MetE) in *Escherichia coli. PLoS Biology*, 2(11), e336.

Hopkinson, B. M., & Morel, F. M. M. (2009). The role of siderophores in iron acquisition by photosynthetic marine microorganisms. *Biometals*, 22(4), 659–669.

Hopkinson, B. M., & Barbeau, K. A. (2012). Iron transporters in marine prokaryotic genomes and metagenomes. *Environmental Microbiology*, 14(1), 114–128.

Hove-Jensen, B., Rosenkrantz, T. J., Zechel, D. L., & Willemoës, M. (2010). Accumulation of intermediates of the carbon-phosphorus lyase pathway for phosphonate degradation in *phn* mutants of *Escherichia coli. Journal of Bacteriology*, 192(1), 370–4.

Hove-Jensen, B., McSorley, F. R., & Zechel, D. L. (2011). Physiological role of *phnP*-specified phosphoribosyl cyclic phosphodiesterase in catabolism of organophosphonic acids by the carbon-phosphorus lyase pathway. *Journal of the American Chemical Society*, 133(10), 3617–3624.

Hu, Z.-L., Bao, J., & Reecy, J. M. (2008). CateGOrizer: a web-based program to batch analyze gene ontology classification categories. *Online Journal of Bioinformatics*, 9(2), 108–112.

Huang, W., & Wu, Q.-Y. (2004). Identification of genes controlled by the manganese response regulator, ManR, in the cyanobacterium, *Anabaena* sp. PCC 7120. *Biotechnology Letters*, 26(18), 1397–1401.

Hunt, B. P. V., Bonnet, S., Berthelot, H., Conroy, B. J., Foster, R. A., & Pagano, M. (2016). Contribution and pathways of diazotroph-derived nitrogen to zooplankton during the VAHINE mesocosm experiment in the oligotrophic New Caledonia lagoon. *Biogeosciences*, 13(10), 3131–3145.

Hutchings, M. I., Palmer, T., Harrington, D. J., & Sutcliffe, I. C. (2009). Lipoprotein biogenesis in Gram-positive bacteria: knowing when to hold 'em, knowing when to fold 'em. *Trends in Microbiology*, 17(1), 13–21.

Hyvönen, M. (2003). CHRD, a novel domain in the BMP inhibitor chordin, is also found in microbial proteins. *Trends in Biochemical Sciences*, 28(9), pp.470–473.

Ito, Y., & Butler, A. (2005). Structure of synechobactins, new siderophores of the marine cyanobacterium *Synechococcus* sp. PCC 7002. *Limnology and Oceanography*, 50(6), 1918–1923.

Ize, B., Gérard, F., Zhang, M., Chanal, A., Voulhoux, R., Palmer, T., Filloux, A. & Wu, L.F. (2002). In vivo dissection of the Tat translocation pathway in *Escherichia coli. Journal of Molecular Biology*, 317(3), 327–335.

Jakuba, R. W., Moffett, J. W., & Dyhrman, S. T. (2008). Evidence for the linked biogeochemical cycling of zinc, cobalt, and phosphorus in the western North Atlantic Ocean. Global Biogeochemical Cycles, 22(4).

James, R. (2005). *Marine Biogeochemical Cycles*. Elsevier Butterworth-Heinemann.

Janson, Wouters, Bergman, & Carpenter. (1999). Host specificity in the *Richelia*–diatom symbiosis revealed by *hetR* gene sequence analysis. *Environmental Microbiology*, 1(5), 431–438.

Jepsoni, B. J. N., Anderson, L. J., Rubio, L. M., Taylor, C. J., Butler, C. S., Flores, E., … Richardson, D. J. (2004). Tuning a nitrate reductase for function. The first spectropotentiometric characterization of a bacterial assimilatory nitrate reductase reveals novel redox properties. *Journal of Biological Chemistry*, 279(31), 32212–32218.

Jiang, H.-B., Lou, W.-J., Du, H.-Y., Price, N. M., & Qiu, B.-S. (2012). Sll1263, a unique cation diffusion facilitator protein that promotes iron uptake in the cyanobacterium *Synechocystis* sp. Strain PCC 6803. *Plant & Cell Physiology*, 53(8), 1404–17.

Jiang, H.-B., Lou, W.-J., Ke, W.-T., Song, W.-Y., Price, N. M., & Qiu, B.-S. (2015). New insights into iron acquisition by cyanobacteria: an essential role for ExbB-ExbD complex in inorganic iron uptake. *The ISME Journal*, 9(2), 297–309.

Jickells, T. D., & Spokes, L. J. (2001). Atmospheric Iron Inputs to the Oceans. *The Biogeochemistry of Iron in Seawater.* (D. . Hunter & K. A. Turner, Eds.). John Wiley & Sons, Ltd, Chichester.

Jickells, T.D., An, Z.S., Andersen, K.K., Baker, A.R., Bergametti, G., Brooks, N., Cao, J.J., Boyd, P.W., Duce, R.A., Hunter, K.A. & Kawahata, H. (2005). Global iron connections between desert dust, ocean biogeochemistry, and climate. *Science*, 308(5718), 67–71.

Jordan, P., Fromme, P., Witt, H. T., Klukas, O., Saenger, W., & Krauß, N. (2001). Three-dimensional structure of cyanobacterial photosystem I at 2.5 Å resolution. *Nature*, 411(6840), 909–917.

Journet, E., Desboeufs, K. V, Caquineau, S., & Colin, J.-L. (2008). Mineralogy as a critical factor of dust iron solubility. Geophysical Research Letters, 35(7).

Jovanovic, M., Rooney, M.S., Mertins, P., Przybylski, D., Chevrier, N., Satija, R., Rodriguez, E.H., Fields, A.P., Schwartz, S., Raychowdhury, R. & Mumbach, M.R. (2015). Dynamic profiling of the protein life cycle in response to pathogens. *Science*, 347(6226).

Juntarajumnong, W., Hirani, T. A., Simpson, J. M., Incharoensakdi, A., & Eaton-Rye, J. J. (2007). Phosphate sensing in *Synechocystis* sp. PCC 6803: SphU and the SphS–SphR two-component regulatory system. *Archives of Microbiology*, 188(4), 389–402.

Kamat, S. S., Williams, H. J., & Raushel, F. M. (2011). Intermediates in the transformation of phosphonates to phosphate by bacteria. *Nature*, 480(7378), 570–3.

Kammler, M., Schön, C., & Hantke, K. (1993). Characterization of the ferrous iron uptake system of *Escherichia coli*. *Journal of Bacteriology*, 175(19), 6212–6219.

Kaneko, T., Sato, S., Kotani, H., Tanaka, A., Asamizu, E., Nakamura, Y., Miyajima, N., Hirosawa, M., Sugiura, M., Sasamoto, S. & Kimura, T. (1996). Sequence analysis of the genome of the unicellular cyanobacterium *Synechocystis* sp. Strain PCC6803. II. Sequence determination of the entire genome and assignment of potential protein-coding regions. *DNA Research*, 3(3), 109–136.

Karl, D. M., Letelier, R., Hebel, D. V., Bird, D. F., & Winn, C. D. (1992). *Trichodesmium* blooms and new nitrogen in the North Pacific gyre. In marine pelagic cyanobacteria: *Trichodesmium* and other Diazotrophs (pp. 219–237). Dordrecht: Springer Netherlands., pp. 219–237.

Karl, D. M., & Björkman, K. M. (2001). Phosphorus cycle in seawater: Dissolved and particulate pool inventories and selected phosphorus fluxes. In B. T.-M. in Microbiology (Ed.), *Marine Microbiology* (Vol. Volume 30, pp. 239–270). Academic Press.

Karl, D., Michaels, A., Bergman, B., Capone, D., Carpenter, E., Letelier, R., Lipschultz, F., Paerl, H., Sigman, D. & Stal, L. (2002). Dinitrogen fixation in the world's oceans. *Biogeochemistry*, 57/58, 47–98.

Karl, D. M. (2014). Microbially mediated transformations of phosphorus in the sea: New views of an old cycle. *Annual Review of Marine Science*, 6(1), 279–337.

Katoh, H., Hagino, N., Grossman, A. R., & Ogawa, T. (2001a). Genes essential to iron transport in the cyanobacterium *Synechocystis* sp. strain PCC 6803. *Journal of Bacteriology*, 183(9), 2779–2784.

Katoh, H., Hagino, N., & Ogawa, T. (2001b). Iron-binding activity of FutA1 subunit of an ABC-type iron transporter in the cyanobacterium *Synechocystis* sp. strain PCC 6803. *Plant and Cell Physiology*, 42(8), 823–827.

Kaufman, A. J. (2014). Early Earth: Cyanobacteria at work. *Nature Geoscience*, 7(4), 253–254.

Kennedy, J., O'Leary, N. D., Kiran, G. S., Morrissey, J. P., O'Gara, F., Selvin, J., & Dobson, A. D. W. (2011). Functional metagenomic strategies for the discovery of novel enzymes and biosurfactants with biotechnological applications from marine ecosystems. *Journal of Applied Microbiology*, 111(4), 787–799.

Keren, N., Aurora, R., & Pakrasi, H. B. (2004). Critical roles of bacterioferritins in iron storage and proliferation of cyanobacteria. *Plant Physiology*, 135(July), 1666–1673.

Khambati, H.K., Moraes, T.F., Singh, J., Shouldice, S.R., Yu, R.H. & Schryvers, A.B. (2010). The role of vicinal tyrosine residues in the function of *Haemophilus influenzae* ferric-binding protein A. *The Biochemical Journal*, 432(1), 57–64.

Kim, Y., Joachimiak, G., Ye, Z., Binkowski, T.A., Zhang, R., Gornicki, P., Callahan, S.M., Hess, W.R., Haselkorn, R. & Joachimiak, A. (2011). Structure of transcription factor HetR required for heterocyst differentiation in cyanobacteria. *Proceedings of the National Academy of Sciences of the United States of America*, 108(25), 10109–10114.

Kim, D., Pertea, G., Trapnell, C., Pimentel, H., Kelley, R., & Salzberg, S. L. (2013). TopHat2: accurate alignment of transcriptomes in the presence of insertions, deletions and gene fusions. *Genome Biology*, 14(4), R36.

Kime, L., Jourdan, S. S., Stead, J. A., Hidalgo-Sastre, A., & McDowall, K. J. (2010). Rapid cleavage of RNA by RNase E in the absence of 5' monophosphate stimulation. *Molecular Microbiology*, 76(3), 590–604.

Kirby, S. D., Gray-Owen, S. D., & Schryvers, A. B. (1997). Characterization of a ferric-binding protein mutant in Haemophilus influenzae. *Molecular Microbiology*, 25(5), 979–987.

Kirchman, D. L. (2015). Growth Rates of Microbes in the Oceans. *Annual Review of Marine Science,* (July), 1–25.

Kneip, C., Lockhart, P., Voß, C., & Maier, U.-G. (2007). Nitrogen fixation in eukaryotes–new models for symbiosis. *BMC Evolutionary Biology*, 7(1), 1.

Kolber, Z., Prasil, O., & Falkowski, P. (1998). Measurements of variable chlorophyll fluorescence using fast repetition rate techniques: defining methodology and experimental protocols. *Biochimica et Biophysica Acta*, 1367(1–3), 88–106.

Kolowith, L. C., Ingall, E. D., & Benner, R. (2001). Composition and cycling of marine organic phosphorus. *Limnology and Oceanography*, 46(2), 309–320.

Kondo, K., Ochiai, Y., Katayama, M., & Ikeuchi, M. (2007). The membrane-associated CpcG2-phycobilisome in Synechocystis: a new photosystem I antenna. *Plant Physiology*, 144(2), 1200–10.

Koropatkin, N., Randich, A. M., Bhattacharyya-Pakrasi, M., Pakrasi, H. B., & Smith, T. J. (2007). The Structure of the iron-binding protein, FutA1, from *Synechocystis* 6803. *Journal of Biological Chemistry*, 282(37), 27468–27477.

Kranz, S. A., Sultemeyer, D., Richtetr, K.-U. & Rost, B. (2009). Carbon acquisition by *Trichodesmium* : The effect of pCO_2 and diurnal changes. *Limnology and Oceanography*, 54(2), 548–559.

Kranzler, C., Lis, H., Shaked, Y., & Keren, N. (2011). The role of reduction in iron uptake processes in a unicellular, planktonic cyanobacterium. *Environmental Microbiology*, 13(11), 2990–2999.

Kranzler, C., Lis, H., Finkel, O. M., Schmetterer, G., Shaked, Y., & Keren, N. (2014). Coordinated transporter activity shapes high-affinity iron acquisition in cyanobacteria. *The ISME Journal*, 8(2), 409–417.

Krewulak, K. D., & Vogel, H. J. (2008). Structural biology of bacterial iron uptake. *Biochimica et Biophysica Acta (BBA) - Biomembranes*, 1778(9), 1781–1804.

Krupke, A., Mohr, W., LaRoche, J., Fuchs, B. M., Amann, R. I., & Kuypers, M. M. M. (2015). The effect of nutrients on carbon and nitrogen fixation by the UCYN-A-haptophyte symbiosis. *The ISME Journal*, 9(7), 1635–47.

Krynická, V., Tichý, M., Krafl, J., Yu, J., Kaňa, R., Boehm, M., Nixon, P.J. & Komenda, J., (2014). Two essential FtsH proteases control the level of the Fur repressor during iron deficiency in the cyanobacterium *Synechocystis* sp. PCC 6803. *Molecular Microbiology*, 94(3), 609–624.

Kuhnert, P., Heyberger-Meyer, B., Nicolet, J., & Frey, J. (2000). Characterization of PaxA and its operon: a cohemolytic RTX toxin determinant from pathogenic *Pasteurella aerogenes*. *Infection and Immunity*, 68(1), 6–12.

Kumar, K., Mella-Herrera, R. A., & Golden, J. W. (2010). Cyanobacterial heterocysts. Cold *Spring Harbor Perspectives in Biology*, 2(4), a000315.

Küpper, H., Šetlík, I., Seibert, S., Prášil, O., Šetlikova, E., Strittmatter, M., Levitan, O., Lohscheider, J., Adamska, I. & Berman-Frank, I. (2008). Iron limitation in the marine cyanobacterium *Trichodesmium* reveals new insights into regulation of photosynthesis and nitrogen fixation. *The New Phytologist*, 179(3), 784–98.

Kurisu, G., Zhang, H., Smith, J. L., & Cramer, W. A. (2003). Structure of the cytochrome b_6f complex of oxygenic photosynthesis: tuning the cavity. *Science*, 302(5647), 1009–14.

Kustka, A. B., Shaked, Y., Milligan, A. J., King, D. W., & Morel, F. M. M. (2005). Extracellular production of superoxide by marine diatoms: Contrasting effects on iron redox chemistry and bioavailability. *Limnology and Oceanography*, 50(4), 1172–1180.

Kustka, A. B., Allen, A. E., & Morel, F. M. M. (2007). Sequence analysis and transcriptional regualtion of iron acquisition genes in two marine daitoms. *Journal of Phycology*, 43(4), 715–729.

Lamb, J. J., Hill, R. E., Eaton-Rye, J. J., & Hohmann-Marriott, M. F. (2014). Functional role of PilA in iron acquisition in the cyanobacterium *Synechocystis* sp. PCC 6803. *PLoS ONE*, 9(8), e105761.

Langlois, R. J., Hummer, D., & LaRoche, J. (2008). Abundances and distributions of the dominant *nifH* phylotypes in the Northern Atlantic Ocean. *Applied and Environmental Microbiology*, 74(6), 1922–1931. 07

Langlois, R., Mills, M. M., Ridame, C., Croot, P., & LaRoche, J. (2012). Diazotrophic bacteria respond to Saharan dust additions. *Marine Ecology Progress Series*, 470, 1–14.

LaRoche, J., Boyd, P. W., McKay, R. M. L., & Geider, R. J. (1996). Flavodoxin as an *in situ* marker for iron stress in phytoplankton. *Nature*, 382(6594), 802–805.

Larsen, R. A., Thomas, M. G., & Postle, K. (1999). Protonmotive force, ExbB and ligand-bound FepA drive conformational changes in TonB. *Molecular Microbiology*, 31(6), 1809–1824.

Larsson, J., Nylander, J. A., & Bergman, B. (2011). Genome fluctuations in cyanobacteria reflect evolutionary, developmental and adaptive traits. *BMC Evolutionary Biology,* 11(1), 187.

Lau, C. K. Y., Ishida, H., Liu, Z., & Vogel, H. J. (2013). Solution structure of Escherichia coli FeoA and its potential role in bacterial ferrous iron transport. *Journal of Bacteriology*, 195(1), 46–55.

Lauro, F.M., McDougald, D., Thomas, T., Williams, T.J., Egan, S., Rice, S., DeMaere, M.Z., Ting, L., Ertan, H., Johnson, J. & Ferriera, S. (2009). The genomic basis of trophic strategy in marine bacteria. *Proceedings of the National Academy of Sciences,* 106(37), 15527–15533

Lea-Smith, D. J., Bombelli, P., Vasudevan, R., & Howe, C. J. (2016). Photosynthetic, respiratory and extracellular electron transport pathways in cyanobacteria. *Biochimica et Biophysica Acta (BBA) - Bioenergetics,* 1857(3), 247–255.

Lee, P. A., Tullman-Ercek, D., & Georgiou, G. (2006). The bacterial twin-arginine translocation pathway. *Annual Review of Microbiology*, 60, 373.

Lee, J.-W., & Helmann, J. D. (2007). Functional specialization within the Fur family of metalloregulators. *Biometals* : An *International Journal on the Role of Metal Ions in Biology, Biochemistry, and Medicine*, 20(3–4), 485–99.

Lee Chen, Y., Chen, H.-Y., Lin, Y.-H., Yong, T.-C., Taniuchi, Y., & Tuo, S. (2014). The relative contributions of unicellular and filamentous diazotrophs to N_2 fixation in the South China Sea and the upstream Kuroshio. *Deep Sea Research Part I: Oceanographic Research Papers*, 85, 56–71.

Lenes, J.M., Darrow, B.P., Cattrall, C., Heil, C.A., Callahan, M., Vargo, G.A., Byrne, R.H., Prospero, J.M., Bates, D.E., Fanning, K.A. & Walsh, J.J. (2001) Iron fertilization and the *Trichodesmium* response on the West Florida shelf. *Limnology and Oceanography*, 46(6), pp.1261-1277.

Lenes, J.M., Darrow, B.A., Walsh, J.J., Prospero, J.M., He, R., Weisberg, R.H., Vargo, G.A. & Heil, C.A. (2008). Saharan dust and phosphatic fidelity: A three-dimensional biogeochemical model of *Trichodesmium* as a nutrient source for red tides on the West Florida Shelf. *Continental Shelf Research*, 28(9), 1091–1115.

Levering, J., Broddrick, J., Dupont, C.L., Peers, G., Beeri, K., Mayers, J., Gallina, A.A., Allen, A.E., Palsson, B.O. & Zengler, K. (2016). Genome-scale model reveals metabolic basis of biomass partitioning in a model diatom. *PLoS ONE*, 11(5), e0155038.

Li, Z., Reimers, S., Pandit, S., & Deutscher, M. P. (2002). RNA quality control: degradation of defective transfer RNA. *The EMBO Journal*, 21(5), 1132–8.

Li, H., Handsaker, B., Wysoker, A., Fennell, T., Ruan, J., Homer, N., Marth, G., Abecasis, G. & Durbin, R. (2009). The Sequence alignment/map format and SAMtools. *Bioinformatics* (Oxford, England), 25(16), 2078–9.

Li, J. J., Bickel, P. J., & Biggin, M. D. (2014). System wide analyses have underestimated protein abundances and the importance of transcription in mammals. *PeerJ*, 2, e270.

Li, J. J., & Biggin, M. D. (2015). Statistics requantitates the central dogma. *Science*,

347(6226), 1066–1067.

Lilie, H., Haehnel, W., Rudolph, R., & Baumann, U. (2000). Folding of a synthetic parallel β-roll protein. *FEBS Letters,* 470(2), 173–177.

Lin, S., Haas, S., Zemojtel, T., Xiao, P., Vingron, M., & Li, R. (2011). Genome-wide comparison of cyanobacterial transposable elements, potential genetic diversity indicators. *Gene*, 473(2), 139–149.

Lindell, D., & Post, A. F. (2001). Ecological aspects of *ntcA* gene expression and its use as an indicator of the nitrogen status of marine *Synechococcus* spp. *Applied and Environmental Microbiology*, 67(8), 3340–9.

Lindell, D., Jaffe, J. D., Johnson, Z. I., Church, G. M., & Chisholm, S. W. (2005). Photosynthesis genes in marine viruses yield proteins during host infection. *Nature*, 438(7064), 86–89.

Lis, H., & Shaked, Y. (2009). Probing the bioavailability of organically bound iron: a case study in the Synechococcus-rich waters of the Gulf of Aqaba . *Aquatic Microbial Ecology*, 56(2–3), 241–253.

Liu, H., HA, N., & Campbell, L. (1997). *Prochlorococcus* growth rate and contribution to primary production in the equatorial and subtropical North Pacific Ocean . *Aquatic Microbial Ecology,* 12(1), 39–47.

Liu, Y., & Aebersold, R. (2016). The interdependence of transcript and protein abundance: new data–new complexities. *Molecular Systems Biology*, 12(1), 856.

Loera-Quezada, M. M., Leyva-González, M. A., López-Arredondo, D., & Herrera-Estrella, L. (2015). Phosphite cannot be used as a phosphorus source but is non-toxic for microalgae. *Plant Science*, 231, 124–130.

Lomas, M. W., Swain, A., Shelton, R., & Ammerman, J. W. (2004). Taxonomic variability of phosphorus stress in Sargasso Sea phytoplankton. *Limnology and Oceanography*, 49(6), 2303–2309.

Lommer, M., Specht, M., Roy, A.S., Kraemer, L., Andreson, R., Gutowska, M.A., Wolf, J., Bergner, S.V., Schilhabel, M.B., Klostermeier, U.C. & Beiko, R.G. (2012). Genome and low-iron response of an oceanic diatom adapted to chronic iron limitation. *Genome Biology*, 13(7), R66.

López-Maury, L., Marguerat, S., & Bähler, J. (2008). Tuning gene expression to changing environments: from rapid responses to evolutionary adaptation. *Nature Reviews. Genetics*, 9(8), 583–93.

Love, M. I., Huber, W., & Anders, S. (2014). Moderated estimation of fold change and dispersion for RNA-seq data with DESeq2. *Genome Biology*, 15(12), 550.

Ludwig, M., & Bryant, D. A. (2011). Transcription Profiling of the model cyanobacterium *Synechococcus* sp. Strain PCC 7002 by Next-Gen (SOLiDTM) sequencing of cDNA. *Frontiers in Microbiology,* 2, 41.1

Ludwig, M., & Bryant, D. A. (2012). *Synechococcus* sp. strain PCC 7002 transcriptome: Acclimation to temperature, salinity, oxidative stress, and mixotrophic growth conditions*. Frontiers in Microbiology,* 3(OCT), 1–14.

Luo, H., Benner, R., Long, R. A., & Hu, J. (2009). Subcellular localization of marine bacterial alkaline phosphatases. *Proceedings of the National Academy of Sciences of the United States of America*, 106(50), 21219–23.

Luo, Y.W., Doney, S.C., Anderson, L.A., Benavides, M., Berman-Frank, I., Bode, A., Bonnet, S., Boström, K.H., Böttjer, D., Capone, D.G. & Carpenter, E.J. (2012). Database of diazotrophs in global ocean: abundance, biomass and nitrogen fixation rates. *Earth Syst. Sci. Data*, 4, 47–73.

Luque, I., Flores, E., & Herrero, A. (1993). Nitrite reductase gene from *Synechococcus* sp. PCC 7942: homology between cyanobacterial and higher-plant nitrite reductases. *Plant Molecular Biology*, 21(6), 1201–5.

Lynch, F., Santana-Sánchez, A., Jämsä, M., Sivonen, K., Aro, E.-M., & Allahverdiyeva, Y. (2015). Screening native isolates of cyanobacteria and a green alga for integrated wastewater treatment, biomass accumulation and neutral lipid production. *Algal Research*, 11, 411–420.

Maeda, S., Badger, M. R., & Price, G. D. (2002). Novel gene products associated with NdhD3/D4-containing NDH-1 complexes are involved in photosynthetic CO_2 hydration in the cyanobacterium, Synechococcus sp. PCC7942. *Molecular Microbiology*, 43(2), 425–435.

Mahaffey, C., Williams, R. G., & Wolff, G. A. (2004). Physical supply of nitrogen to phytoplankton in the Atlantic Ocean. *Global Biogeochemical Cycles*, 18(1), 1–13.

Mahaffey, C., Michaels, A., & Capone, D. (2005). The conundrum of marine N_2 fixation. *American Journal of Science*, 305, 546–595.

Mahaffey, C., Reynolds, S., Davis, C. E., Lohan, M. C., & Lomas, M. W. (2014). Alkaline phosphatase activity in the subtropical ocean: insights from nutrient dust and trace metal addition experiments. *Frontiers in Marine Science,* 1(December), 1–13.

Mahowald, N.M., Baker, A.R., Bergametti, G., Brooks, N., Duce, R.A., Jickells, T.D., Kubilay, N., Prospero, J.M. & Tegen, I. (2005). Atmospheric global dust cycle and iron inputs to the ocean. *Global Biogeochemical Cycles*. 19(4).

Maldonado, M. T., Allen, A. E., Chong, J. S., Lin, K., Leus, D., Karpenko, N., & Harris, S. L. (2006). Copper-dependent iron transport in coastal and oceanic diatoms. *Limnology and Oceanography*, 51(4), 1729–1743.

Marchetti, A., Parker, M.S., Moccia, L.P., Lin, E.O., Arrieta, A.L., Ribalet, F., Murphy, M.E., Maldonado, M.T. & Armbrust, E.V. (2009). Ferritin is used for iron storage in bloom-forming marine pennate diatoms. *Nature*, 457(7228), 467–470.

Marchler-Bauer, A., Derbyshire, M.K., Gonzales, N.R., Lu, S., Chitsaz, F., Geer, L.Y., Geer, R.C., He, J., Gwadz, M., Hurwitz, D.I. & Lanczycki, C.J. (2015). CDD: NCBI's conserved domain database. *Nucleic Acids Research*, 43(Database issue), D222–D226.

Mardis, E. R. (2011). A decade's perspective on DNA sequencing technology. *Nature*, 470(7333), 198–203.

Marguerat, S., & Bähler, J. (2010). RNA-seq: from technology to biology. *Cellular and Molecular Life Sciences* : CMLS, 67(4), 569–79.

Marshall, J.-A., Ross, T., Pyecroft, S., & Hallegraeff, G. (2005). Superoxide production by marine microalgae. *Marine Biology*, 147(2), 541–549.

Martin, J. (1990). Glacial-interglacial CO_2 change: The iron hypothesis. *Paleoceanography*. 5(1), pp.1-13

Martin, J., Coale, K., Johnson, K., Fitzwater, S., Gordon, R., Tanner, S., Hunter, C., Elrod, V., Nowicki, J., Coley, T., Barber, R., Lindley, S., Watson, A., Van Scoy, K., Law, C., Liddicoat, M., Ling, R., Stanton, T., Stockel, J., Collins, C., Anderson, A., Bidigare, R., Ondrusek, M., Latasa, M., Millero, F., Lee, K., Yao, W., Zhang, J., Friederich, G., Sakamoto, C., Chavez, F., Buck, K., Kolber, Z., Greene, R,. Falkowski, P., Chisholm, S., Hoge, F., Swift, R., Yungel, J., Turner, S., Nightingale, P., Hatton, A., Liss, P. & Tindale,. N. (1994). Testing the iron hypothesis in ecosystems of the equatorial Pacific Ocean. *Nature*, 371(6493), 123–129.

Martin, P., Van Mooy, B. A. S., Heithoff, A., & Dyhrman, S. T. (2011). Phosphorus supply drives rapid turnover of membrane phospholipids in the diatom *Thalassiosira pseudonana*. *The ISME Journal,* 5(6), 1057–1060.

Martin, P., Dyhrman, S. T., Lomas, M. W., Poulton, N. J., & Van Mooy, B. A. S. (2014). Accumulation and enhanced cycling of polyphosphate by Sargasso Sea plankton in response to low phosphorus. *Proceedings of the National Academy of Sciences of the United States of America*, 111(22), 8089–94.

Martínez, A., Osburne, M. S., Sharma, A. K., DeLong, E. F., & Chisholm, S. W. (2012).

Phosphite utilization by the marine picocyanobacterium *Prochlorococcus* MIT9301. *Environmental Microbiology*, 14(6), 1363–1377.

Martínez-Garcia, A., Rosell-Melé, A., Jaccard, S. L., Geibert, W., Sigman, D. M., & Haug, G. H. (2011). Southern Ocean dust-climate coupling over the past four million years. *Nature*, 476(7360), 312–315.

Martínez-García, A., Sigman, D.M., Ren, H., Anderson, R.F., Straub, M., Hodell, D.A., Jaccard, S.L., Eglinton, T.I. & Haug, G.H. (2014). Iron fertilization of the Subantarctic Ocean during the last ice age. *Science*, 343(March), 1347–1350.

Martinez-Perez, C., Mohr, W., Löscher, C.R., Dekaezemacker, J., Littmann, S., Yilmaz, P., Lehnen, N., Fuchs, B.M., Lavik, G., Schmitz, R.A. & LaRoche, J. (2016). The small unicellular diazotrophic symbiont, UCYN-A, is a key player in the marine nitrogen cycle. *Nature Microbiology*, 1, 16163.

Massaoud, M. K., Marokházi, J., & Venekei, I. (2011). Enzymatic characterization of a serralysin-like metalloprotease from the entomopathogen bacterium, *Xenorhabdus*. *Biochimica et Biophysica Acta* (*BBA) - Proteins and Proteomics*, 1814(10), 1333–1339.

Massé, E., & Gottesman, S. (2002). A small RNA regulates the expression of genes involved in iron metabolism in *Escherichia coli*. *Proceedings of the National Academy of Sciences of the United States of America*, 99(7), 4620–5.

Maxam, A. M. & Gilbert, W. (1977). A new method for sequencing DNA. *Proceedings of the National Academy of Sciences*, 74(2), 560–564.

Mazard, S. L., Fuller, N. J., Orcutt, K. M., Bridle, O., & Scanlan, D. J. (2004). PCR analysis of the distribution of unicellular cyanobacterial diazotrophs in the Arabian Sea. *Applied and Environmental Microbiology*, 70(12), 7355–7364.

Melvin, J. A., Scheller, E. V., Noël, C. R., & Cotter, P. A. (2015). New Insight into filamentous hemagglutinin secretion reveals a role for full-length FhaB in *Bordetella* virulence. *mBio*, 6(4), e01189-15.

Meng, Q., Wang, Y., & Liu, X.-Q. (2005). An intron-encoded protein assists RNA splicing of multiple similar introns of different bacterial genes. *The Journal of Biological Chemistry*, 280(42), 35085–8.

Metcalf, W. W., & Wanner, B. L. (1991). Involvement of the *Escherichia coli phn* (*psiD*) gene cluster in assimilation of phosphorus in the form of phosphonates, phosphite, Pi esters, and Pi. *Journal of Bacteriology*, 173(2), 587–600.

Metcalf, W. W., & Wolfe, R. S. (1998). Molecular genetic analysis of phosphite and hypophosphite oxidation by *Pseudomonas stutzeri* WM88. *Journal of Bacteriology*, 180(21), 5547–5558.

Mey, A. R., Wyckoff, E. E., Kanukurthy, V., Fisher, C. R., & Payne, S. M. (2005). Iron and Fur Regulation in *Vibrio cholerae* and the Role of Fur in Virulence . *Infection and Immunity*, 73(12), 8167–8178.

Michel, K. P., & Pistorius, E. K. (1992). Isolation of a photosystem-II associated 36 kDa polypeptide and an iron- stress 34 kDa Polypeptide from thylakoid membranes of the cyanobacterium *Synechococcus*-PCC6301 grown under mild iron deficiency. *Z Naturforsch C*, 47(11–12), 867–874.

Michel, K.-P., Thole, H. H., & Pistorius, E. K. (1996). IdiA, a 34 kDa protein in the cyanobacteria *Synechococcus* sp. strains PCC 6301 and PCC 7942, is required for growth under iron and manganese limitations. *Microbiology*, 142(9), 2635–2645.

Michel, K.-P., Exss-Sonne, P., Scholten-Beck, G., Kahmann, U., Ruppel, H. G., & Pistorius, E. K. (1998). Immunocytochemical localization of IdiA, a protein expressed under iron or manganese limitation in the mesophilic cyanobacterium *Synechococcus* PCC 6301 and the thermophilic cyanobacterium *Synechococcus elongatus*. *Planta*, 205(1), 73–81.

Michel, K.-P., Krüger, F., Pühler, A., & Pistorius, E. K. (1999). Molecular characterization of idiA and adjacent genes in the cyanobacteria *Synechococcus* sp. strains PCC 6301 and

PCC 7942. *Microbiology*, 145(6), 1473–1484.

Michel, K.-P., & Pistorius, E. K. (2004). Adaptation of the photosynthetic electron transport chain in cyanobacteria to iron deficiency: The function of IdiA and IsiA. *Physiologia Plantarum*, 120(1), 36–50.

Mikheeva, L. E., Karbysheva, E. A., & Shestakov, S. V. (2013). The role of mobile genetic elements in the evolution of cyanobacteria. Russian *Journal of Genetics: Applied Research*, 3(2), 91–101.

Milligan, A. J., Berman-Frank, I., Gerchman, Y., Dismukes, G. C., & Falkowski, P. G. (2007). Light-dependent oxygen consumption in nitrogen-fixing cyanobacteria plays a key role in nitrogenase protection 1. *Journal of Phycology*, 43(5), 845–852.

Mills, M. M., Ridame, C., Davey, M., La Roche, J., & Geider, R. J. (2004). Iron and phosphorus co-limit nitrogen fixation in the eastern tropical North Atlantic. *Nature*, 429(6989), 292–294.

Mills, M.M., Moore, C.M., Langlois, R., Milne, A., Achterberg, E.P., Nachtigall, K., Lochte, K., Geider, R.J. & LaRoche, J. (2008). Nitrogen and phosphorus co-limitation of bacterial productivity and growth in the oligotrophic subtropical North Atlantic. *Limnology And Oceanography*, 53(2), 824–834.

Mirus, O., Strauss, S., Nicolaisen, K., von Haeseler, A. & Schleiff, E. (2009). TonB-dependent transporters and their occurrence in cyanobacteria. *BMC Biology*, 7(1), 68.

Miyata, K., Maejima, K., Tomoda, K., & Isono, M. (1970). Serratia Protease. *Agricultural and Biological Chemistry,* 34(2), 310–318.

Mizusawa, N., & Wada, H. (2012). The role of lipids in photosystem II. *Biochimica et Biophysica Acta (BBA) - Bioenergetics*, 1817(1), 194–208.

Mock, T., Daines, S.J., Geider, R., Collins, S., Metodiev, M., Millar, A.J., Moulton, V. & Lenton, T.M. (2016). Bridging the gap between omics and earth system science to better understand how environmental change impacts marine microbes. *Global Change Biology*, 22(1), 61–75.

Mohamed, A., & Jansson, C. (1989). Influence of light on accumulation of photosynthesis-specific transcripts in the cyanobacterium *Synechocystis* 6803. *Plant Molecular Biology*, 13(6), 693–700.

Moisander, P.H., Beinart, R.A., Hewson, I., White, A.E., Johnson, K.S., Carlson, C.A., Montoya, J.P. & Zehr, J.P. (2010). Unicellular cyanobacterial distributions broaden the oceanic N_2 Fixation domain. *Science*, 327(5972), 1512–1514.

Momper, L. M., Reese, B. K., Carvalho, G., Lee, P., & Webb, E. A. (2015). A novel cohabitation between two diazotrophic cyanobacteria in the oligotrophic ocean. *The ISME Journal*, 9(4), 882–93.

Montoya, J., Holl, C., Zehr, J., Hansen, A., Villareal, T., & Capone, D. (2004). High rates of N_2 fixation by unicellular diazotrophs in the oligotrophic Pacific Ocean. *Nature*, 430(August), 1027–1031.

Moore, J. K., & Doney, S. C. (2007). Iron availability limits the ocean nitrogen inventory stabilizing feedbacks between marine denitrification and nitrogen fixation. *Global Biogeochemical Cycles,* 21(2).

Moore, J. K., & Braucher, O. (2008). Sedimentary and mineral dust sources of dissolved iron to the World Ocean. *Biogeosciences*, 5(1994), 631–656.

Moore, C.M., Mills, M.M., Achterberg, E.P., Geider, R.J., LaRoche, J., Lucas, M.I., McDonagh, E.L., Pan, X., Poulton, A.J., Rijkenberg, M.J. & Suggett, D.J. (2009). Large-scale distribution of Atlantic nitrogen fixation controlled by iron availability. *Nature Geoscience*, 2(12), 867–871.

Moore, C.M., Mills, M.M., Arrigo, K.R., Berman-Frank, I., Bopp, L., Boyd, P.W., Galbraith, E.D., Geider, R.J., Guieu, C., Jaccard, S.L. & Jickells, T.D. (2013). Processes and patterns of oceanic nutrient limitation. *Nature Geoscience*, 6(9), 701–710.

Morgulis, A., Coulouris, G., Raytselis, Y., Madden, T. L., Agarwala, R., & Schäffer, A. A. (2008). Database indexing for production MegaBLAST searches. *Bioinformatics*, 24(16), 1757–64.

Morris, J. J., Lenski, R. E., & Zinser, E. R. (2012). The black queen hypothesis: Evolution of dependencies through adaptive gene loss. *mBio*, 3(2), e00036-12-e00036-12.

Morrissey, J., Sutak, R., Paz-Yepes, J., Tanaka, A., Moustafa, A., Veluchamy, A., Thomas, Y., Botebol, H., Bouget, F.Y., McQuaid, J.B. & Tirichine, L. (2015). A novel protein, ubiquitous in marine phytoplankton, concentrates iron at the cell surface and facilitates uptake. *Current Biology*, 25(3), 364–371.

Moutin, T., Van Den Broeck, N., Beker, B., Dupouy, C., Rimmelin, P., & Le Bouteiller, A. (2005). Phosphate availability controls *Trichodesmium* spp. biomass in the SW Pacific Ocean. *Marine Ecology Progress Series,* 297(1), 15–21.

Murphy, K. (1985). The trace metal chemistry of the Atlantic aerosol. University of Liverpool.

Nakayama, H., Kurokawa, K., & Lee, B. L. (2012). Lipoproteins in bacteria: structures and biosynthetic pathways. *FEBS Journal,* 279(23), 4247–4268.

Natale, P., Brüser, T., & Driessen, A. J. M. (2008). Sec- and Tat-mediated protein secretion across the bacterial cytoplasmic membrane—Distinct translocases and mechanisms. *Biochimica et Biophysica Acta (BBA) - Biomembranes,* 1778(9), 1735–1756.

Neilands, J. B. (1995). Siderophores: structure and function of microbial iron transport compounds. *Journal of Biological Chemistry* , 270(45), 26723–26726.

Nicolaisen, K., Moslavac, S., Samborski, A., Valdebenito, M., Hantke, K., Maldener, I., Muro-Pastor, A.M., Flores, E. & Schleiff, E. (2008). Alr0397 Is an outer membrane transporter for the siderophore schizokinen in *Anabaena* sp. strain PCC 7120. *Journal of Bacteriology*, 190(22), 7500–7507.

Nicolaisen, K., Hahn, A., Valdebenito, M., Moslavac, S., Samborski, A., Maldener, I., Wilken, C., Valladares, A., Flores, E., Hantke, K. & Schleiff, E. (2010). The interplay between siderophore secretion and coupled iron and copper transport in the heterocyst-forming cyanobacterium *Anabaena* sp. PCC 7120. *Biochimica et Biophysica Acta (BBA) - Biomembranes,* 1798(11), 2131–2140.

Nikaido, H. (2003). Molecular basis of bacterial outer membrane permeability revisited. *Microbiology and Molecular Biology Reviews*. 67(4), 593–656.

Nodwell, L. M., & Price, N. M. (2001). Direct use of inorganic colloidal iron by marine mixotrophic phytoplankton. *Limnology and Oceanography*, 46(4), 765–777.

Notredame, C., Higgins, D. G., & Heringa, J. (2000). T-coffee: a novel method for fast and accurate multiple sequence alignment1. *Journal of Molecular Biology*, 302(1), 205–217.

Nowaczyk, M. M., Hebeler, R., Schlodder, E., Meyer, H. E., Warscheid, B., & Rögner, M. (2006). Psb27, a cyanobacterial lipoprotein, is involved in the repair cycle of photosystem II. *The Plant Cell,* 18(11), 3121–3131.

Nozzi, N. E., Oliver, J. W. K., & Atsumi, S. (2013). Cyanobacteria as a platform for biofuel production. *Frontiers in Bioengineering and Biotechnology*. 1, p.7.

Ohkawa, H., Pakrasi, H. B., & Ogawa, T. (2000a). Two types of functionally distinct NAD(P)H dehydrogenases in *Synechocystis* sp. strain PCC6803. *The Journal of Biological Chemistry*, 275(41), 31630–4.

Ohkawa, H., Price, G. D., Badger, M. R., & Ogawa, T. (2000b). Mutation of ndh genes leads to inhibition of CO_2 uptake rather than HCO^{3-} uptake in *Synechocystis* sp. strain PCC 6803. *Journal of Bacteriology,* 182(9), 2591–6.

Okin, G. S., Mahowald, N., Chadwick, O. A., & Artaxo, P. (2004). Impact of desert dust on the biogeochemistry of phosphorus in terrestrial ecosystems. *Global Biogeochemical Cycles*, 18(2).

Ollis, A. A., Manning, M., Held, K. G., & Postle, K. (2009). Cytoplasmic membrane proton motive force energizes periplasmic interactions between ExbD and TonB. *Molecular Microbiology*, 73(3), 466–481.

Ollis, A. A., & Postle, K. (2012). ExbD mutants define initial stages in TonB energization. *Journal of Molecular Biology*, 415(2), 237–247.

Ollis, A. A., Kumar, A. & Postle, K. (2012). The ExbD periplasmic domain contains distinct functional regions for two stages in TonB energization. *Journal of Bacteriology*, 194(12), 3069–3077.

Orchard, E., Webb, E. & Dyhrman, S. (2003). Characterization of phosphorus-regulated genes in *Trichodesmium* spp. *The Biological Bulletin*, 205(2), 230–1.

Orchard, E. D., Webb, E. A. & Dyhrman, S. T. (2009). Molecular analysis of the phosphorus starvation response in *Trichodesmium* spp. *Environmental Microbiology*, 11(9), 2400–2411.

Orchard, E. D., Benitez-Nelson, C. R., Pellechia, P. J., Lomas, M. W., & Dyhrman, S. T. (2010a). Polyphosphate in *Trichodesmium* from the low-phosphorus Sargasso Sea. *Limnology and Oceanography*, 55(5), 2161–2169.

Orchard, E. D., Ammerman, J. W., Lomas, M. W. & Dyhrman, S. T. (2010b). Dissolved inorganic and organic phosphorus uptake in *Trichodesmium* and the microbial community: The importance of phosphorus ester in the Sargasso Sea. *Limnology and Oceanography*, 55(3), 1390–1399.

Osman, D., & Cavet, J. S. (2010). Bacterial metal-sensing proteins exemplified by ArsR-SmtB family repressors. *Natural Product Reports*, 27(5), 668–80.

Overduin, P., Boos, W., & Tommassen, J. (1988). Nucleotide sequence of the ugp genes of *Escherichia coli* K-12: homology to the maltose system. *Molecular Microbiology*, 2(6), 767–775.

Parages, L. M., Gutiérrez-Barranquero, A. J., Reen, J. F., Dobson, D. A., & O'Gara, F. (2016). Integrated (meta) genomic and synthetic biology approaches to develop new biocatalysts. *Marine Drugs*. 14(3).

Partensky, F., Blanchot, J., & Vaulot, D. (1999). Differential distribution and ecology of Prochlorococcus and Synechococcus in oceanic waters: a review. *BULLETIN-INSTITUT OCEANOGRAPHIQUE MONACO-NUMERO SPECIAL-*, 457–476.

Pasek, M. A., Sampson, J. M., & Atlas, Z. (2014). Redox chemistry in the phosphorus biogeochemical cycle. *Proceedings of the National Academy of Sciences* , 111(43), 15468–15473.

Patti, G. J., Yanes, O., & Siuzdak, G. (2012). Metabolomics: the apogee of the omic triology. *Nature Reviews. Molecular Cell Biology,* 13(4), 263–269.

Paytan, A., Mackey, K.R., Chen, Y., Lima, I.D., Doney, S.C., Mahowald, N., Labiosa, R. & Post, A.F. (2009). Toxicity of atmospheric aerosols on marine phytoplankton. *Proceedings of the National Academy of Sciences*, 106(12), 4601–4605.

Paz, Y., Katz, A., & Pick, U. (2007a). A multicopper ferroxidase involved in iron binding to transferrins in *Dunaliella salina* plasma membranes. *Journal of Biological Chemistry*, 282(12), 8658–8666.

Paz, Y., Shimoni, E., Weiss, M., & Pick, U. (2007b). Effects of iron deficiency on iron binding and internalization into acidic vacuoles in Dunaliella salina. *Plant Physiology*, 144(July), 1407–1415.

Pech, H., Henry, A., Khachikian, C. S., Salmassi, T. M., Hanrahan, G., & Foster, K. L. (2009). Detection of geothermal phosphite using high performance liquid chromatography. *Environmental Science & Technology,* 43(20), 7671–7675.

Pech, H., Vazquez, M.G., Van Buren, J., Foster, K.L., Shi, L., Salmassi, T.M., Ivey, M.M. & Pasek, M.A. (2011). Elucidating the redox cycle of environmental phosphorus using ion chromatography. *Journal of Chromatographic Science*, 49(8), 573–581.

Peers, G., & Price, N. M. (2004). A role for manganese in superoxide dismutases and growth of iron-deficient diatoms. *Limnology and Oceanography*, 49(5), 1774–1783.

Peers, G., & Price, N. M. (2006). Copper-containing plastocyanin used for electron transport by an oceanic diatom. *Nature*, 441(7091), 341–344.

Peters, G. A., & Meeks, J. C. (1989). The *Azolla-Anabaena* symbiosis: Basic biology. *Annual Review of Plant Physiology and Plant Molecular Biology*, 40(1), 193–210.

Petersen, T. N., Brunak, S., von Heijne, G., & Nielsen, H. (2011). SignalP 4.0: discriminating signal peptides from transmembrane regions. *Nature methods,* 8(10), 785–786.

Pfaffl, M. W., Tichopad, A., Prgomet, C., & Neuvians, T. P. (2004). Determination of stable housekeeping genes, differentially regulated target genes and sample integrity: BestKeeper – Excel-based tool using pair-wise correlations. *Biotechnology Letters,* 26(6), 509–515.

Pfreundt, U., Kopf, M., Belkin, N., Berman-Frank, I., & Hess, W. R. (2014). The primary transcriptome of the marine diazotroph *Trichodesmium erythraeum* IMS101. *Scientific Reports*, 4, 6187.

Pfreundt, U. & Hess, W. R. (2015). Sequential splicing of a group II twintron in the marine cyanobacterium *Trichodesmium. Scientific Reports*, 5, 16829.

Pitta, T. P., Sherwood, E. E., Kobel, A. M., & Berg, H. C. (1997). Calcium is required for swimming by the nonflagellated cyanobacterium *Synechococcus* strain WH8113. *Journal of Bacteriology*, 179(8), 2524–8.

Pojidaeva, E., Zinchenko, V., Shestakov, S. V, & Sokolenko, A. (2004). Involvement of the SppA1 peptidase in acclimation to saturating light intensities in *Synechocystis* sp . strain PCC 6803. *Society*, 186(12), 3991–3999.

Polyviou, D., Hitchcock, A., Baylay, A. J., Moore, C. M., & Bibby, T. S. (2015). Phosphite utilization by the globally important marine diazotroph *Trichodesmium*. *Environmental Microbiology Reports*, 7(6), 824–830.

Poole, K., Young, L., & Neshat, S. (1990). Enterobactin-mediated iron transport in *Pseudomonas aeruginosa*. *Journal of Bacteriology* , 172(12), 6991–6996.

Prufert-Bebout, L., Paerl, H. W., & Lassen, C. (1993). Growth, nitrogen fixation, and spectral attenuation in cultivated *Trichodesmium* species. *Applied and Environmental Microbiology*, 59(5), 1367–75.

Ran, L., Larsson, J., Vigil-Stenman, T., Nylander, J.A., Ininbergs, K., Zheng, W.W., Lapidus, A., Lowry, S., Haselkorn, R. & Bergman, B. (2010). Genome erosion in a nitrogen-fixing vertically transmitted endosymbiotic multicellular cyanobacterium. *PLoS ONE,* 5(7), e11486.

Raven, J. A., Evans, M. C. W., & Korb, R. E. (1999). The role of trace metals in photosynthetic electron transport in O_2-evolving organisms. *Photosynthesis Research*, 60(2/3), 111–150.

Reddy, K. J., Haskell, J. B., Sherman, D. M., & Sherman, L. A. (1993). Unicellular, aerobic nitrogen-fixing cyanobacteria of the genus *Cyanothece*. *Journal of Bacteriology*, 175(5), 1284–92.

Reddy, T.B.K., Thomas, A.D., Stamatis, D., Bertsch, J., Isbandi, M., Jansson, J., Mallajosyula, J., Pagani, I., Lobos, E.A. and Kyrpides, N.C. (2015). The Genomes OnLine Database (GOLD) v.5: a metadata management system based on a four level (meta)genome project classification. *Nucleic Acids Research*, 43(Database issue), D1099-106.

Redfield, A. (1958). The biological control of chemical factors in the environment. *American Scientist.* 46(3), pp.230A-221.

Reed, D. C., Algar, C. K., Huber, J. A., & Dick, G. J. (2014). Gene-centric approach to integrating environmental genomics and biogeochemical models. *Proceedings of the National Academy of Sciences*, 111(5), 1879–1884.

Reguera, G., McCarthy, K. D., Mehta, T., Nicoll, J. S., Tuominen, M. T., & Lovley, D. R. (2005).

Extracellular electron transfer via microbial nanowires. *Nature*, 435(7045), 1098–1101.

Rhee, G.-Y. (1973). A continuous culture study of phosphate uptake, growth rate and polyphosphate in *Scenedesmus* sp. *Journal of Phycology*, 9(4), 495–506.

Rich, H. W., & Morel, F. M. M. (1990). Availability of well-defined iron colloids to the marine diatom *Thalassiosira weissflogii. Limnology and Oceanography*, 35(3), 652–662.

Richier, S., Macey, A. I., Pratt, N. J., Honey, D. J., Moore, C. M., & Bibby, T. S. (2012). Abundances of iron-binding photosynthetic and nitrogen-fixing proteins of *Trichodesmium* both in culture and in situ from the North Atlantic. *PloS One*, 7(5), 1–12.

Rippka, R., Deruelles, J., Waterbury, J. B., Herdman, M., & Stanier, R. Y. (1979). Generic assignments, strain histories and properties of pure cultures of cyanobacteria. *Microbiology*, 111, 1–61.

Rivers, A. R., Jakuba, R. W., & Webb, E. A. (2009). Iron stress genes in marine *Synechococcus* and the development of a flow cytometric iron stress assay. *Environmental Microbiology*, 11(2), 382–396.

Robidart, J.C., Church, M.J., Ryan, J.P., Ascani, F., Wilson, S.T., Bombar, D., Marin, R., Richards, K.J., Karl, D.M., Scholin, C.A. & Zehr, J.P. (2014). Ecogenomic sensor reveals controls on N_2 fixing microorganisms in the North Pacific Ocean. *TheISME Journal*, 8(6), 1175–1185.

Rodier, M., & Le Borgne, R. (2008). Population dynamics and environmental conditions affecting Trichodesmium spp. (filamentous cyanobacteria) blooms in the south-west lagoon of New Caledonia. *Journal of Experimental Marine Biology and Ecology*, (1), 35820–32.

Rodier, M., & Le Borgne, R. (2010). Population and trophic dynamics of *Trichodesmium thiebautii* in the SE lagoon of New Caledonia. Comparison with *T. erythraeum* in the SW lagoon. *Marine Pollution Bulletin,* 61(7–12), 349–59.

Roe, K. L., Barbeau, K., Mann, E. L., & Haygood, M. G. (2012). Acquisition of iron by *Trichodesmium* and associated bacteria in culture. *Environmental Microbiology,* 14(7), 1681–1695.

Roe, K. L., & Barbeau, K. A. (2014). Uptake mechanisms for inorganic iron and ferric citrate in *Trichodesmium* erythraeum IMS101. *Metallomics*, 6(11), 2042–2051.

Rose, T., Sebo, P., Bellalou, J., & Ladant, D. (1995). Interaction of calcium with *Bordetella pertussis* adenylate peated sequences of the type GG X G X D X L X (where X represents any amino acid) that are characteristic of the, 270(44), 26370–26376.

Rose, A. L., Salmon, T. P., Lukondeh, T., Neilan, B. a, & Waite, T. D. (2005). Use of superoxide as an electron shuttle for iron acquisition by the marine cyanobacterium *Lyngbya majuscula*. *Environmental Science & Technology*, 39(10), 3708–15.

Rose, A. L., & Waite, T. D. (2005). Reduction of organically complexed ferric iron by superoxide in a simulated natural water. *Environmental Science & Technology*, 39(8), 2645–2650.

Rubin, M., Berman-Frank, I., & Shaked, Y. (2011). Dust- and mineral-iron utilization by the marine dinitrogen-fixer *Trichodesmium*. *Nature Geoscience*, 4(August), 529–534.

Rubio, L. M., Flores, E., & Herrero, A. (2002). Purification, cofactor analysis, and site-directed mutagenesis of *Synechococcus* ferredoxin-nitrate reductase. *Photosynthesis Research*, 72(1), 13–26.

Rudolf, M., Stevanovic, M., Kranzler, C., Pernil, R., Keren, N., & Schleiff, E. (2016). Multiplicity and specificity of siderophore uptake in the cyanobacterium *Anabaena* sp. PCC 7120. *Plant Molecular Biology,* 1–13.

Rue, E. L., & Bruland, K. W. (1995). Complexation of iron(II) by natural organic ligands in the Central North Pacific as determined by a new competitive ligand

equilibration/adsorptive cathodic stripping voltammetric method. *Marine Chemistry*, 50, 117–138.

Rueter, J. G., Hutchins, D. A., Smith, R. W., & Unsworth, N. L. (1992). Iron nutrition of *Trichodesmium* - Marine Pelagic Cyanobacteria: *Trichodesmium* and other Diazotrophs. In E. J. Carpenter, D. G. Capone, & J. G. Rueter (Eds.), (pp. 289–306). Dordrecht: Springer Netherlands.

Rutherford, K., Parkhill, J., Crook, J., Horsnell, T., Rice, P., Rajandream, M. A., & Barrell, B. (2000). Artemis: sequence visualization and annotation. *Bioinformatics*, 16(10), 944–945.

Ryan-Keogh, T. J., Macey, A. I., Cockshutt, A. M., Moore, C. M., & Bibby, T. S. (2012). The cyanobacterial chlorophyll-binding-protein Isia acts to increase the in vivo effective absorption cross-section of PSI under iron limitation. *Journal of Phycology*, 48(1), 145–154.

Sacharz, J., Bryan, S. J., Yu, J., Burroughs, N. J., Spence, E. M., Nixon, P. J., & Mullineaux, C. W. (2015). Sub-cellular location of FtsH proteases in the cyanobacterium *Synechocystis* sp. PCC 6803 suggests localised PSII repair zones in the thylakoid membranes. *Molecular Microbiology*, 96(3), 448–462.

Saito, M. A., Goepfert, T. J., & Ritt, J. T. (2008). Some thoughts on the concept of colimitation: Three definitions and the importance of bioavailability. *Limnology and Oceanography*, 53(1), 276–290.

Saito, M.A., Bertrand, E.M., Dutkiewicz, S., Bulygin, V.V., Moran, D.M., Monteiro, F.M., Follows, M.J., Valois, F.W. & Waterbury, J.B. (2011). Iron conservation by reduction of metalloenzyme inventories in the marine diazotroph *Crocosphaera watsonii. Proceedings of the National Academy of Sciences of the United States of America*, 108(6), 2184–2189

Saito, M.A., McIlvin, M.R., Moran, D.M., Goepfert, T.J., DiTullio, G.R., Post, A.F. & Lamborg, C.H. (2014). Multiple nutrient stresses at intersecting Pacific Ocean biomes detected by protein biomarkers. *Science*. 345(6201), 1173–7

Sánchez-Magraner, L., Viguera, A.R., García-Pacios, M., Garcillán, M.P., Arrondo, J.L.R., de la Cruz, F., Goñi, F.M. & Ostolaza, H. (2007). The calcium-binding C-terminal domain of *Escherichia coli* alpha-hemolysin is a major determinant in the surface-active properties of the protein. *The Journal of Biological Chemistry*, 282(16), 11827–35.

Sandh, G., Ran, L., Xu, L., Sundqvist, G., Bulone, V., & Bergman, B. (2011). Comparative proteomic profiles of the marine cyanobacterium *Trichodesmium erythraeum* IMS101 under different nitrogen regimes. *Proteomics*, 11(3), 406–19.

Sandh, G., Xu, L., & Bergman, B. (2012). Diazocyte development in the marine diazotrophic cyanobacterium *Trichodesmium*. *Microbiology*. 158(Pt 2), 345–52.

Sandström, S., Ivanov, A. G., Park, Y.-I., Oquist, G., & Gustafsson, P. (2002). Iron stress responses in the cyanobacterium *Synechococcus* sp. PCC7942. *Physiologia Plantarum*, 116(2), 255–263.

Sanger, F., Nicklen, S., & Coulson, A. R. (1977). DNA sequencing with chain-terminating inhibitors. *Proceedings of the National Academy of Sciences of the United States of America*, 74(12), 5463–5467.

Santos-Beneit, F. (2015). The Pho regulon: a huge regulatory network in bacteria. *Frontiers in Microbiology*, 6, 402.

Sañudo-Wilhelmy, S.A., Kustka, A.B., Gobler, C.J., Hutchins, D.A., Yang, M., Lwiza, K., Burns, J., Capone, D.G., Raven, J.A. & Carpenter, E.J. (2001). Phosphorus limitation of nitrogen fixation by *Trichodesmium* in the central Atlantic Ocean. *Nature*, 411(6833), 66–69.

Sato, M., Sakuraba, R., & Hashihama, F. (2013). Phosphate monoesterase and diesterase activities in the North and South Pacific Ocean. *Biogeosciences*, 10, 7677–7688.

Sauert, M., Temmel, H., & Moll, I. (2015). Heterogeneity of the translational machinery: Variations on a common theme. *Biochimie*, 114, 39–47.

Scanlan, D. J. (2003). Physiological diversity and niche adaptation in marine *Synechococcus*. *Advances in Microbial Physiology*, 47, 1–64.

Scharek, R., Tupas, L., & Karl, D. (1999). Diatom fluxes to the deep sea in the oligotrophic North Pacific gyre at Station ALOHA. *Marine Ecology Progress Series*, 182, 55–67.

Schauer, K., Rodionov, D.A. & de Reuse, H. (2008). New substrates for TonB-dependent transport: do we only see the 'tip of the iceberg'?. *Trends in biochemical sciences*, 33(7), pp.330-338.

Schink, B., & Friedrich, M. (2000). Bacterial metabolism: Phosphite oxidation by sulphate reduction . *Nature*, 406(6791), 37.

Schink, B., Thiemann, V., Laue, H., & Friedrich, M. W. (2002). *Desulfotignum phosphitoxidans* sp. nov., a new marine sulfate reducer that oxidizes phosphite to phosphate. *Archives of Microbiology,* 177(5), 381–391.

Schneider, D., Volkmer, T., & Rögner, M. (2007). PetG and PetN, but not PetL, are essential subunits of the cytochrome b_6f complex from *Synechocystis* PCC 6803. *Research in Microbiology*, 158(1), 45–50.

Schneider, C. A., Rasband, W. S., & Eliceiri, K. W. (2012). NIH Image to ImageJ: 25 years of image analysis. *Nature Methods*, 9(7), 671–675.

Schrader, P. S., Milligan, A. J., & Behrenfeld, M. J. (2011). Surplus photosynthetic antennae complexes underlie diagnostics of iron limitation in a cyanobacterium. *PloS One*, 6(4), 1–7.

Schuergers, N., Nurnberg, D. J., Wallner, T., Mullineaux, C. W., & Wilde, A. (2015). PilB localization correlates with the direction of twitching motility in the cyanobacterium *Synechocystis* sp. PCC 6803. *Microbiology*, 161(Pt_5), 960–966.

Sebastián, M., Arístegui, J., Montero, M. F., Escanez, J., & Xavier Niell, F. (2004a). Alkaline phosphatase activity and its relationship to inorganic phosphorus in the transition zone of the North-western African upwelling system. *Progress in Oceanography*, 62(2–4), 131–150.

Sebastián, M., Arístegui, J., Montero, M. F., & Niell, F. X. (2004b). Kinetics of alkaline phosphatase activity, and effect of phosphate enrichment: A case study in the NW African upwelling region. *Marine Ecology Progress Series*, 270, 1–13.

Seweryn, P., Van, L.B., Kjeldgaard, M., Russo, C.J., Passmore, L.A., Hove-Jensen, B., Jochimsen, B. & Brodersen, D.E. (2015). Structural insights into the bacterial carbon–phosphorus lyase machinery. *Nature*, 525(7567), 68–72.

Shaked, Y., Kustka, A. B., & Morel, F. M. M. (2005). A general kinetic model for iron acquisition by eukaryotic phytoplankton. *Limnology and Oceanography*, 50(3), 872–882.

Shcolnick, S., Shaked, Y., & Keren, N. (2007). A role for mrgA, a DPS family protein, in the internal transport of Fe in the cyanobacterium *Synechocystis* sp. PCC6803*. Biochimica et Biophysica Acta (BBA) - Bioenergetics*, 1767(6), 814–819.

Sheridan, C. C., Steinberg, D. K., & Kling, G. W. (2002). The microbial and metazoan community associated with colonies of *Trichodesmium* spp.: a quantitative survey. *Journal of Plankton Research,* 24(9), 913–922.

Shi, T., Sun, Y., & Falkowski, P. G. (2007). Effects of iron limitation on the expression of metabolic genes in the marine cyanobacterium *Trichodesmium erythraeum* IMS101. *Environmental Microbiology*, 9(12), 2945–2956.

Shi, D., Kranz, S. a, Kim, J.-M., & Morel, F. M. M. (2012). Ocean acidification slows nitrogen fixation and growth in the dominant diazotroph *Trichodesmium* under low-iron conditions. *Proceedings of the National Academy of Sciences of the United States of America*, 109(45), pp.E3094-E3100.

Shibata, M., Ohkawa, H., Kaneko, T., Fukuzawa, H., Tabata, S., Kaplan, A., & Ogawa, T. (2001). Distinct constitutive and low-CO_2-induced CO_2 uptake systems in cyanobacteria: genes involved and their phylogenetic relationship with homologous genes in other organisms. *Proceedings of the National Academy of Sciences of the United States of America*, 98(20), 11789–94.

Shibata, M., Ohkawa, H., Katoh, H., Shimoyama, M. & Ogawa, T. (2002). Two CO_2 uptake systems in cyanobacteria: four systems for inorganic carbon acquisition in *Synechocystis* sp. strain PCC 6803. Functional Plant Biology, 29(3), 123–129.

Shih, P.M., Wu, D., Latifi, A., Axen, S.D., Fewer, D.P., Talla, E., Calteau, A., Cai, F., de Marsac, N.T., Rippka, R. & Herdman, M. (2013). Improving the coverage of the cyanobacterial phylum using diversity-driven genome sequencing. *Proceedings of the National Academy of Sciences of the United States of America*, 110(3), 1053–8.

Sigman, D. M., & Boyle, E. A. (2000). Glacial/interglacial variations in atmospheric carbon dioxide. *Nature*, 407(October), 859–869.

Simon, N., Cras, A.-L., Foulon, E., & Lemée, R. (2009). Diversity and evolution of marine phytoplankton. *Comptes Rendus Biologies*, 332(2), 159–170.

Singh, A. K., McIntyre, L. M., & Sherman, L. A. (2003). Microarray analysis of the genome-wide response to iron deficiency and iron reconstitution in the cyanobacterium *Synechocystis* sp. PCC 6803. *Plant Physiology,* 132(4), 1825–39.

Singh, A.K., Elvitigala, T., Cameron, J.C., Ghosh, B.K., Bhattacharyya-Pakrasi, M. & Pakrasi, H.B. (2010). Integrative analysis of large scale expression profiles reveals core transcriptional response and coordination between multiple cellular processes in a cyanobacterium. *BMC Systems Biology* 2010 4:1, 4(1), 1354–1365.

Singh, S., & Mishra, A. K. (2015). Unravelling of cross talk between Ca^{2+} and ROS regulating enzymes in Anabaena 7120 and *ntcA* mutant. *Journal of Basic Microbiology*.

Smith, R. J. (1995). Calcium and bacteria. *Advances in Microbial Physiology,* 37, 83–133.

Snow, J.T. (2014). The environmental, elemental and proteomic plasticity of *Trichodesmium* in the (sub) tropical Atlantic (Doctoral dissertation, University of Southampton).

Snow, J.T., Polyviou, D., Skipp, P., Chrismas, N.A., Hitchcock, A., Geider, R., Moore, C.M. & Bibby, T.S. (2015). Quantifying integrated proteomic responses to iron stress in the globally important marine diazotroph *Trichodesmium*. *PloS One,* 10(11), e0142626.

Sohm, J. a, Webb, E. a, & Capone, D. G. (2011). Emerging patterns of marine nitrogen fixation. *Nature Reviews. Microbiology*, 9(7), 499–508.

Spence, E., Sarcina, M., Ray, N., Møller, S. G., Mullineaux, C. W., & Robinson, C. (2003). Membrane-specific targeting of green fluorescent protein by the Tat pathway in the cyanobacterium *Synechocystis* PCC6803. *Molecular Microbiology,* 48(6), 1481–1489.

Spungin, D., Pfreundt, U., Berthelot, H., Bonnet, S., AlRoumi, D., Natale, F., Hess, W.R., Bidle, K.D. & Berman-Frank, I. (2016). Mechanisms of *Trichodesmium* bloom demise within the New Caledonia Lagoon during the VAHINE mesocosm experiment. *Biogeosciences Discuss*., 2016, 1–44.

Stal, L. J. (2009). Is the distribution of nitrogen-fixing cyanobacteria in the oceans related to temperature? *Environmental Microbiology*, 11(7), 1632–1645.

Staal, M., Rabouille, S., & Stal, L. J. (2007). On the role of oxygen for nitrogen fixation in the marine cyanobacterium *Trichodesmium* sp. *Environmental Microbiology*, 9(3), 727–736.

Stearman, R., Yuan, D. S., Yamaguchi-Iwai, Y., Klausner, R. D., & Dancis, A. (1996). A permease-oxidase complex involved in high-affinity iron uptake in yeast. *Science* , 271(5255), 1552–7.

Stevanovic, M., Hahn, A., Nicolaisen, K., Mirus, O., & Schleiff, E. (2012). The components of the putative iron transport system in the cyanobacterium *Anabaena* sp. PCC 7120. *Environmental Microbiology,* 14(7), 1655–70.

Stevanovic, M., Lehmann, C., & Schleiff, E. (2013). The response of the TonB-dependent transport network in *Anabaena* sp. PCC 7120 to cell density and metal availability. *BioMetals*, 26(4), 549–560.

Stevanovic, M. (2015). The putative siderophore-dependent iron transport network in *Anabaena* sp. PCC 7120.

Strzepek, R. F., & Harrison, P. J. (2004). Photosynthetic architecture differs in coastal and oceanic diatoms. *Nature*, 431(7009), 689–692

Su, Z., Olman, V., & Xu, Y. (2007). Computational prediction of Pho regulons in cyanobacteria. BMC *Genomics*, 8(156), 1–12.

Subramaniam, A., Yager, P.L., Carpenter, E.J., Mahaffey, C., Björkman, K., Cooley, S., Kustka, A.B., Montoya, J.P., Sañudo-Wilhelmy, S.A., Shipe, R. & Capone, D.G. (2008). Amazon River enhances diazotrophy and carbon sequestration in the tropical North Atlantic Ocean. *Proceedings of the National Academy of Sciences of the United States of America*, 105(30), 10460–5.

Taniuchi, Y., Chen, Y.L.L., Chen, H.Y., Tsai, M.L. & Ohki, K. (2012). Isolation and characterization of the unicellular diazotrophic cyanobacterium Group C TW3 from the tropical western Pacific Ocean. *Environmental microbiology,* 14(3), pp.641-654.

Thomas, J. D., Daniel, R. A., Errington, J., & Robinson, C. (2001). Export of active green fluorescent protein to the periplasm by the twin-arginine translocase (Tat) pathway in *Escherichia coli. Molecular Microbiology*, 39(1), 47–53.

Thompson, A. W., Huang, K., Saito, M. A., & Chisholm, S. W. (2011). Transcriptome response of high-and low-light-adapted *Prochlorococcus* strains to changing iron availability. *The ISME Journal*, 5(10), 1580–1594.

Thompson, A.W., Foster, R.A., Krupke, A., Carter, B.J., Musat, N., Vaulot, D., Kuypers, M.M. & Zehr, J.P. (2012). Unicellular cyanobacterium symbiotic with a single-celled eukaryotic alga. *Science*. 337(6101), 1546–50.

Thompson, A., Carter, B. J., Turk-Kubo, K., Malfatti, F., Azam, F., & Zehr, J. P. (2014). Genetic diversity of the unicellular nitrogen-fixing cyanobacteria UCYN-A and its prymnesiophyte host. *Environmental Microbiology*, 16(10), 3238–3249.

Toepel, J., Welsh, E., Summerfield, T. C., Pakrasi, H. B., & Sherman, L. A. (2008). Differential transcriptional analysis of the cyanobacterium *Cyanothece* sp. strain ATCC 51142 during light-dark and continuous-light growth. *Journal of Bacteriology*, 190(11), 3904–13.

Tölle, J., Michel, K.-P., Kruip, J., Kahmann, U., Preisfeld, A., & Pistorius, E. K. (2002). Localization and function of the IdiA homologue Slr1295 in the cyanobacterium *Synechocystis* sp. strain PCC 6803. *Microbiology*, 148(10), 3293–3305.

Tommassen, J., de Geus, P., Lugtenberg, B., Hackett, J., & Reeves, P. (1982). Regulation of the pho regulon of *Escherichia coli* K-12: Cloning of the regulatory genes *phoB* and *phoR* and identification of their gene products. *Journal of Molecular Biology,* 157(2), 265–274.

Tripp, H.J., Bench, S.R., Turk, K.A., Foster, R.A., Desany, B.A., Niazi, F., Affourtit, J.P. & Zehr, J.P. (2010). Metabolic streamlining in an open-ocean nitrogen-fixing cyanobacterium. *Nature*, 464(7285), 90–94.

Tsaloglou, M.N., Laouenan, F., Loukas, C.M., Monsalve, L.G., Thanner, C., Morgan, H., Ruano-López, J.M. & Mowlem, M.C. (2013). Real-time isothermal RNA amplification of toxic marine microalgae using preserved reagents on an integrated microfluidic platform. *Analyst*, 138(2), 593–602.

Tsuda, A., Takeda, S., Saito, H., Nishioka, J., Nojiri, Y., Kudo, I., Kiyosawa, H., Shiomoto, A., Imai, K., Ono, T. & Shimamoto, A. (2003). A mesoscale iron enrichment in the western subarctic Pacific induces a large centric diatom bloom. *Science*, 300(5621), 958–61.

Tuit, C., Waterbury, J., & Ravizza, G. (2004). Diel variation of molybdenum and iron in

marine diazotrophic cyanobacteria. *Limnology and Oceanography*, 49(4), 978–990.

Tuo, S., Chen, Y., & Chen, H. (2014). Low nitrate availability promotes diatom diazotroph associations in the marginal seas of the western Pacific. *Aquatic Microbial Ecology*, 73(2), 135–150.

Turner, K. H., Vallet-Gely, I., & Dove, S. L. (2009). Epigenetic control of virulence gene expression in *Pseudomonas aeruginosa* by a LysR-type transcription regulator. *PLoS Genetics*, 5(12), e1000779.

Tyrrell, T. (1999). The relative influences of nitrogen and phosphorus on oceanic primary production. *Nature*, 400(6744), 525–531.

Urbanowski, J. L., & Piper, R. C. (1999). The iron transporter Fth1p forms a complex with the Fet5 iron oxidase and resides on the vacuolar membrane. *Journal of Biological Chemistry*, 274(53), 38061–38070.

Ussher, S. J., Achterberg, E. P., Powell, C., Baker, A. R., Jickells, T. D., Torres, R., & Worsfold, P. J. (2013). Impact of atmospheric deposition on the contrasting iron biogeochemistry of the North and South Atlantic Ocean. *Global Biogeochemical Cycles*, 27(4), 1096–1107.

Valladares, A., Herrero, A., Pils, D., Schmetterer, G., & Flores, E. (2003). Cytochrome *c* oxidase genes required for nitrogenase activity and diazotrophic growth in *Anabaena* sp. PCC 7120. *Molecular Microbiology,* 47(5), 1239–1249.

Van Der Merwe, P., Bowie, A.R., Quéroué, F., Armand, L., Blain, S., Chever, F., Davies, D., Dehairs, F., Planchon, F., Sarthou, G. & Townsend, A.T. (2015). Sourcing the iron in the naturally fertilised bloom around the Kerguelen Plateau: particulate trace metal dynamics. *Biogeosciences*, 12(3), 739–755.

Van Mooy, B. A. S., Moutin, T., Duhamel, S., Rimmelin, P., & Van Wambeke, F. (2008). Phospholipid synthesis rates in the eastern subtropical South Pacific Ocean. *Biogeosciences*, 5(1), 133–139.

Van Mooy, B.A., Fredricks, H.F., Pedler, B.E., Dyhrman, S.T., Karl, D.M., Koblížek, M., Lomas, M.W., Mincer, T.J., Moore, L.R., Moutin, T. & Rappé, M.S. (2009). Phytoplankton in the ocean use non-phosphorus lipids in response to phosphorus scarcity. *Nature*, 458(7234), 69–72.

Van Mooy, B.A., Hmelo, L.R., Sofen, L.E., Campagna, S.R., May, A.L., Dyhrman, S.T., Heithoff, A., Webb, E.A., Momper, L. & Mincer, T.J. (2012). Quorum sensing control of phosphorus acquisition in Trichodesmium consortia. *The ISME Journal*, 6(2), 422–9.

Van Mooy, B.A.S., Krupke, A., Dyhrman, S.T., Fredricks, H.F., Frischkorn, K.R., Ossolinski, J.E., Repeta, D.J., Rouco, M., Seewald, J.D. & Sylva, S.P. (2015). Major role of planktonic phosphate reduction in the marine phosphorus redox cycle. *Science*, 348(6236), 783–785.

Villareal, T. A., & Carpenter, E. J. (2003). Buoyancy regulation and the potential for vertical migration in the oceanic cyanobacterium *Trichodesmium*. *Microbial Ecology*, 45(1), 1–10.

Villareal, T. A., Pilskaln, C. H., Montoya, J. P., & Dennett, M. (2014). Upward nitrate transport by phytoplankton in oceanic waters: balancing nutrient budgets in oligotrophic seas. *PeerJ,* 2, e302.

Vinyard, D. J., Ananyev, G. M., & Charles Dismukes, G. (2013). Photosystem II: The reaction center of oxygenic photosynthesis*. *Annual Review of Biochemistry*, 82(1), 577–606.

Vogel, C., & Marcotte, E. M. (2012). Insights into the regulation of protein abundance from proteomic and transcriptomic analyses. *Nature Reviews Genetics*, 13(4), 227–232.

VonAhlfen, & Schlumpberger. (2010). Effects of low A260/A230 ratios in RNA preparations on downstream applications. *QIAGEN Gene Expression Newsletter*, (15/10).

Wackett, L. P., Wanner, B. L., Venditti, C. P., & Walsh, C. T. (1987). Involvement of the phosphate regulon and the psiD locus in carbon-phosphorus lyase activity of

Escherichia coli K-12. *Journal of Bacteriology,* 169(4), 1753–1756.

Wagener, T., Pulido-Villena, E., & Guieu, C. (2008). Dust iron dissolution in seawater: Results from a one-year time-series in the Mediterranean Sea. *Geophysical Research Letters*, 35(16).

Waldron, K. J., Tottey, S., Yanagisawa, S., Dennison, C., & Robinson, N. J. (2007). A periplasmic iron-binding protein contributes toward inward copper supply. *Journal of Biological Chemistry* , 282(6), 3837–3846.

Walsby, A. E. (1992). The gas vesicles and buoyancy of *Trichodesmium*. In Marine Pelagic Cyanobacteria: *Trichodesmium* and other Diazotrophs (pp. 141–161). Dordrecht: Springer Netherlands.

Walworth, N., Pfreundt, U., Nelson, W.C., Mincer, T., Heidelberg, J.F., Fu, F., Waterbury, J.B., del Rio, T.G., Goodwin, L., Kyrpides, N.C. & Land, M.L. (2015). *Trichodesmium* genome maintains abundant, widespread noncoding DNA in situ, despite oligotrophic lifestyle. *Proceedings of the National Academy of Sciences* , 112(14), 4251–4256.

Walworth, N.G., Fu, F.X., Webb, E.A., Saito, M.A., Moran, D., Mcllvin, M.R., Lee, M.D. & Hutchins, D.A. (2016). Mechanisms of increased *Trichodesmium* fitness under iron and phosphorus co-limitation in the present and future ocean. *Nature Communications*, 7, 12081.

Wang, W., & Dei, R. (2003). Bioavailability of iron complexed with organic colloids to the cyanobacteria Synechococcus and *Trichodesmium*. *Aquatic Microbial Ecology*, 33, 247–259.

Wanner, B. L., & Chang, B. D. (1987). The *phoBR* operon in *Escherichia coli* K-12. *Journal of Bacteriology*, 169(12), 5569–5574.

Watanabe, M., Semchonok, D.A., Webber-Birungi, M.T., Ehira, S., Kondo, K., Narikawa, R., Ohmori, M., Boekema, E.J. & Ikeuchi, M. (2014). Attachment of phycobilisomes in an antenna-photosystem I supercomplex of cyanobacteria. *Proceedings of the National Academy of Sciences*, 111(7), 2512–2517.

Webb, E. A., Moffett, J. W., & Waterbury, J. B. (2001). Iron stress in open-ocean cyanobacteria (*Synechococcus, Trichodesmium*, and *Crocosphaera* spp.): Identification of the IdiA protein. *Applied and Environmental Microbiology*, 67(12), 5444–5452.

Webb, E. A., Jakuba, R. W., Moffett, J. W., & Dyhrman, S. T. (2007). Molecular assessment of phosphorus and iron physiology in *Trichodesmium* populations from the western Central and western South Atlantic. *Limnology and Oceanography*, 52(5), 2221–2232.

Webb, E.A., Ehrenreich, I.M., Brown, S.L., Valois, F.W. & Waterbury, J.B. (2009). Phenotypic and genotypic characterization of multiple strains of the diazotrophic cyanobacterium, *Crocosphaera watsonii*, isolated from the open ocean. *Environmental microbiology*, 11(2), pp.338-348

Welschmeyer, N. A. (1994). Fluorometric analysis of chlorophyll a in the presence of chlorophyll b and pheopigments. *Limnology and Oceanography*, 39(8), 1985–1992.

Werner, T. P., Amrhein, N., & Freimoser, F. M. (2005). Novel method for the quantification of inorganic polyphosphate (iPoP) in *Saccharomyces cerevisiae* shows dependence of iPoP content on the growth phase. *Archives of Microbiology*, 184(2), 129–36.

Westberry, T. K., & Siegel, D. A. (2006). Spatial and temporal distribution of *Trichodesmium* blooms in the world's oceans. *Global Biogeochemical Cycles*, 20(4).

White, A. K., & Metcalf, W. W. (2004). The *htx* and *ptx* operons of *Pseudomonas stutzeri* WM88 are new members of the pho regulon. *Journal of Bacteriology*, 186(17), 5876–82.

White, A. E., Spitz, Y. H., Karl, D. M., & Letelier, R. M. (2006a). Flexible elemental stoichiometry in *Trichodesmium* spp. and its ecological implications. *Limnology and Oceanography*, 51(4), 1777–1790.

White, A. E., Spitz, Y. H., & Letelier, R. M. (2006b). Modeling carbohydrate ballasting by

Trichodesmium spp. *Marine Ecology Progress Series*, 323, 35–45.

White, A. E., Karl, D. M., Björkman, K., Beversdorf, L. J., & Letelier, R. M. (2010). Production of organic matter by *Trichodesmium* IMS101 as a function of phosphorus source. *Limnology and Oceanography,* 55(4), 1755–1767.

Wille, N. (1904). Die Schizophyceen der Plankton-Expedition. In: Ergebnisse der Plankton-Expedition der Humbolt-Stiftung. Lipsius and Tischer, Kiel.

Williams, J. (1988). Construction of specific mutations in photosystem II photosynthetic reaction center by genetic engineering methods in *Synechocystis* 6803. *Methods in Enzymology. 167, pp.766-778.*

Willsky, G. R., Bennett, R. L., & Malamy, M. H. (1973). Inorganic phosphate transport in *Escherichia coli:* involvement of two genes which play a role in alkaline phosphatase regulation. *Journal of Bacteriology*, 113(2), 529–39.

Wolfe-Simon, F., Grzebyk, D., Schofield, O., & Falkowski, P. G. (2005). The role and evolution of superoxide dismutases in algae. *Journal of Phycology*. 41(3), pp.453-465.

Wood, P. M. (1978). Interchangeable copper and iron proteins in algal photosynthesis. Studies on plastocyanin and cytochrome c-552 in *Chlamydomonas*. *European Journal of Biochemistry / FEBS*, 87(1), 9–19.

Wösten, M. M. (1998). Eubacterial sigma-factors. *FEMS Microbiology Reviews*, 22(3), 127–50.

Wu, J., & Luther, G. W. (1995). Complexation of Fe(III) by natural organic ligands in the Northwest Atlantic Ocean by a competitive ligand equilibration method and a kinetic approach. *Marine Chemistry*, 50(1–4), 159–177.

Wu, J., Sunda, W., Boyle, E.A. and Karl, D.M. (2000). Phosphate depletion in the western North Atlantic Ocean. *Science*, 289(5480), 759–62.

Yamasaki, Y., Kim, D.-I., Matsuyama, Y., Oda, T., & Honjo, T. (2004). Production of superoxide anion and hydrogen peroxide by the red tide dinoflagellate *Karenia mikimotoi*. *Journal of Bioscience and Bioengineering*, 97(3), 212–215.

Yan, Y., Wei, C., Zhang, W., Cheng, H., & Liu, J. (2006). Cross-talk between calcium and reactive oxygen species signaling. *Acta Pharmacologica Sinica*, 27(7), 821–6.

Yang, K., & Metcalf, W. W. (2004). A new activity for an old enzyme: *Escherichia coli* bacterial alkaline phosphatase is a phosphite-dependent hydrogenase. *Proceedings of the National Academy of Sciences of the United States of America*, 101(21), 7919–7924.

Yasmin, S., Andrews, S. C., Moore, G. R., & Le Brun, N. E. (2011). A new role for heme, facilitating release of iron from the bacterioferritin iron biomineral. *Journal of Biological Chemistry*, 286(5), 3473–3483.

Yates, J. R. (2011). A century of mass spectrometry: from atoms to proteomes. *Nature Methods,* 8(8), 633–637.

Ye, J., Coulouris, G., Zaretskaya, I., Cutcutache, I., Rozen, S., & Madden, T. L. (2012). Primer-BLAST: A tool to design target-specific primers for polymerase chain reaction. *BMC Bioinformatics,* 13(134), 1–11.

Yeremenko, N., Kouril, R., Ihalainen, J.A., D'Haene, S., van Oosterwijk, N., Andrizhiyevskaya, E.G., Keegstra, W., Dekker, H.L., Hagemann, M., Boekema, E.J. & Matthijs, H.C. (2004). Supramolecular organization and dual function of the IsiA chlorophyll-binding protein in cyanobacteria. *Biochemistry*, 43(32), 10308–13.

Yong, S.C., Roversi, P., Lillington, J., Rodriguez, F., Krehenbrink, M., Zeldin, O.B., Garman, E.F., Lea, S.M. & Berks, B.C. (2014). A complex iron-calcium cofactor catalyzing phosphotransfer chemistry. *Science*, 345(6201), 1170–3.

Yooseph, S., Nealson, K.H., Rusch, D.B., McCrow, J.P., Dupont, C.L., Kim, M., Johnson, J., Montgomery, R., Ferriera, S., Beeson, K. and Williamson, S.J. (2010). Genomic and functional adaptation in surface ocean planktonic prokaryotes. *Nature*, 468(7320), 60–

66.

Yu, X., Geng, J., Ren, H., Chao, H., & Qiu, H. (2015). Determination of phosphite in a full-scale municipal wastewater treatment plant. *Environmental Science: Processes & Impacts*, 17(2), 441–447.

Yun, C. W., Bauler, M., Moore, R. E., Klebba, P. E., & Philpott, C. C. (2001). The role of the FRE family of plasma membrane reductases in the uptake of siderophore-iron in *Saccharomyces cerevisiae*. The *Journal of Biological Chemistry,* 276(13), 10218–23.

Zambolin, S., Clantin, B., Chami, M., Hoos, S., Haouz, A., Villeret, V., & Delepelaire, P. (2016). Structural basis for haem piracy from host haemopexin by *Haemophilus influenzae*. *Nature Communications*, 7, 11590.

Zehr, J. P., Mellon, M. T., & Zani, S. (1998). New nitrogen-fixing microorganisms detected in oligotrophic oceans by amplification of Nitrogenase (*nifH*) genes. *Applied and Environmental Microbiology,* 64(9), 3444–50.

Zehr, J.P., Bench, S.R., Carter, B.J., Hewson, I., Niazi, F., Shi, T., Tripp, H.J. & Affourtit, J.P. (2008). Globally distributed uncultivated oceanic N_2-fixing cyanobacteria lack oxygenic photosystem II. *Science*, 322(5904), 1110–2.

Zehr, J. P., Hewson, I., & Moisander, P. (2009). Molecular biology techniques and applications for ocean sensing. *Ocean Science*, 5(2), 101–113.

Zeidner, G., Bielawski, J. P., Shmoish, M., Scanlan, D. J., Sabehi, G., & Béjà, O. (2005). Potential photosynthesis gene recombination between Prochlorococcus and *Synechococcus* via viral intermediates. *Environmental Microbiology*, 7(10), 1505–1513.